High-Performance Hybrid-Fibre Concrete

- Development and Utilisation -

High-Performance Hybrid-Fibre Concrete

- Development and Utilisation -

Proefschrift

ter verkrijging van de graad van doctor
aan de Technische Universiteit Delft,
op gezag van de Rector Magnificus prof.dr.ir. J.T. Fokkema,
voorzitter van het College voor Promoties,
in het openbaar te verdedigen

op 16 januari 2006 te 13:00 uur

door

Ivan MARKOVIĆ

diplomirani gradjevinski inženjer za konstrukcije
(Universiteit van Belgrado, Servië)

geboren te Aleksandrovac, Servië

S U M M A R Y

High-Performance Hybrid-Fibre Concrete: Development and Utilisation

Although concrete is the most utilised building material on earth, this material has a large shortcoming: it has a good resistance against compressive stresses, but a very low resistance against tensile stresses. When loaded in tension, concrete cracks under very low loads, which means that its tensile strength is low. Moreover, once cracked, cracks in concrete widen and propagate very fast: this means that the so-called "ductility" of concrete is very small.
The usual way to solve this problem is the application of steel reinforcement in concrete structures. Other possibility is the application of different types of fibres in the concrete, for example steel or synthetic fibres: this material is then called "fibre concrete". In the past, many types of fibre concrete have been developed. For many of them, the added value of fibres was rather low: no improvement of tensile strength could be achieved, only the ductility was somewhat higher compared to that of plain concrete.

In the research project presented in this PhD-thesis, an innovative type of fibre concrete is developed, with improved both the tensile strength and the ductility: the Hybrid-Fibre Concrete (HFC). The expression "Hybrid" refers to the "hybridisation" of fibres: short and long steel fibres were combined together in one concrete mixture. This is opposite to conventional steel fibre concretes, which contain only one type of fibre.
The basic goal of combining short and long fibres is from one side to improve the tensile strength by the action of short fibres, and from the other side to improve the ductility by the action of long fibres. In the developed Hybrid-Fibre Concrete, short steel fibres (fibre length = 6-13 mm) and long steel fibres (fibre length = 30-60 mm) are combined. The short fibres are straight, while the long fibres possess hooks at their ends, and both fibre types are made of high-strength steel (f_y = 2500 MPa).

In this research project, all important aspects needed for the development and application of Hybrid-Fibre Concrete have been considered. In total 15 mixtures, with different types and amounts of steel fibres were developed and tested in the fresh state (workability) as well as in the hardened state (uniaxial tensile tests, flexural tests, pullout tests of single fibres and compressive tests). A new analytical model for bridging of cracks by fibres was developed and successfully implemented for tensile softening response of HFC. At the end, the utilisation of HFC in the engineering practice was discussed, including a case-study on light prestressed long-span beams made of HFC.

Pullout tests on single fibres were performed first. Long hooked-end fibres were pulled-out from concretes, in which the following parameters were varied: water-binder ratio, the quantity of short fibres in the concrete and the grading of the aggregate. Both fibres aligned and inclined with respect to the pullout force were tested. The maximum pullout force in the fibres is higher, if the water-binder ratio is lower and the quantity of short fibres in the

surrounding concrete is higher. The fibres inclined at 15° and 30° give an about 20 % better pullout response than aligned ones.

The mixture composition of HFC is one of the decisive factors affecting its mechanical performance. The main goal here was to obtain self-compacting HFC mixtures. The two most important requirements for these mixtures are flowability and stability. Flowablilty can guarantee that the orientation of fibres is always similar for the same way of casting. The stability can guarantee that the number of fibres in each part of the structural element is more-or-less constant, i.e. that no segregation or clustering of fibres takes place. The self-compactability of HFC mixtures is therefore the best possible guarantee for the overall quality of structural elements made of HFC.

The optimisation of mixtures was performed in steps. First, the optimum grading and quantity of aggregate were determined using the concept of packing density of dry aggregate and aggregate-fibre mixtures, as well as the Compressible Packing Model [De Larrard, 1999]. The optimum quantity of cement was related to the applied type and quantity of fibres, and was determined from experimental measurements of the workability. Based on these measurements, a analytical model, which relates the applied fibre type and needed (optimum) quantity of cement for self-compacting HFC mixtures, was developed as well. The water-binder ratio was kept constant at 0.2. The obtained compressive strength of HFC ranged from 100 to 130 MPa.

After the mixture optimisation, the flexural and uniaxial tensile tests of HFC's with different fibre combinations were performed. In both types of tests, special attention was paid to the production of the specimens: a special way of casting was developed in order to achieve the best possible fibre orientation in relation to the tensile behaviour. Moreover, this way of casting was kept constant for all specimens, in order to achieve as low scatter of the results.

Flexural tests were performed as three-point bending tests on notched beams. In the tests, very high values of the flexural strengths of HFC were achieved, for example up to 40 MPa, for hybrid-fibre concrete with in total 2.0 vol.-% of short and long fibres. For comparison, the concrete which contained also 2.0 vol.-% of only short fibres, had a flexural strength of only 25 MPa.

The largest part of the uniaxial tensile tests were performed on un-notched dog-bone shaped specimens. The maximum tensile strengths achieved were 10-12 MPa for hybrid fibre concretes with 2 vol.-% of fibres, and about 15 MPa for concrete with 3 vol.-% of short fibres only.

In both types of tests, it was observed that short fibres are efficient in bridging fine microcracks, which develop in the initial phases of tensile loading, while long fibres are more active in bridging larger macrocracks, which develop later, after the widening and propaga-

tion of the microcracks. Therefore, generally speaking, the short fibres increase the tensile strength and the long fibres increase the ductility of Hybrid-Fibre Concrete.

Moreover, in all tested concretes, the tensile loading continued to increase after the first crack was formed, which is called "strain hardening" and which guarantees a large post-cracking deformation capacity of HFC. Last but not least, in HFC the phenomenon called "multiple cracking" was observed in the initial phases of tensile loading: instead of the formation of a single crack, many very thin cracks were observed. This can be a very large advantage concerning the durability of HFC.

After the tests, the number and orientation of fibres in the specimens were determined using manual and optical methods. In the flexural specimens for example, the average orientation angle of the long fibres (approximaltely 30º) was lower than that of short fibres (approximately 50º), which suggest that long fibres are better oriented. Also, the smaller the specimen, the better fibre orientation can be achieved. The deformability of the hooks of long fibres was analysed as well: the number of the long fibres with deformed hooks is larger (and therefore the total tensile capacity of HFC is higher) if more short fibres are present in the concrete.

"Synergy" is the phenomenon where two subjects acting together, achieve a better result than each of them acting independently from each other. Synergy has been observed in HFC: better flexural and tensile behaviour were achieved using hybrid-fibre concretes, than using reference concretes with only one fibre type.

After the uniaxial tensile tests have been performed, the uniaxial tensile behaviour of HFC was analysed and modelled analytically in detail. The whole tensile response of HFC was divided into 4 main phases: elastic phase, microcracking, macrocrack growth and bridging of macrocrack, according to [Van Mier, 2004a]. The influences of different types of fibres were analytically modelled using existing models for the macrocrack growth phase, with special attention to the multiple cracking [Tjiptobroto & Hansen, 1992]. Own analytical model was developed for modelling of the bridging of macrocrack by fibres (also called "tensile softening phase"). This analytical model is based on the number of fibres present across the crack and their individual pullout responses. The model simulated the experimentally obtained tensile softening behaviour of HFC quite well. The existence of the synergy of short and long fibres was suggested with this analytical model as well.

Finally, in the last chapter of this PhD-thesis, the utilisation of Hybrid-Fibre Concrete in the engineering practice was discussed. Due to the demanding quality control, application of HFC for pre-cast concrete products is recommended. A procedure to relate mechanical properties of HFC at the material level to its behaviour at the structural level has been proposed, with special attention to the design stress-strain relation in the tensile domain. Subsequently, three different types of long-span prestressed beams were designed in HFC and compared to the solutions in conventional concrete C55/65 in terms of self-weight and needed amount of

the reinforcement and prestressing steel. HFC beams are 2.5 up to even 4 times lighter than conventional ones, and no conventional reinforcement is needed in HFC beams. In this way, the higher material costs of HFC can be fully compensated. The expectation is that the durability of the structures made of HFC is better compared to that of conventional concrete structures, which can further decrease the maintenance costs of structures and increase the attractivity of HFC.

Ivan Marković,
Delft University of Technology

S A M E N V A T T I N G

Hoogwaardig Hybride-Vezelbeton: Ontwikkeling en toepassingen

Alhoewel beton het meest gebruikte bouwmateriaal ter wereld is, bezit dit materiaal een groot nadeel: de weerstand tegen drukspanningen is redelijk hoog, maar de weerstand tegen trekspanningen is zeer laag. Indien onderworpen aan de trekbelasting, begint beton al onder zeer lage belasting te scheuren, wat verder betekent dat beton een lage treksterkte bezit. Bovendien, zodra het beton eenmaal gescheurd is, worden de scheuren snel wijder en breiden zich snel uit: dit betekent dat de zogenoemde "taaiheid" of "ductiliteit" van het beton laag is.
Het probleem van lage treksterkte en ductiliteit wordt in de praktijk opgelost door het toepassen van wapening in betonconstructies. Een andere mogelijkheid is het toepassen van verschillende soorten vezels in beton, zoals staal- of synthetische vezels: dit materiaal wordt dan "vezelbeton" genoemd. Veel verschillende types vezelbeton zijn ontwikkeld in het verleden. Toch is in de meeste gevallen de toegevoegde waarde van vezels laag: in vergelijking met ongewapend beton werd meestal verbetering van de treksterkte geregistreerd, alleen was de ductiliteit iets hoger.

In het kader van het onderzoeksproject dat in dit proefschrift gepresenteerd wordt, is een innovatieve betonsoort ontwikkeld, waarbij zowel de treksterkte als ook de ductiliteit verbeterd zijn: het Hybride-Vezelbeton of het HVB (in het Engels "Hybrid-Fibre Concrete"- HFC). De uitdrukking "Hybride" wordt hier gebruikt om te benadrukken, dat het om de "hybridisatie" van de vezels gaat: korte en lange staalvezels zijn samen gebruikt in één betonmengsel. Dit staat in tegenstelling tot conventioneel vezelbeton, waarbij het gebruikelijk is om slechts één soort vezel te gebruiken.
Het hoofddoel van het gelijktijdige gebruik van verschillende soorten vezels is om aan de ene kant de treksterkte door korte vezeltjes te vergroten, en aan de andere kant de ductiliteit door middel van lange vezels te verbeteren. In het hier onderzochte HVB, zijn korte rechte staalvezeltjes (vezellengte = 6-13 mm) gecombineerd met lange gehaakte staalvezels (vezellengte = 30-60 mm).

Alle belangrijke aspecten nodig voor een volledige ontwikkeling en toepassing van Hybride-Vezelbeton zijn geanalyseerd in dit onderzoeksproject. Meer dan 15 mengsels, met verschillende typen en hoeveelheden staalvezels zijn ontwikkeld en beproefd, zowel in de verse toestand (verwerkbaarheid), als ook in de verharde toestand (zuivere trekproeven, buigproeven, uittrekproeven van individuele vezels en drukproeven). Een nieuw analytisch model voor de overbrugging van scheuren door vezels is ontwikkeld en met succes toegepast voor HVB. Ten slotte, het toepassen van HVB in de praktijk werd geanalyseerd, inclusief een case-study waarin de toepassing van HVB voor voorgespannen betonnen liggers met grote overspanningen onderzocht is.

In het begin van dit project zijn uittrekproeven aan individuele vezels uitgevoerd. Lange gehaakte vezels zijn uit beton uitgetrokken, waarbij de volgende parameters gevarieerd zijn: de water-bindmiddel verhouding, de hoeveelheid korte vezels en de korrelgradering van de toeslag. Vezels, met orientatie evenwijdig, als ook onder een hoek ten opzichte van de uittrekkracht, zijn beproefd. De maximale uittrekkracht in de vezels neemt toe, indien de water-bindmiddel verhouding lager wordt, en indien de hoeveelheid korte vezels in beton toeneemt. De vezels die onder de hoeken van 15° en 30° ten opzichte van de uittrekkracht staan, geven een ca. 20 % beter uittrekgedrag, vergeleken met vezels die evenwijdig ten opzichte van de uittrekkracht georienteerd zijn.

De mengselsamenstelling van HVB is één van de belangrijkste factoren ten aanzien van de mechanische eigenschappen. Eén van de hoofddoelen van dit onderzoek was om zelfverdichtende HVB mengsels te produceren. De twee meest belangrijke voorwaarden van zulke mengsels, zijn de vloeibaarheid en de stabiliteit. De vloeibaarheid kan garanderen dat de orientatie van de vezels altijd hetzelfde blijft, indien dezelfde manier van beton storten toegepast wordt. De stabiliteit van het mengsel kan garanderen dat het aantal vezels in elk onderdeel van een constructief element gelijk blijft, d.w.z. dat er geen segregatie of clustering van vezels plaatsvindt. De zelfverdichtende eigenschappen van HVB zijn dus momenteel de beste mogelijke garantie met betrekking tot de kwaliteit van de uit het HVB geproduceerde constructieve elementen.

Het optimaliseren van mengsels is in een aantal stappen uitgevoerd. De optimale korrelgradering en hoeveelheid toeslag zijn eerst bepaald, door middel van het concept van pakking van droge toeslag en pakking van droge toeslag en vezels samen. Het zogenoemde "Compressible Packing Model" [De Larrard, 1999] werd hierbij toegepast. De optimale hoeveelheid cement werd gerelateerd aan het toegepaste type en de hoeveelheid vezels, door middel van experimentele metingen van de verwerkbaarheid. Op basis van deze metingen, werd een analytisch model ontwikkeld, dat het toegepaste type en de hoeveelheid vezels met de optimale hoeveelheid cement relateert, zodat de HVB mengsels zelfverdichtend zijn. Een constante water-bindmiddel verhouding van 0.2 is toegepast voor de meeste mengsels. De druksterkte van het ontwikkelde HVB lag tussen 100 MPa en 130 MPa.

Na de optimalisatie van de mengsels, zijn de buigproeven en zuivere trekproeven op HVB's met verschillende vezelcombinaties uitgevoerd. In beide soorten proeven werd bijzondere aandacht aan de productie van proefstukken gegeven: een bijzondere manier van het storten van HVB werd ontwikkeld, met als doel het bereiken van een zo goed mogelijke oriëntatie van de vezels, d.w.z. een zo goed mogelijk trekgedrag. Bovendien zijn alle proefstukken altijd op dezelfde manier gestort, met de bedoeling een zo laag mogelijke spreiding van de proefresultaten te krijgen.

Buigproeven zijn uitgevoerd als driepuntsbuigproeven op balken met een kerf in het midden. In de proeven zijn zeer hoge buigtreksterkten voor HVB gevonden: bij voorbeeld ca. 40 MPa voor een hybride-vezelbeton met in totaal 2 vol.-% korte en lange vezels. Ter vergelijking, beton met eveneens 2 vol.-%, maar dan alleen korte vezels, had een buigtreksterkte van ca. 25 MPa.

Zuivere trekproeven zijn uitgevoerd op proefstukken met de zogenoemde "dog-bone" vorm, waarbij de meeste geen kerf hadden. De maximale bereikte treksterkte was ca. 10 - 12 MPa voor hybride-vezelbeton met 2 vol.-% vezels, en ca. 15 MPa voor beton met 3 vol.-% van uitsluitend korte vezels.

Een van de meest belangrijke conclusies uit beide soorten proeven, is dat de korte vezeltjes efficiënt voornamelijk de kleine microscheurtjes overbruggen, die zich in de initiële fasen van de trekbelasting ontwikkelen, terwijl lange vezels voornamelijk actief zijn in het overbruggen van grotere scheuren (macroscheuren), die als resultaat van het uitbreiden en verspreiden van de microscheuren ontstaan. In het algemeen wordt dus de treksterkte door de korte vezeltjes, en de ductiliteit door de lange vezels verhoogd.

Bovendien, in alle beproefde HVB's neemt de trekbelasting toe, ook nadat de eerste scheur gevormd is. Dit verschijnsel is bekend als de "strain hardening" en daardoor wordt een gunstig nascheur gedrag van HVB gegarandeerd. Uiteindelijk, in de initiële fasen van de trekproeven op HVB werd ook het verschijnsel dat bekend staat als de "multiple cracking" geobserveerd: in plaats van het ontstaan van één enkele scheur, ontstaan er heel veel kleine microscheurtjes. Dit kan een groot voordeel van HVB zijn met betrekking tot de duurzaamheid.

Na het uitvoeren van de proeven zijn het aantal en de oriëntatie van vezels in de proefstukken bepaald door middel van handmatige en optische methoden. Geconcludeerd werd, dat de oriëntatie van de lange vezels iets beter was dan die van de korte vezels: in de buigbalken was de gemiddelde oriëntatiehoek van de lange vezels ca. 30°, en van de korte ca. 50°. Hoe kleiner het proefstuk is, des te beter wordt de oriëntatiehoek. De vervormbaarheid van de haakjes van de lange vezels is ook geanalyseerd: het aantal lange vezels met vervormde haakjes is groter (en daardoor ook de totale trekcapaciteit van HVB) indien er meer korte vezels in het beton aanwezig zijn.

"Synergie" is een verschijnsel waarbij twee mechanismen die samen werken een beter resultaat bereiken, in vergelijking met het resultaat dat ze onafhankelijk van elkaar zouden bereiken. De synergie werd in HVB geobserveerd: het buiggedrag en het zuivere trekgedrag van HVB waren beter dan buiggedrag en zuiver trekgedrag van betons met alleen korte of alleen lange vezels (die als referentie gebruikt zijn).

Nadat de zuivere trekproeven uitgevoerd waren, is het zuivere trekgedrag geanalyseerd en tot in detail gemodelleerd. Het gehele trekgedrag van HVB werd volgens [Van Mier, 2004a] verdeeld in 4 fasen, te weten: elastisch gedrag, de vorming van microscheuren, het groeien van macroscheur en het overbruggen van macroscheur door vezels. Een bestaand analytisch model [Tjiptobroto & Hansen, 1992], werd gebruikt om de vorming van microscheuren en "multiple cracking" te modelleren. Een nieuw analytisch model werd ontwikkeld voor de modellering van het overbruggen van macroscheur door vezels (de zogenoemde "tensile softening" fase). Dit analytische model is gebaseerd op het aantal vezels die de scheur overbruggen en op hun individuele uittrekgedrag. Het uit de proeven verkregen trekgedrag van HVB in de "tensile softening" fase, kon met succes gemodelleerd worden door middel van dit analytische model. De synergie van de korte en de lange vezels volgt ook uit dit analytische model.

Aan het einde, in het laatste hoofdstuk van dit proefschrift, zijn de toepassingen van Hybride-Vezelbeton in de praktijk geanalyseerd. Het gebruik van HVB voornamelijk in de sector van prefab-industrie werd aanbevolen, aangezien de noodzakelijke strenge eisen met betrekking tot de kwaliteit van producten. Een volledige procedure om de mechanische eigenschappen van HVB op materiaalniveau te verbinden met het gedrag van HVB op constructieniveau is voorgesteld, met bijzondere aandacht voor het spanning-rek diagram van HVB onder trek.

Ten slotte zijn drie verschillende voorgespannen balken met grote overspanningen ontworpen in HVB, en vergeleken met balken van dezelfde overspanning in beton C55/65. De parameters die vergeleken zijn, waren het eigengewicht van de balken en de hoeveelheden staal- en voorspanwapening. De HVB balken zijn ca. 2.5 tot zelfs 4 keer lichter dan de balken in C55/65, en bovendien is in de HVB balken geen passieve staalwapening nodig. Op deze manier worden de hoge materiaalkosten van HVB volledig gecompenseerd. Naar verwachting is ook de duurzaamheid van HVB veel beter dan die van gewoon beton, wat verder kan resulteren in lagere onderhoudskosten van constructies en attractieve toepassingsmogelijkheden.

Ivan Marković,
Technische Universiteit Delft

A C K N O W L E D G E M E N T S

TABLE OF CONTENTS

Chapter 3: Tensile Properties

Chapter 4: Analytical Modelling of Tensile Behaviour

Chapter 6: Conclusions and future prospects

CHAPTER 1:

INTRODUCTION

1.1 Scope of the research

Concrete is the mostly utilised building material nowadays. Although most of the structures which surround us are made of concrete, there are still some serious problems related to the utilisation of this material:

− Concrete possesses a very low tensile strength and almost no ductility. Therefore, the utilisation of steel reinforcement is always required, to bridge the cracks and to cope with the tensile forces larger than the tensile capacity of concrete. The reinforcement shares a substantial part of the total costs of concrete structures, including the material costs, the labour costs and the time needed for its placing;

− The self-weight of concrete structures is couple of times higher compared to steel structures with the same carrying capacity. This requires large support structures and increases significantly the production, transport and handling costs;

− Concrete is not a maintenance-free material: harmful substances penetrate from its surface through cracks and pores, which may cause the corrosion of reinforcement. The maintenance is therefore necessary, and this may create significant additional costs during the service life of concrete structures.

With regard to the previously mentioned disadvantages, a very suitable solution can be the utilisation of <u>High-Performance Hybrid-Fibre Concretes (HFC)</u>. This is a whole range of fibre concretes, which were developed within the research project presented in this PhD-Thesis. They contain different combinations of short and long steel fibres in optimised high-strength concrete matrices. Hybrid-Fibre Concretes are characterised by high tensile and flexural strengths and high ductility, as well as by a high compressive strength and a very good workability.

This concrete originates from three initially independent types of concrete:

− High- and Ultra-high-strength-concrete (UHSC or UHPC): possesses highly optimised mixture composition, a very dense inner structure and a very high compressive strength (f_{cc} > 100 MPa).

− Self-compacting concrete (SCC): flows under its own weight and does not require any additional mechanical compaction; the self-compactability improves the homogeneity of the inner matrix structure and reduces the production time.

− Fibre-reinforced concrete (FRC): contains discontinuous steel or synthetic fibres, which bridge cracks in concrete loaded in tension; in this way, the ductility of concrete can be increased;

Combining the properties of these types of concrete, the Hybrid-Fibre Concretes (HFC) can rightfully be denoted not only as "high-performance", but rather as "multiple-performance concretes". These concretes are designed in such a way, that they can successfully respond to all demands during production, construction and service life of structures.

By virtue of its improved tensile and compressive resistance, the structural elements made of Hybrid-Fibre Concrete can be much thinner and lighter than those made of conventional concrete, which simplifies transport and erection and decreases the size of the supporting structure. The production of such elements is simplified as a result of good workability (self-compactability). This material is therefore very suitable for the utilisation in the precast concrete industry. When combined with prestressing, often no conventional reinforcement is necessary, which additionally decreases the cost of structures. Taking into account that the development of a very fine narrow pattern of multiple cracks is possible (by virtue of the action of fibres as micro-reinforcement), it may be expected that the durability will be satisfactory as well. However, like all other types of high-performance concrete, also Hybrid-Fibre Concrete requires a high level of quality control during production.

1.2 Research goals

The goals of this research are:
− to create and optimise the mixture compositions of Hybrid-Fibre Concretes on the basis of their tensile properties and workability;
− to find the appropriate combinations of fibres, which can ensure an optimum tensile response of the concrete, with regard to uniaxial tensile strength, flexural strength, first-cracking stress and ductility;
− to be able to model the tensile behaviour of Hybrid-Fibre Concretes with different combinations of fibres, on the basis of performed uniaxial tensile tests
− to create the fundamentals for the utilisation of Hybrid-Fibre Concretes in the engineering practice, on the basis of determined tensile properties; subsequently, to perform a study on its utilisation in the engineering practice and to evaluate this utilisation from engineering, technical and economical point of view.

This research covers the whole concept of the development of Hybrid-Fibre Concrete, from its raw materials, up to its utilisation in the engineering practice.

1.3 Research strategy

Mixture composition of HFC

The orientation of fibres in the structural elements is one of the key factors regarding the applications of Hybrid-Fibre Concrete. In an ideal case, one should be able to design and to control the orientation of fibres in structural elements, in order to optimise their load-carrying capacity. The best possible way to achieve this, is to create flowable and stable HFC mixtures, with constant rheological properties. By flowing only under their own weight, such mixtures would allow to design and control the fibre orientation rather well. The self-compacting HFC-mixtures would most probably satisfy this demand.

In order to obtain flowable (self-compacting) HFC mixtures, the composition of concrete matrix must be adapted and optimised, so that the applied types and quantities of fibres can be "accommodated" in a proper way in the matrix. This means that an optimum quantity and type of cement, and an optimum quantity and grading of aggregate should be determined, always with respect to the combination and quantities of all applied fibre types.

On the microlevel, the concrete matrix around each fibre must be dense enough to ensure efficient utilisation of fibres in their pullout during opening and bridging of crack.

The bridging of a crack by fibres will initially be simulated by pullout tests on single short and long fibres. The main goal of these tests is to find the concrete matrix (i.e. here the pullout medium), from which the most efficient pullout response of the fibres can be obtained. The main parameters in these tests are: the composition of the concrete from which the fibres are pulled out, the presence of short "secondary" fibres in that concrete, and the inclination angles of the fibres which are pulled out.

Tensile behaviour of HFC

The selection of the optimum combinations of fibres, requires testing and determination of the tensile properties of different Hybrid-Fibre Concretes (HFC). The basic demand here is to achieve the best possible tensile properties with a minimum applied quantity of fibres. Flexural tests will be performed firstly, in order to find the combinations of fibres, which fulfil this demand. Subsequently, uniaxial tensile tests on selected Hybrid-Fibre Concretes will be performed, in order to enable the final evaluation of the tensile properties. This will also create a basis for the utilisation of HFC in practice. However, not only the applied type and quantity of fibres affect the tensile properties, but also parameters like the number and orientation of fibres. Therefore, also these parameters will be analysed in detail and related to the tensile behaviour of fibre concrete.

Analytical modelling of the tensile behaviour of Hybrid-Fibre Concretes can provide an insight into the behaviour of HFC with many other combinations of fibres, as well as a better understanding of the fracture processes during tensile loading. The uniaxial tensile behaviour will be modelled on the basis of the results of single fibre pullout tests and uniaxial tensile tests, accompanied by the analysis of the number and orientation of the fibres.

The first step needed for the utilisation of Hybrid-Fibre Concretes on the structural level, is the creation of appropriate stress-strain relations. This will be done using the results of the uniaxial tensile tests on HFC. Moreover, appropriate relations between the tensile properties determined by testing on the material level, and tensile properties of HFC in real structures, will be provided. Here, the number and orientation of fibres play the most important roles.

In order to evaluate all the advantages of the utilisation of Hybrid-Fibre Concrete in engineering practice, prefabricated concrete beams with different spans and cross-sections will be designed in HFC, as well as in conventional concrete, and subsequently compared to each other. This example of utilisation will be evaluated from the engineering, technical and economical point of view.

1.4   Outline of this PhD-Thesis

This PhD-thesis consists of six chapters, and its structure is given in Fig. 1.1. As a rule, each chapter begins with a short literature overview, followed by more sub-chapters, which contain the results and the evaluation of appropriate experiments and analytical studies. In the end of each chapter, the concluding remarks are given.

In the Introduction (Chapter 1), basic facts are given on the development and utilisation of Hybrid-Fibre Concretes, on the goals of this research and on the research methodology.

In Chapter 2, methods used to design mixtures of Hybrid-Fibre Concrete, for given types and quantities of fibres, are presented. The sub-chapters include the determination of the packing densities of dry aggregate-fibre mixtures, the workability characterisation of HFC with different fibre combinations, the recommendations on the mixture composition of HFC using the "Excess-paste model", and the single fibre pullout tests using different types of concrete as pullout medium. Each of these sub-chapters begins with a short literature overview.

In Chapter 3, a general literature overview on the tensile behaviour of different high-performance fibre concretes is given first, focusing on tensile strength, strain hardening and ductility. The results of the flexural tests on different types of Hybrid-Fibre Concrete are given subsequently. From these tests, the concretes with the best flexural behaviour are selected, and tested in uniaxial tension. Both types of tests are accompanied by the analysis of the number and orientation of fibres in the specimens, and by their relation to the tensile properties.

In Chapter 4, the stages of the tensile fracture of fibre concrete are first described in detail. A short literature overview on the existing modelling techniques for both the strain hardening and the strain softening of fibre concretes is also provided. Subsequently, the analytical modelling of the strain hardening and the strain softening stage of tensile fracture of Hybrid-Fibre

Concrete is performed. Both analytical models are based on the single fibre pullout tests and on the number and orientation of fibres in the tensile specimens.

1. Hybrid-Fibre Concrete (HFC) - Introduction

↓

2. Mixture composition of HFC
- methodology for mixture design
- workability characterisation
- pullout tests on single fibres

↓

3. Tensile properties of HFC
- flexural behaviour
- uniaxial tensile behaviour
- number and orientation of fibres

↓

4. Modelling of tensile behaviour of HFC
- strain hardening
- strain softening

↓

5. Utilisation of HFC
- design fundamentals
- case-study on slender precast-concrete beams

↓

6. Conclusions and recommendations

Fig. 1.1: Structure of this PhD-Thesis

In Chapter 5, the fundamentals of the structural design using fibre concrete are given first. A special attention is put on the fibre orientation on the material level (testing specimens) and on the structural level (structural elements). This is followed by the case study on the utilisation of Hybrid-Fibre Concrete for slender prefabricated concrete beams, with variable spans and shapes of cross-sections. The comparisons with the similar structural elements made of conventional concrete on engineering, technical and economical basis, is provided as well.

In Chapter 6, the conclusions on the development and utilisation of Hybrid-Fibre Concrete will be made. Based on the results of this research project, the needs and the recommendations for future activities in the field of high- and ultra-high-performance concrete, will be provided as well.

Notations of applied types of fibres

In this research project, different types of Dramix® - steel fibres were used: short straight steel fibres and long steel fibres with hooked ends. All of them are shown in Fig. 1.2, with appropriate notations.

The original producer notations contain two numbers and two or four letters (Fig 1.2). For short straight fibres, these numbers represent the ratio: *fibre length / fibre diameter* (e.g. for fibre OL 13/0.20, fibre length = 13 mm, fibre diameter = 0.2 mm)). For long hooked-end fibres, they represent the ratio: *[fibre aspect ratio (length/diameter)] / [fibre length]* (e.g. for fibre RC-80/60-BP, fibre aspect ratio = 80, fibre length = 60 mm).

In order to simplify the notation, all fibres in this thesis will be denoted according to the ratio: *fibre length / fibre diameter* (Fig. 1.2). This will be abbreviated in the text as *l/d* (e.g. *l/d = 60/0.7,* is a fibre with a length = 60 mm and a diameter = 0.7 mm, which is in the original notation RC-80/60-BP). The maximum applied fibre length is 60 mm. It should also be kept in mind that here, the fibres shorter than 30 mm are always straight, whereas the fibres longer than 30 mm have always hooked ends.
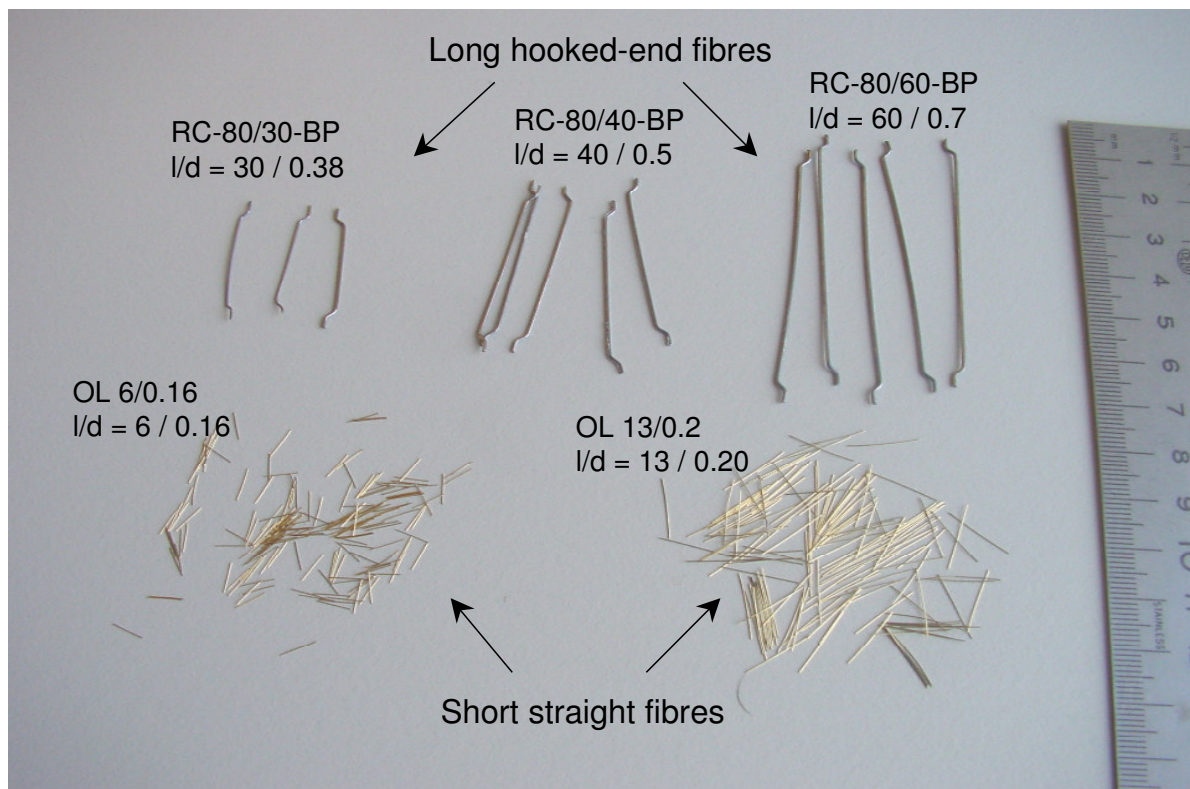
Fig. 1.2: Applied types of steel fibres in this research project, with their original notations (Dramix®), and with ratios l/d (fibre length / fibre diameter, both in [mm])

CHAPTER 2:

MIXTURE COMPOSITION

2.1 Introduction

The mixture design of high-performance concrete is the key factor, which to a large extent determines its performance on the structural level. Also, a standard mixture design for high-performance concrete does not exist – for each specific application a different mixture design is required.

In this chapter, the methods for mixture design and mixture compositions of different types of Hybrid-Fibre Concrete (HFC) will be presented. The basic principle of combining different types of steel fibres together in a "hybrid-fibre concrete" mixture will be given first. After that, a short literature overview of mixture design principles of different high- and ultra-high-performance concretes will be presented.

Subsequently, the methodology of mixture design of HFC will be given, based on fixed values of the water/binder-ratios, and fixed fibre combinations. The interactions between the applied quantities and types of steel fibres, with the aggregate grains, will be analysed first. In this step, the packing densities of different dry aggregate-fibre mixtures will be determined experimentally and analytically. This will be followed by the determination of the optimum aggregate and cement content, which will be done by workability studies on fresh HFC mixtures. The basic demand here, is that all HFC mixtures must be self-compacting, homogeneous and stable. The "Excess-paste model", will subsequently be applied to the mixtures with one and more fibre types, in order to determine and to recommend the optimum quantities of aggregate and cement, for given fibre combinations. This model is based on the thickness of the layer of cement paste around grains and fibres.

Subsequently, the optimum concrete mixtures will be selected, and applied as a pullout medium in the pullout tests on different short straight and long hooked-end steel fibres. The main goal of the fibre pullout tests, is the further optimisation and selection of concrete mixtures, on the basis of the utilisation of tensile capacity of fibres during their pullout. The mixture composition of the pullout medium, the presence of short "secondary" steel fibres in it, as well as the fibre inclination angle, will be the main testing parameters. The results of the fibre pullout tests, will also be used later, in the modelling of tensile behaviour of Hybrid-Fibre Concrete.

2.2 Hybrid-Fibre Concrete (HFC): basic principles

Basic principles of the mixture design of Hybrid-Fibre Concrete are:

- the application of short and long steel fibres together in one same concrete mixture;
- on the structural level: to ensure that all these fibres are homogeneously distributed in each part of the structural element;
- on the material level: to ensure that all the fibres are as effective as possible in crack bridging.

Application of different types of steel fibres

The application of different types of steel fibres, i.e. of short straight steel fibres and long hooked-end steel fibres (Fig. 2.1), is related directly to the fracture mechanics of concrete.

According to [Van Mier, 1997], the fracture processes of concrete loaded in tension, begin by the formation of numerous fine microcracks in the interfacial zones around aggregate grains. If the tensile load continues to increase, these microcracks connect with each other and form larger cracks, which subsequently leads to failure.
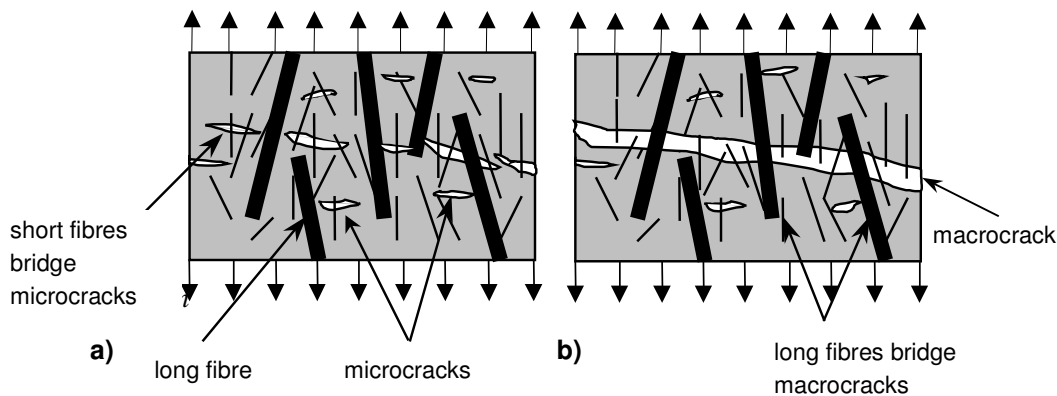
Fig. 2.1: The main principle of Hybrid-Fibre Concrete: a) The influence of short thin fibres on the bridging of microcracks and the increase of tensile strength;   b) the influence of long thick fibres on the bridging of macrocracks and the increase of ductility

The idea of the utilisation of short and long fibres together is given in Fig. 2.1. Short fibres can bridge microcracks more efficiently, because they are very thin and their number in concrete is much higher than that of the long thick fibres, for the same fibre volume quantity (Fig. 2.1.a). Taking into account that microcrack formation and crack bridging by fibres, occurs in the first phases of tensile loading, the short fibres can have a significant influence on the increase of the tensile strength.

As the microcracks grow and join into larger macrocracks, the long hooked-end fibres become more and more active in crack bridging (Fig. 2.1.b). In this way, primarily the ductility can be improved, and partly also the tensile strength. Long fibres can therefore provide a stable post-peak response. Short fibres will be less and less active, because they are being more and more pulled out, as the crack width increases.

From a mechanical point of view, the combination of fibres seems to be an optimum solution to increase both the tensile strength and the ductility. The application of different types of fibres together in a concrete mixture, was proposed for the first time by [Rossi et al., 1987], as the so-called multi-modal fibre reinforced concrete (MMFRC).

Optimisation with respect to structural level
On the structural level, it is important to achieve a homogeneous distribution of the fibres in all parts of a structural element. The distances between neighbouring fibres should be as equal as possible, whereas too large spaces without fibres, as well as the fibre segregation should be avoided. The best possible way to fulfil all these requirements, is to produce self-compacting fibre concrete. This concrete flows under its own weight, and fibres therefore may orient in appropriate directions during flowing in the formwork of a structural member. This may further have a decisive influence on the tensile response of such a structural member. Moreover, this concrete must have stable consistence, so that no danger of fibre segregation exists. As no additional compaction is required, the fibres will remain in their original positions. Clearly, all these advantages guarantee the most homogeneous fibre distribution.

However, stiff steel fibres with a cylindrical shape, very often have a significant negative influence on concrete workability, especially if applied in higher percentages. Therefore, the interactions between fibre and aggregate grains will be studied in this research project. Basic parameters, such as average fibre spacing and the packing density of dry aggregate-fibre mixtures will be determined, and used in mixture optimisation. It will be shown that it is possible to maintain the self-compactability of concrete, up to relatively large fibre quantities (from e.g. 1.5 up to 5 vol.-%).

Optimisation with respect to material level
Concrete cracks under the action of tensile stresses. If fibres are present in the concrete, they can bridge these cracks and provide an appropriate resistance to the crack opening. The degree of this resistance depends basically on the utilisation of the available tensile strength of each single fibre during crack bridging. Clearly, this so-called efficiency of fibres, depends mostly on the mixture composition of the pullout medium, i.e. of the concrete matrix, which surrounds the fibres. The efficiency of the fibres will here be determined in single fibre pull-out tests. The most important parameters in these tests will be: the type, the embedded length and the inclination angle of the fibres, as well as the w/b-ratio, the quantity of cement and the presence of short secondary fibres in the pullout medium (concrete matrix).

2.3   Literature overview of mixture design of high- and ultra-high-performance concretes

As mentioned in the Introduction, the Hybrid-Fibre Concrete combines the properties of three, at the first sight independent types of concrete:
−   self-compacting concrete,

−   fibre-reinforced concrete, and

−   high- and ultra-high-strength concrete.

In this subchapter, the basic principles of the mixture design of these types of concrete, as well as the impact of their mixture composition on the mechanical properties will be explained.

2.3.1 Self-compacting concrete (SCC)

Self-compacting concrete is flowable and does not require any compaction after casting. It has such a viscosity, that the air-bubbles can migrate to the outer surface of the fresh concrete. The fundamental idea of SCC, is to lubricate the aggregate grains with a thin layer of cement paste (Fig. 2.2.a), so that the shear stresses between them in the fresh mixture can be decreased, and mixture can become flowable [Walraven, 2002]. Two most important design methods – the Japanese method [Okamura et al., 2000], and the Swedish method [Billberg, 2002], are based on a constant quantity of fluid in the concrete, as well as on an increased quantity of binder materials compared to conventional concretes. The porosity and the micro-structure of SCC are improved in comparison to conventional concrete [Wallevik, 2002].
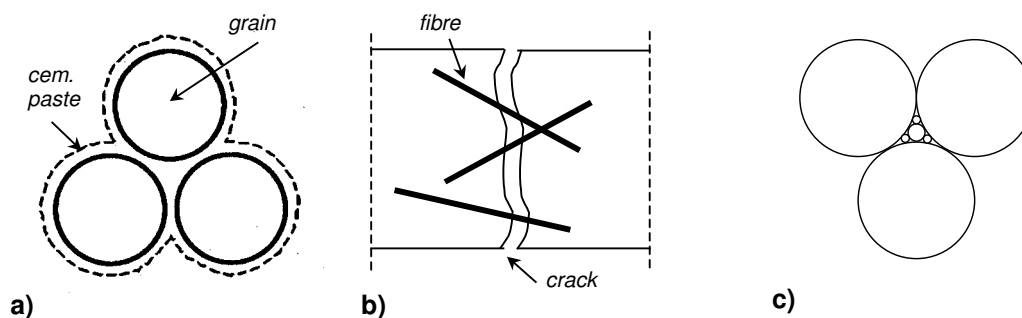
Fig. 2.2: a) Self-compacting concrete (SCC): a layer of cement paste surrounds each grain, after [Walraven, 2002];   b) Fibre-reinforced Concrete (FRC): crack bridging mechanism by fibres;   c) Ideal packing arrangement (Apollonian packing) where each grain fills the voids between larger grains, used as the basic principle for Reactive Powder Concrete (RPC)

2.3.2 Fibre reinforced concrete (FRC)

The basic idea of the application of discontinuous fibres in concrete (Fig. 2.2.b), is that they can bridge cracks, similarly like conventional steel bar reinforcement [Romualdi et al., 1964]. However, although the number of fibres across a crack is much higher compared to the number of steel bars, the fibre action can never be that effective, as that of steel bars. The main reasons for this are:

−   steel bars are continuous and have much larger diameter compared to fibres; the tensile capacity of steel bars and the bond of steel bars and concrete will therefore be much stronger compared to the bond between fibres and concrete;

- in a structural element, the steel bar reinforcement can always be placed in the direction of the main tensile stresses, while the fibres are in general randomly oriented.

Conventional fibre concrete without steel bar reinforcement can therefore not be used for most load-carrying elements in the engineering practice [Pfyl, 2003].

Addition of fibres in a standard concrete mixture without modifications in the mixture proportion, results almost always in a decreased workability [Kooiman, 2000]. As a consequence, the structure of the concrete around the fibres is not homogeneous and compact, and therefore the fibres are not well bonded to the concrete. Their efficiency during pullout can therefore not be high enough under such circumstances. Furthermore, the fibres will be distributed in a random way in the concrete elements, with an orientation that usually does not correspond to the direction of the main tensile stress. The ductility of such a conventional fibre concrete will be somewhat higher compared to plain concrete, but the tensile strength may remain the same, or will even be lower [Brite-Euram Project on FRC, 2002].

An alternative to conventional fibre concrete, is self-compacting fibre concrete [Nemeger, 1999], [Groth, 2000], [Grünewald et al., 2000]. Similar to self-compacting concrete, these concrete types are characterised by an optimised granular composition and a higher quantity of cement and fine filler materials. The workability is therefore much better compared to conventional fibre concrete. The fibres may therefore be better oriented and may therefore have a better efficiency in crack bridging. Both the flexural strength and the ductility could therefore be enhanced, as stated in [Groth, 2000] and [Grünewald et al., 2002 b].

2.3.3   Ultra-high-strength concretes (UHSC)

Reactive Powder Concrete (RPC)
Concretes with a compressive strength up to 100 MPa, were in the past usually obtained using low water/binder-ratios, high-strength aggregate and special filler materials, such as micro-silica. A tremendous brake-through in the development of ultra-high-strength concretes, was obtained by the introduction of Reactive Powder Concrete (RPC) [Richard et al., 1995], with very high compressive strengths of 200 MPa and more. The basic principles of mixture design of RPC are:

1. low values of the water/binder-ratio (e.g. w/b = 0.12 to 0.20): all present water is used for the hydration of one part of the total cement quantity, the remaining unhydrated cement particles act as fillers on the micro-level;
2. the enhancement of homogeneity by the elimination of coarse aggregates, i.e. by the application of only very fine sand as aggregate. The microcracks, whose development starts around the aggregate grains, will therefore be of much smaller sizes compared to those in conventional concrete with large gravel grains;

3. a limited content of sand, so that the aggregate is like a set of inclusions entrapped in the cement paste, without direct contact between the grains. The global paste shrinkage is therefore not blocked by the aggregate grains;

4. the maximised packing density of all grains (fine sand, cement, and silica fume), so that each class of grains fills the voids of the larger class (Fig. 2.2.c). The rest of the voids should be filled with water, which results in a very low water-cement ratio of about 0.14.

5. the eventual enhancement of the microstructure by heating during hardening at an optimum temperature (between 90ºC and 200ºC), which enhances the pozzolanic reaction of microsilica, and also results in a significant reduction of porosity [Cheyrezy et al., 1995].

6. the eventual application of compression during hardening, which if combined with the appropriate heat-treatment, creates a concrete with almost zero porosity [Cheyrezy et al., 1995].

All these factors together contribute to significantly high values of compressive strength of RPC. Nevertheless, the RPC showed an extremely high brittleness as well. The short thin steel fibres were added to the original mixtures, in order to enhance the ductility under the compressive loading.

Ultra-high-strength concretes reinforced with fibres

The RPC was further developed only with fibres, and this resulted not only in an improved ductility under compression, but also in an increased tensile strength and ductility under tensile loading ([Richard, 1996], [Behloul, 1996 a, b]). Since then, many different types of so-called ultra-high-performance fibre concrete (UHPFC), were derived from the initial RPC mixture composition. The most important examples are Ductal®- concretes in [Orange et al., 2000], [Chanvillard, 2003], Multi-Modal Fibre Reinforced Concretes (MMFCR) in [Rossi et al., 1996], and [Sato et al., 1999, 2000] as well as the Ultra High Performance Fibre Concrete developed at the University of Kassel [Schmidt et al., 2001].

In almost all mentioned concretes, the initial original mixture composition of RPC was not changed a lot. The consequence of this is, that the ratio between their compressive and tensile strengths ranges up to 20 - 30, depending on the applied fibre quantity. This is much higher than in any conventional concrete, where this ratio reaches values of 10 - 12 as a maximum.

Also, the addition of fibres causes the disturbance of granular skeleton. Therefore, the optimum packing of particles in the initial plain RPC should probably be optimised in another way, so that it can accept fibres of appropriate type and quantity.

Therefore, near all previously mentioned requirements, two additional very important goals in the mixture design of Hybrid-Fibre Concrete, are:

− to decrease the large difference which exists between compressive and tensile strength of UHPFC

−   to analyse the interactions between the aggregate skeleton and the applied combinations of fibres, and to design appropriate HFC mixtures applying the results of this analysis.

2.4   Methodology for mixture design of Hybrid-Fibre Concrete

In this sub-chapter, the methods used to determine the optimum mixture compositions of Hybrid-Fibre Concrete, in order to satisfy the criteria stated in the introduction of this chapter, will be presented (Fig. 2.3).

Firstly, the water-binder ratio was kept constant for all produced mixtures (values of w/b = 0.40, 0.30 and 0.20). Therefore, the methodology of mix design does not correspond to the usual methods for mix design of self-compacting concrete, such as the "Japanese" method [Okamura et al., 2000], or the "Swedish" method [Billberg et al., 2002], which are both based on experimental finding of the optimum amount of fluid in a concrete mixture. As binder materials, two types of local Dutch cement were applied: portland cement CEM I 52.5 R, and blast furnace slag cement CEM III/A 52.5 N, both produced by the ENCI Factories, Maastricht, Netherlands.

Secondly, all the combinations of different types and amounts of steel fibres, which will be applied, were fixed as such in the beginning. These combinations were partly based on own experience, and partly on the results of previous research on different high-performance fibre concretes, such as those on multi-modal fibre concrete [Rossi et al., 1995], [Sato et al., 1999, 2000], on reactive powder concrete [Richard et al., 1995], as well as on self-compacting fibre reinforced concrete [Grünewald et al., 2000].

On the basis of these two initial parameters, the mixture compositions were further adjusted and optimised. All applied steps will be discussed in detail in the following sub-chapters.

The next step was the estimation of the maximum size of the aggregate grain (D_{max}). This has been done on the basis of the average distance of the applied fibres, for the actual fibre volume. After the D_{max} was determined, the aggregate grading which gave the highest dry packing density was found, both experimentally and by using the "Compressible packing model" [De Larrard, 1999].

This was followed by numerous workability studies on fresh HFC-mixtures. The main goal of those studies was the determination of the appropriate quantity of aggregate, (i.e. of cement), for the applied types and quantities of fibres, so that the mixtures are self-compacting. The optimum quantities of the viscosity agent (superplasticizer), were determined in these studies as well.

```
┌─────────────────┐        ┌──────────────────────┐
│  w/b = const.   │        │     Steel fibres     │
└─────────────────┘        │ (chosen - given types and │
                           │     quantities)      │
                           └──────────────────────┘
                                     │
                           ┌──────────────────────┐
                           │  Determine D_max     │
                           └──────────────────────┘
                                     │
                           ┌──────────────────────┐
                           │ Determine aggregate  │
                           │      grading         │
                           └──────────────────────┘

          ┌────────────────────────────────────────────┐
          │ Determine: Vol. aggregate i.e. Vol. cement  │
          └────────────────────────────────────────────┘
                           │
                  ┌──────────────────────┐
                  │ Determine amount of  │
                  │   viscosity agent    │
                  └──────────────────────┘

  adjusting              requirements

                  ┌──────────────────────┐        ┌────────────┐
        NO        │ Slump flow > 60 cm   │  YES   │ Testing of │
                  │ No segregation of fibres│─────▶│ mechanical │
                  │ No clustering of fibres │      │ properties │
                  └──────────────────────┘        └────────────┘
```
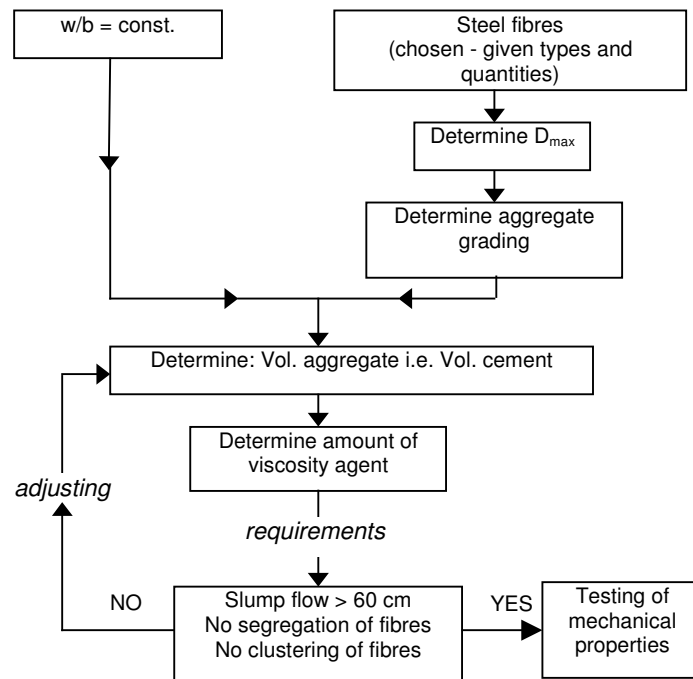
Fig. 2.3: The methodology applied for the design of self-compacting hybrid-fibre concrete mixtures

2.5 Interactions between aggregate grains and steel fibres

In this sub-chapter, the maximum applicable grain size, based on the average distance between the fibres, will be determined first. The optimum granular composition of aggregate, based on the maximum achievable packing density, will be determined subsequently. Different types of steel fibres will then be combined with this granular composition. The packing densities of such dry mixtures will be determined, in order to evaluate the interaction of aggregate grains and fibres.

2.5.1 Homogeneous distribution of fibres and size of aggregate grains

The homogeneous distribution of steel fibres in concrete is one of the most important demands, taking into account the function of the fibres itself. In an ideal case, the same amount of fibres should be present in each cross section of a structural element made of fibre concrete. Moreover, the fibres should then be alligned in the direction of the main tensile stress, if possible in a regular array, like a square or a triangular array (Fig. 2.4.a and b). In both of these ideal cases, the longitudinal axis of neighbouring fibres will be at constant spacing *S* from each other, and the fibres will also be oriented in an optimal direction with respect to the main tensile stresses.
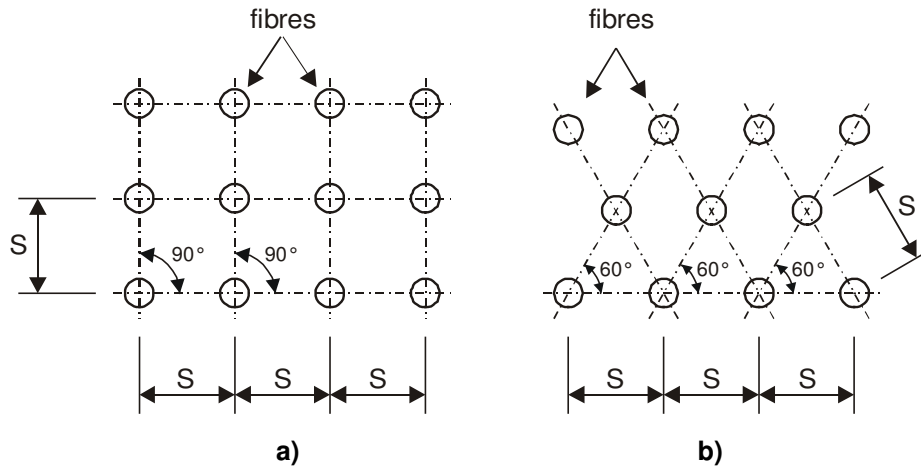
Fig. 2.4: Two examples of ideal arrangements of fibres in a cross-section of a FRC-element: a) regular square array; b) regular triangular array

In order to achieve such a fibre arrangement, the aggregate grains must be packed between the fibres, without disturbing their pattern. The conditions to achieve this are:

- the aggregate grains with the most appropriate maximum size D_{max}, must fit between the fibre surfaces (Fig. 2.5.a);
- the aggregate grains of an average grain size, must be placed so, that they are in contact with each other (Fig. 2.5.b).

If both conditions are satisfied, the fibre concrete will be able to accommodate an appropriate aggregate composition, for a given number of fibres in a cross-section (i.e. for given fibre volume quantity) regarding their geometrical properties (fibre length and diameter).
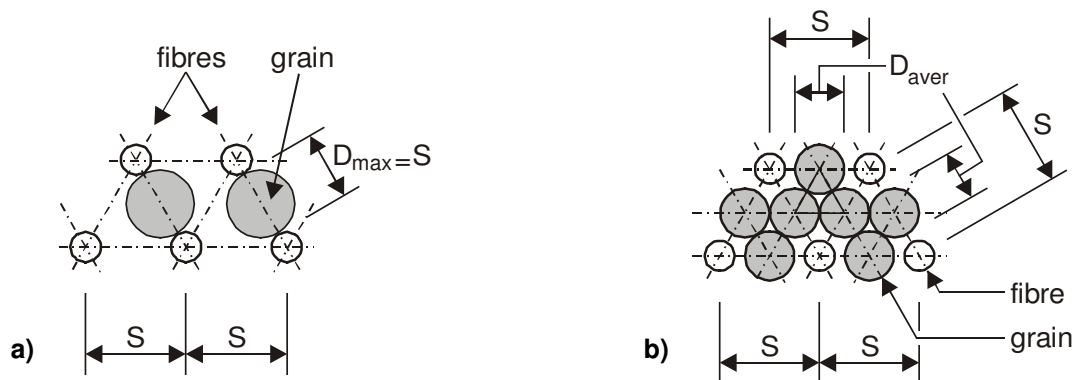
Fig. 2.5: Possibilities of placing aggregate grains between the fibres with spacing S, in a regular triangular array;   a) grains of maximum size (D_{max});   b) grains of an arithmetically average size (D_{aver})

Maximum grain size (D_{max})

In reality, the fibres can never be arranged in the described way, due to their discontinuous nature, as well as due to the production process of the fibre concrete itself. Therefore, a random orientation of fibres should be taken into account, and the average fibre spacing, obtained in such a way, should be the basis for the selection of D_{max}.

Numerous formulas for the calculation of the average spacing S between fibres, were published elsewhere. Here follows a set of five equations of different authors, where S represents the average surface-to-surface spacing between neighbouring fibres in a cross-section of a FRC element, with the following basic symbols:

d = fibre diameter

l = fibre length

V_f = applied volume content of fibres in %,

1. $S = d\left(\sqrt{\dfrac{\alpha}{V_f/100}} - 1\right),$ [Kelly, 1974], where: (2.1)

$\alpha = \pi/2\sqrt{3}$, for triangular fibre array

$\alpha = \pi/4$, for square fibre array

2. $S = \sqrt[3]{A_{f,1}\dfrac{l_f}{V_f/100}} - d$,   [McKee, 1969], where: (2.2)

$A_{f,1}$ is the surface area of the cross section of a single fibre

3. $S = 13.8\,d\,\sqrt{\dfrac{1}{V_f}} - d$,   [Romualdi et al., 1964]   (2.3)

4. $S = 5\sqrt{\dfrac{\pi}{\beta}\dfrac{d}{\sqrt{V_f}}} - d$,   [Kobayashi et al., 1976], where: (2.4)

the fibre orientation factor $\beta = 0.002\,l/d + 0.4$

5. $S = \beta\,\dfrac{d}{\sqrt{V_f/100}}$,   [Krenchel, 1976],   (2.5)

$\beta = 1.12$ for random fibre orientation.

The average surface-to-surface fibre spacing, for cylindrical fibres with diameters $d = 0.16$ to 0.60 mm (standard "Dramix" sizes), for a constant fibre volume content of $V_f = 4.0$ vol.-%, is given in Fig. 2.6.a. This volume content corresponds approximately to the maximum content of fibres, which will be used in this research.

Obviously from Fig. 2.6, there is no firm relation for the average fibre distance, i.e. every mentioned researcher has different results. Comparing the influence of fibre orientation, it can be concluded that randomly oriented fibres lay on larger average distances compared to uniform arrays of fibres (square and triangular).
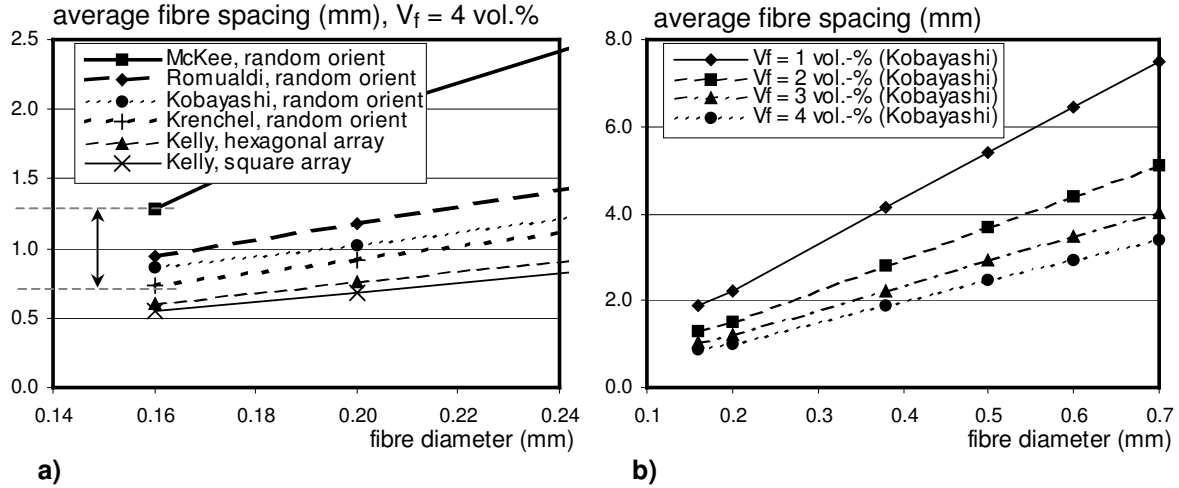
Fig. 2.6: a) Different relations between fibre diameter and average fibre spacing (i.e. possible maximum grain size), for the same volume quantity of fibres (V_f = 4 vol.-%); b) Relations between fibre diameters and average fibre spacing (i.e. possible maximum grain size), for different volume quantities of fibres (V_f = 1.0 to 4.0 vol.-%), according to the equation of [Kobayashi, 1976]

The normative fibre distance for the selection of the maximum grain size of the aggregate, will be the one for the maximum applied volume content of the fibres with the smallest diameter. In this case (Fig. 2.6.a), that is the fibre type with d = 0.16 mm, where the fibre spacing ranges from 0.55 mm for the regular square fibre array [Kelly, 1974], i.e. from 0.74 for random fibre orientation [Krenchel, 1976], up to 1.28 mm for random fibre orientation [McKee, 1969].

The average of the two limit values for random fibre orientation, is S = 1.02 mm. Therefore, the maximum aggregate size of D_{max} = 1.0 mm was selected. It was also decided to produce a couple of mixtures with D_{max} = 0.5 mm, in order to observe the influences of D_{max} on the workability and possibly also on the mechanical properties of hybrid-fibre concrete.

In this way selected maximum grain size, should be able to provide a homogeneous fibre distribution in extreme cases of rather high content of short thin fibres (4.0 vol.-%). Many concrete mixtures, both with only one and with more types of fibres, will not contain that high fibre volume contents. Also, fibres with larger diameters have a larger average spacing. Therefore, the average fibre spacing will in many produced types of HFC, be larger than 1.02 mm, as calculated here. This is also clear from Fig. 2.6.b, where the average fibre spacings for different fibre volume contents are presented. The equation of [Kobayashi, 1976] has been

used here, because it approximately corresponds to the mean value of data of all other researchers given in Fig. 2.6.a.

However, $D_{max} = 1$ mm (i.e. 0.5 mm) will be applied for all mixtures, independent of the applied fibre volume. This will be done in order to isolate the influence of the fibres on the tensile behaviour and on the workability of HFC.

Average grain size (D_{aver})

Only a very limited number of grains possess the maximum grain size. Therefore, the mean arithmetical value of all grain sizes is certainly more representative, if these grains have to be packed between the fibres (Fig. 2.5.b). Following the geometrical arrangement of aggregate grains between the fibres given in Fig. 2.5.b, it may be concluded that the average grain size (D_{aver}), is in such a case equal to one half of the fibre spacing S:

$$D_{aver} = S / 2.$$

Taking into account that for a random fibre orientation, the average fibre spacing S equals 1.02 mm, the average grain size should then be equal to $D_{aver} = 0.5$ mm. After the final aggregate grading is chosen, the average grain size will be calculated using the simple arithmetical mean value, and subsequently compared to the value of $D_{aver} = 0.5$ mm.

2.5.2 Optimum grading of the aggregate: Compressible packing model

After the maximum grain sizes D_{max} has been chosen, the volume quantities of the appropriate aggregate fractions can be determined, using the standard ISO-sieve sizes. The basic demand here is to achieve the maximum possible packing density of the applied aggregate particles, similarly as in the case of RPC [Richard et al., 1995], and UHPC [De Larrard et al., 1994]. Such an approach can theoretically guarantee the highest possible density of the concrete, and therefore the significantly improved mechanical properties, compared to conventional concrete. In this sub-chapter, the packing process of aggregate particles itself, including the compressible packing model [De Larrard, 1999], will be presented.

Packing density of aggregate particles

The packing density of any mixture of aggregate particles is defined as a content of the solid volume Φ in a unit total volume [De Larrard, 1999]. The packing density depends on three main parameters:
− the size and volume content of each ISO - class of aggregate grains under consideration
− the shape of the grains
− the method of creating and processing an appropriate packing of the grains.

The **virtual packing density** is defined as the maximum packing density, which can be achieved only by placing each particle one by one, in appropriate positions (e.g. RPC in Fig. 2.2 c). In reality, it is not possible to control the positions of the grains, and therefore the dis-

tribution of the particles is random. For any random packing arrangement, a value called the **actual packing density** may be calculated [de Larrard, 1999].
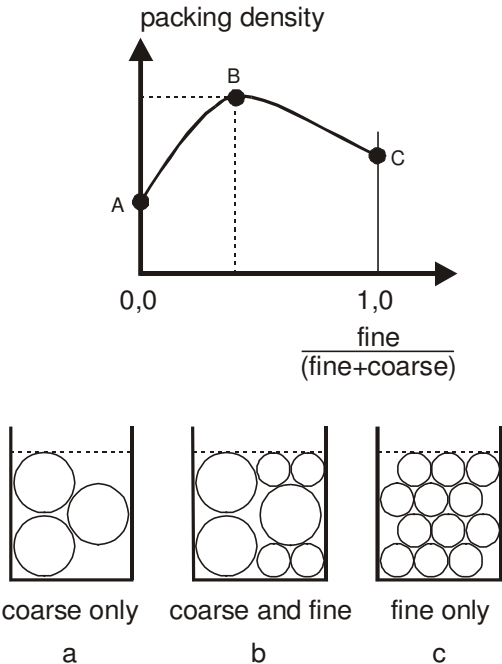
Fig. 2.7: A general case of the evolution of the packing density of granular mixtures with only coarse (a), only fine (c), and the combined fine and coarse aggregate grains (b)

A general case of the evolution of the packing density Φ of a dry mixture with two classes of aggregate particles (one large, another small), is given in Fig. 2.7. Border conditions are $\Phi = \Phi_1$ for $\Phi_1 = 100$ vol.-% (only coarse particles), and $\Phi = \Phi_2$ for $\Phi_2 = 100$ vol.-% (only fine particles). The maximum value of packing density appears only for one appropriate combination of these two classes of particles, when the empty spaces between larger particles are fully filled with the smaller particles.

Compressible packing model [De Larrard, 1999]

The compressible packing model is an efficient tool for the determination of the packing density of any granular mixture, for a given process of compaction. The granular mixture is firstly divided into n quasi-monosized classes i, the size of which is d_i. The packing density is then governed by:

- y_i, the volume of i-grains divided by the total solid volume
- α_i is the experimental packing density of i grains, separately packed
- K_i is the compaction index of the grain class i (dimensionless value). This parameter represents the energy, which is applied during the process of compaction of an appropriate grain class, i.e. the energy needed to create an appropriate packing density. It is possible to determine the compaction index for any compaction process, by comparing the values of

the packing densities obtained in analytical and experimental way. Some values recommended by [De Larrard, 1999] are:

$K = 3.5 - 4.2$, for simple pouring the grain material into the container

$K = 4.5$, for pouring and compacting the grain material with the rod

$K = 4.5 - 5.0$, for vibration the grains in the container

$K = 9.0$, for combined vibration and external pressure.

The procedure for the calculation of the packing density for an aggregate composition is:

1. determine experimentally the packing densities α_i of the quasi-monosized grain classes (e.g. for each of the ISO - aggregate fractions 0.125 - 0.25, 0.25 - 0.50, . . . , 16.0 - 32.0 mm, for a mixture with $D_{max} = 32.0$ mm).

2. the virtual packing densities β_i should then be calculated from:

$$K_i = \frac{1}{\beta_i / \alpha_i - 1} \tag{2.6}$$

3. the packing density Φ can subsequently be obtained from the following system of equations:

$$\gamma_i = \frac{\beta_i}{1 - \sum_{j=1}^{i-1} [1 - \beta_i + b_{ij}\beta_i(1 - 1/\beta_j)] - \sum_{j=i+1}^{n} [1 - a_{ij}\beta_i / \beta_j] y_j} \tag{2.7}$$

$$K = \sum_{i=1}^{n} K_i = \sum_{i=1}^{n} \frac{y_i / \beta_i}{1/\Phi - 1/\gamma_i}, \tag{2.8}$$

where a and b are the loosening (opening) and wall-effect coefficients respectively. These coefficients are taken into account for all smaller ($j = 1$ to (i-1)) and all larger fractions ($j = (i+1)$ to n), with respect to the fraction under consideration, i.e. to the fraction i. This calculation has to be repeated for all present fractions.

These coefficients depend on the diameter of the neighbouring grain fractions and may be calculated as follows [De Larrard, 1999]:

$$a_{ij} = \sqrt{\frac{d_j}{d_i}} \quad \text{and} \quad b_{ij} = \frac{d_i}{d_j}. \tag{2.9}$$

2.5.3 Determination of packing density of aggregate mixtures

In this sub-chapter, first, the experimental and analytical determination of dry packing density of aggregate particles will be presented, together with the procedure for the estimation of the compaction index and the wall-effect. Afterwards, the influence of different fibre types on the packing of the optimum aggregate mixture will experimentally be measured and evaluated.

A cylindrical container made of steel (diameter = 20 cm, height = 25 cm, weight of the empty container = 5.94 kg), was used for the experimental measurements of packing density. After the weight of the container completely filled with aggregate and fibres, is measured, the packing density can be calculated as:

$$\Phi = \frac{m_{full} - m_{cont}}{V_{cont} \left(\gamma_{agg} \cdot Vol_{agg} + \gamma_{fib} \cdot Vol_{fib} \right)},$$ (2.10)

where:

Φ = the packing density of an aggregate-fibre mixture;

m_{cont} = the weight of the empty container (kg);

m_{full} = the weight of the full container (kg);

V_{cont} = the volume of the container (dm^3);

γ_{agg} = 2.60 kg/dm^3 = specific weight of aggregate;

γ_{fib} = 7.85 kg/dm^3 = specific weight of fibre steel;

Vol_{agg} = the volume content of aggregate in a unit volume of the mixture (in vol.-%);

Vol_{fib} = the volume content of fibres in a unit volume of the mixture (in vol.-%).

Experimental measurements of packing density of aggregate fractions

The packing density of each aggregate fraction on its own was measured first. Taking into account the chosen D_{max} = 1.0 mm, and adopting to the standard ISO sieve sizes, three aggregate fractions were selected: 0.125 - 0.25, 0.25 - 0.50, and 0.50 - 1.00 mm.

As explained in chapter 2.5.2, different compaction methods (pouring, tamping, vibrating and/or combinations of them), with different compacting energies (index K) can be used. One of the standard methods is that defined by the British Standard [BS 812: Part 2, 1975], and it was used in a slightly modified form for the measurements of the packing density of numerous aggregate-fibre mixtures, given by [Hoy, 1998] and [Grünewald, 2000]. This method consists of pouring and tamping of the material, after which the vibration under compression should be applied.

In this research project, first a couple of different methods were applied, in order to find the one, that gives the highest packing densities. Simple pouring of sand at once gave lower values than pouring and tamping in 3 layers. Vibrating of the filled container turned out to be very efficient: pouring and tamping in 3 layers and vibration of each of them for 30 sec., gave an about 20% higher packing density, compared to pouring. A longer vibration time (3 sequences by 60 sec.) improved only slightly the values of packing density. A slightly simpli-

fied procedure consisting of pouring and tamping in 3 layers, followed by only one vibration period of 90 sec. (instead of 3 vibration periods, where each lasts for 30 sec.), resulted in even higher values of the packing density. This procedure was therefore chosen and was further used for the measurements of the packing density of all other mixtures.

In all cases, the container was filled with an additional surplus of the material and was kept full in such a way, covered by a square plexiglas plate on its top. No compression was applied. Tamping was performed with a 15-mm diameter stick, with a falling height of about 50 mm. For the vibration of the material, the filled container was placed in a standard Ve-Be tester for concrete workability.

Somewhat higher values of the packing density were obtained for larger particles. According to [De Larrard, 1999], the compaction by vibration is more efficient for larger particles, due to fewer contacts between them per unit volume, compared to small particles.

Estimation of the compaction index K

The compaction index K, may be determined by comparing, at one side the experimentally determined packing density of a granular mixture and at the other side, the results of the analytical calculation of the packing density of the same granular mixture. This process should be repeated for different granular mixtures. The most simple way to perform this procedure, is the utilisation of binary or ternary mixtures, i.e. mixtures composed of 2 and/or 3 fractions of aggregate particles, such as in [De Larrard, 1999] or [Grünewald, 2004].

Within the scope of this research, different combinations of two sand fractions (0.125 - 0.250 mm, and 0.250 - 0.500 mm) were utilised for the determination of the compaction index K. The packing densities of these fractions were calculated for three different values of K (K = 1.5, 2.0 and 2.5), and subsequently compared to the experimentally measured packing densities. Fig. 2.8 shows that the experimentally determined packing densities are in a rather good agreement with the analytically determined packing densities, for the compaction index K = 2.3. All further analytical calculations will be based on this value. Also, the higher the level of compaction, the higher packing density of a granular mixture can be reached.

The estimated value of K is about 50 % lower than that recommended by [De Larrard, 1999], which is probably a consequence of the absence of compression during compaction. Anyhow, the packing density that can be reached, i.e. the level of compaction that one applies, is actually not that important. From Fig. 2.8, it is clear that all the curves (independent of the K-value) reach their maximum value for approximately the same value of the quantity of finer sand fraction.

Therefore, there is one optimum combination of aggregate fractions (with about 35 - 40 % of finer fraction in it), for which the maximum packing density will be reached, and this combination does not depend on the applied compaction level. Indeed, from a practical point of view, the correct combination of fractions is actually much more important than the value of their dry packing density.
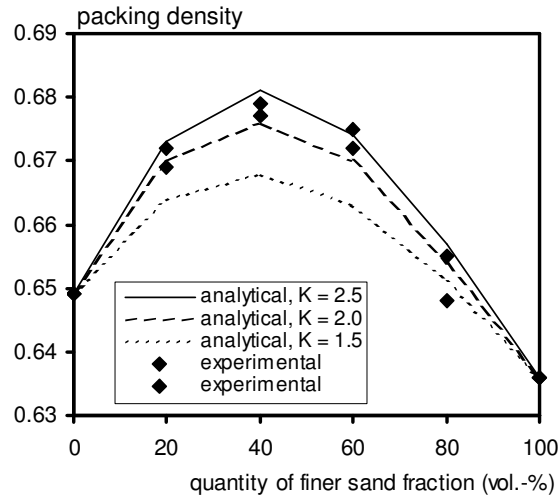
Fig. 2.8: Comparison between experimentally and analytically (for 3 different values of the compaction index K) determined packing densities, of dry mixtures with two fractions of fine sand (0.125 - 0.25 mm and 0.25 - 0.50 mm)

Determination of the optimum grading curve of the aggregate

After the maximum grain size D_{max} is chosen, and the compaction index K estimated, it is possible to determine both experimentally and analytically the grading curve of the aggregate, which gives the maximum possible packing density. This grading curve will be used as the optimum one for all future concrete mixtures with fibres.
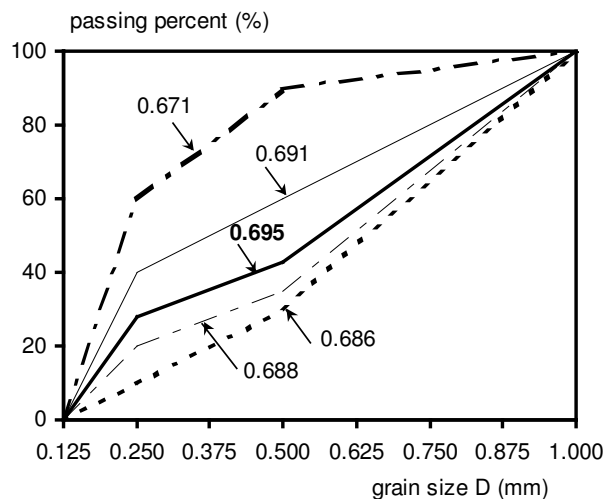
Fig. 2.9: Different grading curves of aggregate composition with D_{max} = 1 mm, with analytically determined packing densities for each of them

Different grading curves for 3 aggregate fractions, with a maximum grain size D_{max} = 1 mm, are given in Fig. 2.9. For each grading curve, the values of the analytical packing densities are given. For the calculation of all analytical values, the compaction index K = 2.3 was applied.

The maximum value of packing density is 0.695, for a grading (28% + 15% + 57%), of first three ISO-aggregate fractions. However, no large differences in packing density exist, compared to "similar" neighbouring grading curves (e.g. curve 20% + 15% + 65%), whereas the difference compared to a "non-similar" grading curve (60% + 30% + 10%) is rather large (about 8 %).

The arithmetical mean size of the aggregate grains for the combination (28% + 15% + 57%), is about 0.53 mm. This size is almost equal to the required average grain size of 0.50 mm, as explained in the sub-chapter 2.5.1, and in Fig. 2.5.b. This means that these grains will be able to pack without problems between the rather densely arranged fibres (4.0 vol.-% of the shortest fibres with $l/d = 6/0.16$), and of course between all other fibre combinations with lower volume quantities as well.

2.5.4 Packing density of aggregate-fibre mixtures

Introduction
Compared to aggregate grains, whose shape can in most cases be approximated with a sphere or ellipsoid, stiff steel fibres have usually a cylindrical shape, with a much higher aspect ratio (length/diameter) and slenderness. For an aggregate mixture, whose all grains have approximately the same size (mono-sized mixture), the influence of steel fibres on the packing density of such grains, depends on the ratio between the length of the fibres and the diameter of the grains. Four limit situations are given in Fig. 2.10, where D_{agg} is the diameter of the aggregate grains, and L_{fib} is the length of applied fibre.

Obviously, if the difference between the fibre length and the aggregate diameter increases, the lower is the influence of the fibres on the packing of the aggregate (cases 2 and 4 in Fig. 2.10). Very small grains can pack very efficiently around long thick fibres (case 2), and also the packing of very large grains will not be much disturbed by the presence of very short thin fibres between them (case 4). Contrary to these cases, if the length of fibres and the diameter of the grains are in the same order of magnitude (cases 1 and 3), the grains cannot pack efficiently any longer, due to the slender fibrous inclusions. This is even more obvious if one compares case 4 (almost undisturbed packing) with case 3 (very disturbed packing).

Concerning the practical mixture design of fibre concrete, the mixtures with disturbed packing contain more empty spaces, which has to be filled with cement paste. Therefore, the addition of fibres will in these cases indirectly cause a significant increase of needed quantity of cement, which is rather non-practical. Also, the probability of clustering of fibres in fresh concrete mixtures, is rather high in such a situation. However, with the right combinations between the fibre length and the average grain size, almost no influence on the packing density exists, which makes such aggregate-fibre combinations very suitable for practical mixture design.
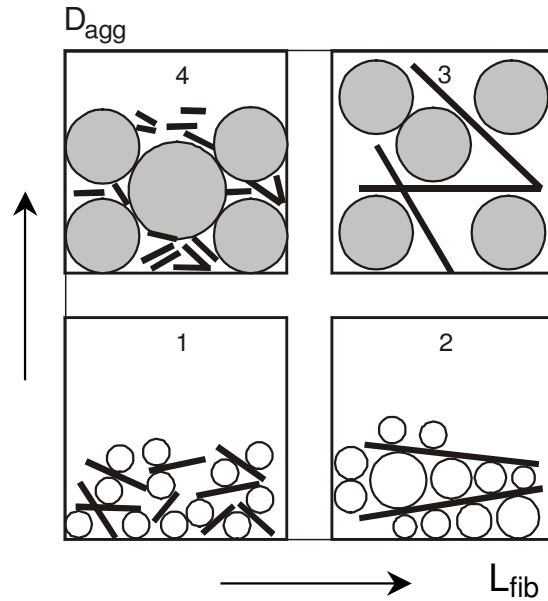
Fig. 2.10: Interaction between fibres of different lengths (L_{fib}) and aggregate grains of different diameters (D_{agg})

Determination of the packing density of aggregate-fibre mixtures

The packing density of aggregate-fibre dry mixtures was measured using the same method as for aggregate grains, which means that the influence of different types of steel fibres on the packing density of the aggregate grains may correctly be estimated.

Only the optimum aggregate grading curve (28% + 15% + 57%), determined in previous sub-chapter (Fig. 2.9), was used in all performed measurements. The initial value of the packing density was equal to 0.695.

First, the packing densities of the aggregate mixtures with one type of fibre were measured. Three types of steel fibres were applied for this, independent from each other: short straight fibres with $l/d = 6/0.16$ and $l/d = 13/0.2$, and long hooked-end fibres with $l/d = 60/0.7$, with volume percentages ranging from 0 to 4 vol.-% for each of them.

After that, the packing densities of the aggregate with two types of fibres together, were measured. The volume percentage of long hooked-end fibres ($l/d = 60/0.7$) was fixed to 1.0 vol.%, whereas the volume percentage of short straight fibres with $l/d = 13/0.2$ was varied from 0.0 to 2.0 vol.%. In this way, the maximum total applied volume quantity of fibres was 3.0 vol.-%.

The results of the measurements of packing density of different aggregate-fibre mixtures are given in Fig. 2.11 a and b.
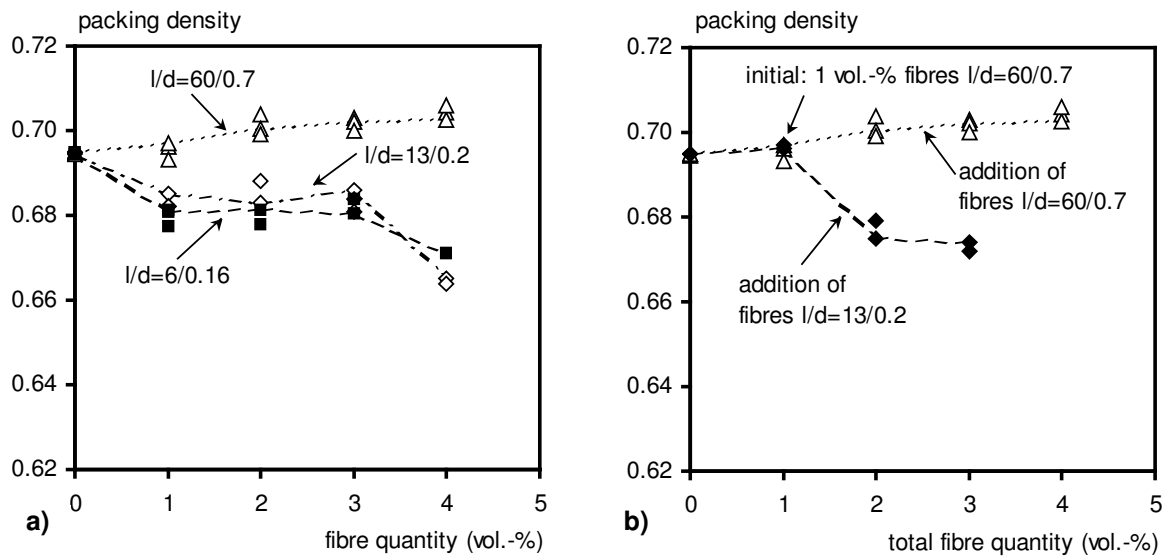
Fig. 2.11: The influence of the volume quantity of steel fibres, with different length/diameter (l/d) ratios, on the packing density of the aggregate mixture with $D_{max} = 1$ mm, for: a) three types of fibres (short and long) are combined with aggregate, independent of each other;   b) the addition of short fibres in the mixture which initially contains 1 vol.-% of long fibres, and the comparison to the mixture with long fibres only

In general, for the granular composition with $D_{max} = 1$ mm applied herein, the fibres did not have a significant negative effect on the packing density. The presence of long fibres only, caused even a slight increase of the packing density, from 0.695 up to 0.704 (Fig. 2.11.a). When only short fibres were mixed with aggregate, a slight decrease of the packing density was registered, from 0.695 up to 0.662 (Fig. 2.11.a). Slightly higher values of packing density were registered for fibres with l/d = 13/0.2, compared to shorter fibres with l/d = 6/0.16. Similar results were found by [Hoy, 1998]. All mentioned results correspond to possible situations of aggregate-fibre packing (cases 2 and 1, respectively), given in Fig. 2.10.

When both long and short fibres were present together in one granular mixture (Fig. 2.11.b), a decrease of the packing density, from 0.695 up to 0.670 was registered. This is another approval that the packing arrangement of grains is more disturbed by shorter than by longer fibres. Obviously, somewhat more cement paste will be necessary for the mixtures with only short and both short and long fibres, compared to the mixtures with only long fibres.

It is also interesting to note, that long thick fibres in combination with very fine grains, fill the space better that the grains self. In such a case, the volume of each cylinder (i.e. of the fibre) will always be bigger than the volume of the spheres (i.e. aggregate grains), which fill that cylinder. Therefore, the total packing density will automatically be higher if long fibres

are present in the container. Another reason for this phenomenon is the local internal action of the fibres during compaction by vibration. As the weight of long steel fibres is much larger than the weight of each aggregate grain, the long steel fibres will move more intensively during vibration. This may cause a better compaction of grains around each fibre, which suggests that these fibres may act additionally as internal vibrators.

Estimation of the wall-effect of the container on the packing density
Disturbances in the packing of particles always appear near bodies or surfaces with (much) larger volume and surface area. For example, the wall of a container is such a surface. This phenomenon is called the "wall-effect".

In [Ben-Aim, 1970], two different zones (volumes) in a container are introduced: a disturbed zone, adjacent to the container walls, with a lower packing density, and a non-disturbed zone in the middle, with a higher packing density. The experimentally determined packing density is actually a mean value of the packing densities in these two zones. The undisturbed packing density should be normative for mixture proportioning.

According to [Ben-Aim, 1970], the size of the disturbed zone spreads up to a distance equal to $D_{max}/2$, measured from the container wall. This was recently proven by [Nordenswan, 2002] as well. For the mixtures with both fibres and aggregates, it may be assumed that the size of the disturbed zone spreads up to a distance of $L_f/2$ from the container wall, where L_f is the fibre length.

Therefore, the packing density in the undisturbed zone of the container (PD_{nd}), can be obtained from:

$$PD_{exp} = V_{nd} \cdot PD_{nd} + k_w \cdot V_d \cdot PD_{nd}, \quad \text{thus} \quad PD_{nd} = PD_{exp} / (V_{nd} + k_w \cdot V_d), \qquad (2.11)$$

where:

PD_{exp} = experimentally determined (i.e. mean) value of the packing density
PD_{nd} = non-disturbed packing density
V_{nd} = ratio of non-disturbed volume of container and total volume of container
V_d = ratio of disturbed volume of container and total volume of container
k_w = disturbance coefficient, $k_w < 1.0$.

However, in [Hoy, 1998], no wall-effect at all could be registered, for fibre lengths varying from 30 up to 60 mm, while in [Grünewald, 2004] it was possible to register the wall-effect, and the differences between disturbed and undisturbed packing densities ranged up to about 25 %.

In this research project, the influence of the wall-effect on the packing density will not be taken into account. The size of the container is much larger, than both the maximum aggregate size (D_{max} = 1 mm), and the dimensions of the short fibres (l/d = 13/0.2). Therefore, the

wall effect for these two cases can be neglected. Nevertheless, the wall-effect probably play a role for mixtures with long fibres ($l/d = 60/0.7$). However, the measured packing densities of such mixtures will be lower than the undisturbed packing densities. This will result in slightly higher quantities of needed cement paste. The utilisation of somewhat more cement paste in FRC, can indeed have only positive influences both on its workability [Okamura, 2000], and on its tensile properties [Van Mier, 2004 a].

2.6 Characterisation of workability of Hybrid-Fibre Concretes

As already explained in the introduction of this chapter, the first requirement concerning the mixture composition of Hybrid-Fibre Concrete, was the creation of self-compacting mixtures. The main and the most important feature of self-compacting fibre concrete is a much better and more uniform distribution of the fibres in comparison to conventional fibre concrete. The absence of any additional compaction, as well as the possibility to align the fibres in the direction of the flow, are unique characteristics of self-compacting fibre concrete.

2.6.1 Applied concrete mixtures, mixing sequence and testing procedure

For a given water/binder-ratio and a chosen combination of fibres, the optimum aggregate grading was determined in previous sub-chapters. The next step, is the determination of the most appropriate quantity of the sand (i.e. of cement), that should be applied for a given quantity and given types of fibres. This was realised by numerous workability studies on fresh concrete mixtures. These studies were followed by the determination of the compressive and the splitting tensile strength, which will provide the first estimation of the mechanical properties of Hybrid-Fibre Concrete.

According to the order of development, all mixtures can be divided into two main groups, given in Tab. 2.1:

−   preliminary mixtures: these are mortars with fibres, characterised by a rather low volume quantity of the aggregate ($V_{agg} < 30$ vol.-%), two maximum grain sizes of $D_{max} = 4$ mm and 1 mm and two selected values of the w/b-ratio ($w/b = 0.4$ and 0.3). The procedure for optimisation of the granular composition, described in the previous sub-chapters, was not applied in this preliminary phase. These mixtures will be used only in the fibre pullout tests (Tab. 2.1, mixtures 1 - 10);

−   optimised mixtures: these are very fine mortars, whose granular composition was developed completely on the basis of the procedure described in the previous sub-chapters. The maximum grain size of $D_{max} = 1$ mm was used, the quantity of aggregate is somewhat higher compared to preliminary mixtures ($V_{agg} < 50$ vol.-%), with a rather low value of the w/b-ratio ($w/b = 0.2$). These optimised mixtures will be used first in the fibre pullout tests,

and will serve as a basis for all the mixtures which will be used subsequently in the flexural, and finally in the uniaxial tensile tests on HFC (Tab. 2.1, mixtures 11 - 25).

The complete overview of all the mixtures is given in Tab. 2.1, together with the slump flow and an estimation of the visual appearance of the fresh mixtures (clustering of fibres).

Tab. 2.1: Scheme of the composition of developed concrete mixtures, with their workability characteristics (slump flow and clustering)

No	w/b	microsilica vol.% cem.	aggregate (vol.-%)	D_{max} (mm)	short fibres (vol.-%) 6/0.16	13/0.20	long fibres (vol.-%) 60/0.70	slump flow (cm)	clustering of fibres
1	0.40	0.0	30.0	4	0.0			67.5	no
2	0.40	0.0	26.0	4	4.0			59.0	no
3	0.40	0.0	24.0	4	4.0	2.0		27.0	yes
4	0.30	0.0	30.0	4	0.0			81.0	no
5	0.30	0.0	26.0	4	4.0			64.5	no
6	0.30	0.0	24.0	4	4.0	2.0		28.0	yes
7	0.30	0.0	30.0	1	0.0			85.0	no
8	0.30	0.0	28.0	1	2.0			81.5	no
9	0.30	0.0	26.0	1	4.0			69.0	no
10	0.30	0.0	26.0	1	4.0	2.0		45.0	yes
11	0.20	4.0	50.0	1		0.0		90.0	no
12	0.20	12.0	50.0	1		0.0		94.0	no
13	0.20	4.0	48.0	1		1.0		81.5	no
14	0.20	4.0	46.0	1		2.0		76.0	no
15	0.20	4.0	38.0	1		3.0		75.0	no
16	0.20	4.0	35.0	1		4.0		53.0	yes
17	0.20	4.0	40.0	1	2.0	2.0		70.0	no
18	0.20	4.0	42.0	1	1.0	3.0		56.0	partly
19	0.20	4.0	45.0	1		0.0	1.0	64.5	no
20	0.20	4.0	40.0	1	2.0		1.0	68.0	no
21	0.20	4.0	41.0	1	4.0		1.0	48.0	yes
22	0.20	4.0	40.0	1		0.5	1.0	70.0	no
23	0.20	4.0	40.0	1		1.0	1.0	58.0	partly
24	0.20	4.0	41.0	1		2.0	1.0	47.0	yes
25	0.20	4.0	35.0	1		2.0	1.0	56.0	partly

All designed mixtures were mixed in the same way (Fig. 2.13): aggregate and cement were premixed first for 20 sec., after which water and viscosity agent (superplasticizer) were added. After about 1 min. of mixing, the microsilica was added (for mixtures 11 - 25), and such a mixture was subsequently mixed, until it became flowable. It took mostly from 3 to 6 minutes for this, depending on the value of the *w/b*-ratio, and on the total volume of the mixture. The lower is the *w/b*-ratio, the more cement is present, and therefore the longer is the time needed for the viscosity agent to react with the cement and to improve the flowablity of cement paste. Concerning the total volume of the mixture, the more cement the mixture contains, the faster and more effective the viscosity agent will react with it.

When a mixture became flowable, the fibres were added in it and mixed additionally for 2 to 3 minutes, depending on the fibre type. The long hooked-end fibres are glued to strips, and for them about 3 minutes of mixing were enough to dissolve the glue and distribute the fibres in the mixer. The workability was tested subsequently.
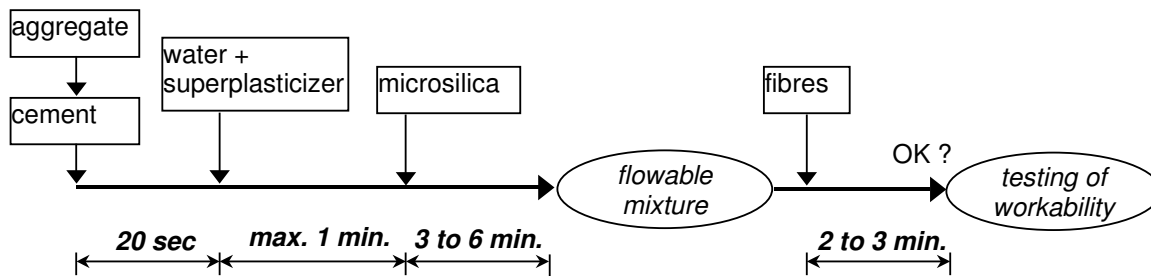
Fig. 2.13: Scheme of the mixing process for Hybrid-Fibre Concrete

For the characterization of the workability, the following methods were used:

- the slump flow test, or the slump test (depending on the workability), using a standard Abrams cone (height = 30 cm, upper diameter = 20 cm, lower diameter = 10 cm). The requirement for self-compactability was a slump flow higher than 60 cm;
- the visual appearance of concrete; the requirements for self-compactability were: an approximately round shape of the flow area of fresh fibre concrete mixture, without clustering and/or segregation of fibres and/or aggregate grains;
- the determination of the so-called "t_{50} time", i.e. the time needed for a flowing mixture to reach on the testing table a circle with a diameter of 50 cm;
- the determination of the so-called "V-funnel time", i.e. the time needed for concrete to flow out of a funnel, with dimensions: height = 60 cm, thickness = 7.5 cm, upper width = 51.5 cm, lower width = 6.5 cm. This method was used only for mixtures intended for the flexural and for the uniaxial tensile tests (mixtures 11 – 25, Tab. 2.1).

2.6.2   Determination of the optimum quantities of aggregate and cement

The reference mixture in each set of mixtures contained no fibres. In the mixtures with fibres, the volume quantity of the aggregate was decreased, as the volume quantity of the fibres was increased. The principle that an appropriate quantity of aggregate can be replaced by a same quantity of fibres, was applied for all preliminary mixtures (Tab. 2.1, mixtures 1 - 10). It is also possible to decrease the aggregate quantity to a larger portion than the quantity of added fibres, which was applied in all optimised mixtures (Tab. 2.1, mixtures 11 - 25).

It should be emphasised, that the slump flow will not depend only on the applied fibre types and quantity, but also on the applied quantity of the viscosity agent (superplasticizer). The quantity of it was always adjusted in such a way, that no segregation of fibres appeared. Too high quantities of the viscosity agent resulted in too flowable cement paste, which then simply flows through the fibre skeleton, while the fibre skeleton remains in the middle of the testing table. As the optimum quantity of the viscosity agent depends on many influencing factors (type of the viscosity agent, type and fineness of the cement and of the other applied filler materials, aggregate grading and quantity, mixed volume of the concrete, mixer, tem-

perature, mixing sequence and time, and also the applied fibre types and volume quantities in the case of FRC), it will not be analysed here.

Fig. 2.14.a shows the influence of short fibres on the slump flow, for different maximum grain sizes D_{max} = 4.0 mm, and D_{max} = 1.0 mm, and for w/b = 0.3 for all mixtures. The applied volume quantity of aggregate (in vol.-%) is given near each point on the diagram. The underlined values represent the mixtures, where clustering of fibres was observed. There is not a big difference in workability, up to a fibre factor $V_f * L_f / D_f$ = 1.5 (corresponding to 4.0 vol.-% of short fibres with l/d = 6/0.16).

The addition of another 2.0 vol.-% of short fibres with l/d = *13/0.2*, caused a significant decrease of the slump flow, for the mixture with D_{max} = 4.0 mm. This decrease was however much smaller for the mixture with D_{max} = 1.0 mm. This suggests that the granular composition must be refined, in order to be able to accommodate large quantities of fibres. No long fibres were applied in the preliminary mixtures.
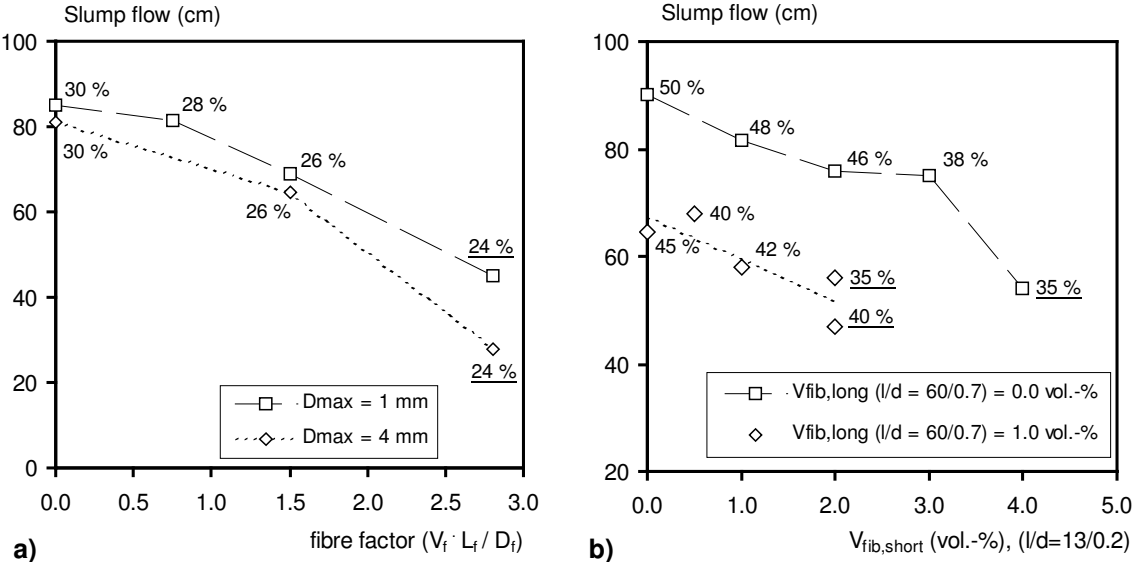
Fig. 2.14 :   a) The influence of the applied quantity of short fibres l/d = 6/0.16 on the slump flow of concrete, for two different maximum sizes of the aggregate grains (D_{max});   b) The influence of the applied quantity of short fibres (l/d = 13/0.2) on the slump flow of concretes without and with 1.0 vol.-% of long fibres, with l/d = 60/0.7;   In both figures, the label near each point represent the applied volume quantity of aggregate, and the underlined label values represent the mixtures, where clustering of fibres was registered

Fig. 2.14.b shows the influence of both short and long fibres on the slump flow of the second group of mixtures (optimised mixtures), with D_{max} = 1 mm, and w/b = 0.2. The applied quantity of aggregate (in vol.-%) is given near each point on the diagram. The underlined values represent the mixtures, in which clustering of fibres was observed. Short fibres with l/d =

13/0.2 could be applied up to rather high volume quantities of about 3 vol.-%, keeping the workability on a satisfactory level.

Compared to these mixtures, the mixtures with both short (l/d = 13/0.2), and long fibres (l/d = 60/0.7), had a smaller slump flow. This was mostly due to the presence of the long fibres, which tend to form clusters when applied in larger quantities. In combination with 1 vol.-% of these fibres, the maximum applicable quantity of short fibres with l/d = 13/0.2 is about 0.5 to 1 vol.-%, in order to keep the workability on a satisfactory level.

The application of higher fibre quantities causes clustering of fibres, although the mixtures still possess a rather good workability. If the quantity of the aggregate is decreased (e.g. from 40 to 35 vol.-%, Fig. 2.14.b), the flowability and the appearance may become somewhat better. However, it is not possible to obtain such mixtures, which can satisfy all mentioned criteria of self-compactability.

The comparison in applied volume quantities of aggregate in Fig. 2.14.a and b, shows that it is not necessary to decrease them significantly (i.e. to increase the applied quantity of cement), in order to force the mixtures to accommodate large quantities of steel fibres.

Both Fig. 2.14.a and b, show a rather constant trend in slump flow, up to an appropriate volume quantity of fibres. After this quantity has been reached, a sudden decrease of workability appears. This suggests that there is a defined maximum applicable quantity of fibres (for each type of fibres), in combination with appropriate granular composition and amount of aggregate. Increasing the fibre content above this value cannot result in self-compacting, stable and homogeneous mixtures.

2.7 Modelling the optimum quantity of aggregate in Hybrid-Fibre Concretes ("Excess-paste Model")

2.7.1 Introduction

There are many different types of steel fibres (Fig. 1.2), and they can be used in many different amounts in Hybrid-Fibre Concrete. It would therefore be practical to know which quantity of aggregate should be used with which combination of steel fibres.

The so-called "Excess-paste Model", which is based on the thicknesses of the layers of cement paste around aggregate grains and fibres, can be used to predict the needed quantity of aggregate. This model will be developed and calibrated in this sub-chapter, for a general case of mixtures with different types of fibres. With calibrated parameters, the model can be used in practice for an approximate prediction of the aggregate quantity for given combination of steel fibres, which is also its main goal.

2.7.2 "Excess-paste Model"

The so-called "Excess-paste Model", developed for ordinary and self-compacting concrete in [Kennedy, 1940], and [Midorikawa et al., 2001], can be applied to self-compacting fibre con-

crete as well. According to this model, the <u>necessary</u> amount of cement paste in self-compacting concrete, consists of two components:

- <u>the minimum paste amount</u> (V_p), which fills the voids in a dry fully compacted mixture of aggregate and fibres;
- <u>the additional paste amount</u> ($V_{pa} + V_{pf}$), which covers all aggregate particles (V_{pa}) and all fibres (V_{pf}), in order to "lubricate" them and to create a flowable viscous mixture.

According to the Fig. 2.15 a, the composition of the fibre concrete mixture with dry packing density *PD*, which consists of *m* fractions of aggregate (according to ISO standard sieve sizes), and *n* types of fibres, may be represented as:

$$V_a + V_{pa} + V_f + V_{pf} + V_p + V_{air} = 1, \text{ which is equal to:} \tag{2.12}$$

$$V_a + \sum_{i=1}^{m} n_i \cdot V_{pa,i}^{(1)} + V_f + \sum_{j=1}^{n} n_j \cdot V_{pf,j}^{(1)} + (1 - PD) + V_{air} = 1, \tag{2.13}$$

where $V_{pa,i}^{(1)}$ and $V_{pf,j}^{(1)}$ represent the volume of the excess paste around a single aggregate particle and single fibre respectively (Fig. 2.15 b). With the assumption of a spherical shape of the aggregate particles, and a constant thickness of the cement paste layers (c_a and c_f), these volumes may further be expressed as:

$$V_{pa,i}^{(1)} = \pi/6 \cdot (6d_{a,i}^2 c_{a,i} + 12d_{a,i}c_{a,i}^2 + 8c_{a,i}^3), \text{ and} \tag{2.14}$$

$$V_{pf,j}^{(1)} = \pi \cdot l \cdot (d_{f,j}c_{f,j} + c_{f,j}^2). \tag{2.15}$$
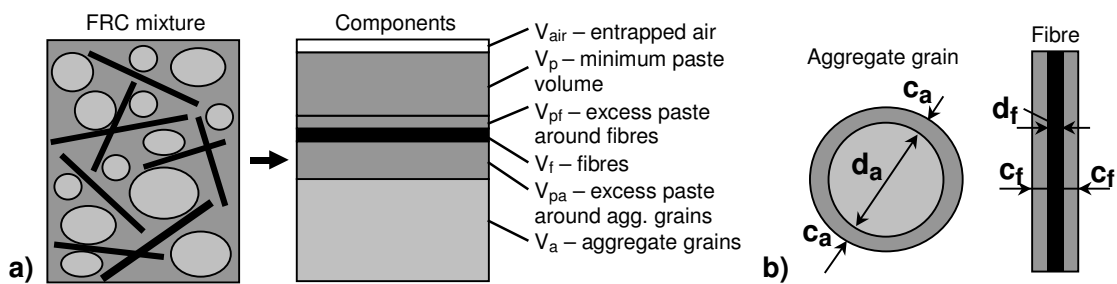
Fig. 2.15: a) Composition of a (self-compacting) fibre concrete mixture, with three different roles of the cement paste; b) layers of cement paste around single aggregate grain and single fibre

From the known dry packing density of the aggregate-fibre mixture *(PD)*, one may easily obtain the minimum necessary paste volume V_p, as $V_p = 1 - PD$. For a given volume and grading

of the aggregate, and known amount and types of applied fibres, it is possible to calculate the additional paste volume, which is necessary to cover all grains and all fibres. By summing-up the minimum and the additional paste volume, the total paste content can be obtained. This forms a basis for the mix design of any self-compacting fibre concrete.

In order to be able to carry out calculations with this model, the following additional assumptions are made:

- The thickness of the paste layer (c_a and c_f) is proportional to the diameter of the grain, i.e. diameter and length of the fibre, with the proportionality factor k, so that:

  - for paste layer around grains: $c_a = k \cdot d_a$, and $\hspace{2cm}$ (2.16)

  - for paste layer around fibres: $c_f = k \cdot d_f \cdot l_f^m$, $\hspace{2cm}$ (2.17)

  where m is a parameter, which should be calibrated using the results of the workability experiments;

- No entrapped air is present in the fresh mixtures.

2.7.3 Application of "Excess Paste Model" to Hybrid-Fibre Concretes

Procedure for calculation

The procedure of determining the paste thickness and the aggregate volume content necessary for the fibre reinforced self-compacting concrete (FRSCC) is given in Fig. 2.16. First, self-compacting mixtures with sand only are developed, and the coefficient k is calculated. In this way, the needed paste thickness around each aggregate grain can be obtained. Knowing the packing density of the aggregate-fibre mixture, it is possible to compute the paste amount (V_{paste}) of the fibre concrete mixtures, which is necessary to keep the coefficient k constant. The paste thickness around the grains is obtained using equation 2.16, and the paste thickness around the fibres using equation 2.17, with the parameter m ranging from 0 to 2. The maximum applicable amount of aggregate follows then directly from here.
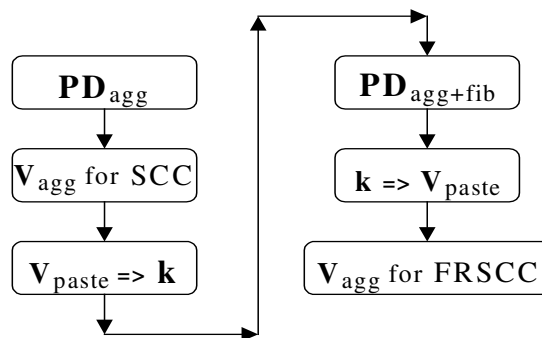
Fig. 2.16: Procedure applied for the calculation of the amount of aggregate required for the creation of self-compacting fibre concrete

Calibration of parameters

For an initial quantity of aggregate of 55.0 vol.-% in plain self-compacting concrete, the obtained value of the parameter k is $k = 0.0404$. This means, that the average paste thickness around aggregate grains ranges from 0.007 mm for an average grain size of 0.175 mm (smallest fraction), up to 0.03 mm for an average grain size of 0.75 mm (largest fraction in this case).

The results of these calculations, for mixtures with short and long fibres, for different values of the parameter m, are presented in Fig. 2.17.a and b. The maximum applicable contents of sand obtained experimentally by mixing, are presented in Fig. 2.17. a and b as well. By a comparison of the two models, it is possible to calibrate the value of the parameter m needed for the optimal fitting of the existing curve.

Short straight fibres usually do not have a significant influence on the workability, except in case of very large fibre volume percentages ($V_f > 3.0$ vol.-%) . This is mostly due to their small length and diameter, and follows both from the theoretical (modelled) and from the experimental curves (Fig. 2.17.a). No significant decrease of the volume content of the aggregate is necessary in order to keep the workability at a satisfactory level. The best fit for the coefficient m is $m = 1.2 - 1.3$, so that for further modelling of hybrid-fibre mixtures the average value $m = 1.25$ will be applied.
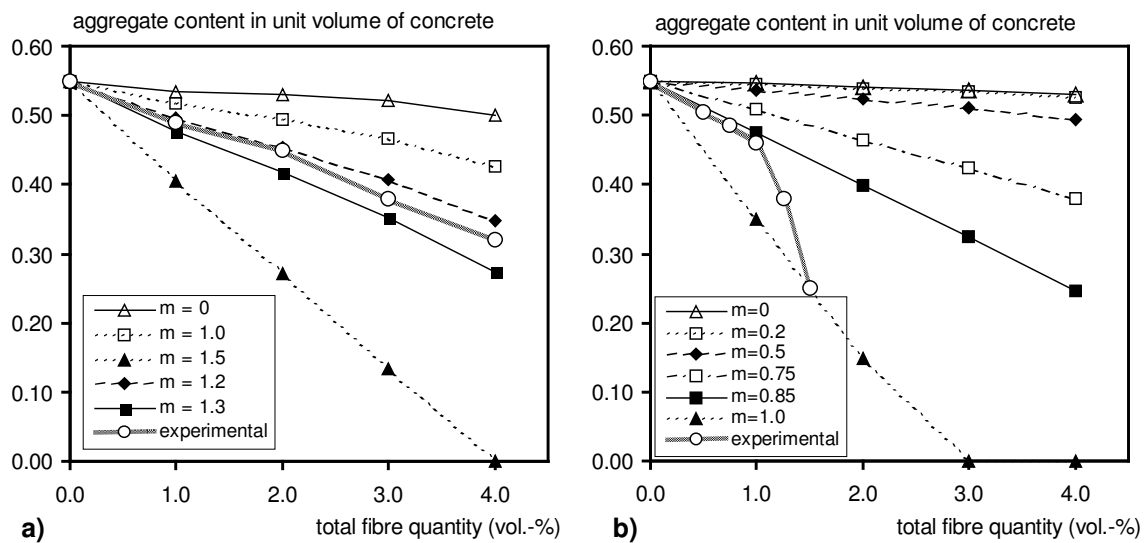
Fig. 2.17: The quantity of aggregate required to create self-compacting fibre concrete for different types and quantities of steel fibres, with calibration of the thickness of the paste layer around the fibres (parameter "m"): a) short fibres (l/d = 13/0.2); b) long fibres (l/d = 60/0.7)

On the contrary, long fibres may influence the workability already at lower volume contents. All values of the coefficient *m* from 0 to 0.75, lead to unrealistic results for the aggregate content (Fig. 2.17.b). The value of *m* = 0.85 fits the maximum applicable aggregate volume quite well for the lower volume contents of fibres (up to 1.0 - 1.25 vol.%). According to the model, it is possible to apply higher fibre contents as well, with a further decrease of the aggregate content. Practically, clustering of the long fibres appears and the mixtures cannot be regarded as self-compacting any longer.

Application of the model to hybrid-fibre concrete

When the parameters *m* are calibrated in this way, independently for short and long fibres, the model could be applied to hybrid-fibre mixtures (with both short and long fibres). The results of this analysis are given in Fig. 2.18. As it can be observed, excellent agreement between the analytically and the experimentally determined quantities of aggregate exists. The initial mixture contained 1.0 vol.-% of long fibres only. The effects of the addition of both short and long fibres to this initial mixture, may be observed in Fig. 2.18 as well. Clearly, the addition of short fibres to the mixture with long fibres, assures a good workability up to rather high fibre quantities. By increasing only the quantity of long fibres, this is not possible. As it will be shown later, good workability will have a positive effect on the mechanical properties as well.
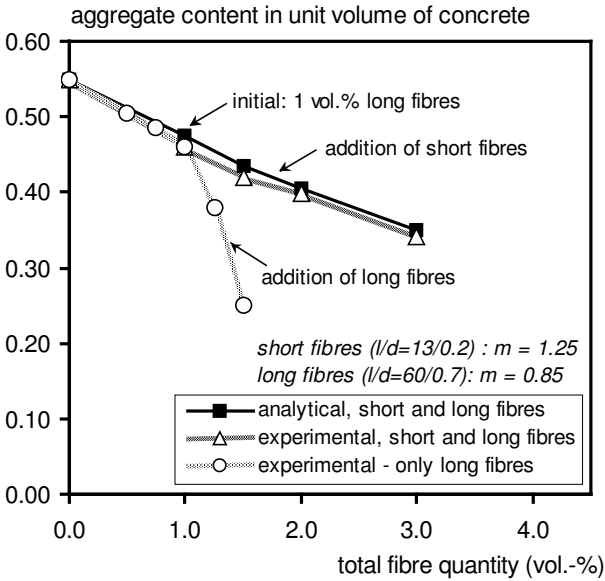
Fig. 2.18: Comparison between analytically and experimentally determined quantities of aggregate, needed to create self-compacting hybrid-fibre concrete (with both long and short fibres)

The satisfactorily agreement between analytically and experimentally obtained values, shows that the "Excess-paste Model" can be applied for other fibre combinations as well. This model can serve efficiently for an approximate estimation of the needed quantities of aggregate, for

many other combinations of fibres. The quantities of aggregate given in Fig. 2.17 and 2.18 are the maximum recommended quantities, required for self-compactability of fresh HFC mixtures. Lower quantities of aggregate may be applied as well.

2.7.4 Discussion of the "Excess-paste Model"

Although the "Excess-paste Model" can be regarded as an universal tool for the mixture composition of self-compacting concretes with different types and combinations of fibres, it should be kept in mind that this model contains a number of simplifications:

− In reality, the aggregate grains are never perfectly spherical, and therefore the thickness of the paste layer around them may vary. These factors have a stochastic nature and are difficult to quantify;

− The values of the dry packing density may vary significantly depending on the measuring procedure. Having in mind that the model is based on dry packing density, it should always apply a constant procedure for its determination;

− The wall-effect in the measuring container is always present. It increases significantly if particles and fibres are large in comparison to the container dimensions. As explained in the sub-chapter 2.5.4, the influence of the wall-effect was not taken into account here. Therefore, the calculated minimum necessary paste volume (V_p) is somewhat higher for disturbed packing. If some more cement paste is required, the disturbed packing density may be considered as the one being at the "safe side";

− The application of long fibres causes the most serious problems for workability. The present model works efficiently for contents of long fibres up to 1.0 vol.%. Theoretically, the additional paste content may be estimated also for larger fibre contents. Practically, the quantity of long fibres is limited to an appropriate value, in order to assure self-compactability of the fibre concrete. Any increase of the fibre content above these values leads to clustering and grouping of the fibres, so that such a concrete cannot be applied in practice.

In spite of this, the Excess-Paste Model can be used very efficiently in the initial phases of the mix design process of Hybrid-Fibre Concrete with various fibre types and combinations. Using this model, the optimum quantities of cement and aggregate can be estimated rather accurately. When these parameters are known, it is necessary to continue the further mixture optimisation with respect to the quantity of the viscosity agent.

2.8 Summary and concluding remarks on mixture composition

In the previous sub-chapters the mixture compositions of different types of fibre concrete, with one and two types of fibres, are presented. The basic requirement was to produce self-compacting hybrid-fibre concrete. It was shown that with an appropriate mixture composition, it is possible to produce self-compacting fibre concrete, with relatively high volume quantities of both long and short steel fibres (from 1.0 vol.-% up to 5.0 vol.-%). The detailed procedures

for the mixture design have been given as well. They are based on the interaction between steel fibres and aggregate grains. The "Excess-paste Model" was also applied to these mixtures, in order to recommend the optimum quantities of aggregate for given types and quantities of fibres.

From the previous sub-chapters the following may be concluded:

1. Aggregate grains must be able to pack between the fibres, for the given quantity and type of fibres. The maximum and the average grain size follow from the distance between neighbouring fibres.

2. For an aggregate composition consisting of very fine sand only, no large differences in packing density are obtained with variations in aggregate grading.

3. The packing density of dry aggregate-fibre mixtures depends on types and quantities of the applied fibres. Compared to the reference value (only aggregate, without fibres), the packing density increases if long fibres are applied and decreases if only short, or both short and long fibres are applied.

4. Short steel fibres do not have a significant influence on the workability. They may be applied up to 4.0 – 5.0 vol.-%, maintaining the concrete self-compacting. Long steel fibres (l/d = 60/0.7) form clusters if applied in quantities higher than 1.0 vol.-%, independent of the applied concrete mixture composition. Such concretes can therefore not be regarded as self-compacting.

5. In the "Excess Paste Model", the existence of the layer of cement paste around each aggregate grain and fibre is assumed. This cement paste enables the flow of concrete. The parameters of the model were calibrated for mixtures with one single type of fibre, and after that successfully tested on hybrid-fibre mixtures. In this way, recommendations for the needed quantity of aggregate in self-compacting Hybrid-Fibre Concrete with many different fibre combinations, can be derived.

In the following part of this research, appropriate mixtures will be selected and used as a pullout medium, in the pullout tests on single fibres. The fibre efficiency will be determined in these tests, and the results will be presented in the following sub-chapter.

2.9 Pullout behaviour of steel fibres

2.9.1 Introduction

Concrete cracks under the action of tensile stresses. In order to prevent brittle failure, appropriate load-carrying mechanisms must be provided across the cracks. In reinforced concrete, the reinforcing bars continue to carry tensile stresses across the cracks and provide structural reliability after cracking. Similar to this, in the fibres in fibre concrete bridge cracks, transmit tensile stresses and prevent brittle failure in this way.

During bridging of a crack by steel fibres, two main fracture processes occur:
- the debonding on the interface between fibre and matrix, and subsequently,
- the pullout of fibre.

The distribution of stresses in a single straight fibre, which bridges a crack, and in the surrounding concrete, is given in Fig. 2.19.a. For the sake of simplicity, only one fibre aligned in the direction of the main tensile stress is presented here. It is further supposed that debonding occurs only at one (the right-hand) side of the fibre. Elastic elongation of the fibre will occur as well, but its effect will be neglected for small crack widths. Therefore, the debonding slip of the fibre L_{db}, the slip of the fibre across the crack Δ, and the crack width w will approximately be equal to each other.
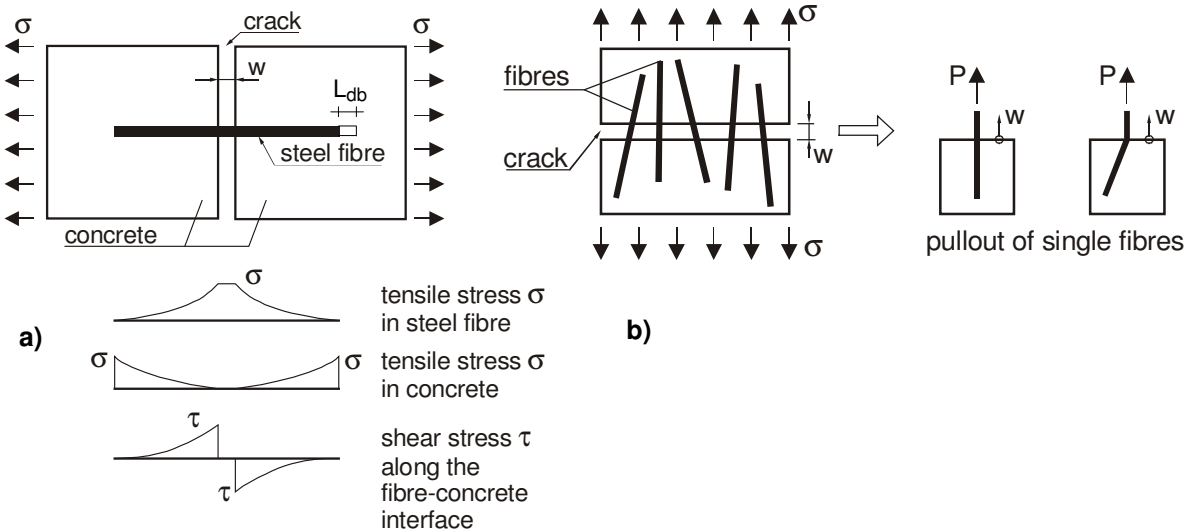
Fig. 2.19: Cracked fibre concrete under the action of a uniaxial tensile stress σ: a) Bridging of a crack by a single aligned fibre, with distribution of stresses in fibre and in concrete (normal stress σ), and along the fibre-concrete interface (shear stress τ), at a crack width w (i.e. at fibre slip Δ), and for a fibre debonding slip L_{db}; b) Real case of bridging of a crack by a group of randomly oriented fibres and simulation of this process by the pullout tests on single fibres, aligned and inclined with respect to the pullout force P, i.e. to the tensile strength σ

The fibre takes over the total tensile force over the crack, and transfers it stepwise into the surrounding concrete, along its interface. In this simple case, the total tensile capacity of the fibre-concrete composite depends on the tensile stress, which can develop in the fibre during crack bridging. The higher this stress, the better will the tensile response. The mechanics of fibre reinforced concrete including crack bridging mechanisms, is described in detail in [Bentur & Mindess, 1990], and [Shah et al., 1993].

The bridging of a crack by fibres is in the reality (Fig. 2.19.b) somewhat different, compared to the idealized case shown in Fig. 2.19.a. Fibres act in and as a group, close to each other. Moreover, they are randomly oriented with respect to the uniaxial tensile stress σ, i.e. with respect to the crack surface.

Pullout tests on single fibres (Fig. 2.19.b) are an efficient way of simulating such a bridging of cracks by fibres. The main goal of fibre pullout tests is the determination of the efficiency of fibres in crack bridging process. Fibres are fully efficient only then, when their tensile capacity is utilized up to an optimum limit during crack bridging. This can be e.g. up to 80-90 % of the total tensile capacity (tensile strength) of the material of the fibre.

The efficiency of fibres depends basically on the coherence between the applied type of fibre and the concrete which surrounds the fibres (pullout medium). In such a pullout medium, the quantities of all ingredients (cement, water, aggregate, etc.) may be varied. It is also possible to utilize additionally short fibres as a "secondary" reinforcement. Such a case may be used for the simulation of the pullout behaviour of the long fibres in Hybrid-Fibre Concrete, which contains both types of fibres. It is also possible to vary the angle of fibre inclination with respect to the pullout force. The influence of all these parameters will be explained in detail in section 2.9.2, and evaluated experimentally in section 2.9.3 and 2.9.4. Before this, the characteristic phases of the pullout behaviour of the fibres (adhesion, debonding and frictional pullout) will be described in detail.

Fibre-matrix interface and adhesion

Adhesion bond is the mutual bond between each fibre and the concrete which surrounds it. It is directly related to the quality (i.e. strength) of the material in the interfacial zone between each fibre and the concrete matrix. Under the action of the tensile stresses on a fibre, debonding between fibre and matrix occurs. The debonding process as such never occurs at the surface of the fibre. Actually, very fine cracks spread at a certain very small distance from the fibre, in and through the interfacial zone [Bentur & Mindess, 1991]. This is a consequence of the structure of this zone, which is qualitatively similar to that of the aggregate-cement paste interface. Due to non-efficient packing of the finest cement particles in the fresh state, that space will only partly be filled with hydration products. Also, just like around any other inclusion, there is a somewhat higher water entrapment around the fibres.

All these phenomena result in a somewhat higher porosity around fibres than in the bulk concrete matrix, and also in an increased amount of calcium-hydroxide (CH) crystals, which can be detected by a microscope (Fig. 2.20.a). The width of the interfacial zones determined in such a way by a SE Microscope ranges from 20-50 μm [Bentur et al., 1985]. The micro-

hardness of concrete around the fibre (Fig. 2.20.b), is generally 30-50 % lower than in the bulk concrete matrix, which also implicates a higher porosity [Wei et al., 1986]. The lower the w/b-ratio, the higher is the hardness of the interface zone. The estimated widths of the interface zones from these measurements are of similar size (about 75 μm), independent on the w/b-ratio.
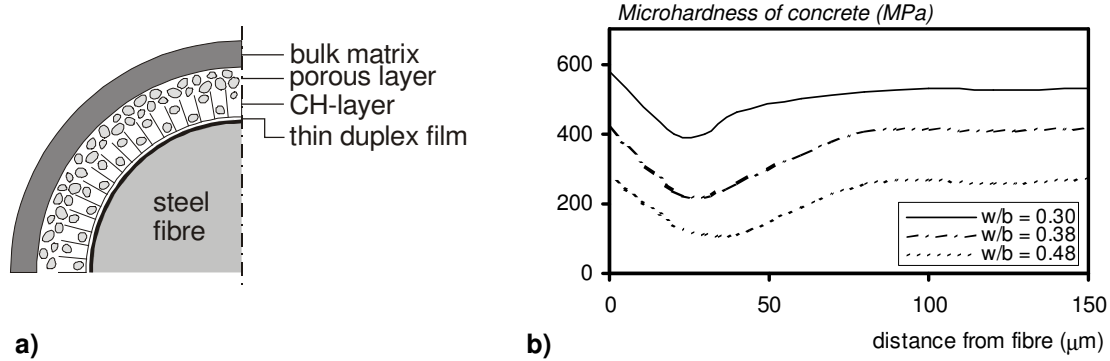
Fig. 2.20: a) Transverse cross-section through a steel fibre, interfacial zone with pores and calcium-hydroxide crystals (CH-layer) and bulk concrete matrix, which surrounds them, after [Bentur, Mindess, 1991]; b) Results of microhardness tests around steel fibres, for different water/binder ratios of concrete (after [Wei et al., 1986])

Debonding and pullout behaviour of straight and hooked-end steel fibres

The total pullout process of a fibre consists basically of 2 stages: debonding and frictional pullout. An overview of all the phases of the total pullout process, for straight and hooked-end steel fibres, is given in Fig. 2.21. The debonding process has generally the same character for both types of fibres. However, rather large differences between these two fibre types exist in frictional pullout.

As explained in the previous sub-chapter, debonding can be understood as a cracking process inside and along the fibre-matrix interface zone. The pullout force P increases during this process (*phase a*, Fig. 2.21 and 2.22.a), up to an appropriate value. When the adhesion bond along a fibre is fully destroyed , the pullout force, as a rule, decreases (straight fibres), or continues to increase (hooked-end fibres), like presented in Fig. 2.22.a. Depending on the applied fibre type, length (l), diameter (d) and embedded length (l_{emb}), the debonding will finish at fibre slips (w) from about 0.005 mm (polypropylene fibre, l/d = 6/0.01, l_{emb} = 3 mm, [Li & Stang, 1997]), up to 0.08 mm (steel fibre, l/d = 60/0.7, l_{emb} = 30 mm, [Van Gysel, 2000]). After that, the fibre is being pulled out of the concrete matrix, if the crack width (i.e. the fibre slip) further increases.

During the pullout process of a fibre, the frictional stresses develop along the interface zone. For steel fibres, the frictional stage for two fibre geometries (straight and hooked-end steel fibres) will be discussed.

The frictional stage of both types of fibres, is characterized by the following phenomena:

1. Basically, during slipping of a straight steel fibre through its channel, abrasion and compaction processes inside and along the interfacial zone occur, which generates frictional stresses;

2. The "fibre-matrix misfit" [Pinchin & Tabor, 1978] causes the contact pressure as well. The fibre-matrix misfit is a consequence of the hindered shrinkage of the concrete matrix around a fibre, and it is defined as the difference between the fibre radius and the radius of the hole in the absence of the fibre (Fig. 2.22.b). According to [Naaman et al., 1991], the fibre-matrix misfit deteriorates and decreases as the fibre is pulled out, because of the abrasion and compaction processes in the interfacial zone. According to [Li & Stang, 1997], this contact pressure depends also on the curing conditions of concrete, as well as on the concrete mix composition: a higher shrinkage (i.e. contact pressure) will develop, if the concrete contains more silica fume;

3. During its pullout, the fibre is subjected to a tensile stress in the longitudinal direction, which causes the Poisson's contraction in the transverse direction.
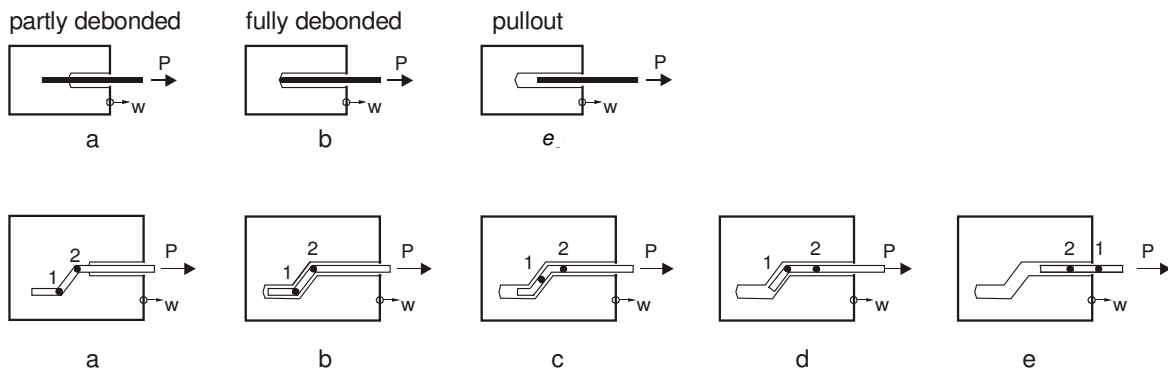
Fig. 2.21:   First row: debonding and pullout process of straight steel fibre;   Second row: debonding, plastic deformation of fibre hook (i.e. of the curvatures 1 and 2) and pullout of hooked-end steel fibre; (in both cases, the relation of the pullout force P and the fibre slip w can be determined)

The pullout process of hooked-end fibres is somewhat more complex than that of straight steel fibres. Basically, the same phenomena (debonding, followed by frictional pullout) present for straight fibres, are valid for hooked-end fibres as well.

However, there is one additional deformation mechanism: plastic deformation of the fibre hooks. Fibre hooks provide mechanical interlock and their plastic deformation occurs in the first phases of the pullout process. This is also suitable with regard to the initial phases of tensile loading of fibre-concrete composites. During these phases, fibre concrete is reaching its tensile strength, which is one of its most important mechanical properties. In most cases, only the deformation of one fibre hook happens, usually at the side where the fibre has smaller embedded length with respect to the position of the crack.

The total pullout process of a hooked-end fibre consists of 5 phases (Fig. 2.21, second row, *phases a to e*). First, debonding along the interface takes place (*phase a to b*). After the fibre has been fully debonded (*phase b*), bending of both curved parts of one of the fibre hooks begins (curvatures marked as *1* and *2*, *phase b to c*). The larger is the fibre diameter, the more energy has to be invested in this process, due to the increased bending stiffness of the fibre. Also other factors, such as the hook dimensions, the interface properties and the shear strength, have an important influence on the energy needed to deform the hook [Van Gysel, 2000].

As fibre pullout continues, the pullout load reaches its maximum value (Fig. 2.22.a), both curvatures *1* and *2* are deformed, which causes a decrease of the pullout force (*phase c to d*). The ex-curvature *1* slips already through the straight part of the channel, while the ex-curvature *2* has to be bent another time in the opposite direction, at the place where the curvature *1* previously used to be. This results in a slight increase of the pullout force (Fig. 2.22 a), and this corresponds to *phase d*. Finally, after the ex-curvature *2* has also been straightened, the fibre continues to slip through the channel (*phase e*).
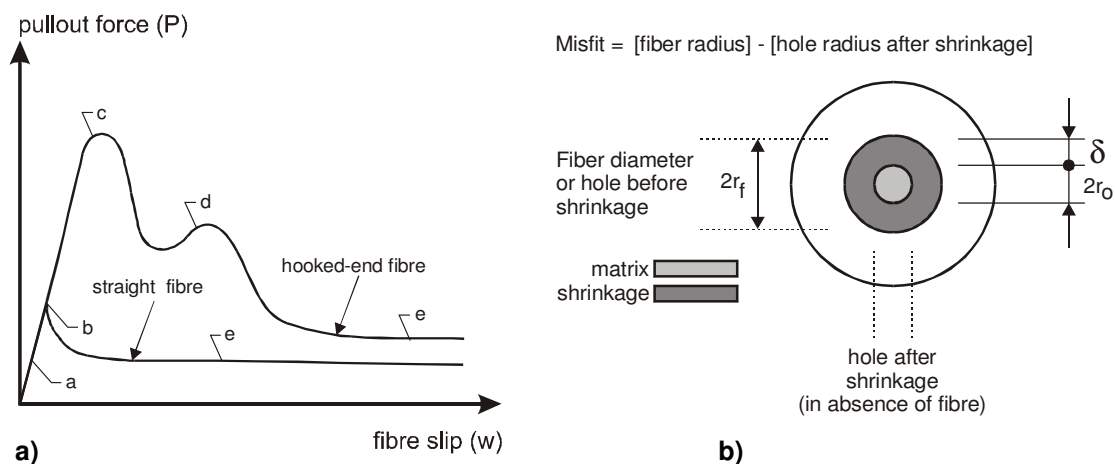
Fig. 2.22: a) Typical pullout response (relation fibre slip - pullout force) for straight and hooked-end steel fibres, with debonding and pullout phases (a to e) corresponding to Fig. 2.21; b) Fibre-matrix misfit, i.e. the pressure of concrete matrix on a fibre due to shrinkage, after [Pinchin & Tabor, 1978].

The rest of the pullout process (*phase e*, Fig. 2.21, second row) is similar to the frictional pullout of straight fibres (*phase e*, Fig. 2.21, first row), with one important difference: the fibre hook (i.e. the curvatures 1 and 2), is usually not completely straightened. This generates an additional effect on the pullout resistance by increasing the frictional stresses, as shown in Fig. 2.22.a [Van Gysel, 2000].

Fig. 2.21 and 2.22.a, make clear that hooked-end fibres possess a much higher tensile capacity than straight fibres. As it will be shown later, the mechanical interlock provided by

fibre hooks has a significant importance, not only for the tensile capacity of a single fibre, but also for the total tensile capacity of the fibre-concrete composite.

2.9.2 Factors which affect the pullout behaviour of steel fibres

The pullout behaviour of a single steel fibre depends on the following factors:

1. Fibre shape i.e. fibre geometry (straight, hooked-end, wave-shaped, twisted, with indented surface, etc.):

Due to the plastic deformation of fibre hooks as anchoring mechanisms, a considerably higher maximum pullout force may develop in hooked-end steel fibres (4 to 6 times higher), than in straight steel fibres, if all other influencing factors are the same, according to [Naaman et al., 1991a] and [Van Gysel, 2000].

Wave-shaped fibres have usually more curved parts than hooked-end fibres, so that somewhat more energy is needed to deform them, in comparison with hooked-end fibres, if all other properties are the same ([Chanvillard, 1993] and [Groth, 2000]).

Twisted fibres with triangular cross-section [Naaman, 1999], possess improved interfacial bond and significantly improved ductility during pullout, compared to the classical straight smooth steel fibres with a circular cross-section. The full deformation of these fibres implies the untwisting, which improves the ductility during pullout. After the maximum value of the pullout force has been reached, the force remains almost constant up to very large fibre slips.

Fibres with indented surface [Groth, 2000] show a higher pullout resistance than smooth fibres. It should be noted that the combination of indents on the fibre surface and hooked-ends is possible as well, which results in very large values of the maximum pullout force.

2. The material out which the fibre is made (medium- or high-strength steel, different synthetic materials, glass, etc); The fibre material is of great importance, especially for steel fibres with hooked ends. The utilization level of fibres made of high-strength steel (tensile strength f_y = 2200-2600 MPa) in [Van Gysel, 2000], resulted in 50-100 % higher maximum pullout forces, than it was obtained for the fibres made of medium-strength steel (f_y = 1200 MPa).

3. Fibre diameter; In general, the larger is the diameter, the higher are the tensile stresses that can be developed in a fibre, if the material is the same and all other properties constant [Groth, 2000], [Van Gysel, 2000]. The fibre diameter determines not only the fibre tensile capacity, but has also a very important influence on the bending stiffness of fibre hooks, i.e. on the energy required for their plastic deformation.

4. Fibre embedded length; For the same fibre geometry, a larger fibre embedded length results in a larger surface area of the fibre in contact with the cement matrix. Therefore, a

somewhat higher maximum pullout force and the total pullout capacity of a fibre can be expected. However, while this holds mostly true for straight steel fibres [Li & Stang, 1997], it is usually not the case for hooked-end steel fibres. It even may happen, that for the same type of hooked-end fibres, a higher pullout force for shorter embedded length is obtained [Van Gysel, 2000]. It seems that the plastic deformation of the fibre hook is the most dominant fracture mechanism for hooked-end fibres, so that the fibre embedded length is not of a great importance any longer.

5. The inclination angle of the fibre with respect to the direction of the main tensile stresses; In fibre concrete, the fibres can almost never be aligned in the same direction. This is a logical consequence of the discontinuous nature of the fibres and of the current production process of fibre concrete. Basically, inclined fibres have to be partly bent at the end of the fibre channel at the crack face. Therefore, further to the frictional pullout resistance, also the additional bending resistance of the fibres is present. This generally increases the total frictional resistance during fibre pullout. The bending resistance depends on the angle of inclination of the fibre, type of fibre and also on the composition of the surrounding concrete.
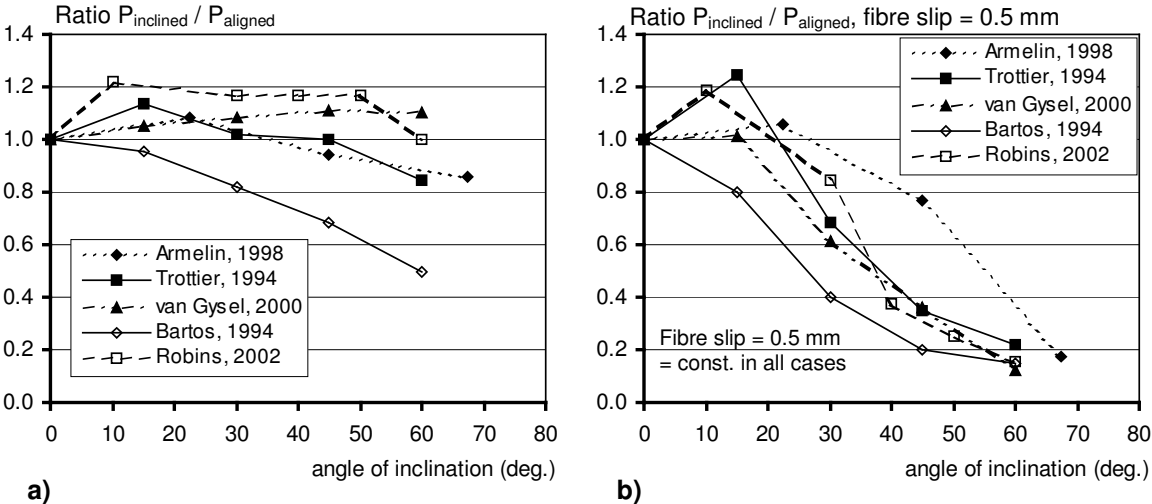
Fig. 2.23:   a) Relations between the angle of fibre inclination and the normalized maximum registered pullout force in hooked-end inclined steel fibres, for fibre slips at which this maximum force was achieved;   b) Relations between the angle of fibre inclination and the normalized pullout force in inclined fibres, at a chosen constant fibre slip (i.e. at an approximate crack width) of w = 0.5 mm

 Fig. 2.23.a represents different relations between the angle of fibre inclination and the normalized values of the maximum achieved "inclined" pullout force ($P_{inclined}$) in hooked-end steel fibres, for angles of inclination ranging from 0° to 67.5°. The values of the forces are given relatively to the pullout force at the angle of fibre inclination = 0° ($P_{aligned}$). In most cases somewhat higher forces are necessary to pull the inclined fibres out, with a maximum

for an angle of about 15º. Even at very large inclination angle of 60º, no significant differences comparing to the aligned fibre could be found, except in case of [Bartos et al., 1994]. However, the values of the fibre slips for which the maximum pullout force was reached, were always a number of couple of times larger for inclined fibres than for aligned fibres.

Such observations do not say much about the performance of fibres in real structures. Instead of observing only the maximum pullout force, one should rather observe the values of the fibre pullout force for an appropriate constant fibre slip. Translated to a structural scale, this would be at an appropriate crack width. This chosen normative crack width (fibre slip) has to be small enough, regarding either the durability or the ultimate load-bearing capacity, which means that the chosen value should for instance lay between 0.1 mm - 1.0 mm.

Fig. 2.23.b represents the relations between the angle of fibre inclination and the pullout force, registered at a fibre slip (i.e. at crack width) of 0.5 mm. Obviously, the maximum values of the pullout forces (about 20% higher compared to aligned fibres), are achieved at inclination angles of about 10º - 15º. In most cases, the fibres with inclination angles larger than 20º, show drastically lower pullout forces than aligned fibres. For example, the force in a fibre inclined at 45º, is only about 30% of the force, which is present in the aligned fibre, for the same fibre slip, i.e. crack opening.

Another phenomenon that may occur during the pullout of inclined steel fibres, is the rupture of the fibres, due to stress concentrations. In e.g. [Van Gysel, 2000], all hooked-end steel fibres under inclination angles of 45º and 60º, ruptured in the first phase of their pullout. This is a consequence of the relatively high stress concentrations in the fibre at the bending point (i.e. near the crack surface). In some of these cases, rupture of the matrix around the fibre bending point, in the form of a splitting fracture, could be observed as well.

Therefore, as a conclusion, the optimum angles of fibre inclination lay between 0º and 20º. Higher angles lead to a lower tensile capacity in the first phases of tensile loading, which is also the most important one, taking into account the role of fibres and their performance in the structure. In some cases, rupture of fibres at high inclination angles is possible as well, due to high stress concentrations.

6. The quality of the concrete matrix, which includes factors such as:
- **water/cement-ratio or water/binder-ratio** (i.e. indirectly the compressive strength of the applied concrete matrix); As given in Fig. 2.20.b, lower values of the w/b-ratio result in a higher density and a higher microhardness of the fibre-concrete interfacial zone (Wei et al., 1986]. Therefore, a better pullout behaviour of fibres can be expected, keeping all other properties constant. The observed improvement of the maximum pullout force was about 30 - 40 % in [Van Gysel, 2000], for a decrease of the *w/b*-ratio from 0.45 to 0.29;
- **the type and the quality of the cement;** the type of cement (in terms of its compressive strength) as well as its grading and fineness, its specific area and chemical composition (e.g. the amount of clinker and/or slag), may have a rather large influence on the properties of

the interfacial zone. However, no thorough investigation of the effect of different cement types on the fibre pullout capacity has been carried out up to now.

      - the presence of fine filler materials (silica fume, fly ash, metakaolin, latex etc.); the size of the particles of these materials is about one order of magnitude lower than the size of cement particles (e.g., for silica fume, the average grain size is about 0.1 μm). Therefore, they can efficiently fill the empty spaces between cement particles and fibres in the interface zone, which increases both the packing density of the interface. Moreover, silica fume exhibits a so-called pozzolanic reaction. During this reaction, the conventional calcium-hydroxide crystals are partly replaced by much stronger calcium silicate crystals. This improves the overall strength and the quality of the interfacial zone [Bentur, Mindess, 1991]. Also, the shrinkage of a concrete with silica fume may be 2 - 3 times higher compared to a concrete without it. This means that the clamping pressure to the fibre due to the matrix shrinkage will also be higher if silica fume is present in the concrete matrix [Li & Stang, 1997]. This may also additionally improve the debonding and frictional resistance during fibre pullout. In [Guerrero et al., 2000], the addition of fly ash (20 vol.-%) improved the maximum pullout force of hooked-end steel fibres for about 20%, while the addition of metakaolin (10 vol.-%) led to the full utilization of the fibre tensile capacity (i.e. to fibre rupture).

     - **aggregate grading and maximum grain size (D_{max});** due to the utilization of mortar which contained only very fine sand with D_{max} = 14 μm [Guerrero et al., 2000], the maximum pullout force of hooked-end steel fibres increased with 10 - 20 %, and also the frictional stresses were somewhat higher, compared to the mortar with the ASTM grading 50/70, with D_{max} = 7.0 mm. The debonding process is localized in a very narrow zone around the fibre. Therefore, the aggregate composition can also have an indirect influence on the fibre pullout capacity, through the overall workability of the concrete and the entrapped air.

     - **the presence of fibres in the pullout medium**, in the form of secondary fibre reinforcement; for example, a single steel fibre can be pulled out from the concrete matrix, which already contains other steel or polypropylene fibres. These fibres increase the (splitting) tensile strength of the pullout medium, providing in such a way a confinement to the pulled-out fibre. This may additionally improve its pullout capacity. Especially the frictional resistance during fibre pullout can be improved, even up to 200% [Naaman et al., 1991a and c], with utilization of SIFCON with about 11.0 vol.-% of steel fibres, as a pullout medium.

7. Pullout rate; for hooked-end steel fibres, a higher pullout rate (2.12 mm/sec) resulted in an increase of the maximum pullout force with about 10 - 40 %, compared with a much lower pullout rate of about 8.5 μm/sec [Banthia et al., 1991]. A high pullout rate changed in some cases the failure mode as well: instead of fibre pullout, the rupture of the fibre occurs. High pullout rates of fibres can appear in structures subjected to impact loading.

2.9.3 Pullout tests on single fibres: test set-up and parameters

The main goal of the pullout tests conducted within the scope of this research project, is the optimisation of the mixture compositions of concrete, so that different types of steel fibres,

which are pulled out of them, give an optimum pullout response. A pullout response of a fibre is optimal, if its tensile capacity is utilised up to about 80 - 90 %. The knowledge obtained in this way may further be used for:

− further adjustment of appropriate mixture compositions of concretes, in order to improve and optimise the efficiency of fibres during pullout (i.e. during bridging of a crack);

− modelling the uniaxial tensile response of different types of hybrid-fibre concrete, which will be presented in detail in Chapter 4.

Test set-up and testing procedure

The pullout tests on single steel fibres were performed using cylindrical concrete specimens, glued to a thick round plate made of steel (Fig. 2.24.a). This plate was fixed to the platform of the frame of the "Instron" testing machine.

In order to produce the specimens, a special mould was designed, able to accommodate 8 fibres fixed at its bottom [Markovic et al., 2002 b]. After casting, the concrete was cured at a temperature of 20ºC and a relative humidity of about 95 %. After 3 weeks, the concrete was demoulded, and the cylindrical specimens containing each one single fibre were drilled out. They were cured for another 4 weeks under the same conditions as from the beginning, after which the fibre pullout tests were performed. The diameter of each specimen was 65 mm, and its height 50 mm. The standard "Instron" tensile grip could successfully be applied for the fibres, even though the applied fibres were made of very high-strength steel, with a relatively high hardness. For the measurement of the slip of the fibre from the grip, one LVDT (Solarton A6G, linear stroke +/- 1mm) was used. A light aluminium plate, which was fixed to the fibre with two fine screws, was used as a support for this LVDT (detail in Fig. 2.24.a). In all pullout tests, the same displacement rate of 5 μm/sec was used.
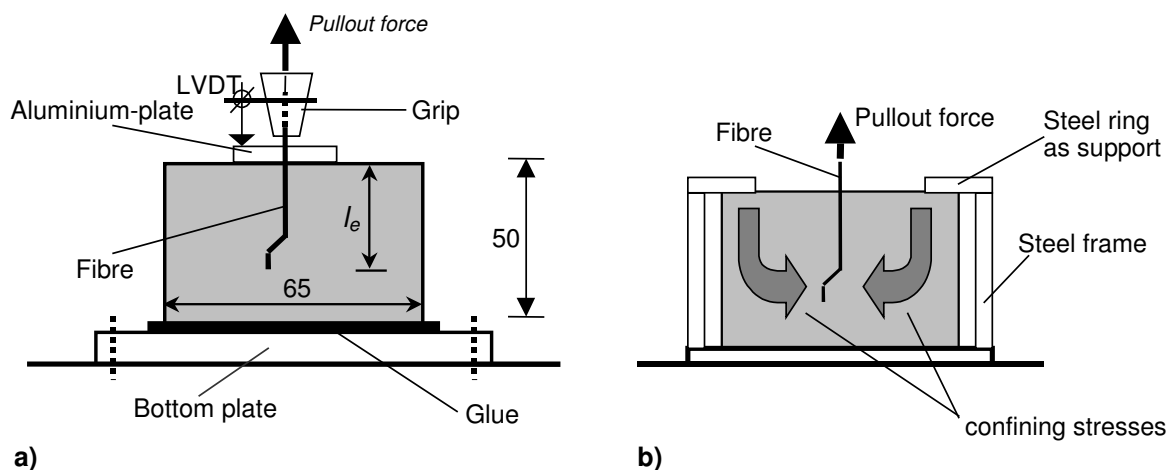
Fig. 2.24:   a) Scheme of the test set-up for the pullout tests on single short and long steel fibres;   b) Scheme of the distribution of confining compressive stresses in the pullout specimens, depending on the boundary conditions

When designing a test-set-up for fibre pullout tests, special attention should be paid to the state of stresses around fibre. It is very important to simulate a realistic situation, reflecting the conditions in fibre concrete loaded in tension. This means that no lateral confinement of any part of the fibre by compressive stresses should exist. Such a confinement appears if a steel ring at the upper side of the specimen is used as a support, like in [Van Gysel, 2000]. For such a case, a linear-elastic finite element simulation (Fig. 2.24.b) showed the development of arch action by the compressive stresses. This can unrealistically improve the pullout behaviour of the fibre. The solution of gluing the specimen at its bottom is much more suitable and it was applied in this research project. With such a solution, no compressive stresses around the fibre develop; moreover, the handling of the specimens is much easier.

Experimental parameters

The fibre pullout tests, performed within the scope of this research project, may be divided into two main groups, according to the properties of the concrete matrices from which the fibres were pulled out:

− in the first group, rather innovative concretes were used (mostly very fine mortars, with low w/b-ratios and a high amount of cement).
− in the second group, concretes with standard mixture compositions were applied. An overview of the mixture compositions is given in the following sub-chapters.

The complete overview of all the fibres applied in the pullout tests, with reference to their type, geometry, embedded length, inclination angle and minimum tensile capacity, is given in Tab. 2.2. In all performed pullout tests, only the "Dramix" fibres, made of high-strength steel with increased content of carbon, were used [Bekaert BV, 2000]. The minimum guaranteed tensile strength of the basic steel wire from which the fibres were made, varies from about 2300 MPa for a diameter of 0.75 mm, to 2500 MPa for a diameter of 0.20 mm.

Tab. 2.2: Overview of applied fibre types, embedding lengths and inclination angles, with their mechanical properties

fibre type (l / d)	mixture no.	embedding length (mm)	inclination angle (º)	minimum tensile capacity	
				stress (MPa)	tens. force (N)
30 / 0.4	CC & SCC	10	0	2610	280
60 / 0.7	CC & SCC	10 and 30	0	2340	925
13 / 0.2	12 (Tab. 2.1)	7	0	2900	90
40 / 0.5	1 to 6 (Tab. 2.1)	20	0 and 15	2610	515
60 / 0.7	7, 8 and 9 (Tab. 2.1)	20	0, 15 and 30	2340	925
60 / 0.7	10 and 11 (Tab. 2.1)	30	0, 15 and 30	2340	925

For each applied mixture, the workability characterisation was performed first, as explained in sub-chapter 2.6.1. This was followed by the measurements of the compressive and the splitting tensile strengths after 28 days, on cubes with an edge length of 150 mm, according to the Dutch NEN-standards.

2.9.4 Results of the first group of fibre pullout tests: influence of mix design parameters and fibre characteristics on fibre pullout

Goals of pullout tests and experimental parameters

In this group of fibre pullout tests, the basic parameters are the mix composition of the concrete from which the fibres were pulled out, and the type, geometry and orientation of the fibres. The main goals of the first group of fibre pullout tests were:

−   the optimisation of the mixture compositions of the concretes from which the fibres are pulled out, so that these fibres give an optimum pullout response. The utilisation of the tensile capacity of the fibres at different values of the fibre slip (i.e. of crack width), was the most important criterion in the analysis of the results.

−   the determination of the influence of the fibre orientation on its pullout response

−   the determination of the influence of short steel fibres in the pullout medium, on the pullout behaviour of the long fibres

−   the application of the results of these tests for analytical modelling of the uniaxial tensile behaviour of different types of Hybrid-Fibre Concrete.

The main variables of the concrete mixtures used in the first group of the pullout tests were:

−   the water/binder ratio of the concrete mixtures (0.40, 0.30 and 0.20);

−   the content and the composition of the aggregate (from 30 to 50 vol.-% of concrete);

−   the amount and type of short fibres in the concrete matrix (secondary reinforcement), which varied from 0.0 up to 6.0 vol.-%

−   the maximum grain size (D_{max} = 1.0 mm or 4.0 mm)

The complete overview of the experimental parameters for the 12 concrete mixtures applied in this group of tests, together with the types of fibres which were pulled out, is given in Tab. 2.3. An extensive overview of all experimental parameters and all results of this group of tests, is also given in [Markovic et al., 2002 a] and in [Markovic et al., 2003 b].

Tab. 2.3: Second series of fibre pullout tests: composition of applied concrete mixtures and their basic properties (workability, compressive strength f_{cc} and splitting tens. strength f_{spl})

Mix. No.	w/b-ratio	cement type	aggregate (vol.-%)	D max (mm)	short fibres (vol.-%) 6/0.16	13/0.2	fibre type used in pullout tests	slump flow (cm)	f cc (MPa)	f spl (MPa)
1	0.40	PC 52.5	30	4	0	0	RC-80/40-BP	67.5	74.0	4.1
2	0.40	PC 52.5	26	4	4	0	RC-80/40-BP	59	77.3	8.3
3	0.40	PC 52.5	24	4	4	2	RC-80/40-BP	27	85.1	10.3
4	0.30	PC 52.5	30	4	0	0	RC-80/40-BP	81	102.0	7.8
5	0.30	PC 52.5	26	4	4	0	RC-80/40-BP	70	106.6	14.0
6	0.30	PC 52.5	24	4	4	2	RC-80/40-BP	28	118.4	17.3
7	0.30	PC 52.5	30	1	0	0	RC-80/60-BP	85	108.2	7.7
8	0.30	PC 52.5	28	1	2	0	RC-80/60-BP	81.5	105.8	12.1
9	0.30	PC 52.5	26	1	4	0	RC-80/60-BP	67	108.5	14.2
10	0.20	CEM III 52.5	50	1	0	0	RC-80/60-BP	114.5	95.1	9.6
11	0.20	CEM III 52.5	46	1	0	2	RC-80/60-BP	90.5	96.2	10.1
12	0.20	CEM III 52.5	46	1	0	0	OL 13/0.20	89.5	103.1	11.8

All values of the tensile stresses in fibres in the diagrams in Fig. 2.25 and Fig. 2.27, are given as a mean value of 2 or 3 test results.

Results: Fibres aligned with respect to tensile load (Fig. 2.25)

The smaller type of hooked-end fibres, with *l/d* = 40/0.5 (RC-80/40-BP), is pulled out from the concretes No. 1 to No. 6 (Tab. 2.3), with *w/b* = 0.4 and *w/b* = 0.3 and with a maximum grain size of D_{max} = 4 mm. The volume content of short steel fibres in the concrete was varied from 0.0 to 6.0 vol.-%.

The level of the tensile stress in the fibres 40/0.5 during their pullout, and the comparison with the minimum guaranteed tensile capacity of this fibre type, are shown in Fig. 2.25. Decreasing the w/b-ratio causes an increase of the tensile stress in fibre, especially when plain concrete is used as a pullout medium. So, the difference in the tensile stress in fibre is about 20%, when mixture No. 4 (*w/b* = 0.3) was used as a pullout medium instead of mixture No. 1 (*w/b* = 0.4),. The presence of 4.0 vol.-% of short "secondary" fibres (type OL, *l/d* = 6/0.16) in the pullout medium, improved the stress in fibre further with about 25% (mixture No. 5) with respect to plain concrete matrix (mixture No. 4). In this situation, the tensile capacity of the fibres 40/0.5 was utilised for about 90-95 %. The further addition of short fibres (another 2 vol.-% of fibre type OL, *l/d* = 13/0.2), did surprisingly not resulted in a further improvement of the pullout capacity of the long fibres (both in mixtures No. 3 and No. 6). This is most probably due to bad workability of the concrete with this fibre content (Tab. 2.3), i.e. due to the higher content of entrapped air in the pullout medium.
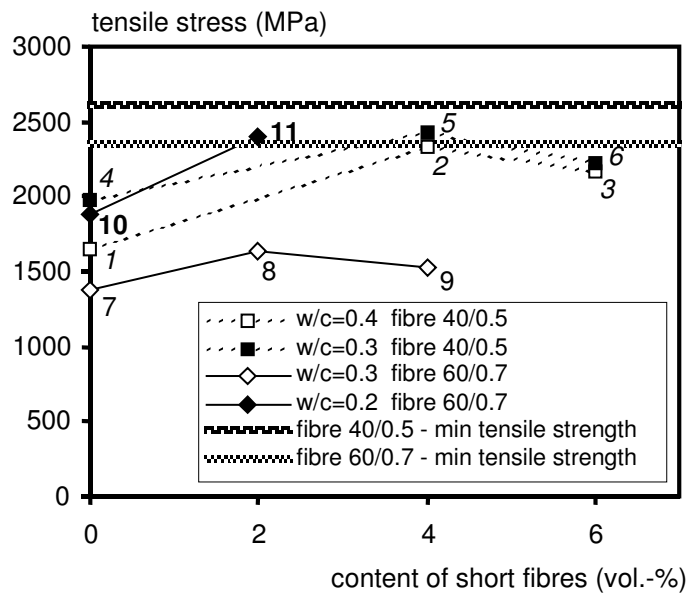
Fig. 2.25: Relations between the maximum tensile stress in the long hooked-end fibres (l/d = 40/0.5 and 60/0.7) aligned with respect to the pullout load, and the volume quantity of short fibres in the pullout medium (concrete mixtures No. 1 - 11 (Tab. 2.3)); the minimum guaranteed tensile strengths of both fibre types are presented with horizontal lines above

Taking into account that the tensile capacity of the fibres with $l/d = 40/0.5$ is almost fully utilised here, it would not be optimal to combine these fibres with lower w/b-ratios and with concretes with additional short fibres. It was therefore decided to use larger fibres (RC-80/60-BP, with $l/d = 60/0.7$) for the pullout tests from concretes with lower w/b-ratios, with and without short fibres. It is also obvious that the quantity of short straight fibres does not have to be that high. This is due to its negative influence on the workability and therefore on the pull-out resistance of long hooked-end fibres. The next set of mixtures (No. 7 to No. 12, Tab. 2.3), was composed considering these conclusions.

The larger type of hooked-end fibres, with $l/d = 60/0.7$ (RC-80/60-BP), was pulled out from the concretes No. 7 to No. 11 (Tab. 2.3), with $w/b = 0.3$ and $w/b = 0.2$, and with a maximum grain size of $D_{max} = 1$ mm. The volume quantity of the short steel fibres in the concrete was varied from 0.0 to 4.0 vol.-%.

The level of tensile stress during pullout in fibre 60/0.7, and its comparison with the minimum guaranteed tensile capacity of this fibre, is shown in Fig. 2.25. The pullout tests from the concrete with $w/b = 0.3$, showed that only about 65 % of the tensile capacity of these fibres was utilised (mixture No. 7). The presence of short straight fibres in the pullout medium (mixtures No. 8 and No. 9) increased the tensile stress in the fibre with 10 - 15 % compared to the plain matrix, which is also a lower increase than in the case of fibre type 40/0.5.

A further decrease of w/b-factor to $w/b = 0.2$, improved significantly the level of the tensile stress in the fibres. For the plain matrix as a pullout medium, this improvement was about 25 - 30 % (mixture No. 10). The presence of 2.0 vol.-% of short straight fibres (type OL, $l/d = 13/0.2$), further improved the tensile stress in the fibre for about 20 - 25 %.

The effect of the addition of short fibres may also be observed directly at the pullout curves, given in Fig. 2.26. The first part of the curves has a somewhat higher slope and a higher maximum pullout force for the pullout medium with the short fibres (mixture No. 11). After that, it runs almost parallel to the reference curve (mixture No. 10, i.e. the pullout medium without short fibres), with a slight difference in the frictional stresses. In this case (mixture No. 11), the minimum guaranteed tensile capacity of the fibres with $l/d = 60/0.7$ was exceeded, i.e. the utilisation of the minimum tensile capacity of the fibres was larger than 100 % (Fig. 2.25). In this figure, one can also recognise the specific phases of the fibre pullout process, which were already schematically given in Fig. 2.21 and 2.22.a.

Such an improved pullout behaviour of the hooked-end steel fibres, observed for the concretes which contain short steel fibres, is most probably a consequence of the improved (splitting) tensile properties of these concretes. As registered in the microscopy observation of epoxy-impregnated concrete in the vicinity of the (former) fibre hook after the pullout [Markovic et al., 2002 a], a number of microcracks in concrete around the fibre hook develop. Short fibres bridge those microcracks, and decrease their further opening and propagation. This increases the energy (i.e. the pullout force) needed to deform the curvatures of the hook, in the first phases of the fibre pullout process. The slope of the pullout curves and the maximum pullout

force, will therefore be higher if short fibres are used in the pullout medium in a suitable concrete mixture. Later, when the fibre is almost straightened and it slips through the matrix channel, no such a significant influence of the short fibres can exist any longer.
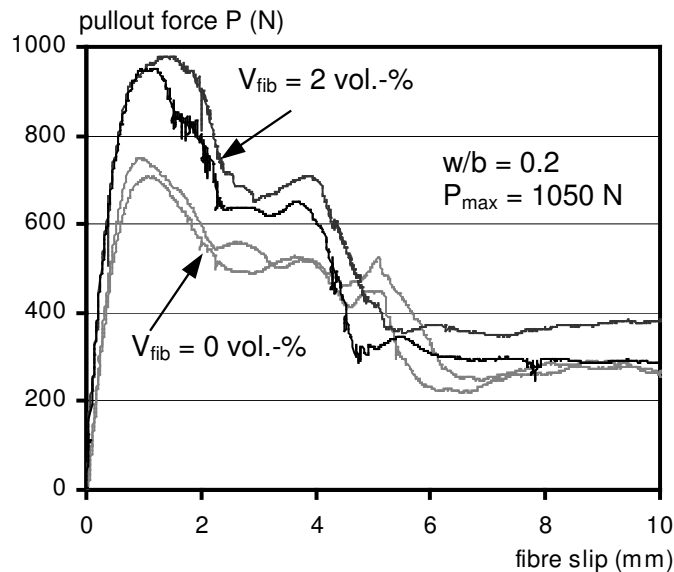
Fig. 2.26: Influence of volume quantity short fibres (V_{fib}) in the pullout medium on the pullout behaviour of the long fibres, for the same w/b-ratio: both fibres are parallel to the pullout force, where P_{max} is the minimum guaranteed tensile force in fibre

Results: Fibres inclined with respect to tensile load (Fig. 2.27)

The smaller type of hooked-end fibres, with l/d = 40/0.5 (RC-80/40-BP), was pulled out from the concretes No. 1 to No. 6 (Tab. 2.3) under an inclination angle of 15° only.

The level of the tensile stress in the inclined fibre 40/0.5 during its pullout, and its comparison with the minimum guaranteed tensile capacity of this fibre, are shown in Fig. 2.27. This inclination caused a similar level of improvement of the tensile stress in the fibres, for both pullout mediums (with w/b = 0.4 and w/b = 0.3). The improvement was substantially larger in the case of plain concrete as a pullout medium. For the concrete mixtures No. 1 and No. 4 as pullout mediums (Fig. 2.27), an increase of the fibre stress of about 15 % can be registered, with regard to the aligned fibres (Fig. 2.25, mixture No. 1 and No. 4).

Contrary to this, in the case of pullout mediums reinforced with short fibres, the fibre inclination caused an improvement of the fibre stress of only 5 % compared to the aligned fibres. This suggests that in the case of fibres 40/0.5, the addition of short fibres in the pullout medium, can improve the fibre pullout behaviour in a larger proportion than the inclination of the fibre. However, the minimum tensile capacity of this type of fibre was almost reached, when the pullout medium contained both 4 and 6 vol.-% of short straight fibres (mixtures No. 2, 3,

5 and 6). Fibre failure was registered in the case of mixture No. 5. Similarly to aligned fibres, the decrease of the *w/b*-ratio caused an increase in fibre stress. The application of too high fibre contents (6.0 vol.-%), caused bad workability of concrete, and therefore did not result in any improvement of the pullout behaviour of fibres from such a concrete.
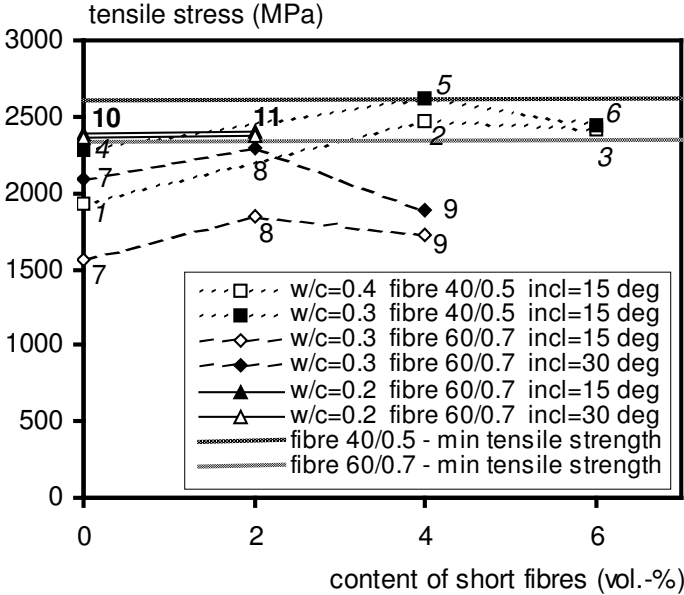
Fig. 2.27: Relations between the maximum tensile stress in the long hooked-end fibres inclined at 15° and 30° with respect to the tensile (pullout) load, and the volume quantity of short fibres in the pullout medium from 0 to 4 vol.-% (concrete mixtures 1 - 11 (Tab. 2.3)); the minimum guaranteed tensile strengths of both fibre types are given with horizontal lines

The larger type of hooked-end fibres, with l/d = 60/0.7 (RC-80/60-BP), was pulled out from the concretes No. 7 to No. 11 (Tab. 2.3), under the inclination angles of 15° and 30°.

The level of the tensile stress in inclined fibre 60/0.7 during pullout, and its comparison with the minimum guaranteed tensile capacity of this fibre, are shown in Fig. 2.27. For mixtures with w/b = 0.3 as a pullout medium (mixtures No. 7, 8 and 9), the stresses in the fibre improved with about 12 % by virtue of the inclination of 15°. The increase of inclination angle of fibres to 30°, caused a further increase of the tensile stress in the fibres. In comparison with the aligned fibres, a rather large increase of about 30 - 35 % was registered.

The improvement of the fibre pullout behaviour as a result of its inclination, can also be observed in Fig. 2.28.a, where the pullout curves of fibres inclined at 0° and 30°, for the same concrete mixture as a pullout medium, are given. The first part of all the curves is almost identical, after which the pullout force of the inclined fibre becomes higher, and remains almost parallel to the one of aligned fibre, with a rather high difference in frictional stresses of about 70-100 %. In the case of the inclined fibre, both the plastic deformation of the whole fibre hook, and the continuous plastic deformation at the fibre bending point, must occur. The

latter is even more pronounced when short fibres are present in the concrete. Similarly to all previous cases, a too high volume content of short fibres in the pullout medium did not improve the pullout behaviour of the long fibres.
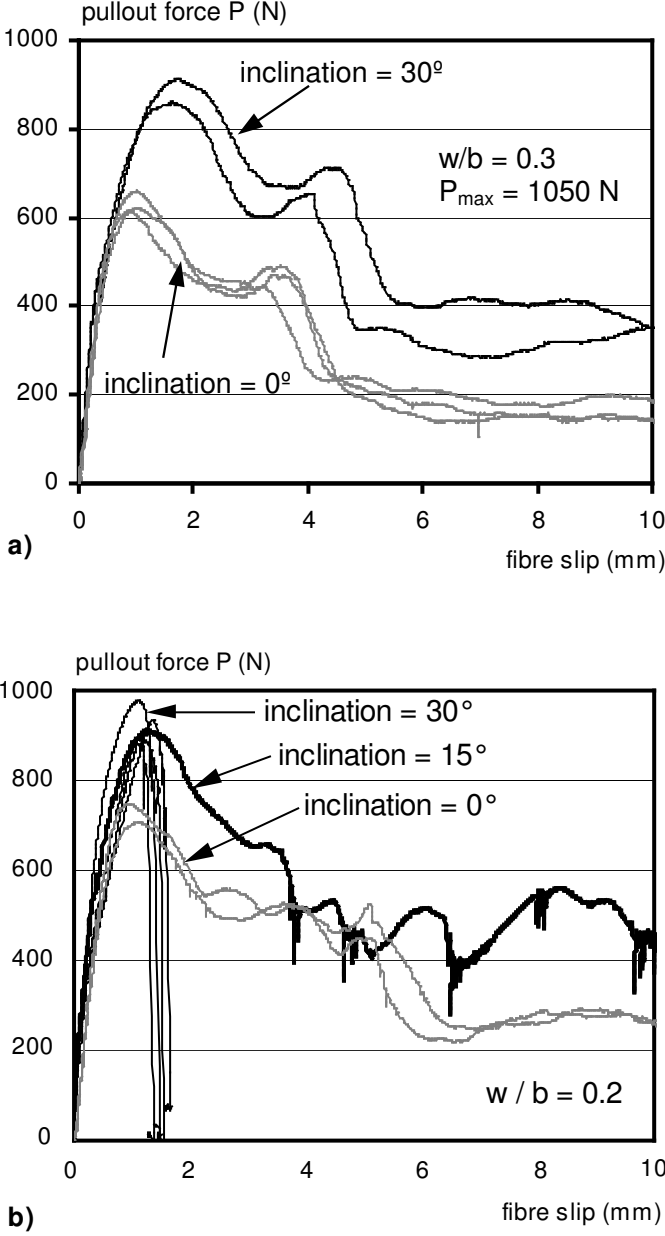
Fig. 2.28.:   Influence of the angle of fibre inclination on the fibre pullout behaviour, for pull-out from the same type of concrete, where P_{max} is the minimum guaranteed tensile force in the fibre: a) concrete matrix: w/b = 0.3;   fibre inclination angles 0° and 30°;   b) concrete matrix: w/b = 0.2;   fibre orientation angles 0°, 15° and 30°

The maximum content of short fibres was therefore decreased from 4.0 to 2.0 vol.-%, and this quantity was applied in the mixtures No. 10 and 11. The results of the pullout tests of fibres

inclined at 0°, 15° and 30° are given in Fig. 2.28.b. In case of fibre inclinations angles of 15° and 30°, the pullout stress exceeded the minimum guaranteed tensile strength of fibres. It was however possible to pullout the fibres inclined under 15°, whereas all fibres inclined under 30° fractured in the vicinity of the curved part at the exit from the pullout specimens, a couple of moments after reaching the maximum value of the pullout force (pullout behaviour given with thin black curves in Fig. 2.28.b). The fibre failure is a result of a strong concrete matrix and a good fibre anchoring in it, but partly probably a result of the stress concentrations and eigen stresses, which are present in the bent part of the fibre.

The normalised values of the tensile stress in the fibres, at fibre slips (i.e. at crack widths) of Δ = 0.1 mm, Δ = 0.25 mm, Δ = 0.5 mm and Δ = 1.0 mm, are given in Fig. 2.29.a. The corresponding tensile stress in the fibres, must also be determined at these "normative" values of the fibre slip, i.e. of the crack width, and not only at the maximum stage. In fact, the determined maximum tensile stresses, which develop in the fibres during the pullout, are normative only for the general observation of the efficiency of fibres in concrete. These values are reached mostly at fibre slips of 0.95-1.30 mm, depending on the applied type of fibre and its inclination angle, and they are anyhow given previously (Fig. 2.25 and 2.27).
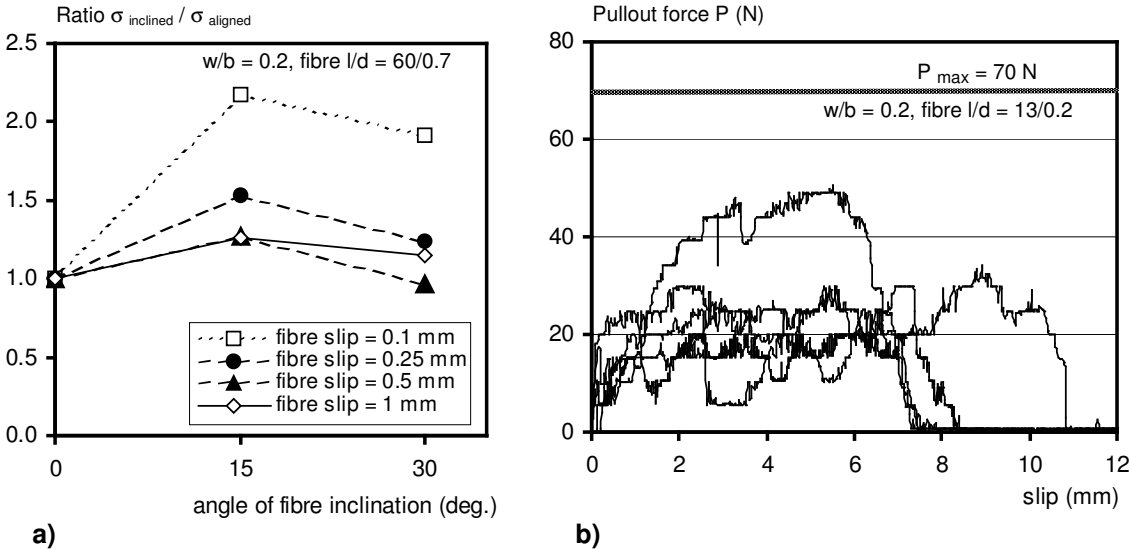
Fig. 2.29:   a) Normalised values of the tensile stresses in aligned and inclined fibres (0°, 15°, and 30°), at different fibre slips, related to tensile stress in aligned fibres;   b) Pullout curves for short straight fibres OL 13/0.2, with their minimum guaranteed tensile force given above

Fig. 2.29.a shows, that fibres inclined at 15° possess the largest efficiency at all fibre slips (i.e. at all crack widths). Especially in the beginning of tensile loading, for small fibre slips (i.e. crack widths) of Δ = 0.1 and 0.25 mm, fibres inclined at 15° are respectively 2.2 and 1.5 times more effective compared to fibres aligned to the tensile load. At higher fibre slips, somewhat lower differences occur.

- 56 -

An inclination of 30º has a positive effect only at very small fibre slips (Δ = 0.1 mm). Later, no large differences compared to aligned fibres, can be observed. A similar situation is given previously in Fig. 2.23.b, where a comparison of the results of different researchers, at different inclination angles is given. The highest efficiency could also there be observed at an angle of about 15º.

Results: Pullout behaviour of straight steel fibres

Due to the absence of the hook as an interlocking mechanism, straight steel fibres develop much lower values of the pullout forces than hooked-end steel fibres [van Gysel, 2000]. Within the scope of this research project, the pullout tests on fibre type OL 13/0.2 were performed, using only concrete mixture No. 12 as a pullout medium.

During these tests, the values of the fibre slip at debonding, the corresponding debonding force, and the value of the frictional stresses were observed. The pullout response of the short straight fibres 13/0.2 will later be used for analytical modelling of the tensile response of concretes, which contain this type of fibre.

The pullout response of the short straight fibres OL 13/0.2 is given in Fig. 2.29.b. It is characterised by rather low values of the pullout force, and by a low level of utilisation of the tensile capacity of the fibres (only about 15-30 %, except in one case). Therefore, also a steel wire with a somewhat lower tensile strength might be used for the production of these fibres.

No strong relation between fibre embedded length and maximum pullout force could be observed. The variations in the results were also larger, compared to all previously presented results on hooked-end fibres. This is rather normal phenomenon for low values of the pullout forces (i.e. of the load in general).

2.9.5 Second group of fibre pullout test: SCC versus non-SCC concrete matrix

Goals of pullout tests and experimental parameters

In the flexural tests on small beams performed by [Grünewald, 2002b], it became clear that the self-compacting fibre concrete (SCC) had somewhat higher flexural strength and lower scatter in the results, compared to conventional fibre concrete (CC), for the same compressive strength of the concrete, and for equal fibre volume contents.

Both flexural and tensile responses of any type of fibre concrete, depend basically on 2 factors:
− pullout response of each single fibre which bridges a crack(s) during tensile loading
− number and orientation of fibres across the crack(s).

Single-fibre pullout tests were performed in order to determine the influence of the first factor (fibre pullout) on the flexural response of both SCC and CC, i.e. in order to establish why rather large differences in flexural responses of these two types of fibre concrete exists.

The goals of this group of tests are:
- determination of the influence of the workability, compressive strength and fibre embedded length on the pullout response of the fibres
- comparison with the pullout response of the same fibres from the optimised concrete mixtures, performed previously in the first group of the pullout tests
- utilisation of the results of the pullout tests for the analytical modelling of the flexural response of self-compacting fibre concrete, performed in [Grünewald, 2004].

In the second group of fibre pullout tests, the experimental parameters were:
- the compressive strength of concrete matrix (B45, B65 and B105, i.e. C35/45, C53/65 and C90/105 according to EN 206-1),
- the workability of the concrete (self-compacting vs. non-self-compacting for each strength class).

An extensive overview of all the experimental parameters and all results of this group of tests, is given in [Markovic et al., 2002 b]. All types of mixtures were already developed and used in three-point bending tests in [Kooiman, 2000] and [Grünewald, 2004].

Test results

The utilisation of the tensile capacity for both types of fibres, when three different types of self-compacting concrete were used as a pullout medium, is given in Fig. 2.30.a. All given values represent the average value of two or three test results. The utilisation level is given as a ratio of the maximum tensile stress registered in the fibre during its pullout (σ_{max}) and the tensile strength of the fibre steel (f_y), see Tab. 2.2.

The average utilisation levels are similar for both fibre types and range from about 60 % when B45 was used as a pullout medium, up to about 75 % when the fibres were pulled out from a concrete B105. The smaller fibres with $l/d = 30/0.4$ have a degree of utilisation which is about 10 - 15 % higher compared to the larger fibres with $l/d = 60/0.7$.

The fibre pullout curves follow the usual pattern for hooked-end fibres, explained in sub-chapter 2.9.1. About three times lower pullout forces were registered for the fibres 30/0.4, compared to larger fibre type 60/0.7, due to their smaller diameter and smaller hook. This does not mean that the concrete with smaller fibres has worse tensile properties. On the contrary, the number of smaller fibres in the concrete is about 3 times higher for the same fibre volume content, compared to the number of larger fibres. This means that no weaker tensile response should be expected, if shorter fibres would be applied.

The comparison of the utilisation levels of the long fibres 60/0.7, when different types of conventional (CC) and self-compacting (SCC) concrete were applied as pullout media, is given in Fig. 2.30.b. For both B45 and B105, almost the same stresses in fibres were achieved, no matter if conventional or self-compacting concretes were utilised as pullout media. The tensile stress in the fibres was higher only in the case of SCC B65, for about 10 %, compared to CC B65. On the basis of this, it can be concluded that in the case of a single fibre, the differences in the quality of the concrete around it, are not very high. Such a phenomenon appears most probably because in single-fibre pullout tests, the fibre is isolated from the other fibres, making the compaction process of conventional concrete very efficient.

A rather different situation may be expected in real fibre concrete, where each fibre is surrounded by many other fibres. During the compaction of conventional fibre concrete, the bubbles of entrapped air are obstructed in their movement upwards to the surface of the concrete, because fibres act as obstacles. During this process, many air bubbles concentrate under and around the fibres, so that the overall density and strength of the fibre-concrete interfaces are undoubtedly lower, compared to those in single fibre pullout tests.
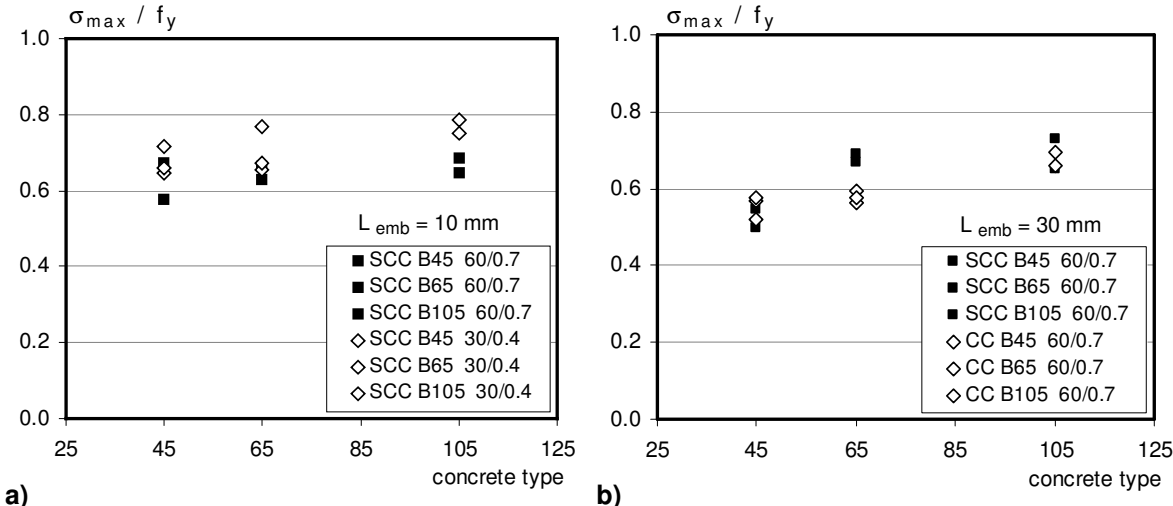
Fig. 2.30:   a) Comparison between the maximum achieved tensile stress in the fibres (σ_{max}) and fibre tensile strength (f_y), for pullout of two fibre types (l/d = 60/0.7 and 30/0.4), with the same embedded length (L_{emb} = 10 mm), from different types of self-compacting concrete (B45, B65 and B105);   b) Same comparison in pullout response of fibres with l/d = 60/0.7, with an embedded length of L_{emb} = 30 mm, from 3 different types of self-compacting (SCC) and conventional concrete (CC)

With self-compacting fibre concrete, the concentration of entrapped air is lower, compared to conventional fibre concrete. In SCC with fibres, there is also a natural movement of the bubbles of entrapped air upwards. Fibres may also here act as obstacles, but the concentration of air around them will for sure be lower, compared to that in conventional fibre concrete. There-

fore, a higher fibre efficiency during pullout and crack bridging may be expected if the fibres are applied in self-compacting concrete.

The quality of the concrete in terms of its compressive strength, surprisingly did not have a large influence on the maximum pullout force of the fibres, especially for the fibre embedded length of 10 mm (Fig. 2.30.a). For a fibre embedded length of 30 mm (Fig. 2.30.b), a difference of about 20 % could be observed between SCC B45 and SCC B105. Compared to the first group of tests (concretes No. 10 and 11), a somewhat lower utilisation level of the fibre tensile capacity, can be observed here (SCC B105), for a similar compressive strength of pullout medium.

The fibre embedded length does not play a significant role concerning the maximum tensile stress in the fibres neither. In the case of SCC B45 about 10% higher pullout forces could be achieved (Fig. 2.30.a), if the fibre had a shorter embedded length (L_{emb} = 10mm). Although many references point out that straight fibres with larger embedded lengths develop higher tensile stresses during pullout, it seems that in the case of hooked-end fibres, the plastic deformation of the fibre hook is the most dominant resistance mechanism, i.e. the fibre embedded length is more-or-less irrelevant.

2.9.6 Summary and concluding remarks on fibre pullout tests

Pullout tests on single steel fibres have been introduced here, as an efficient simulation of the bridging of the cracks by fibres, in a concrete element loaded in uniaxial tension. An overview of the factors which affect the pullout behaviour of steel fibres is given first. Subsequently, the results of the pullout tests on hooked-end and straight steel fibres, pulled out from different concrete matrices as pullout mediums, are presented.

The basic goal of the tests is to optimise in steps the mixture compositions of the concretes, from which the fibres are pulled out, so that the fibres give an optimum pullout response. The utilisation of the tensile capacity of the fibres at different values of the fibre slip (i.e. of crack width), was the most important criterion in the analysis of the results.

According to the mixture composition of the pullout medium, all performed fibre pullout tests are divided into 2 groups. In the first group, rather innovative concretes were used (mostly very fine mortars, with low w/b-ratios and high amount of cement). In the second group, concretes with standard mixture compositions were applied.

In the first group, some of the most important testing parameters were the w/b-ratio of the concrete, the presence of short fibres in the concrete (as a secondary reinforcement), and the inclination angles of the long fibres, which were pulled out. The results of these tests will be used later for the analytical modelling of the tensile behaviour of different types of Hybrid-Fibre Concrete. In the second group of tests, the most important experimental parameters were the concrete workability (conventional concrete versus SCC), its compressive strength and the embedded length of fibres.

From the performed fibre pullout tests, the following may be concluded:

1. In general, both the under-utilisation of the fibre tensile capacity and the rupture of fibres due to their over-utilisation, should be avoided.

2. The decrease of the w/b-ratio of concrete mixtures has a positive effect on the value of the tensile stress in fibres at pullout. Optimum combinations of the w/b-ratio of the concrete and the fibre type to be applied in it, were proposed on the basis of these tests. In general, the larger the fibre diameter and hooks are, the lower the w/b-ratio should be.

3. The utilisation of the tensile capacity of the long hooked-end fibres, was in average 20-30 % higher, if short steel fibres were used as "secondary" reinforcement in the pullout medium (concrete matrix). Short steel fibres increase the (splitting) tensile strength and the ductility of the concrete around the long fibres by creating a confinement around them. This improves their pullout behaviour. However, a too high volume content of short fibres may result in bad workability of the concrete, and therefore in a worse pullout response of the long fibres.

4. The optimum inclination angle of long fibres is about 15°, which was proven for different values of the fibre slip (i.e. of crack width). This is in accordance with the results of other researchers.

5. Straight steel fibres showed a much lower level of utilisation, compared to hooked-end fibres. Therefore, fibre hooks are a very efficient and important interlocking mechanism. Their plastic deformation occurs in the early beginning of the fibre pullout process, and this is very important for the tensile response of the fibre concrete as a whole.

6. In the standard concrete mixtures (second groups of fibre pullout tests), no large influence of any of the factors (workability, compressive strength and fibre embedded length), on the fibre pullout behaviour, could be observed. A higher utilisation of the tensile capacity of the fibres was observed in the first group of tests, for a similar compressive strength of the concrete.

Fibre pullout tests proved themselves to be an efficient tool in the optimisation of the mixture composition of the fibre concrete. However, up to a certain limit, they represent a rather idealised situation, because only the pullout behaviour of a single isolated fibre was observed. The situation could, however, be rather different in real fibre-concrete composites, where each fibre acts in a group, near many other fibres. Appropriate corrections of the fibre pullout response will then be necessary in such a case. This will be explained in Chapter 5.

CHAPTER 3:

TENSILE PROPERTIES

3.1 Introduction

In the previous chapter, the methodology for the designing of different mixtures of Hybrid-Fibre Concrete (HFC) was given. A number of the HFC-mixtures was developed on the basis of this methodology, and the workability was tested. Pullout tests of long hooked-end and short straight steel fibres were performed, as a simulation of the bridging mechanism of the cracks by fibres in structural elements made of fibre concrete. The main goal of these tests was to find the best combination of applied type of fibre and concrete matrix, based on the utilization of the fibre tensile capacity during the pullout.

The next step is the testing of the mechanical properties of different types of Hybrid-Fibre Concrete in bending and in uniaxial tension. A literature overview of the influence of steel fibres on the tensile and flexural behaviour of different types of fibre concrete, will be given first in this chapter. Subsequently, the results of three-point-bending tests on different Hybrid-Fibre Concretes, will be presented and analysed. After that, the concretes with the best flexural performance and a fibre quantity as low as possible will be selected, and tested in uniaxial tensile tests. The influence of short and long fibres on the tensile behaviour of hybrid-fibre concrete will be explained. For both flexural and tensile tests, the number and the orientation of the fibres in the testing specimens will be determined and related to flexural and tensile strength and ductility.

All this will form the basis for the analytical modelling of the tensile behaviour of different types of hybrid-fibre concrete, which will be presented in the next chapter.

3.2 Tensile properties of high-performance fibre concretes (HPFC) – a literature overview

3.2.1 Introduction: high-performance versus conventional fibre concrete

The firstly developed high-performance fibre concretes (HPFC) were SIFCON (Slurry Infiltrated Fibre Concrete) and Fibre Reinforced DSP Concrete (Concrete with Densified Small Particles), and they were followed by Reactive Powder Concrete (RPC) with short steel fibres. An exact overview on this topic is given in [Naaman & Reinhardt, 1995].

Although the mixture compositions of these concretes differ a lot, their uniaxial tensile response is rather similar. Fig. 3.1 represents the uniaxial tensile response of plain concrete,

conventional fibre concrete and high-performance fibre concrete (HPFC). Tensile loading of all these concretes is accompanied by cracking. Basically, two types of crack may be introduced [Van Mier, 1997], [Van Mier, 2004 a]:

1. <u>Microcracks:</u> they develop in the very early phases of tensile loading, mostly in the weak interface zones between fibres and aggregate; the lengths of these cracks are similar to the diameter of the aggregate grains, their width is a couple of microns (e.g. 1 - 5 μm);

2. <u>Macrocracks:</u> they develop as a result of connecting of microcracks, and represent larger discontinuities, spread across the surfaces (much) larger than the surface of an aggregate grain; the length of these cracks may be such, that they cover the whole cross-section of a specimen (the so-called "through-cracks"), or a part of it; the width may vary from couple of microns (e.g. 5 - 10 μm), up to very large values.
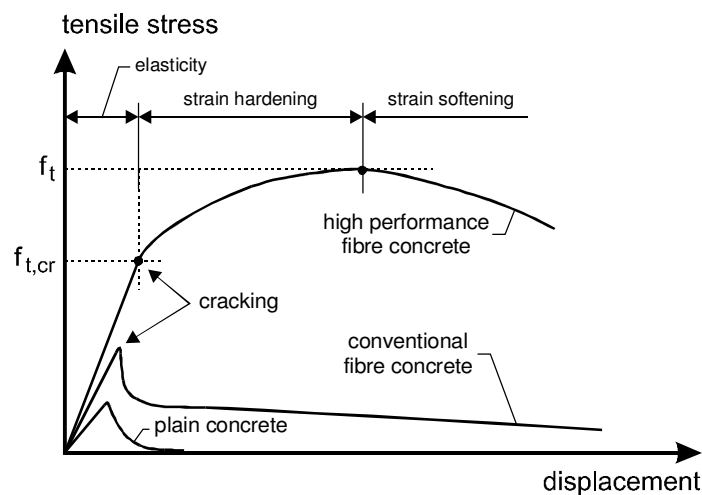
Fig. 3.1: Comparison of uniaxial tensile behaviour obtained in testing of plain concrete, conventional fibre concrete, and high-performance fibre concrete

From Fig. 3.1, the following may be concluded:
1. The microcracking is much more pronounced in HPFC, especially if it contains high quantities of short thin fibres. If these fibres are thin and act at small distances, they can very efficiently bridge microcracks. Therefore, the first larger cracks appear at much higher levels of tensile load in HPFC, than in conventional fibre concrete.
2. After the first large crack(s) (macrocrack(s)) have appeared, the tensile load still continues to increase. This is in complete contrast to any other conventional fibre concrete, where a significant drop of the tensile capacity appears after the first cracking. The increase of the tensile load after cracking is the so-called "strain hardening", or "plastic hardening" [Naaman & Reinhardt, 1995]. The "strain hardening" guarantees that a structural element made of HPFC will maintain its stability also after cracking. This is to a certain amount

similar to the tensile stiffening of classical structural reinforced concrete. The "strain hardening" creates therefore a necessary basis for the utilisation of HPFC in the engineering practice. This is a decisive difference between all conventional, and high-performance fibre concretes.

3. As a consequence of the strain hardening, the tensile strength of HPFC is much higher than that of conventional fibre concrete. After the tensile strength has been reached, the tensile load starts to decrease. The crack continues to open, and the fibres are being pulled out of the matrix, which still generates some resistance to crack opening. This is the so-called "tensile softening". When all fibres are completely pulled out, no resistance has left, i.e. the tensile stress is equal to zero.

All mentioned phases of tensile behaviour are applicable to Hybrid-Fibre Concrete as well. All of these phases will be analysed in detail in Chapter 4 of this PhD-thesis.

3.2.2 Reactive Powder Concretes with fibres (RPC)

In the previous Chapter 2, a detailed overview of the principles of mixture design of RPC is given. Although in this case the initial role of the steel fibres was the improvement of ductility under compressive loading, a significant improvement of the tensile response, compared to all previously known conventional concretes, was achieved [Richard et al., 1996]. Tensile strengths of about 14 MPa could be reached, with utilisation of 4 vol.-% of short steel fibres [Behloul, 1996].
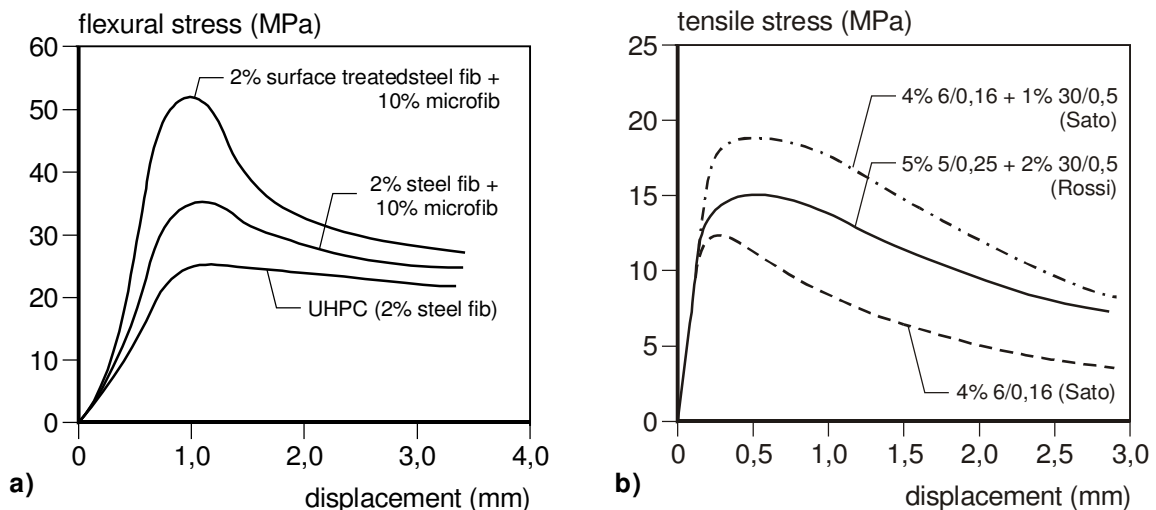
Fig. 3.2: a) Flexural behaviour of different Ductal®-concretes (after [Orange et al., 2000]); b) Comparison in uniaxial tensile behaviour of different types of multi-modal fibre reinforced concrete (MMFRC) (after [Rossi et al., 1996] and [Sato et al., 1999, 2000]).

The original mixture composition of RPC with fibres, was further modified and presented in [Orange et al., 2000] as the concrete type Ductal®. The flexural behaviour of different types of

this concrete, with the optimisation steps and the effects of the application of fibres, is given in Fig. 3.2.a. The initial concrete contained 2.0 vol.-% of short straight steel fibres.

The first optimisation step consisted of the improvement of the ductility of the concrete matrix itself, by the addition of 10 vol.-% of inorganic micro-fibres, which increased the flexural strength with about 40 %, from 25 MPa to 35 MPa. The next optimisation step was the chemical treatment of the short steel fibres, so that their surface becomes rough. This contributed to further increase of the flexural strength from 35 MPa to 52 MPa, which is about twice as high, as the initial flexural strength of 25 MPa.

One of the first developments of Ultra High Performance Fibre Concrete (UHPC) in Germany was reported in [Schmidt et al., 2001] and [Borneman et al., 2002]. Those concrete mixtures contained 1.5 to 2.5 vol.-% of short straight steel fibres, which resulted in tensile strengths up to 12.0 MPa, with strain hardening. On the contrary to the RPC where the mixture optimisation was directed to the applied amount and type of fibres, the optimisation of the granular skeleton and of the powder materials was applied for German UHPC. This resulted in improved compressive strength and decreased amount of cement, as well as in somewhat improved tensile behaviour.

3.2.3 Multi-modal fibre reinforced concretes (MMFRC)

The idea of using different types of steel fibres, in combination in the same concrete mixture, was for the first time postulated in [Rossi et al., 1987], and in [Rossi et al., 1996], as multi-modal fibre reinforced concrete (MMFRC). According to this concept, the fibres should namely be active at two levels: at material level and at structural level. A higher percentage of short fibres can improve the tensile strength and the ductility at the material level, when smaller cracks are present. The transition from the material to the structural level, is marked by the coalescence of the smaller into the larger cracks. At a structural level, longer fibres should be used for bridging of the large cracks, in order to improve the load bearing capacity and the ductility of the structures.

A comparison of different types of MMFRC is given in Fig. 3.2.b. The mixture composition of MMFRC was partly based on the composition of ultra-high performance concrete, by [De Larrard et al., 1994], where the concept of maximum packing density was used for aggregate grading, with a maximum grain size of 0.6 mm. The water/binder-ratio was equal to 0.155. Two types of steel fibres were used: 5.0 vol.-% of short straight fibres (l/d = 5/0.25 mm/mm), and 2.0 vol.-% of long hooked-end fibres (l/d = 25/0.3 mm/mm). The tensile strength ranged from 12 to 16 MPa, and strain hardening was present as well (Fig. 3.2.b).

MMFRC was developed in the Netherlands as well, using locally available Dutch materials [Sato et al., 1999], [Sato et al., 2000], with a maximum grain size of 0.5 mm, and with a w/b-ratio of 0.25. Three types of short straight fibres were used (with l/d = 6/0.16; 13/0.20; 20/0.25 mm/mm), together with one type of long hooked-end fibres (l/d = 30/0.5 mm/mm). The tensile strength of these fibres was about 1.5 to 2 times higher than those used in [Rossi et al., 1996], which also may produce a better tensile response of concrete with a lower applied quantity of fibres [Van Gysel, 2000].

The achieved tensile strength of these concretes varied from 11 MPa for 4.0 vol.-% of short fibres (*l/d* = 6/0.16 mm/mm) to 25 MPa, for a combination of 4.0 vol.-% of fibres with *l/d* = 6/0.16 mm/mm and 1.5 vol.-% of fibres with *l/d* = 30/0.5 mm/mm (Fig.3.2.b). This is one of the highest achieved tensile strengths of steel fibre concrete ever. Also, the strain hardening was much more pronounced in the case of concrete with both short and long fibres, than in the case of concrete with short fibres only.

3.3 Production of specimens and testing methods

3.3.1 Relation between casting process and tensile behaviour of fibre concrete

The casting process and the flowability of fibre concrete has a decisive influence on the orientation of the fibres in the testing specimens, and therefore also on the tensile and flexural behaviour of fibre concrete, as well as on the scatter in it. A comparison of the flexural behaviour of conventional fibre concrete and self-compacting fibre concrete, for the same casting process, is given in Fig. 3.3.
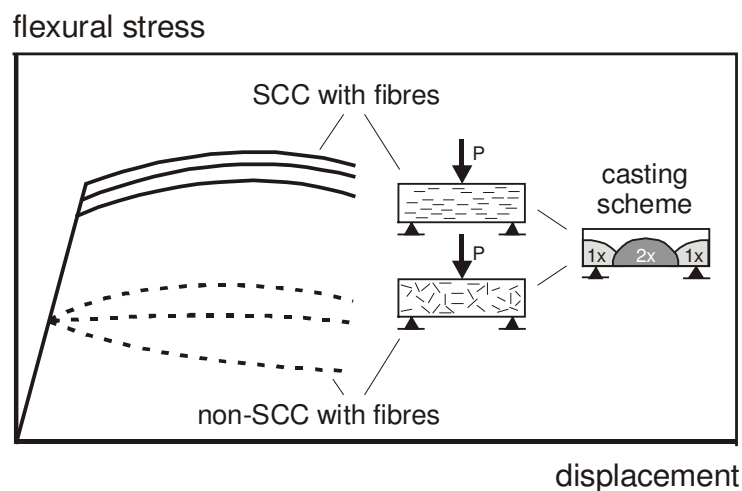
Fig. 3.3: Comparison of flexural behaviour of conventional FRC and self-compacting FRC, with the same fibre quantity and same compressive strength, after [Kooiman, 2000], and [Grünewald, 2004]

The flexural behaviour of conventional (non-SCC) fibre concrete is usually characterized by a rather large scatter of the results, which decreases significantly the characteristic values of the strength, needed for structural design [Kooiman, 2000]. Taking into account the rather bad workability of such concretes, the fibres possess always a different orientation, even if one does his best to apply an uniform casting process.

On the other hand, the same uniform casting process of self-compacting fibre concrete, results in a better and more uniform fibre orientation, by virtue of the good flowablity of such a concrete (Fig. 3.3). Therefore, better flexural behaviour could be observed, with a much lower scatter of the results, in [Grünewald, 2002]. This is in concordance with some findings, that fibres tend to orient in the direction of flow of concrete [Behloul, 1996]. This suggests that by means of the concrete flowability, one could possibly control the tensile properties of fibre concrete, which would open a whole new perspective for the utilization of fibre concrete in the engineering practice.
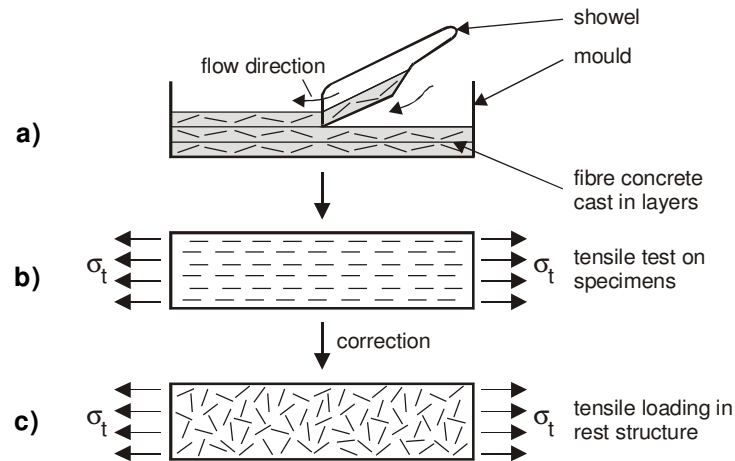
Fig. 3.4:   *a) The scheme of applied casting process of HFC;   b) The fibre orientation in specimens for tensile and flexural tests, as a circumstance of such a casting process;   c) Possible fibre orientation in a real structure, for which calculation a correction of the fibre orientation values can be made (explained in Chapter 5)*

In this research project, the casting of all Hybrid-Fibre Concretes was performed in layers (Fig. 3.4.a), so that the fibres could be oriented as much as possible in the direction of the main tensile stress (Fig. 3.4.b). This casting procedure will be applied in preparation of both the flexural and the tensile specimens. This also makes an exact comparison of the results of both types of tests possible.

Such an "optimum" fibre orientation will result in probably the highest obtainable tensile and flexural strength and ductility. In real structures in practice (Fig. 3.4.c), the casting can never be performed like in these tests. This suggests that the orientation of fibres, and therefore the whole tensile and flexural behaviour of structural elements, will be different than in these specimens. However, it is possible to relate in a rather simple way, the tensile properties of these test specimens, with the tensile properties of real structural elements made of HFC. In Chapter 5, which is dedicated to the utilization of HFC in practice, the simple relations between the behaviour of HFC in test specimens and in structures will be developed and explained.

3.3.2 Testing methods for the tensile properties of fibre concretes

The experimental tensile characterization of any type of fibre concrete, consists usually on the measuring of the relation between the opening of one or more cracks, and the corresponding tensile load. For completely the same mixture composition of fibre concrete, this relation may differ significantly, if two different test set-ups and types and shapes of the specimens are applied. Also in many other types of tests, keeping all other material parameters constant, the experimental set-up and the applied testing methods, may have a tremendous influence on the obtained results [Van Mier, 1997].

Some of the previously used test-set-ups for different types of fibre concrete are given in Fig. 3.5. The RILEM Technical Committee on fibre reinforced concrete [RILEM TC-162 TDF, 2000], recommended the following tests for the tensile characterization of conventional fibre concretes (fibre concretes without strain hardening):

−   three-point bending test on notched beams (beam dimensions 150*150*600 mm), for the characterization of the flexural behaviour (Fig. 3.5.a), and

−   uniaxial tensile test on notched cylinders, with a diameter of 100 mm and a height of 150 mm, for the characterization of the tensile behaviour (Fig. 3.5.b).

The wedge splitting tensile test (Fig. 3.5.c) is often used as an alternative for the tensile characterization of conventional fibre concretes, by [Stang, 1998] or [Löfgren, 2004]. Recently, a round-plate test for FRC was also proposed by [Vandewalle et al., 2004].
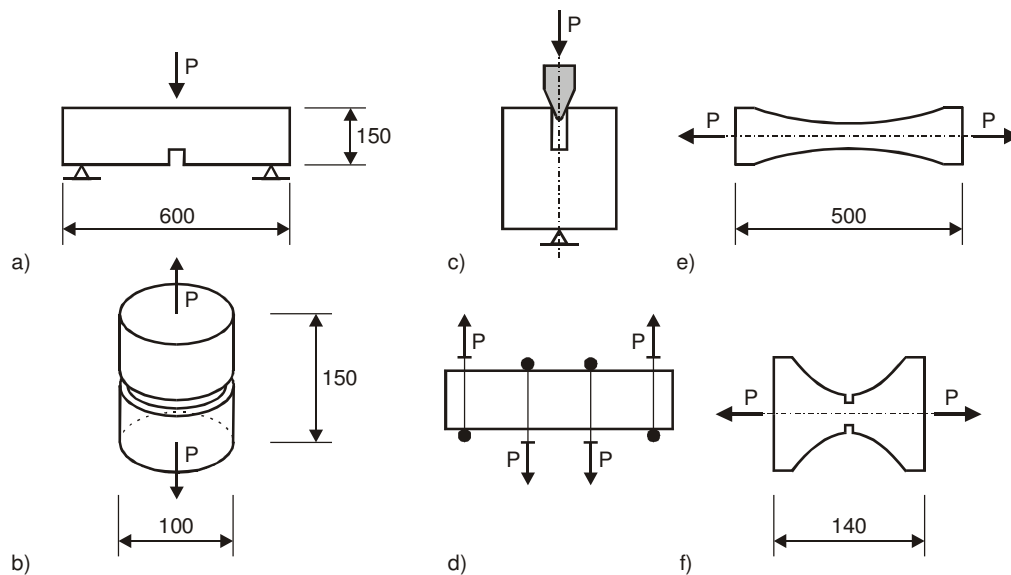
Fig. 3.5: Possible test set-ups for tensile (b, c, e, f) and flexural tests (a, d) on conventional and high-performance fibre concretes

However, there are still no recommendations for the tensile characterization of high-performance fibre concretes (HPFC). The possibilities are however relatively large. The flexural tests on RPC were performed as 4-point bending tests on plates without notch, with di-

mensions 15*100*400 mm in [Behloul, 1996]. The similar tests on the Dutch version of MMFRC, were performed as three-point-bending tests on notched beams, with dimensions 150*150*600 mm, by [Sato et al., 1999, 2000]. In [Stähli & Van Mier, 2004], four-point bending tests were performed, using the test set-up with pendulum bars (Fig. 3.5.d).

Uniaxial tensile tests on HPFC were performed mostly on dog-bone-shaped specimens, with different thicknesses and lengths, ranging from 50*50*500 mm in [Behloul, 1996] (Fig. 3.5.e), to 30*20*140 mm in [Sato, 2000] (Fig. 3.5.f). In the research of Sato, the dog-bone-shaped specimens were notched as well.

In cases of concrete reinforced with synthetic fibres (PVA- or PVE-fibres), plate-formed specimens without or with notches were applied for the so-called Engineered Cementitious Composites (ECC), in [Li et al., 1998]. Dog-bone-shaped specimens for testing concrete with polyvinyl microfibres were used in [Shah et al., 1996].

With all these different types and dimensions of testing specimens, the comparisons of the obtained results is almost impossible. One of the urgent matters in further research activities with HPFC should therefore be a development of appropriate test set-ups and testing procedures for uniaxial tensile and flexural tests.

3.3.3   Testing method for HFC: notched or un-notched specimens?

Basic facts about notches

In plain concrete, the notched specimens are usually applied for uniaxial tensile tests [Van Mier, 1997]. In theory, the notches pre-define the place of crack localization, and in such a way, make the measurement of the crack width during the test possible.

In fibre concrete the situation is rather different. At the surface of the specimen, the fibres are usually fully aligned to it (Fig. 3.6.a), and due to the notch, cracking begins at a certain distance from that surface, where the fibres should be more-or-less randomly oriented (Fig. 3.6.c). In theory, this should give a realistic flexural (tensile) response of the material, because the wall-effect on the fibre orientation (Fig. 3.6.a) is eliminated. In contrast to this, for the specimens without notch, the obtained flexural or tensile characteristics may be over-estimated, due to the agreeable alignment of fibres near the surface of the specimen.

However, the place where the crack appears, and partly its propagation path, will also be pre-described by the notch itself. In real structures made of fibre concrete, there are no notches, i.e. the crack(s) searches the easiest way to propagate through the concrete (Fig. 3.6.b).

This suggests, that tests on un-notched specimens may be more realistic in describing the behaviour of fibre concrete. Recent results of [Stähli & Van Mier, 2004], suggest that even about 40 % lower flexural strengths can be registered in four-point bending tests on beams without a notch, compared to three-point bending tests on beams with a notch, for the same types of fibre concrete. The concrete contained both short and long fibres.

In contrast to this, in [Chanvillard et al., 2003], only slightly lower tensile and flexural strengths were obtained on un-notched specimens. The tensile strengths obtained using notched specimens were about 5 - 10 % higher than those obtained on un-notched specimens in this case. In [Habel et al., 2002], even somewhat better tensile behaviour was observed using the un-notched specimens. In both last two cases, the tested concretes contained only short steel fibres (l/d = 13/0.2, made of high-strength steel).
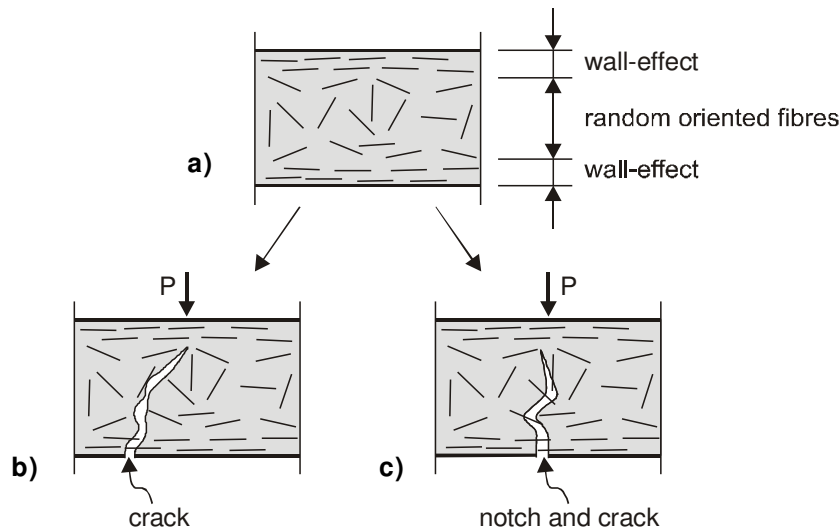
Fig. 3.6:   a) Possible orientation of fibres in a specimen with 2 borders;   b) crack propagation in un-notched specimen   b) crack propagation in notched specimen

The differences in tensile behaviour do not depend only on notches. They are in each case also a consequence of the different number and orientation of the fibres in the testing specimens. Moreover, concrete with short fibres only is much more homogeneous than concrete with both long and short fibres. Short fibres are also more randomly oriented, so that probably a similar cracking pattern develops always, no matter if there is a notch in the specimen or not. Therefore, in this case the notch will not have a significant influence on tensile behaviour.

In concrete which contains long fibres, the notch probably plays a much more important role. It pre-determined the crack pattern significantly, and with that the tensile response as well. It can therefore be expected, that the presence of a notch can lead to a significant overestimation of the tensile characteristics of fibre concrete with long fibres.

As a conclusion, testing of tensile properties of fibre concrete, both using notched and un-notched specimens, has its advantages and disadvantages. There is still no ideal testing method and test set-up. However, standard test methods should be designed so, that the material is tested as it appears in the structure [Van Mier, 2004 b].

Selection of testing methods applied for Hybrid-Fibre Concretes

In this research project, the selection of test set-up and of type and shape of specimens, was done on the basis of the specifically defined purposes of the appropriate tests.

Flexural tests on HFC were performed firstly, and their basic goal was the selection of concretes with best flexural properties, to be applied further in uniaxial tensile tests. The results of the flexural tests do not have that important practical meaning, except maybe to determine the first-cracking stress. Therefore, the qualitative side of the flexural behaviour will be of most interest. In such a case, it is actually not that important which type of specimen (notched or un-notched) is used. Therefore, it was decided to use the three-point bending test on notched beams, according to [RILEM TC-162 TDF, 2000].

The basic goal of the uniaxial tensile tests on HFC, was to obtain a reliable (tensile stress)-(crack width) relation, i.e. tensile stress-strain relation, which can later be used in structural design. The presence of a notch would probably lead to over-estimation of the tensile properties. In this research project, it will later be shown that this indeed happens. Therefore, un-notched dog-bone specimens were chosen for the uniaxial tensile tests. Only a few of these tests were performed on notched specimens, in order to compare the results to those obtained using un-notched specimens.

3.3.4 Determination of number and orientation of fibres in specimens

As already stated, the tensile properties of any type of fibre concrete, depend mostly on 2 parameters:

− the number of fibres in the cracking zone, and
− the orientation of fibres in the cracking zone, with respect to main tensile stresses.

These parameters will be determined in this research, for a number of different types of HFC.
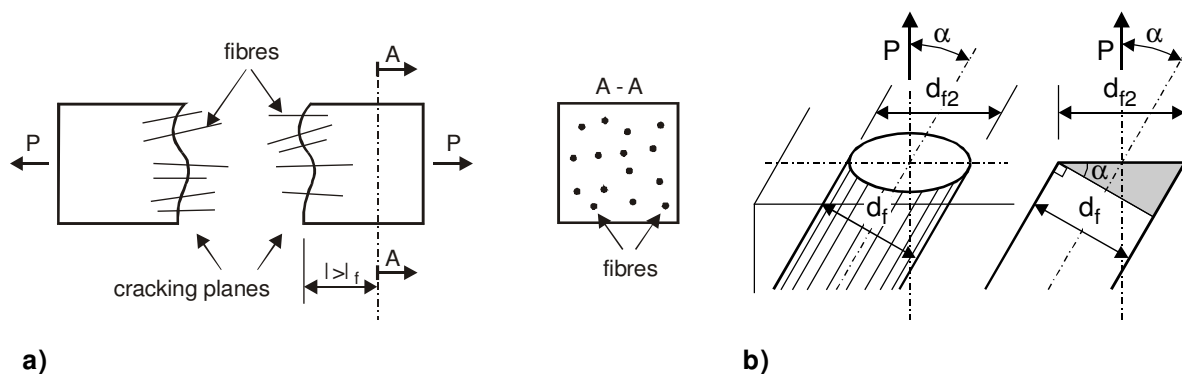
Fig. 3.7:   a) Fractured parts of the tensile specimen with fibres, used for the determination of the number and the orientation of the fibres by manual (on cracking planes self) and optical methods (in cross-section A-A);   b) Orientation of single fibres in a cross-section of a FRC-element: aligned and inclined fibres and their measurement

The determination of the number and the orientation of fibres has more goals:

- the tensile and the flexural behaviour of fibre concrete can be explained on the basis of these parameters;
- analytical modelling of the tensile response of HFC can be performed knowing these parameters;
- a relation can be created between the tensile properties of HFC on the material and on the structural level.

The number and the orientation of fibres were determined using two methods, for both flexural and uniaxial tensile tests on HFC:

- **Manual method**: consists of counting of the fibres present at both cracking planes after the test; this will be done only for long hooked-end fibres (Fig. 3.7.a). The determined number of fibres will be used as such, both for the characterisation and the modelling of the tensile (flexural) behaviour.

   Another two parameters, which will be determined for hooked-end fibres are:

   - **the visible lengths of the fibres at both cracking planes (fracture surfaces) i.e. the pulled-out lengths of the fibres** (Fig. 3.7.a). The number of the fibres, which possess an appropriate visible length (l_{vis}), will be classified in intervals of 10 mm, e.g. from 0-10 mm, 10-20 mm, etc.. This analysis can provide information on the relation between the fibre distribution and the cracking paths through fibre concrete, and will be used later for analytical modelling of the tensile response of HFC;

   - **the deformability of the fibre hooks, i.e. the number of fibres whose hooks are fully plastically deformed**. These fibres will be denoted as "fully active fibres", while fibres with non- or partly-deformed hooks, will be denoted as "partly active fibres". This will later be related to the visible length of the same fibres, and used for analytical modelling of the tensile response of HFC.

- **Optical method**, (after [Schönlin, 1988], and [Grünewald et al., 2002]), which consists of taking photos of the cross-section of the beam specimens with a flash camera, and by subsequent analysis of them in the image-analysis programme "Optimas". When subjected to the flesh light, the fibres reflect it, whereas the surrounding concrete absorbs it. In such a way, an image is produced where each fibre can clearly be distinguished as an individual surface, with appropriate geometrical characteristics. This method enables the estimation of both the number and the orientation of the fibres, for each applied fibre type (for both short and long steel fibres).

Fibres aligned to the main tensile stresses have a circular cross-section with a diameter D_f, while all other fibres have an elliptical cross-section. According to Fig. 3.7.b, the fibre orientation coefficient η may be calculated as:

$$\eta = \frac{1}{N} \cdot \sum_{i=1}^{N} \cos \alpha_i \quad , \quad \text{where:} \tag{3.1}$$

N = total number of fibres in the cross section

α_i = the angle of inclination of each single fibre i with respect to the direction of the main tensile stress, where $\cos \alpha = D_f / D_{f2}$, with (Fig. 3.7.b):

   D_f = nominal fibre diameter

   D_{f2} = length of the longer axis of the elliptical cross-section of a fibre.

However, in order to make a representative cross-section for the analysis, the beam must be cut at a certain distance $l > l_f$ from the macro-cracking plane, in order to ensure that no spaces with pulled-out fibres are present in the cross-section (Fig. 3.7.a). This distance was 60 mm if long fibres are present, and 15 mm if only short fibres are present. Therefore, the number and orientation of the fibres determined by the optical method, do not exactly correspond to those, which take part in the crack bridging.

One of the possible methods for the determination of the orientation of the fibres in the cracking zone, is the X-ray technique [Van Gysel, 2000].

3.4 Flexural behaviour of Hybrid-Fibre Concrete

3.4.1 Introduction

In Chapter 2, mixture compositions for different types of Hybrid-Fibre Concrete were determined, after which the workability was tested. The main requirement of this was, that the mixtures should be self-compacting. However, good mechanical properties are much more important than good workability, and they are therefore the main point of this whole research project. The workability is only a necessary pre-requisite, for achieving a uniform fibre distribution and therefore the best possible mechanical properties.

Flexural tests were carried out first for the evaluation of the behaviour of different types of Hybrid-Fibre Concrete exposed to tensile stresses. It was decided to use standard three-point-bending tests on notched beams, as defined by [RILEM, 2000].

The main goals of the flexural tests on different Hybrid-Fibre Concretes, performed in the scope of this research, were:

1. to select the optimum Hybrid-Fibre Concretes and to test them subsequently in the uniaxial tensile tests; the basic criteria for this selection is, that a concrete should possess the best possible flexural behaviour, for the lowest possible fibre quantity;

2. to observe the influence of different types of fibres on the first-cracking stress, strain hardening, flexural strength and ductility, accompanied with the analysis of number and orientation of the fibres in the beam specimens;

3. to determine analytically the uniaxial tensile behaviour of HFC by inverse analysis, using the flexural behaviour as a basis.

In this sub-chapter, a summary of the results of the flexural tests will be given, with the first-cracking stress and the flexural strength as the most important parameters. With these parameters the strain hardening will be characterized. These results will subsequently be related to applied type and quantity of the fibres, as well as to their number and orientation.

3.4.2 Applied concrete mixtures and testing procedure

A schematic overview of the mixture composition of the concretes applied in the flexural tests, together with their basic properties (workability, compressive and splitting tensile strength), is given in Tab. 3.1. These mixtures were composed on basis of the workability characterization, explained in Chapter 2 (Tab. 2.1 and 2.2).

Tab. 3.1: Scheme of the mixture compositions of the concretes tested in flexural tests

No.	w/b	D_{max}	microsilica	aggregate	fibres l/d (vol.%)				fibres	slump flow	strength (MPa)	
		(mm)	(vol.%)	(vol.%)	6/0.16	13/0.2	40/0.5	60/0.7	(kg)	(cm)	compr.	spl. tens.
1	0.2	1.0	4.0	50					0	74.0	118.2	10.1
2	0.2	1.0	4.0	46		2			160	75.0	127.9	14.7
3	0.2	1.0	4.0	40	2	2			320	72.5	132.4	16.6
4	0.2	1.0	4.0	48				1	80	72.0	120.2	12.1
5	0.2	1.0	4.0	40		0.5		1	120	79.0	118.6	14.5
6	0.2	0.5	12.0	40		0.5		1	120	62.0	126.5	14.8
7	0.2	0.5	12.0	35		0.5		1.5	160	50.0	119.8	14.3
8	0.2	1.0	4.0	38		1		0.5	240	72.0	122.3	16.2
9	0.2	1.0	4.0	35		2		1	240	55.0	135.2	21.3
10	0.2	1.0	4.0	45	2			1	240	74.0	127.7	16.7
11	0.2	1.0	4.0	35		1	1		160	71.0	124.5	17.1
12	0.2	1.0	4.0	35	4		1		400	66.5	124.5	19.1

The w/b-ratio, the quantity of silica fume and the aggregate grading were kept the same in most of the concretes. An exception was made only in two mixtures, in order to investigate if more improvements were possible by variations in these parameters. A reference concrete without fibres, as well as concretes with only short, only long, and with both short and long fibres, were tested. In total, 4 types of fibres were applied, in 12 different concrete mixtures.

All flexural tests were performed as three-point bending tests on notched beams, according to the procedure defined in [RILEM, 2000]. Beams with dimensions 150*150*600 mm, with a span of 500 mm and a notch with a depth of 25 mm in the middle, were used (Fig. 3.8). All specimens were cured at 20ºC, and 95 - 100 % relative humidity. The notch was made about 3 weeks after casting, while before that the specimens were turned for 90º with respect to the casting direction. For each type of concrete four specimens were tested. The loading speed

was 11.1 µm/s for the reference (plain) concrete beams, and 55.5 µm/s for all fibre concrete beams. During the tests the crack opening was registered by means of 2 LVDT's, placed on both sides of the notch.
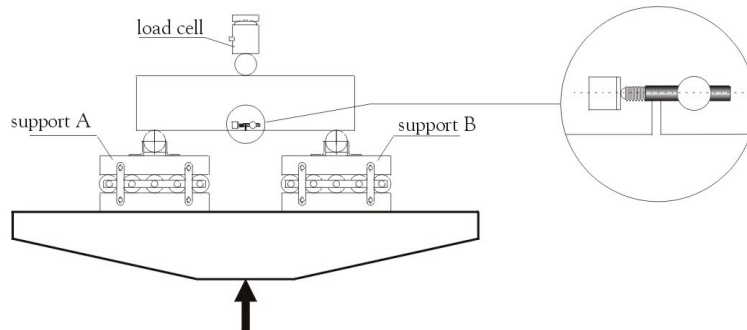
Fig. 3.8: Test set-up for three-point bending tests on HFC beams (after [Kooiman, 2000])

This test-set-up is very practical and easy for utilisation, but its disputable point is the friction at the supports. Although rolling supports have been chosen to reduce as much as possible the friction, the negative influence of it can never totally be eliminated. Also, the outer bending forces do not remain perpendicular to the specimen at larger crack openings. Both "short-comings" of the present test set-up may result in slightly higher values of the bending force and the displacement. A better alternative would be the innovative test set-up with pendulum bars (Fig. 3.5.d), as recently proposed by [Stähli & Van Mier, 2004], where all these negative influences are completely eliminated.

3.4.3   Results of the flexural tests

An overview of the results of the flexural tests on HFC will be presented in this sub-chapter. Detailed results of the flexural tests are given in [Markovic et al., 2003-a], and [Markovic et al., 2003-c] as well. Each type of concrete will be denoted according to the volume quantity of the fibres, and the corresponding fibre length. For example: 1.0% (13) + 0.5% (60), refers to the concrete No. 8, which contains 1.0 vol.-% of fibres with l/d = 13/0.2, and 0.5 vol.-% of fibres with l/d = 60/0.7.

Also, instead of the experimentally measured flexural force, all results will be presented using the equivalent flexural stress. This stress is derived from the flexural force, assuming linear elastic flexural behaviour (i.e. $\sigma = M / W$). Since the compressive strength of all applied concretes varied only slightly, it will not be regarded as an experimental parameter.

Flexural strength

An overview of the values of the flexural strengths, for different combinations of fibres, is given in Fig. 3.9. First of all, the achieved flexural strengths of all types of fibre concrete, were substantially higher compared to those of plain concrete. This was not the case for conventional fibre concrete [Kooiman, 2000]. The scatter of the test results was also much lower

than in the same conventional fibre concrete. The flexural strength ranged from about 7 MPa for plain concrete, up to about 45 MPa for Hybrid-Fibre Concrete with total fibre quantity of 5.0 vol.-%.

It is however not necessary to use that high quantities of fibres: Fig. 3.9 shows that only slightly lower flexural strength of about 40 MPa can be obtained with a Hybrid-Fibre Concrete, which contains only 2.0 vol.-% of fibres. Similarly, the flexural strengths achieved by concretes with 3 or 4 vol.-% of fibres, are almost equal to the flexural strength of the concrete with 5 vol.-% of fibres. Therefore, the applied combination of fibres is far more important than the applied volume quantity of fibres in an absolute sense.

In the case of the two concretes with in total 1.5 vol.-% of fibres, the highest flexural strength was achieved if concrete contained more long fibres. The flexural strength was higher with fibre combination 0.5% (13) + 1.0% (60) than with 1.0% (13) + 0.5% (60).

A similar conclusion could be drawn as well for all concretes with 2 vol.-% of fibres. In this case, the application of a combination of short and long fibres (1% (13) + 1% (40)), resulted even in a 50 % higher flexural strength, than achieved by the concrete with the same volume quantity of the short fibres only (2% (13)). Obviously, the combining of different types of fibres has very positive effects in this case.
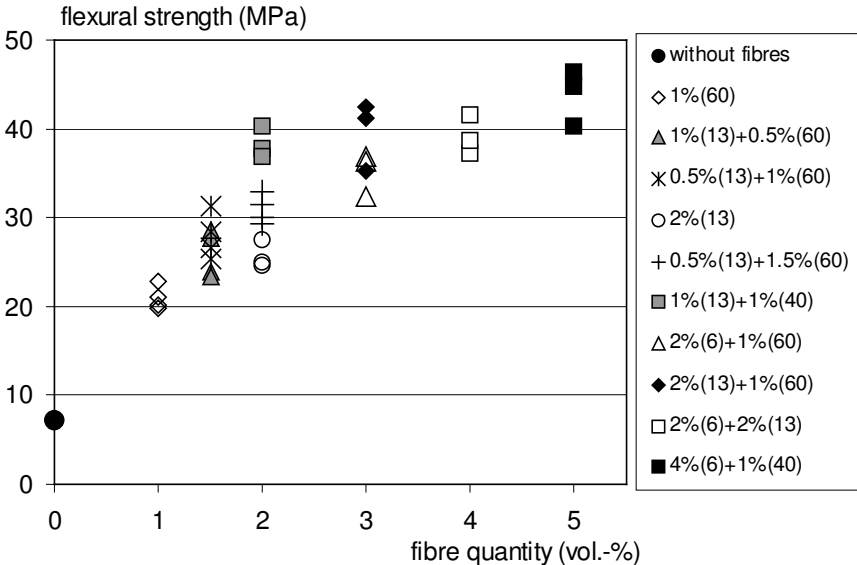
Fig. 3.9: Flexural strengths of applied concretes with one and two types of steel fibres (the results of each single test are presented)

Concretes with one and with two types of fibres

A comparative overview of the flexural behaviour of plain concrete, mono-fibre concretes with 2 vol.-% of only short straight fibres, 1.0 vol.-% of only long hooked-end, and of hybrid-

fibre concrete with both 2.0 vol.-% of short and 1.0 vol.-% of long fibres, is given in Fig. 3.10.

The concrete with 2.0 vol.-% of short fibres had a rather high flexural strength (26 MPa), but soon after it was reached, the softening began. The concrete with 1.0 vol.-% of long fibres, had somewhat lower flexural strength (20 MPa) compared to the concrete with short fibres, but its ductility was much better. The Hybrid-Fibre Concrete, which contained both types of fibres, had a very high flexural strength (42 MPa), with significantly improved ductility.

The addition of the flexural stresses (i.e. diagrams) of both concretes with one type of fibre results in an arithmetical value, which is lower (or approximately equal), compared to experimentally obtained flexural stresses. Therefore, the two types of fibres are "helping" each other in achieving higher flexural stresses, when they are combined together in Hybrid-Fibre Concrete. This phenomenon is known as "synergy". This shows that the whole concept of the utilization of more fibre types together in one concrete, is completely legitimate. The fibres act better when they are together, than when they act on individual basis.
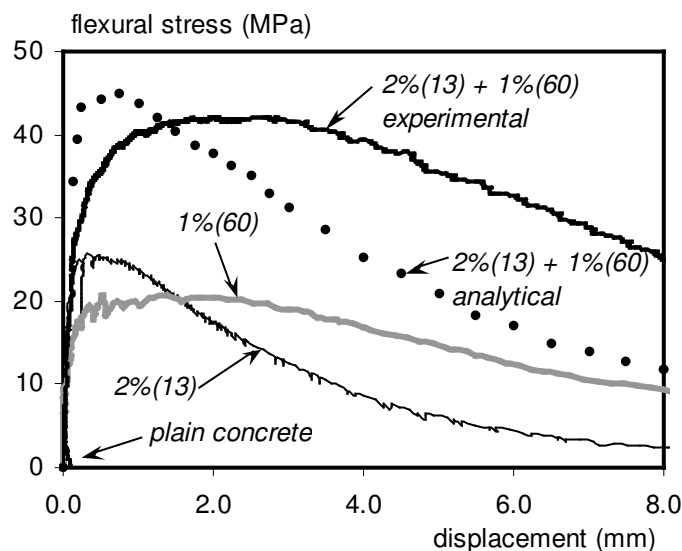
Fig. 3.10: Flexural behaviour of concretes with only short, only long, and both short and long fibres, and the synergy effects of fibre combination (experimentally obtained stress in HFC is larger than the analytical sum of stresses in concretes with one fibre type)

A very suitable example of all the benefits of combining fibres is given in Fig. 3.11. The initial concrete contains 2 vol.-% of short fibres with l/d = 13/0.2. In the Hybrid-Fibre Concrete, 1 vol.-% of short fibres is exchanged with 1 vol.-% of long hooked-end fibres with l/d = 40/0.5. This resulted in tremendously higher flexural strength for about 50 % (from 25 MPa up to 38 MPa), even though the same volume content of fibres was applied. Therefore, the combining of fibres offers a much higher potential for the optimisation of the tensile properties, than just increasing the volume of a single type of fibres in concrete.
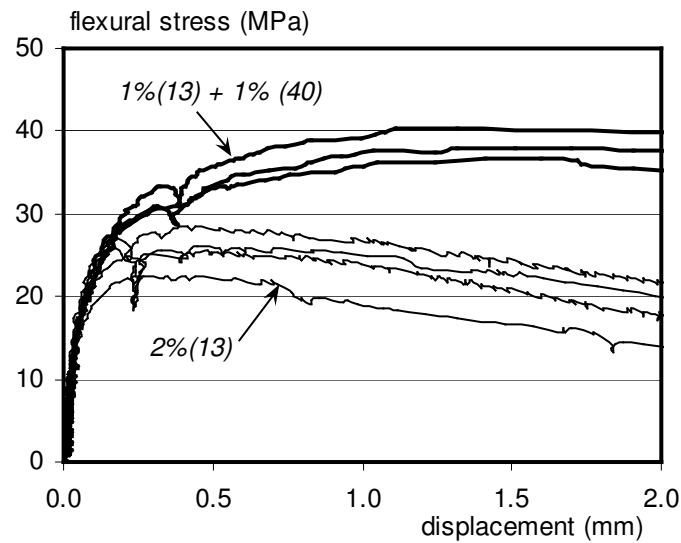
Fig. 3.11: Example of optimisation of fibre combinations: the mixture with both short and long fibres possess almost 50% higher flexural strength and much more expressed ductility, compared to a mixture with short fibres only, and with the same total fibre volume quantity (2.0 vol.-%)

The influence of the presence of different quantities of short fibres with l/d = 13/0.2, in a concrete which initially contains 1.0 vol.-% of long fibres with l/d = 60/0.7 is given in Fig. 3.12.b. Due to the presence of 0.5 vol.-% of short fibres, both the first-cracking stress and the flexural strength are improved, the latter for about 50 %. Further addition of 1.5 vol.-% of short fibres resulted again in an improvement of the flexural strength with about 50 %. This is not proportional to the applied fibre quantity, i.e. a higher flexural strength could be expected for this concrete. The reason for this is probably a non-completely satisfying workability of this concrete, with a slump flow of 55 cm.

First-cracking flexural stress and strain hardening
The first-cracking flexural stress is used here only for the characterisation of strain hardening. It cannot be used for certain predictions of the first-cracking stress on the structural level, because the here used flexural beams possess notches. The place of cracking is therefore fixed. In un-notched beams, probably lower values of the first-cracking stress might occur.

The values of the flexural stress at the formation of the first macrocrack (initial crack width taken as w = 0 mm), and the values of the flexural stress at a crack width w = 0.2 mm, are given in Fig. 3.12.a. All stresses are the mean of four measured values.

These two values are an indication of the intensity of the strain hardening, for concretes with short, with long and with both short and long fibres. The chosen crack width of 0.2 mm is often denoted as the limit crack width for rather unsuitable environmental conditions, according to many recommendations on design of concrete structures [e.g. Dutch NEN 6720].
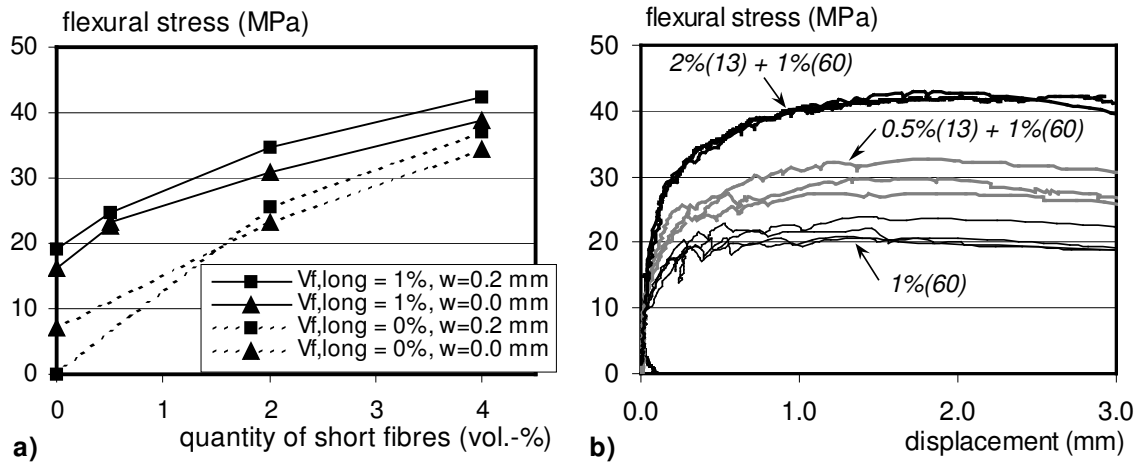
Fig. 3.12: a) First-cracking flexural stress (at crack width w = 0 mm), and flexural stress at crack width w = 0.2 mm, for concretes with only short (V $_{f, long}$ = 0.0 vol.-%), and concretes with both short and long fibres (V $_{f, long}$ = 1.0 vol.-%),; b) The influence of different short fibres in the concrete which initially contains only long fibres, on the flexural behaviour

In general, the higher is the fibre quantity, the higher the first-cracking stress and the more pronounced the strain hardening will be. Higher flexural stresses are always obtained at the crack opening of $w = 0.2$ mm, by virtue of the strain hardening. If concrete contains only short fibres, this difference is not that high (about 10 %), which means that the strain hardening is not very pronounced.

If concrete contains long fibres, both values of the stress are higher compared to the concrete with short fibres only. This is valid both for the concrete with only long, as well as for the concrete with both short and long fibres. The strain hardening will also be somewhat more pronounced for these concretes as well. Finally, it is important that a stable flexural behaviour is obtained after cracking, and this is always fulfilled here, no matter which type of fibres has been applied in the concrete.

Influence of mixture composition on flexural behaviour
As stated in Tab. 3.1, the maximum grain size $D_{max} = 1.0$ mm and the amount of microsilica of 4.0 vol.-% of the cement volume quantity, were kept constant in all, except in two concretes (concretes No. 6 and 7). In these two cases, the maximum grain size was decreased to $D_{max} = 0.5$ mm, and a 3 times higher quantity of microsilica was applied, in order to refine the mixture. It can be expected, that better bond can be developed between fibres and concrete in such a way, and therefore that a better total flexural behaviour can be obtained.

However, no differences at all were observed in the flexural behaviours of normal and refined concretes, for the same fibre volume quantity (Fig 3.13.a). The flexural curves were almost identical [Markovic et al., 2003-c]. Therefore, it seems that the bond between the fibres and the surrounding concrete, does not improve significantly with increased quantity of silica fume. Even larger quantities of microsilica (25.0 vol.-% of the applied cement quantity), also did not lead to a much better flexural behaviour of RPC [Behloul, 1996], or MMFRC [Sato, 1999]. Therefore, in all further mixtures, the quantity of microsilica will be 4 vol.-% of the applied cement quantity.
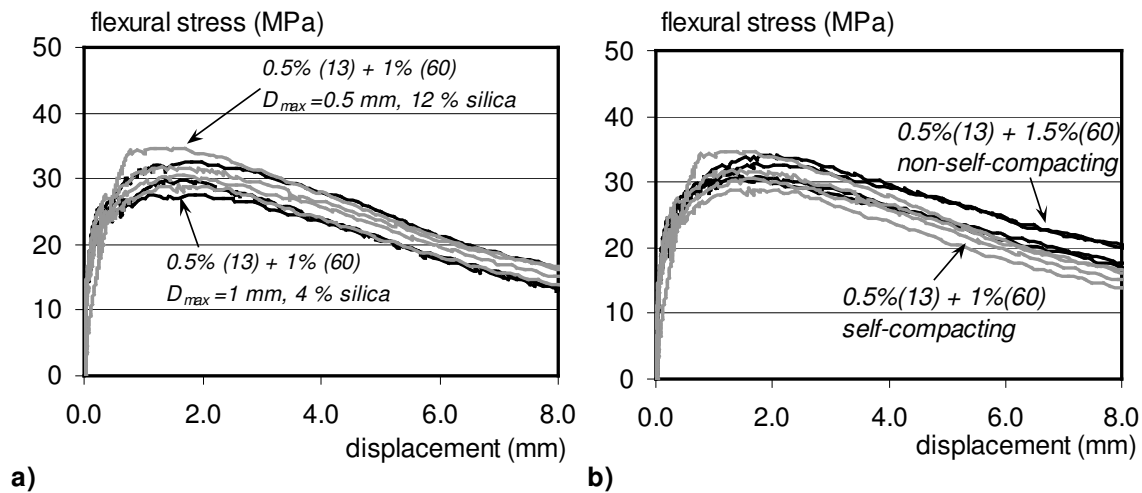
Fig. 3.13:   a) Influence of the refinement of the mixture composition on the flexural behaviour, for concretes with the same quantity and type of fibres;   b) Influence of the workability of HFC on the flexural behaviour

Influence of workability on the flexural behaviour

A comparison of the flexural behaviour of self-compacting HFC and non-self-compacting HFC is shown in Fig. 3.13.b. In both cases, the same refined mixture composition was used (Tab. 3.1, concretes No. 6 and 7), the only difference being the quantity of long fibres (1.0 vol.-% in self-compacting, versus 1.5 vol.-% in non-self-compacting concrete). For such a relatively high difference in fibre quantity, an obvious difference in flexural behaviour could have been expected.

However, Fig. 3.13.b suggests that there is no difference at all in flexural behaviour of these two concretes. The quality of the fibre-concrete interface is probably much lower in the case of non-self-compacting HFC, due to the higher content of entrapped air. The orientation of the fibres is also probably worse than in self-compacting HFC. Therefore, no improvement of the flexural behaviour is obtained, in spite of the higher applied fibre quantity.

3.4.4. Summary and concluding remarks on the flexural behaviour of HFC

In this sub-chapter, the results of flexural tests on 12 different types of concretes, reinforced with one and two different types of steel fibres have been presented. All flexural tests were performed as three-point bending tests on notched beams. It was possible to obtain very high values of the flexural strength, with relatively low volume quantities of fibres. The first-cracking stresses were also very high, with significantly pronounced strain hardening and ductility. The tests were accompanied with the analysis of the number and the orientation of the fibres in the beams.

On basis of the performed tests, the following may be concluded:

1. The flexural strength depends much more on the applied combination of fibres, than on the applied total volume content of fibres. Hybrid-Fibre Concrete offers actually much more possibilities for the optimization of fibre combinations, than any fibre concrete with only one type of fibres.

2. Concretes with only short fibres have a high flexural strength but a relatively low ductility; concretes with only long fibres have lower flexural strength but a higher ductility; finally, the Hybrid-Fibre Concretes, which contain both short and long fibres, have a significantly improved both the flexural strength and the ductility. A strong synergy of fibre action is obvious.

3. The higher is the quantity of short fibres in the concrete, the higher first-cracking stress of concrete will be obtained; the higher is the quantity of long fibres in the concrete, the more pronounced the strain hardening will be.

4. The refinement of the aggregate grading and utilization of rather large quantities of micro-silica, did not have any significant influence on the improvement of the flexural behaviour, for the same fibre combination.

5. The workability can have a very large influence on the flexural behaviour of Hybrid-Fibre Concrete. If Hybrid-Fibre Concretes are not self-compacting, no improvements in flexural behaviour are obtained, in spite of the increase in fibre quantity.

3.5 Uniaxial tensile behaviour of Hybrid-Fibre Concrete

3.5.1 Introduction

Results of flexural tests on 12 different Hybrid-Fibre Concretes (HFC), were given in the previous sub-chapter. The main goal of flexural tests was the optimisation of the fibre combinations. The main requirement for that optimisation, was that a concrete should possess the best possible flexural behaviour, with a fibre quantity as low as possible. The concretes with the best performances were chosen on basis of flexural tests, and will be tested further in uniaxial tensile tests.

The uniaxial tensile tests were performed on dog-bone shaped specimens. All of them were un-notched. A couple of additional specimens with notches were tested as well, for the sake of comparison. In total 7 different concretes have been tested, with one and two types of fibres, and also without fibres (reference concrete).

The main goals of the uniaxial tensile tests are:

1. to determine appropriate σ - w (tensile stress - crack width), i.e. σ - ε (tensile stress - tensile strain) curves, for different types of HFC, on the basis of the results of these tests;
2. to develop an analytical model for the tensile behaviour of different types of HFC on the basis of the results of these tests; to be able to predict the tensile properties of other types of HFC (with other combinations and quantities of fibres) on the basis of this model;
3. to analyse the influence of different types of fibres (only short, only long and both short and long fibres together) on the tensile behaviour of HFC; to compare subsequently the uniaxial tensile behaviour with the flexural behaviour of HFC, for the same fibre combinations and quantities, and to find the appropriate relations between them, if they exist.

In this chapter, the preparation of the specimens and the test-set up will be presented first. The summary of the results of the uniaxial tensile tests will be given subsequently. The main parameters will be the uniaxial tensile strength, the first-cracking stress and the ductility. The influence of the notches will be shown as well. After that, the cracking patterns will be studied, including multiple cracking. The determination of number and orientation of fibres in tensile and flexural specimens will be given at the end of this chapter.

3.5.2 Applied concrete mixtures

A schematic overview of the mixture compositions of the concretes applied in the uniaxial tensile tests, together with their basic properties (workability, compressive and splitting tensile strength), is given in Tab. 3.2. These mixtures were chosen on the basis of the results of the flexural tests (sub-chapter 3.4). The basic criterion for the selection was the best possible flexural behaviour (flexural strength, ductility), using a fibre quantity as low as possible. Another important criterion was the workability: all tested mixtures had to be self-compacting, according to the criteria described in sub-chapter 2.6.

The w/b-ratio, the quantity of silica fume and the aggregate grading were kept the same in most of the concretes. The reference concrete without fibres, as well as the concretes with only short, only long, and with both short and long fibres were tested. In total, 3 types of fibres were applied, in 7 different concrete mixtures.

Tab. 3.2: Applied concrete mixtures in uniaxial tensile tests

No.	fibres (vol.-%)			w/b	D_{max}	microsilica	slump flow	strength	
	straight	hooked-end						f_{cc}	f_{spl}
	13/0.2	40/0.5	60/0.7		(mm)	(vol.-% cem.)	(cm)	(MPa)	(MPa)
1				0.2	1.0	4.0	82 / 85	119.7	9.6
2	2			0.2	1.0	4.0	81 / 76	133.0	14.3
3	3			0.2	0.5	12.0	80 / 70	134.1	20.4
4	1		0.5	0.2	1.0	4.0	84 / 88	125.0	15.7
5	0.5		1	0.2	1.0	4.0	68 / 72	120.1	14.0
6	1	1		0.2	1.0	4.0	73 / 75	113.0	15.3
7			1	0.2	1.0	4.0	57 / 61	124.4	11.6

The maximum applied fibre volume quantity ranges up to 2.0 vol.-%. This choice is equally based on the workability requirements and on the feasibility of utilisation of HFC for pre-cast concrete products (based upon [Simon et al., 2002] and [Grünewald et al., 2002 c]). The economical feasibility of HFC will be analysed in detail in Chapter 5 of this thesis.

Only the concrete No. 3 (Tab. 3.2), contains more than 2.0 vol.-% of fibres. In this concrete, 3.0 vol.-% of short fibres 13/0.2 have been applied, in order to compare its tensile behaviour with the tensile behaviour of other concretes with lower fibre quantity. The granular composition was also refined in this concrete ($D_{max} = 0.5$ mm, higher quantity of microsilica).

3.5.3   Test set-up and testing procedure

Test set-up

For the uniaxial tensile tests, a testing frame with fixed boundaries was used (Fig. 3.15.c). This frame was developed for uniaxial tensile and fatigue tests on plain concrete, in [Hordijk, 1985]. The shape and the dimensions of the specimens were therefore dependent, in the first line on the available space in the testing frame, between the loading plates. So, the height was limited to 180 mm, and width and depth to 160 mm. Moreover, the total tensile capacity of the machine is 100 kN. This limited the dimensions of the normative cross-section, making sure that the specimen can reach its tensile strength. At the same time, the maximum tensile force should not exceed the maximum of 95 % of the full tensile capacity of the machine.

After linear and non-linear finite-element simulations have been performed, the so-called dog-bone shape of the specimens was chosen (Fig. 3.15.a), with a height of 180 mm, and a width 160 mm at the top and bottom, and 70 mm in the middle. The chosen depth of the specimen was 70 mm. Therefore, during testing, in the pre-peak period about 2.25 times higher tensile stresses develop in the middle of the specimen, than at the top and the bottom. All cracking activities can therefore be expected in the middle zone, where they can be regis-

tered with LVDT's. Moreover, the normative cross section, with dimensions 70 x 70 mm^2, allows to reach the maximum tensile stress of 20 MPa. Taking into account the results of the flexural tests on HFC (sub-chapter 3.4), and the applied fibre quantities, no higher stresses from this one should be expected.

Wall-effect of fibres in tensile specimens

At first sight, the dimensions of the specimens may seem rather small. The normative cross section (70 x 70 mm^2), may seem rather narrow, taking into account that the length of the fibres goes up to 60 mm. The so-called "representative volume element" (RVE) in concrete, should indeed be at least a couple of times larger, than the largest particle and/or fibre. If not, the fibres will surely be aligned in one direction.

However, structural elements made of high-performance fibre concrete are often very thin ([Toutlemonde, 2002], [Simon et al., 2002], [CPCI, 2003]). The thickness of some structural members maybe even limited up to 1.25 cm, as presented in [Behloul et al., 2004]. The fibres, especially the long ones, will therefore definitely be oriented in plane (2D) or longitudinally (1D) in such elements. Therefore, no mistake is made, if the specimens for the tensile tests of HFC are narrow. Indeed, the obtained tensile behaviour in the tests using such specimens, will be representative for the real tensile behaviour of concrete in a structure. This is also in accordance with the recent recommendation to test these types of concrete in such a way, as they appear in the structure [Van Mier, 2004 b]. However, the results of these uniaxial tensile tests can be used also for thicker and larger structural elements. In such a case, a correction for the orientation and the number of fibres should be made (Fig 3.4, sub-chapter 3.3.1). This will be explained in detail in Chapter 5.

Testing procedure

One of the most important requirements for a successful performance of tensile tests on HFC, is that the fibres should be homogeneously distributed throughout the whole specimen. The best solution is to cast HFC in moulds, which are longer and higher than the final specimens. Taking this into account, the initial height of the specimens was 380 cm (Fig. 3.15.b). The final specimens for testing (Fig. 3.15.a), were obtained by cutting off the 100-mm-high pieces from both top and bottom of the initial specimen. The goal is to achieve uniform orientation of fibres in all parts of the specimen, i.e. both in the middle- and in the end-zones (top and bottom). This is especially important for long fibres (Fig 3.15.b).

Without applying this method, the fibres in the end-zones of the specimen, at the top and bottom, would most probably be aligned horizontally to the walls of the mould. The normative tensile strength of such an end-zone, will for sure be lower than the tensile strength of the middle zone. Therefore, the fracture might occur outside the middle zone, in many cases near and along the glue layer (the so-called "glue-fracture"). In such a case, the goals of uniaxial tensile tests would not be fulfilled at all.

In order to ensure additionally that no glue-fracture takes place, the bottom- and the top-zone of the specimens, were stiffened by four thin steel strips. In both zones, two of them

were glued laterally outside (Fig 3.15.c), and two in grooves, inside. In the case of notched specimens, the notches were made about 3-4 weeks after casting. The notch depth was 5 mm, and the notches were cut from all 4 sides of the specimen.

The curing regime was the same for all specimens: 26 days at 20 ºC at a relative humidity of 95 - 100 %. After cutting of un-necessary pieces and attaching the steel strips, each specimen was glued to the upper and lower platen of the testing machine under a low compressive load (1 - 2 kN).
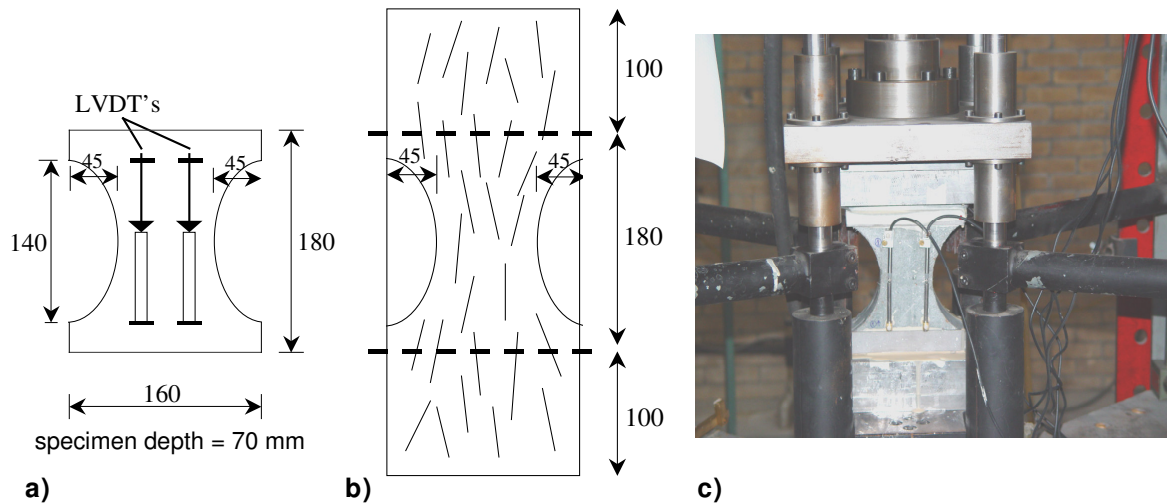
Fig. 3.15: a) Measurements of specimens for the uniaxial tensile tests, with positions of the LVDT's (in mm); b) Initial mould (length = 380 mm), and cutting lines, so that the final specimen height is equal to 180 mm; c) Specimen glued to the loading plates of the testing frame, with steel strips at top and bottom zone, and with LVDT's

A minimum of three samples was tested for each concrete composition, at an age of 28 days, in a deformation-controlled way. The crack opening was registered by 4 LVDTs ("Schlumberger", linear stroke +/- 1 mm), attached at the front and the back of the specimen (Fig. 3.15. a and c). A measuring length of 110 mm for fibre reinforced and of 35 mm for plain concrete specimens was used. In all cases two displacement rates were applied: 2 μm/s up to a displacement of 10 mm, and after that 20 μm/s, until the end of the test.

3.5.4 Results of uniaxial tensile tests

An overview of the results of the uniaxial tensile tests on HFC, will be presented in this sub-chapter. A more detailed overview of the results of these tests is given in [Markovic et al., 2004 a], and [Markovic et al., 2004 b]. Each type of concrete will be denoted according to the applied volume quantity of fibres, and to the corresponding fibre length. For example: 1.0% (13) + 0.5% (60), is concrete No. 5 (Tab. 2.3), which contains 1.0 vol.-% of fibres with l/d = 13/0.2, and 0.5 vol.-% of fibres with l/d = 60/0.7.

Also, instead of the experimentally measured tensile force, all results will be presented using the equivalent tensile stress. This stress (σ) will be derived from the tensile force (N), taking into account the linear elastic tensile behaviour and full cross section in the middle (A), as $\sigma = N / A$. Taking into account that the compressive strength of all concretes is rather similar, it will not be treated as an experimental parameter.

Uniaxial tensile strength

The uniaxial tensile strengths of all tested samples are given in Fig. 3.16. Obviously, the concrete which contains only long fibres, has only a slightly improved tensile strength compared to the reference plain concrete. On the contrary, whenever short fibres were present in the concrete, the tensile strength was always significantly improved (Fig. 3.16).
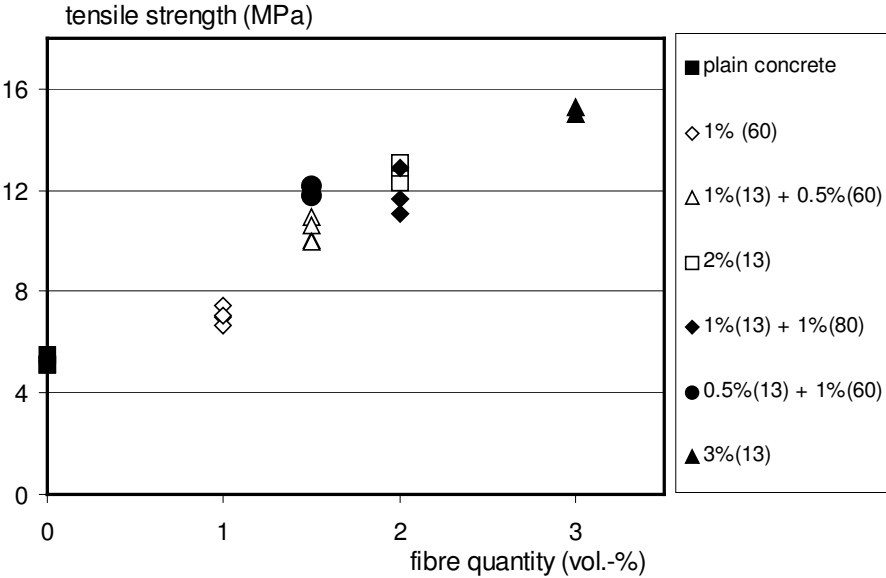
Fig. 3.16: Uniaxial tensile strengths of the applied concretes with one or two different types of fibres (the results of all single test are presented)

Similar values of the tensile strength (about 12 MPa) were obtained, if the concrete contained 1.5 vol.-% of both short and long fibres, and 2.0 vol.-% of only short fibres. For the same fibre volume content (1.5 vol.-%), if more long fibres were present, a slightly higher tensile strength could be achieved. The exchange of 1.0 vol.-% of short fibres $l/d = 13/0.2$, by 1.0 vol.-% of long fibres $l/d = 40/0.5$, did not result in a further increase of tensile strength.

A further increase of the fibre volume quantity leads to further improvement of the tensile behaviour. The maximum value of the tensile stress of about 15.2 MPa, was reached with the concrete that contained 3.0 vol.-% of short fibres. After this, a glue-fracture occurred. This value can therefore not be considered as the final tensile strength. As it will be shown later, the shape of the tensile diagram suggests, that even higher stresses could have been reached in this case.

All tensile strengths, given in Fig. 3.16, are obtained on un-notched specimens. Tensile tests on notched specimens were performed only for the concretes No. 5 and 6 (Tab. 2.3). Both the tensile strength and the ductility obtained with notched specimens, were higher than obtained with the un-notched ones. The tensile behaviour for both types of specimens will be presented and compared later in this sub-chapter.

Tensile behaviour of concretes with one type of fibre

The tensile behaviour of plain concrete (concrete No. 1, Tab. 3.2), serves as a reference for the tensile tests, taking into account that almost the same mixture composition was used (Fig 3.17.a). Almost the same value of tensile strength (about 4.5 - 4.8 MPa) could be registered in all tests on plain concrete. The softening branch could be registered only in one case, due to a slight bending of the specimen.
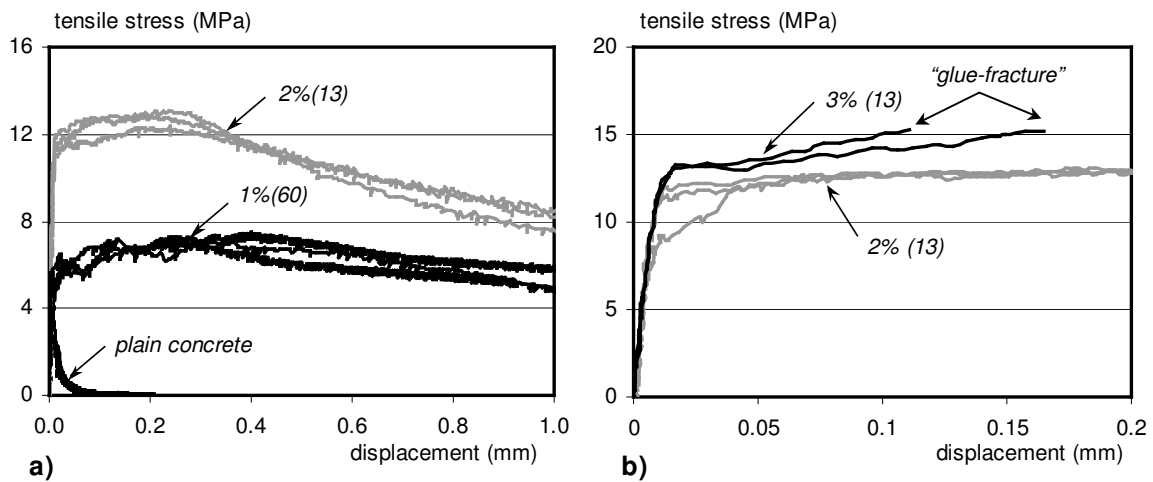
Fig. 3.17:   a) Tensile behaviour of plain concrete and concretes with only long (l/d = 60/0.7) and only short fibres (l/d = 13/0.2);   b) Tensile behaviour of concretes with 2.0 and 3.0 vol.-% of short fibres (l/d = 13/0.2)

The concrete with 1.0 vol.-% of long hooked-end fibres with *l/d* = 60/0.7 (concrete No. 7, Tab. 3.2), had a tensile strength of about 6.5 - 7.5 MPa (Fig. 3.17.a). This is an increase of about 20 % compared to the reference plain concrete. However, the first-cracking stress remained almost the same as the tensile strength of the plain concrete (about 5.0 MPa). The accompanied displacement was about 0.0025 mm. Naturally, the ductility of this concrete was significantly larger than that of the plain concrete. Strain hardening occurred up to 0.30 - 0.45 mm, after which tensile softening started. The tensile capacity was totally exhausted at a displacement of about 20 mm, which corresponds to 1/3 of the fibre length (*l* = 60 mm). The scatter in the tensile behaviour was extremely low.

The concrete with 2.0 vol.-% of short straight fibres l/d = 13/0.2 (concrete No. 2, Tab. 3.2), had a tensile strength of about 12.0 - 13.0 MPa (Fig. 3.17.a). This is an increase of about 150 % with regard to the reference plain concrete, and of about 100 % compared to the concrete with 1.0 vol.-% of long fibres only. The first-cracking stress was also significantly improved to about 11 MPa. This is mostly due to the presence of short fibres. They obviously bridge the microcracks much more efficient than the long fibres. This is due to their small diameters, large number and relatively small distances. Similar effects were observed in the flexural tests as well.

Strain hardening occurred up to a displacement of about 0.2 - 0.3 mm, after which the strain softening began. The tensile capacity was totally exhausted at a displacement of about 4 mm, which corresponds to 1/3 of the fibre length (l = 13 mm), like for the concrete with the long fibres. The total area under the stress-displacement diagram (i.e. the fracture energy) was about 1.4 times higher in the case of the concrete with the long fibres. Similarly as for concrete with long fibres, the scatter in the tensile behaviour was extremely low.

A comparison of tensile behaviour of the concretes with 2.0 vol.-% and 3.0 vol.-% of short fibres (concretes No. 2 and 3, Tab. 3.2), is given in Fig. 3.17.b. Just like concluded before, the more short fibres are present in the concrete, the higher is the first-cracking stress. In this case, the addition of another 1.0 vol.-% of short fibres, increased the average value of the first-cracking stress with about 20 %. The maximum tensile stress that could be registered, was about 15.3 MPa. A clear tendency of further growth of the tensile stress existed. However, at this stress level, a glue fracture occurred.

Tensile behaviour of Hybrid-Fibre Concretes

A comparison between the uniaxial tensile behaviour of hybrid-fibre concrete with 1% long and 0.5 % short fibres and the concrete with 2.0 vol.-% of short fibres only, is given in Fig. 3.18 (concretes No. 5 and 2, Tab. 3.2). Long fibres have a l/d = 60/0.7, and short fibres l/d = 13/0.2. The first-cracking stress is about 30 % lower for the hybrid-fibre concrete. This is mostly due to the 4 times lower quantity of short fibres (0.5 vol.-%), compared to concrete with 2.0 vol.-% of short fibres.

However, the strain hardening phase is much more pronounced for the hybrid-fibre concrete (Fig. 3.18). Therefore, the tensile strength of this concrete (on average about 11.75 MPa) is only slightly lower, than the tensile strength of the concrete with only short fibres (on average about 12.5 MPa). Due to the large pullout capacity of the long hooked-end fibres, the ductility of the hybrid-fibre concrete, will also be higher, than the ductility of concrete with only short straight fibres.

It should also be noted that the applied volume quantity of the fibres is 0.5 vol.-% lower in the case of hybrid-fibre concrete. The obtained tensile strength is however almost the same as for the concrete with 2.0 vol.-% of short fibres only, and the ductility is higher. Only the first-cracking stress is somewhat lower. Thus, the mechanical properties of the hybrid-fibre con-

crete are in general very similar to the concrete with larger volume quantity of short fibres only. Its price is however lower. Therefore, the hybrid-fibre concrete can be more suitable for the utilisation in the engineering practice in many cases.
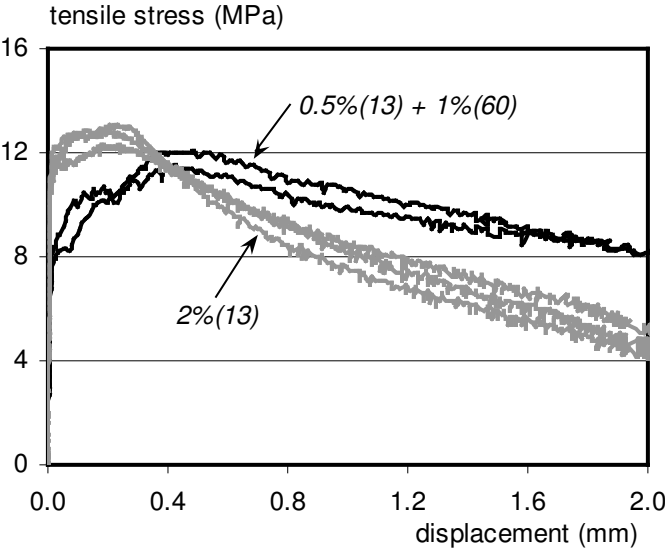
Fig. 3.18: Comparison of tensile behaviour of concrete with 2.0 vol.-% of only short fibres (l/d = 13/0.2), and concrete with in total 1.5 vol.-% of both short and long fibres (l/d = 13/0.2 and 60/0.7, respectively)
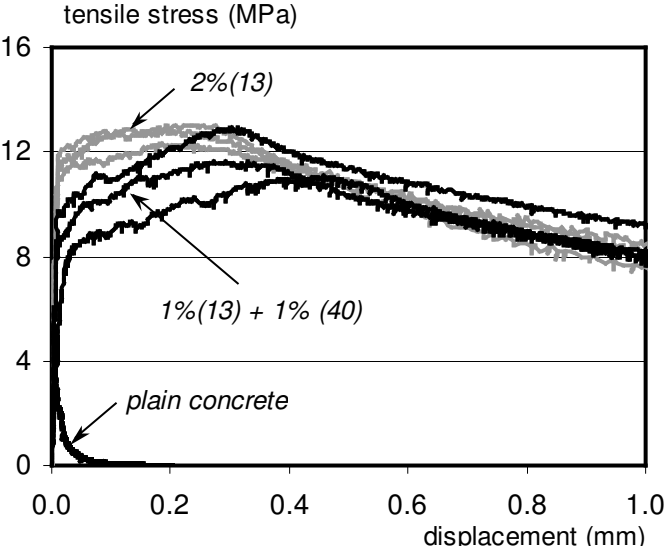
Fig. 3.19: Comparison of the tensile behaviour of concrete with only short fibres (l/d = 13/0.2), and concrete with the same amount of short and long fibres (a combination of l/d = 13/0.2 and l/d = 40/0.5)

A comparison of the tensile response of hybrid-fibre concrete and concrete with only short fibres, which both contain 2.0 vol.-% of fibres, is given in Fig. 3.19 (concretes No. 6 and 2, Tab. 3.2). The long fibres, applied in the hybrid-fibre concrete, have a $l/d = 40/0.5$, and the short fibres a $l/d = 13/0.2$. In the hybrid-fibre concrete, 1.0 vol.-% of the short fibres is thus exchanged with 1.0 vol.-% of the long fibres, in order to observe possible differences in the tensile behaviour.

Similarly to all previous cases, the first-cracking stress was somewhat lower for the hybrid-fibre concrete, which contained less short fibres compared to the concrete with only short fibres. However, the strain hardening was much more pronounced for hybrid-fibre concrete. A similar situation can be observed in Fig. 3.18 as well. The average tensile strength that could be reached with hybrid-fibre concrete, was almost the same as the one with concrete with short fibres only. The ductility is more pronounced for hybrid-fibre concrete.

Concretes No. 4 and 5 (Tab. 2.3), are both hybrid-fibre concretes with 1.5 vol.-% of fibres. The applied long fibres have $l/d = 60/0.7$, and short fibres $l/d = 13/0.2$. The concrete No. 4 contains more short fibres, and the mixture No. 5 more long fibres. For this combination of fibres, no large differences in the first-cracking stress could be observed. The variation in volume quantity of short fibres was not that high, and this was probably the reason that no differences could be observed. Strain hardening was somewhat more pronounced for concrete with long fibres. Also, somewhat higher tensile strength was registered for this concrete.

Tensile behaviour: un-notched vs. notched specimens

Rather controversial differences in tensile behaviour of specimens with and without notches, were discussed in the sub-chapter 3.3.3. While some researchers observed significant differences, the other obtained almost identical tensile behaviour of notched and un-notched specimens.

The specimens in laboratory tests, should simulate as much as possible the real situation in the structures. As already pointed-out, real structures do not have notches. All tensile tests in this research project, were therefore performed using the un-notched specimens. The tests using notched specimens, were performed only for concretes No. 5 and 6 (Tab. 3.2), in order to observe possible differences.

The comparisons in tensile behaviour of un-notched and notched specimens, is given in Fig. 3.20.a and b. In both cases, the values of the first-cracking stress were only slightly higher for notched specimens. Therefore, the similar amount of short fibres is active in bridging of microcracks in un-notched and in notched specimens. This points out, that the microcracking zone probably has approximately the same size in both types of specimens, although rather large stress concentrations are present around notches. Therefore, in this case, the first-cracking stress can be considered as a material property, because it is independent of the applied type of specimen. However, this is valid only if the number and orientation of fi-

bres are similar in un-notched and notched specimens, i.e. if the production process of specimens is constant.
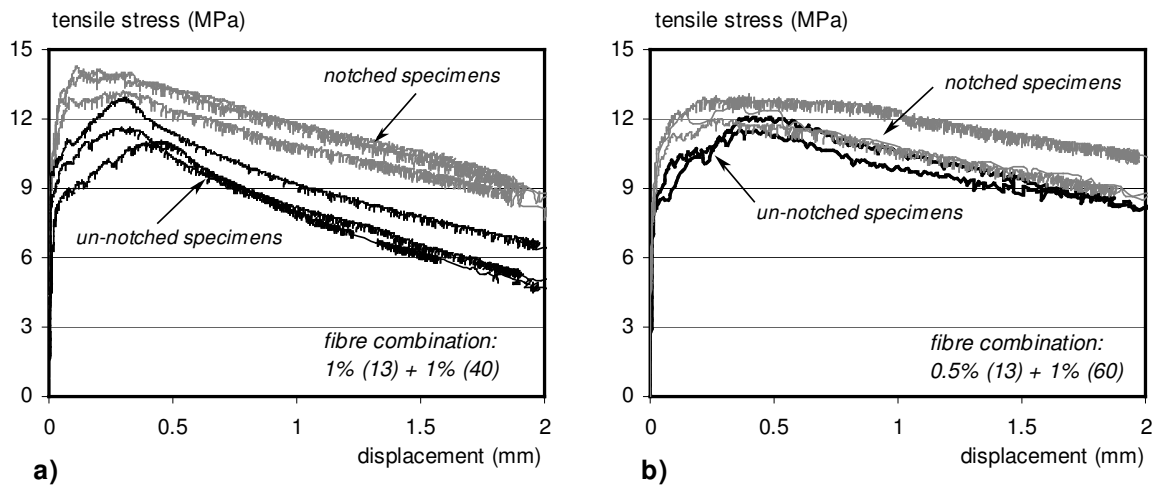
Fig. 3.20: Comparisons of tensile behaviour of notched and un-notched specimens, for hybrid-fibre concretes with: a) 1.0 vol.-% of short fibres (l/d = 13/0.2) and 1.0 vol.-% of long fibres (l/d = 40/0.5);   b) 0.5 vol.-% of short fibres (l/d = 13/0.2) and 1.0 vol.-% of long fibres (l/d = 60/0.7)

In both cases, the strain hardening is somewhat more pronounced for notched specimens. Also, the tensile strength was about 10-15 % higher for notched specimens in both cases. In fibre concrete, the crack path, i.e. the fibres which cross it, determine the tensile behaviour. Obviously, in notched specimens, this path is strongly predetermined by the notches self. The notches exist at all four sides of the specimens.

In specimens without notches, the cracking takes place there, where the minimum resistance exists. Therefore, somewhat worse tensile behaviour can be expected in this case, when no notches are present. The tensile behaviour of un-notched specimens, is however the most realistic one, and should therefore be used as a basis for structural design. A detailed analysis of the crack path and fibre distribution in un-notched and notched specimens, will be presented in section 3.6.7.

3.5.5   Summary and concluding remarks on uniaxial tensile behaviour of HFC

In this sub-chapter, the results of uniaxial tensile tests on 7 different types of concretes, reinforced with one and two different types of steel fibres, are presented. All uniaxial tensile tests were performed using the "dog-bone-shaped" specimens. The maximum volume quantity of fibres was limited to 2.0 vol.-% in all concretes, except in one, where 3 vol.-% of fibres were applied. It was possible to obtain high values of tensile strength (maximum of more than 15 MPa) and first-cracking stress (maximum up to 12 MPa). The significant level of strain hard-

ening was registered in all tested concretes, except in plain concrete. The scatter in registered tensile behaviours, was very low.

On the basis of performed tests, the following may be concluded:

1. An approximately equal number and orientation of the fibres must be must be provided in the tensile specimens, especially if long fibres are applied. This is important to avoid the "glue-fracture" during the uniaxial tensile tests on fibre concrete.

2. No large difference between the uniaxial tensile strength of plain concrete and concrete with only long fibres was observed. On the contrary, the concrete with only short fibres, had significantly higher tensile strength and first-cracking stress. This shows that short thin fibres bridge the microcracks in the concrete much more efficiently than long fibres. However, the strain hardening of the concrete with long fibres was more pronounced.

3. Hybrid-fibre concretes possess a somewhat lower first-cracking stress than concretes with short fibres only. The strain hardening is however more pronounced for hybrid-fibre concretes. This is the reason why the hybrid-fibre concretes and the concrete with short fibres only possess almost the same tensile strengths, in spite of a 0.5 vol.-% lower volume content of fibres in the hybrid-fibre concrete. Hence, the hybrid-fibre concrete possesses a similar tensile response as concrete with short fibres only, whereas its material costs are rather lower.

4. The tensile behaviour of the notched specimens was better than that of the un-notched specimens, for the same quantity and combination of fibres and the same production process. This is a consequence of the pre-defined cracking path in the notched specimens.

3.6 Number, orientation and deformability of fibres

3.6.1 Introduction

The number, orientation and deformability of fibres in the specimens, have significant influence on the tensile behaviour of any fibre concrete. These parameters were determined using both the manual and the optical approach, as explained in the sub-chapter 3.3.4. In this sub-chapter, the results for both the flexural specimens (beams), and the tensile specimens (dog-bone-shaped specimens) will be presented.

Tab. 3.3.: Number and orientation of short and long fibres in flexural and tensile specimens, determined by optical and manual method

No.	applied fibres (vol.-%)			number of fibres per cm²			orientation coeff. of fibres			orient. angle of fibres (degrees)			manually counted total number of long fibres		
	6/0,16	13/0,2	60/0,7	6/0,16	13/0,2	60/0,7	6/0,16	13/0,2	60/0,7						
FLEXURAL TESTS															
1		2.0			32.19			0.637			50.5				
2		0.5	1.0		8.88	1.33		0.691	0.912		46.3	24.2	317	370	290
3		0.5	1.0		8.23	1.40		0.703	0.921		45.4	22.9	299	257	273
4		2.0	1.0		27.77	1.95		0.721	0.853		43.9	31.5	422	349	285
5	2.0		1.0	33.16		1.60	0.596		0.862	53.4		30.5	329	299	301
6			1.0			1.46			0.770			39.7	306	333	313
						average:	0.596	0.688	0.864	53.4	46.6	30.3			
TENSILE TESTS															
7		2.0			42.63			0.770			39.7				
8		2.0			40.91			0.826			34.3				
9		2.0			42.91			0.927			22.0				
10		2.0			40.34			0.787			38.1				
11		0.5	1.0		10.43	2.06		0.805	0.917		36.4	23.5	112	98	110
12		0.5	1.0		11.87	1.50		0.841	0.872		32.8	29.3	112	98	110
13			1.0			2.50			0.832			33.7	107	101	95
14			1.0			2.30			0.856			31.1	107	107	95
						average:		0.826	0.869		33.9	29.4			

In Tab. 3.3, the overview of optically and manually determined number of fibres, and of the optically determined orientation of fibres, is given. In the table, a difference is made between concretes with only one fibre type, and hybrid-fibre concretes. In the manual approach, only long fibres were counted in 3 specimens belonging to the same concrete type (last column of the Tab. 3.3).

3.6.2 Number of fibres

The number of both short and long fibres per cm², determined by optical method, both in flexural beams and in tensile specimens, is given in Fig. 3.21.a and b. The exact values are given in Tab. 3.3.

Slightly higher number of fibres per cm² could be found in tensile specimens. In both types of specimens, the number of short fibres per cm² is much higher than the number of long fibres (Fig. 3.21). The registered number of short fibres in tensile specimens, showed a very low scatter (in specimens No. 7, 8, 9 and 10, Tab. 3.3.). In flexural specimens, this scatter was somewhat higher (in specimens 1 and 5, Tab. 3.3.).
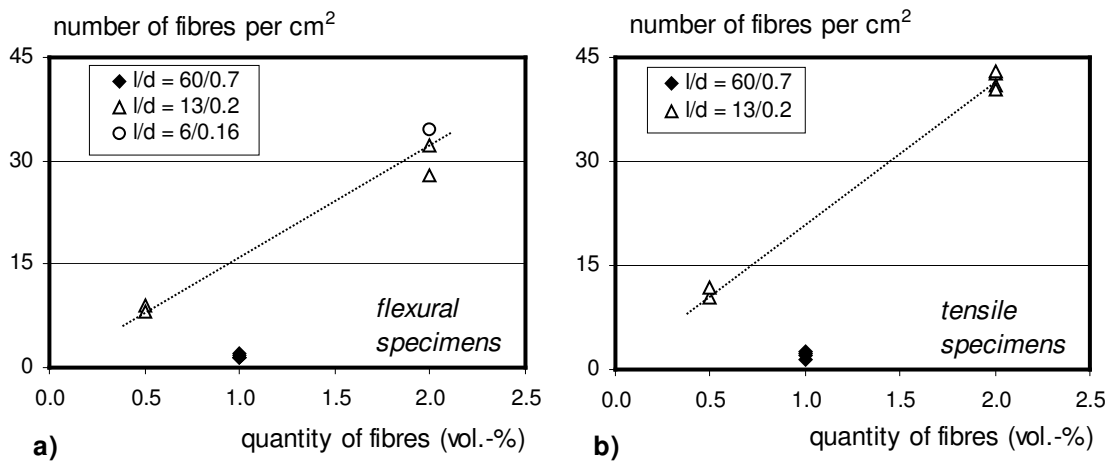
Fig. 3.21: Number of short (l/d = 13/0.2 and l/d = 6/0.16) and long fibres (l/d = 60/0.7), per cm² of the cross-sections of: a) Flexural specimens (beams);   b) Tensile specimens

For the same volume quantity of short and long fibres (e.g. 1.0 vol.-%), about 10 times higher number of short fibres per cm² may be expected. With that much larger number per cm², it is natural that short fibres are much more active in bridging of microcracks. The registered number of short fibres (l/d = 13/0.2), followed with approximate linear proportion their applied volume quantities (0.5 vol.-% and 2.0 vol.-%, in Fig.3.21, in both flexural and tensile specimens.

3.6.3   Orientation of fibres and its relation to the production process of specimens

The orientation angls of both short and long fibres, determined by optical method, both in flexural beams and in tensile specimens, are given in Fig. 3.22.a and b. The exact values are given in Tab. 3.3. The ideal orientation angle of fibres is theoretically equal to 0°. In such a case, all fibres are fully aligned in the direction of main tensile stress.

The long fibres (*l/d* = 60/0.7) had extremely high orientation coefficients, both in flexural and in tensile specimens. The orientation coefficients of these fibres, range from 0.77 to 0.917 (Fig. 3.22, and Tab. 3.3.), with an average value of 0.867. Also, the long fibres have similar orientation in both flexural and tensile specimens, in spite of more than 4.5 times larger cross-section of flexural specimens. The long fibres have much more space to rotate in flexural specimens, but this is not happening.
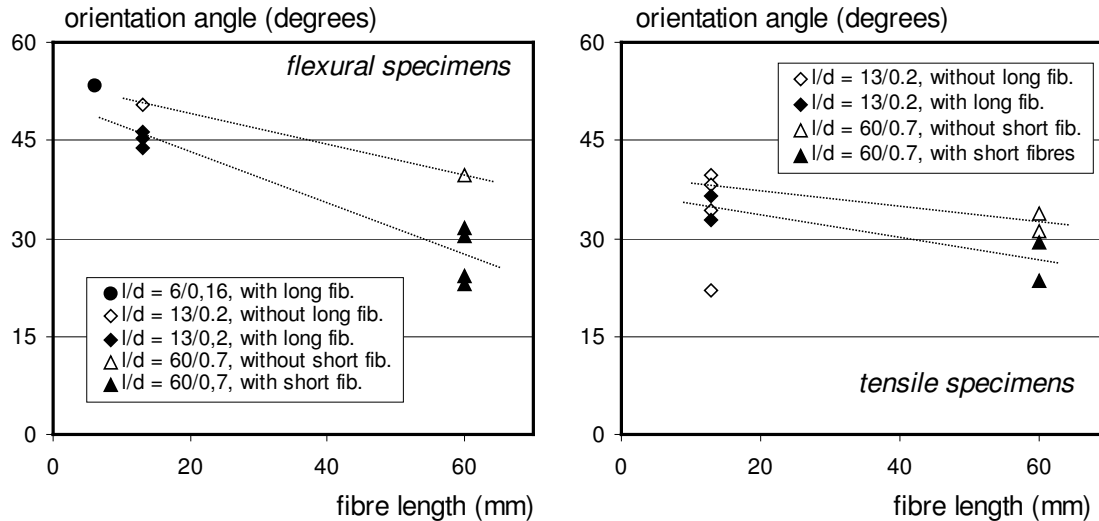
*Fig. 3.22: Average angles of orientation of short (l/d = 13/0.2 and l/d = 6/0.16) and long fi-
bres (l/d = 60/0.7), in the cross-sections of: a) Flexural specimens (beams);   b) Tensile
specimens (for orientation angle of 0º, all the fibres are aligned with the main tensile stress)*

The reason for this is most probably the applied method of casting of the fresh self-
compacting fibre concrete layers (Fig. 3.4), which was applied both for flexural and tensile
specimens. The thickness of each layer is couple of times smaller than the fibre length, so that
there is not much possibility for the long fibres to rotate in the vertical plane (Fig. 3.23.a).

Long fibres also cannot rotate much horizontally, in the plane of each layer. The reason for
this is probably the rather narrow shovel, which has been used for casting (Fig 3.23.b). It has
been observed during casting, that long fibres are more-or-less aligned, while they are already
in such a shovel. Therefore, they will remain aligned also in each type of mould where they
are cast.

Therefore, the method of casting in layers can guarantee the fibres have very good alignment
to the main tensile stress, no matter of the shape and the size of the specimen. The scatter of
the orientation coefficients was also rather low, again due to the constant casting process. It
can be concluded, that through the casting in layers, the orientation of long fibres can be con-
trolled on a very satisfying level in laboratory conditions.

It is however somewhat more difficult to control the orientation of short fibres through the
casting process. These fibres are about 5 times shorter compared to long fibres (*l/d = 13/0.2*),
and can therefore rotate in each single layer of cast fresh concrete, both in vertical and in
horizontal direction (Fig. 3.23). The orientation coefficients of short fibres are therefore lower
than those of long fibres, and vary from 0.630 to 0.927, with an average value of 0.754.
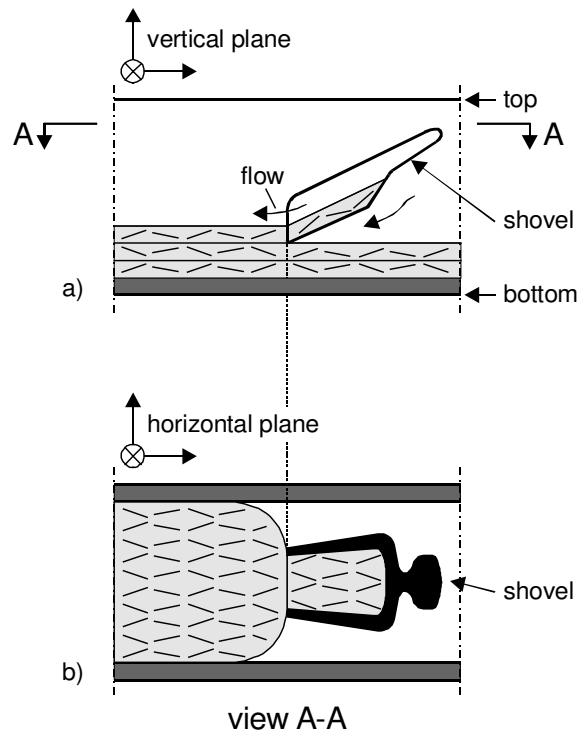
Fig. 3.23: The orientation of long fibres during casting of self-compacting fibre concrete in layers with a shovel: a) in the vertical plane of the mould;   b) in the horizontal plane of the mould

The short fibres (*l/d* = 13/0.2), are somewhat better oriented in tensile, than in flexural specimens (Fig 3.22). This is most probably by virtue of the smaller layers of fresh concrete in tensile specimens, i.e. by virtue of the smaller cross-section area of tensile specimens. Also, shorter fibres (*l/d* = 6/0.16) possess lower orientation coefficients than longer fibres (*l/d* = 13/0.2).

No clear relations between fibre orientation and tensile behaviour could be find. The most possible reason for this, is a large similarity of the orientation coefficients self. The scatter in the tensile behaviour was also very small, especially in concretes with only short and only long fibres. This is directly related to such a similar number and orientation of fibres. It should however bear in mind, that the estimated orientation by optical method, does not perfectly match to the actual orientation of fibres in the cracking zone and across the crack.

3.6.4   Influence of long and short fibres on each other's orientation

In each hybrid-fibre concrete, there is an interaction of long and short fibres during casting of concrete specimens, which is of special interest in this analysis.

In Fig. 3.22.a and b, the black symbol represents hybrid-fibre concretes, and the white symbols concretes with one type of fibre. Both figures clearly show, that the long fibres are somewhat better oriented, if also the short fibres are present in concrete. Similarly, short fibres are better oriented, if long fibres are present in concrete. This could be observed in all analysed specimens, both tensile and flexural.

In Fig. 3.24, the possible orientation of short fibres with and without long fibres in concrete, is presented. Long fibres are always well oriented between the two imaginary borders, if casting of concrete in layers was applied (these borders may also be the walls of the mould). With such positions, the long fibres form a kind of a barrier for short fibres, and limit their space for rotation. The short fibres will therefore be somewhat better oriented when combined together with long fibres, than on their own.

However, according to the situation given in Fig. 3.24, this limitation is mostly present in the vertical plane. Short fibres may still rotate in other directions (in 3D), where no long fibres exist in the vicinity. Therefore, the positive influence of long fibres is not that high, but it exists in both types of tested specimens, and should not be neglected as such.
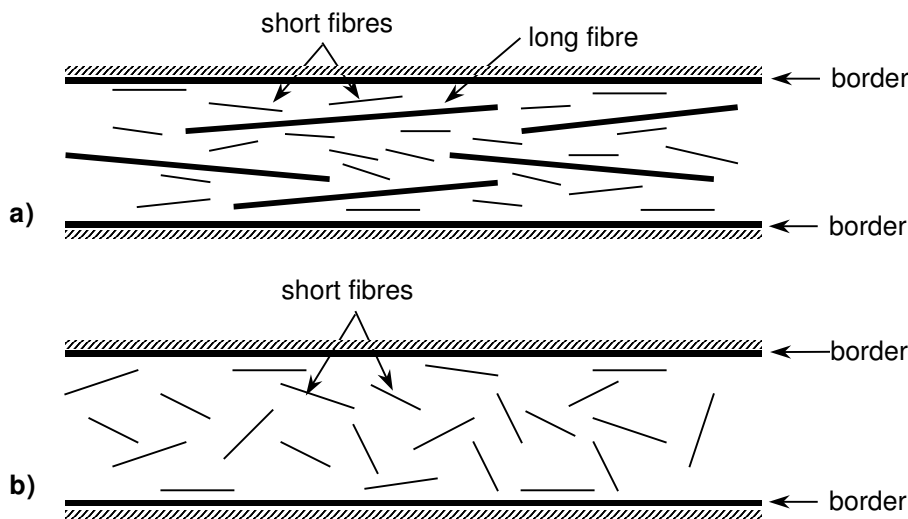
Fig. 3.24: Orientation of short fibres between the walls of the mould (or any other borders in general), in combination with long fibres (a), and when they are alone on their own (b)

3.6.5 Visible (pulled-out) lengths of fibres

The visible (pulled-out) lengths of fibres and the deformability of fibre hooks, are determined only for long hooked-end fibres, as explained in the sub-chapter 3.3.4. This has been done for specimens with long fibres only, as well as for specimens with both short and long fibres (hybrid-fibre concrete).

In Fig. 3.25, the probability $p(l_{vis})$ is denoted, that a fibre with a visible length l_{vis} may be found on a fracture plane, i.e. that a fibre will cross a crack on the distance l_{vis} from one of

fibre ends. This probability was determined only for long fibres with $l/d = 60/0.7$, firstly for all, and then only for active fibres. This has been done both for flexural specimens (Fig. 3.25.a), as well as for tensile specimens (Fig. 3.25.b).

It should take into account that flexural specimens possess notches, while tensile specimens are un-notched. The cross-section of flexural specimens is also about 4.5 times larger than the cross-section of tensile specimens. Therefore, some differences in the analysed parameters may be expected.

In flexural specimens (Fig. 3.25.a), there is almost the same probability $p(l_{vis})$ of about 25 %, that fibres with visible lengths between 10 and 30 mm can be found on the fracture plane. This does not depend on applied fibre combination (only long or both short and long fibres).

A rather different situation was observed in tensile specimens (Fig 3.25.b). In these specimens, for the concrete specimens with both short and long fibres (hybrid-fibre concrete), more fibres with longer visible lengths can be found on the fracture plane, compared to concrete specimens with only long fibres. So was the most frequent visible length $l_{vis} = 20\text{-}30$ mm in hybrid-fibre concrete, and $l_{vis} = 10\text{-}20$ mm in concrete with long fibres only. The differences between flexural and tensile specimens are caused by different sizes and type of the specimens (notched vs. un-notched).
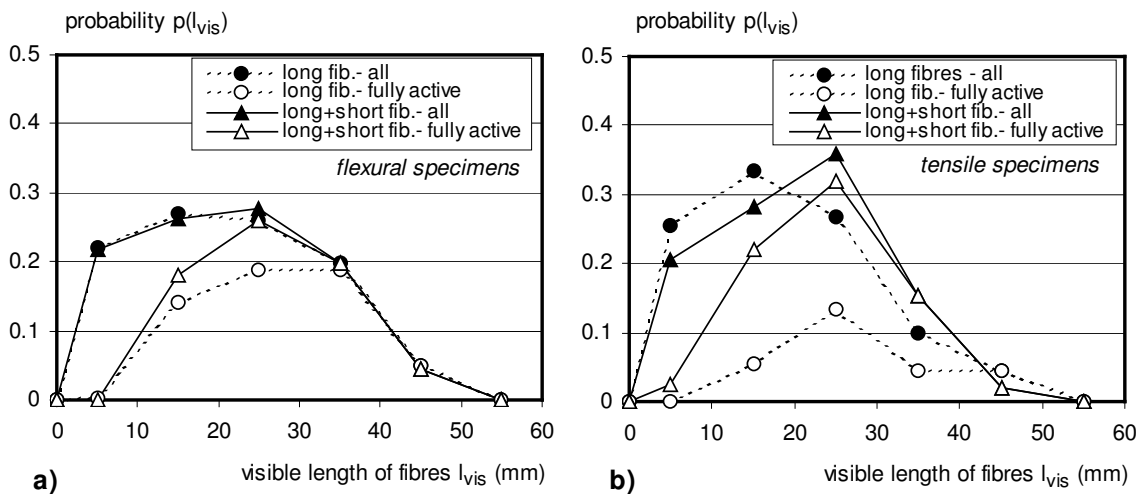
Fig. 3.25: Probability p(l$_{vis}$), that a fibre with a visible (pulled-out) length l$_{vis}$, can be found on the fracture plane of the: a) flexural specimens;   b) tensile specimens;   (these specimens contain only long or both short and long fibres; if the hook of long fibre is fully deformed, than is that fibre "fully active" in crack bridging)

If the fibre is longer, the probability is higher, that its hook will be fully deformed. This was observed in both flexural and tensile specimens. The fibre is then considered as "fully active" (i.e. fully effective in crack bridging).

If concrete contains both short and long fibres, the probability of hook deformation is also higher. This was observed for both types of specimens. However, this probability was higher in flexural than in tensile specimens. This is most probably, the circumstance of different types and sizes of flexural and tensile specimens. A detailed analysis of the deformability of fibre hooks will be given in the following sub-chapter.

Also, in both types of specimens, about 20% of long hooked-end fibres possess a higher visible (pulled-out) length than the half of their full length l, $l = 60$ mm. Therefore, the pullout process of long hooked-end fibres is not governed only by shorter embedded length, but also by the microstructure of concrete around each fibre.

3.6.6 Deformability of fibre hooks

The probability that the hook of a fibre with a visible length l_{vis}, will have a fully deformed hook, is denoted as $p(d)$. This probability for flexural and tensile specimens is given in Fig. 3.26.a and b. For eventual comparisons, it should again take into account different sizes and types of these specimens.

In both types of specimens, the fibres with short visible lengths (< 10 mm), where the crack passed almost near the fibre end, cannot deform the hook in about 0-15 % of cases. If crack passed near the middle of the fibre or even further, this probability becomes much higher.
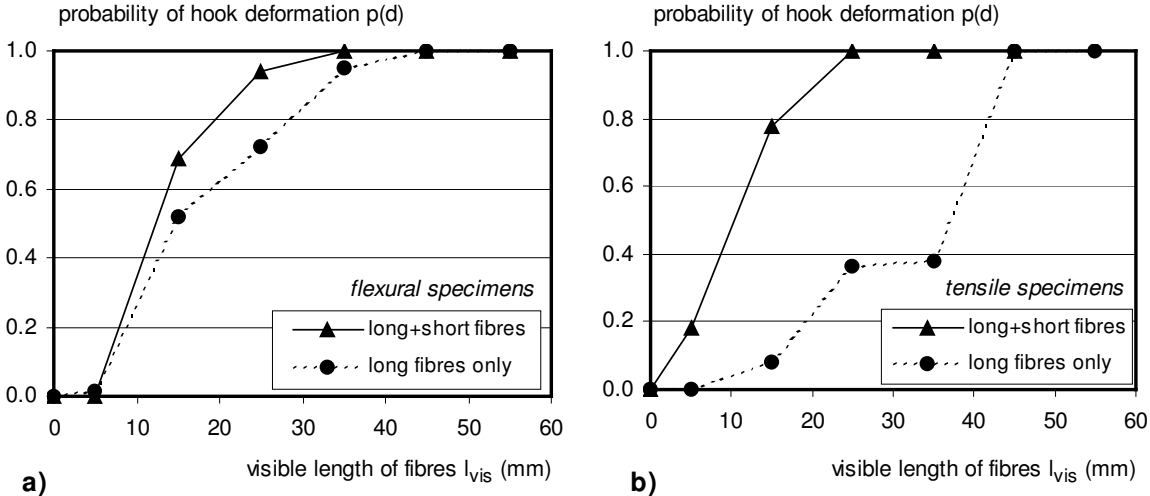
Fig. 3.26: The probability that a hooked-end fibre on a fracture plane, with a visible length l_{vis}, will have fully deformed hook, for specimens with only long, and with both short and long fibres, tested in: a) flexural tests;   b) tensile tests

In both tensile and flexural specimens, the presence of short fibres has very positive effects on the deformation of hooks of long fibres (Fig. 3.26. a and b). Concretes with only long, as well as with both short and long fibres, were analysed. In flexural specimens, for visible lengths of long fibres ranging from 20-30 mm, about 95% of fibres had fully deformed hooks, when

combined with short fibres (Fig. 3.26.a). When the concrete contained only long fibres, this number was about 70%. The refinement of the mixture composition contributes further to the improvement of the deformability of fibre hooks [Markovic et al., 2003-d].

In tensile specimens, the influence of short fibres on deformability of the hooks of long fibres, is much higher than in flexural specimens (Fig. 3.26.b). For visible lengths of long fibres ranging from 20-30 mm, all long fibres (100%) had fully deformed hooks, if the concrete contained also short fibres. If the concrete contained only long fibres, only about 40% of fibres possessed fully deformed hooks. Such a large difference in the deformation of fibre hooks in flexural and tensile specimens, were similarly as before, the circumstance of the different types and dimensions of these specimens.

Therefore, the role of short fibres is not only to bridge microcracks. They are also increasing the efficiency of long fibres during crack bridging, by the deformation of the hooks of these fibres. The similar phenomenon was observed in the pullout tests on long hooked-end fibres, from concretes, which contain also short fibres (Fig 2.26, sub-chapter 2.9.4).

3.6.7 Differences between un-notched vs. notched specimens; Segregation potential of fibres

The differences in visible lengths and deformability of fibres, between notched and un-notched specimens, were analysed as well (Fig. 3.27.a). This analysis is provided for concrete No. 6 (Tab. 3.2), which contains both short and long fibres (1%(13) + 1%(40)). Rather large differences in tensile behaviour of notched and un-notched specimens made of this concrete, were observed (Fig.3.20.a).

As mentioned in the sub-chapter 3.3.3, the crack searches and follows the path of the lowest resistance in the un-notched specimen. Indeed, the dominant visible (pulled-out) length of long fibres in un-notched specimens ranges from 0 to 10 mm (Fig. 3.27.a). The chance for the full deformation of fibre hook is therefore automatically smaller. Similarly as in all other tensile and flexural specimens, if the crack passes on larger distance from the fibre hook, the chance of hook deformation gets higher. This was very pronounced in notched-specimens. These specimens were notched from all 4 sides. Therefore, the crack has almost no possibility to deviate from the, by the notches, pre-described path.

The number of fibres with deformed hook is therefore higher in notched, than in un-notched specimens. For example, if the visible length of fibres is from 10 to 20 mm, almost 90 % of them will have fully deformed hooks in notched specimens. In case of un-notched specimen, only about 50 % of fibres have fully deformed hooks, for the same visible length (Fig. 3.27.a).

The notched-and un-notched specimens were here produced in the same way and with the same fibre combinations and quantities. The fibres along the cracking path in notched specimens, are thus always more active, compared to fibres at the cracking path of un-notched specimens. The fibres in notched specimens will therefore produce much higher tensile resistance during crack bridging (Fig 3.20. a and b).
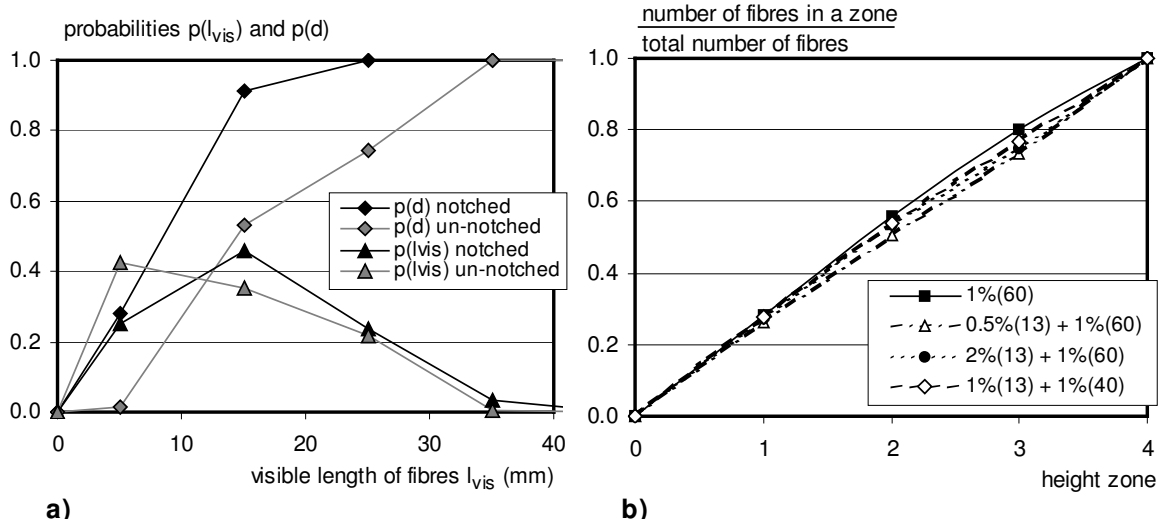
Fig. 3.27:   a) Differences in visible lengths and hook deformations of long fibres, expressed as probabilities p(l_vis) and p(d), for notched and un-notched specimens made of hybrid-fibre concrete, tensile responses of both types of specimens given in Fig. 3.20.a;   b) Number of fibres along the 4 height zones of the HFC beam specimens (cumulative distribution), which illustrates the segregation potential of fibres

The segregation potential of long fibres in flexural specimens, is given in Fig. 3.27.b. All presented values are an average of 4 values, one for each tested beam. In total 4 different concretes are tested, one with only long and 3 with both short and long fibres. Each fracture plane is divided in 4 height zones, and the fibres in each of them were counted. The first zone is the bottom zone, and the fourth zone is the top zone of the specimen. On the vertical axis, the cumulative relative number of fibres is given. Every distribution line is almost a straight line. Therefore, there is obviously no segregation of long fibres, i.e. all applied concretes are very stable.

3.6.8   Summary and concluding remarks on the number, orientation and deformability of fibres in flexural and tensile specimens

In this sub-chapter, the number, orientation and deformability of fibres in flexural and tensile specimens were determined and analysed. The analysis was performed using two methods: manual (counting of the fibres on the fracture planes), and optical (mathematical analysis of the photos of appropriate cross-sections of the specimens).

On the basis of performed analysis, the following may be concluded:

1. For the same applied fibre volume quantity, about 10 times more short than long fibres, are there in the cross-section of a HFC specimen. This explains the already proven ability of short thin fibres to bridge numerous microcracks in concrete.

2. Very good orientation of fibres, with respect to the direction of main tensile stress, were found. The orientation coefficients ranged up to 0.921 (orientation coefficient = 1.00 for ideal fibre orientation). The reasons for such a good orientation are the self-compactability of applied fibre concretes, as well as the specific method of casting in layers.

3. Long fibres were very well oriented both in flexural and in tensile specimens. Short fibres were somewhat better oriented in tensile specimens, because these specimens are smaller.

4. No clear relation between the orientation and number of fibres and tensile behaviour of tested concretes, could be found. This was due to the very low scatter in the complete tensile behaviour and also due to the low scatter in the orientation coefficients and observed number of fibres.

5. There is a tendency, that short fibres are better oriented when also long fibres are present in concrete, than when they are alone on their own. Long fibres may indeed act as barriers, and force the short fibres to align with them. This could be another advantage of Hybrid-Fibre Concrete.

6. If short fibres are present in concrete, the higher chance exist that the hook of long hooked-end fibres will be deformed. The long fibres are therefore much more effective in crack bridging. This was especially expressed in tensile specimens.

7. Similarly, if the visible length of long hooked-end fibre (on the fracture plane) is larger, the higher probability exist that the fibre hook will be deformed. The difference in visible fibre lengths (and therefore in fibre effectivity), is especially pronounced between notched and un-notched specimens.

8. In flexural beams, no segregation of long fibres at all, could be observed.

CHAPTER 4:

ANALYTICAL MODELLING OF TENSILE BEHAVIOUR

4.1 Introduction

In the previous chapter, the uniaxial tensile and flexural behaviour of Hybrid-Fibre Concretes (HFC) with different combinations and quantities of steel fibres were determined. This was followed by the determination of the number and the orientation of fibres in the applied testing specimens.

In this chapter, the qualitative and quantitative observation of the tensile fracture of Hybrid-Fibre Concrete will be given. Analytical modelling of the tensile behaviour of HFC will be presented. A literature overview of the existing analytical and numerical models will be given first in this chapter. This will be followed by the analysis of fracture processes during tensile loading of HFC. Subsequently, the analytical model for the softening behaviour of HFC will be introduced and explained. The modelling will be carried out at the meso-level, taking the pullout response of the fibres, as well as their number and orientation across the crack(s), as basic parameters. The modelling will initially concentrate on concretes with only short and only long fibres, in order to calibrate the appropriate modelling parameters. After that, these parameters will be implemented to the HFC with both short and long fibres. The modelled tensile response of this HFC will subsequently be compared with its tensile behaviour observed in the experiments. This will be followed by an evaluation of the analytical model.

The main goal of this modelling is to be able to predict the softening behaviour of Hybrid-Fibre Concretes, with different types and combinations of fibres.

Qualitative observation of tensile fracture of HPFRCC

4.2.1 Introduction

In chapter 3, the results of flexural and uniaxial tensile tests on different types of HFC were presented in a quantitative way, without going deeper into the tensile fracture processes. In this chapter, a detailed analysis of the tensile fracture process of HPFRCC will be given. The tensile response of HPFRCC and ordinary FRC will be compared as well.

According to [Van Mier, 2004 a], and [Van Mier, 2004 b], the tensile fracture of <u>any type</u> of concrete (actually also of almost all other building materials), can be subdivided into 4 main stages:

0) Elastic stage

A) Microcracking

B) Macrocrack growth

C) Bridging of macrocrack

It is important to notice that the tensile fracture of concrete is a continuous process, and that there are no firm limits between these stages.

The scheme in Fig. 4.1 represents the tensile fracture of Hybrid-Fibre Concrete, and it is partly based on [Van Mier, 2004 a and b]. In the following, each stage of the tensile fracture will be analysed in detail.
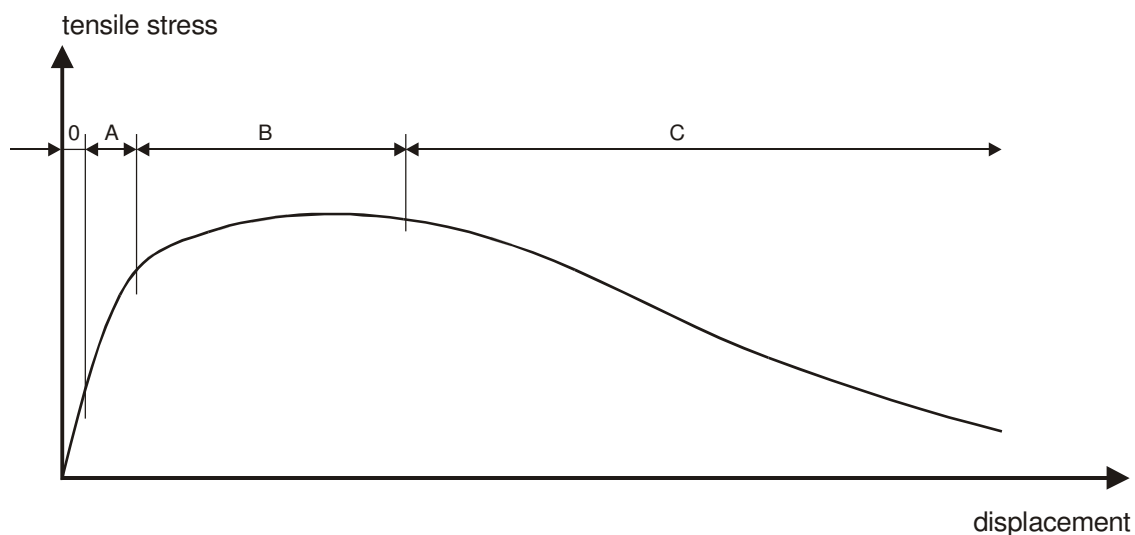
Fig. 4.1: Stages in the tensile fracture of Hybrid-Fibre Concrete: 0) Elastic stage; A) Microcracking; B) Macrocrack growth; C) Bridging of macrocrack

4.2.2 Stages in tensile fracture of concrete

0) Elastic stage

The tensile response in the elastic stage is almost linear elastic, and will not be analysed here.

A) Microcracking stage

What are microcracks?

The microcracking stage is probably the most important one in the tensile response of concrete. During this stage, the material is being prepared to break macroscopically [Van Mier,

2004 a]. Therefore, the tensile strength of the material depends strongly on its response during the microcracking stage. Also, on the structural level, the durability and permeability depend on the size and the number of microcracks.

A crack can be understood as a displacement-discontinuity in the structure of the material, characterised by separated crack planes. In cement-based materials, cracks can have different sizes (e.g. micro- and macrocracks). It is however still not generally accepted when a crack can be called micro- and when macrocrack.

In this thesis, the term "microcracks" will be used for those cracks, whose length is approximately equal to the average diameter of the applied aggregate composition. In the case of Hybrid-Fibre Concrete, this will be about 0.5 mm The width of a microcrack in plain concrete is dependent on its length, but in fibre concrete, also on the available resistance to crack opening. The experimentally observed microcrack widths in fibre concrete are about 8.0 μm in [Mobasher et al., 1990], or they vary from 1.5 to 13.6 μm, as reported in [Mihashi et al., 2002].

Why do microcracks occur?
The main reasons for the formation of microcracks are:
− the initial drying shrinkage and temperature gradients: by virtue of these phenomena, the cracks occur in any type of concrete even before it is loaded;
  For example, in hybrid-fibre concrete with polyethylene and steel fibres [Mihashi et al., 2002], many very fine cracks, generated by virtue of drying shrinkage, were observed even before the mechanical loading was applied. These initial cracks formed a clear path for the subsequent development of larger cracks in the loaded specimen. Similar initial cracking can be observed in ordinary concrete and cement paste as well, such as in e.g. [Shiotani et al., 2003], and [Bisschop et al., 2002].
− after the applied loading (tensile or compressive), the microcracks occur around inclusions (aggregate grains, fibres), due to the weak structure of the interfacial zone between cement paste and these inclusions [Van Mier, 1997].
− the presence of air-bubbles (or generally any other inclusions) in concrete may create stress concentrations under tensile loading, and therefore lead to the formation of microcracks [Kabele, 2004]. To the author's knowledge, there are still no experimental evidences for this.

How to increase the tensile strength of concrete?
In order to increase the tensile strength of concrete, the growth and widening of microcracks should be stopped or eventually constrained by an appropriate resisting mechanism.

In plain concrete, the only resisting mechanism is the cement paste (Fig. 4.2.a and b). Having somewhat higher tensile strength compared to the interface zone, the cement paste can provide some resistance to further propagation of microcracks, but this occurs to a relatively small extent.

The higher the applied volume quantity of aggregate, the smaller the distance between the aggregate grains will be. Consequently, according to [Prado & Van Mier, 2003], the microcracks can propagate faster and easier in a plain concrete with a higher volume quantity of aggregate (Fig. 4.2.a), compared to the concrete with lower volume of aggregate (Fig. 4.2.b).
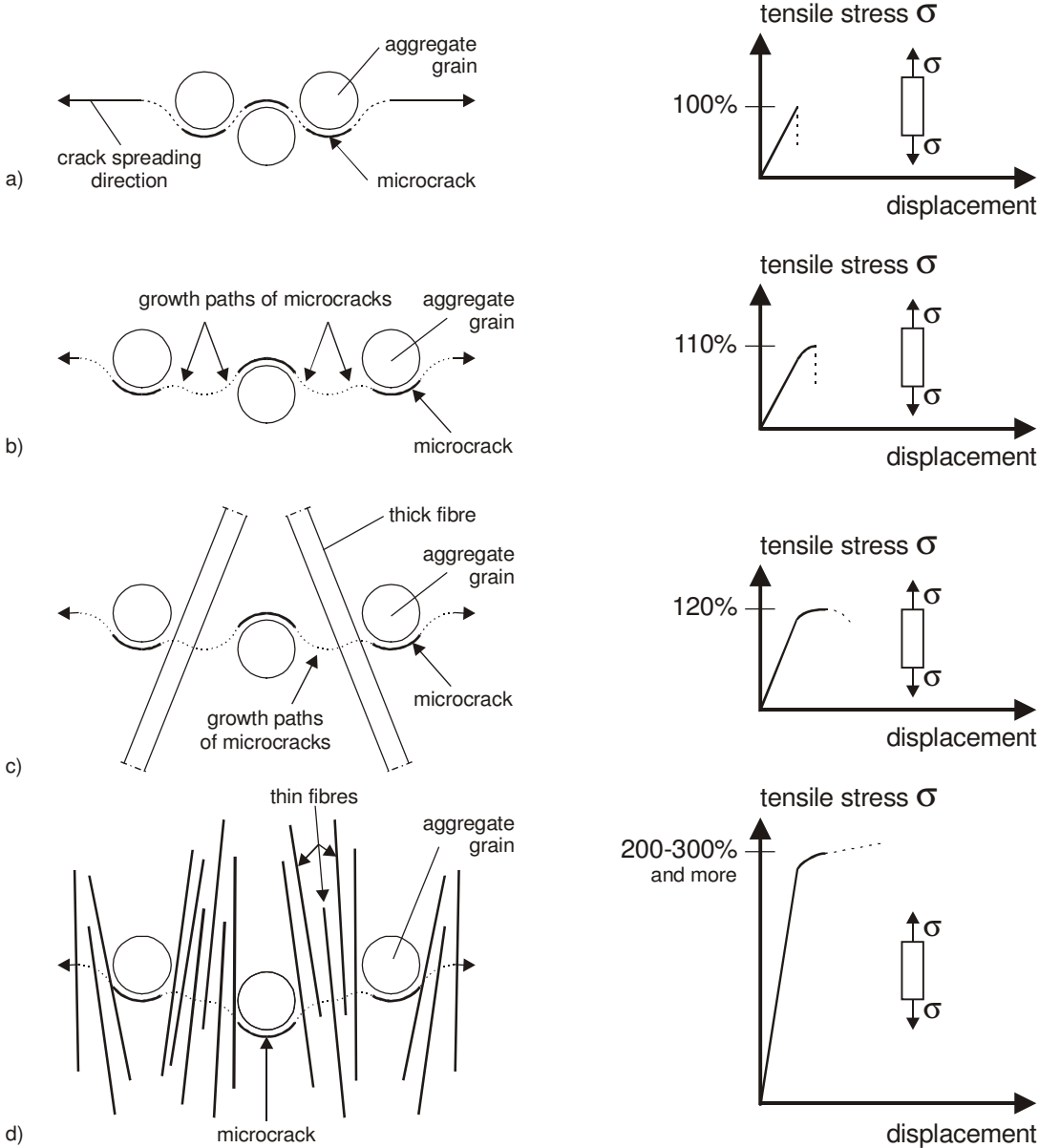
Fig. 4.2: The initial stages of uniaxial tensile fracture characterized by microcracking, and appropriate schematic diagrams of the uniaxial tensile response, for: a) plain concrete with high aggregate quantity;   b) plain concrete with low aggregate quantity;   c) fibre concrete with low quantity of thick fibres;   d) fibre concrete with high quantity of thin fibres;   (the numerical values given on the diagrams in %, serve only for an approximate orientation regarding the first-cracking tensile stresses in these concretes)

In the case of fibre concrete (Fig. 4.2.c, d), the development of microcracks can be very efficiently controlled, if more fibres with as smallest fibre spacing as possible and with an optimum orientation would be present in the microcracking zones. The smaller the fibre distance, the slower the propagation of the microcracks will be [Van Mier, 2004 a and b]. As a consequence, the first macrocrack develop at higher tensile stress (first-cracking stress), i.e. the higher tensile strength can be reached (Fig. 4.2.d).

This was experimentally proven first by [Romualdi et al., 1963], and later on also by e.g. [Mobasher et al., 1990], [Betterman et al., 1999] and [Akkaya et al., 2001], for fibre concretes with polypropylene fibres. In the latter, it was also observed, that the fibre-free areas in the specimen made of polypropylene-fibre concrete, reduce its tensile strength, because these fibre-free areas actually act as a sort of "defects" in the material.

However, not only the fibre spacing (i.e. the number of fibres), but also their orientation with respect to the tensile stress, and the quality of the fibre-matrix bond, are very important factors as well, when considering microcracking. Up to now, only a few studies partly dealt experimentally and/or analytically with these factors, such as [Karihaloo, 1995], and [Karihaloo et al., 1997].

B) Macrocrack growth

During this stage, an overpass must be made, from the microcracking stage, with many very fine cracks distributed throughout the specimen, to the crack-bridging stage, with usually one dominant crack. If the tensile loading of concrete continues after the formation of microcracks, the microcracks will propagate and connect with each other, creating bigger, so-called macrocracks. At the first instance, it can be supposed that a macrocrack has a length, which is couple of times higher than the largest grain diameter.

Within this dissertation, a macrocrack will be defined on the basis of the performed uni-axial tensile tests on HFC, as a crack that is spread across the whole cross section of the tensile specimen, i.e. as the so-called "through-crack". The tensile stress, which corresponds to the formation of the first through-crack, will be called the "first-cracking (tensile) stress".

Therefore, the macrocrack growth stage start at the moment, when the first "through-crack" has formed in the tensile specimen. This moment corresponds most probably to the first bent point on the tensile diagrams of HFC, which follows after the ascending branch (Fig. 4.1). There are however still no experimental evidences for this.

During the formation and growth of the macrocracks, the tensile load must be transferred from the cement matrix to other elements of the material, possessing the same or higher carrying capacity [Van Mier, 2004 b].

Both in ordinary concrete, as well as in conventional steel fibre concrete, this stage is accompanied with a fast and sudden loss of tensile carrying capacity (Fig. 4.3). In both cases, usually one single macrocrack appears.

In the case of ordinary concrete, almost no stress transfer is possible, because of the relative non-efficiency of the cement paste as a resistance mechanism. The macrocrack growth stage is therefore extremely short.

In conventional steel fibre concrete, there is a delay in transmission of tensile stresses from the cement matrix to the fibres during the propagation of the macrocrack [Van Mier, 2004 b]. This is a consequence of:

−   the relatively low number of fibres present in the cracking zone(s) – conventional fibre concretes usually contain rather low amounts of thick steel fibres. This means that the fibre distance within the cracking zones will be rather large, and that the macrocrack can propagate rather fast. Also, the applied fibres are thick, which does not "match" with the size of very fine and thin microcracks.

−   the relatively weak interface zone between the fibres and the cement matrix, causes a non-efficient stress transfer from concrete matrix to fibre.
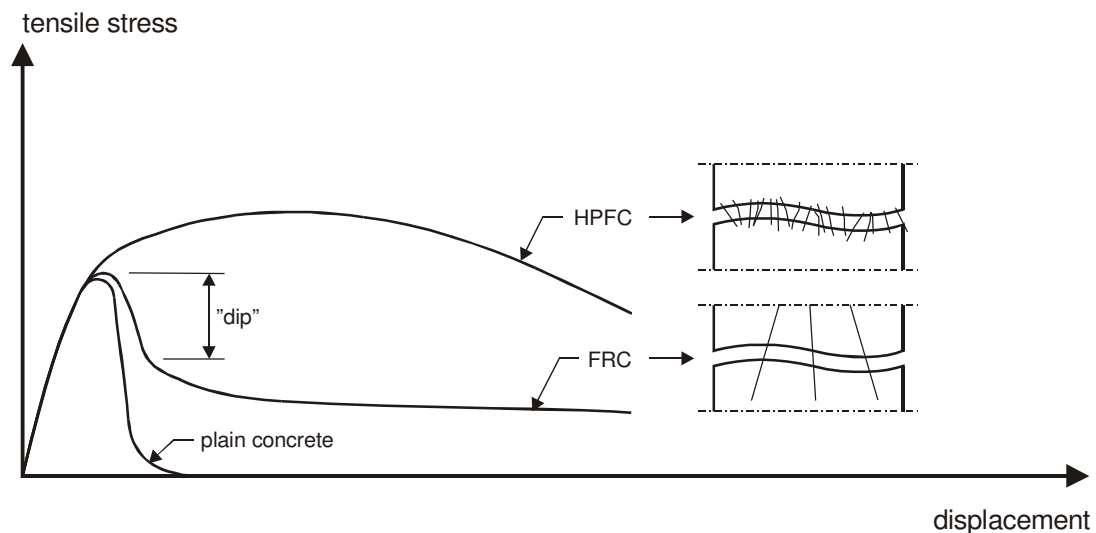
Fig. 4.3: Tensile responses with macrocrack growth stage for HPFRCC, conventional fibre concrete and plain concrete (the last two possess a characteristic "dip" in carrying capacity, due to a non-efficient stress transfer from matrix to fibres) (after [Van Mier, 2004b])

These two phenomena are the reasons for the "dip" in the uniaxial tensile diagram of conventional steel fibre concrete, which appears immediately after the tensile strength has been reached. Therefore, conventional fibre concrete does not possess sufficient ductility, and must be combined with steel reinforcement for structural purposes [Marti et al., 2002].

In high-performance fibre concrete (HPFC), both the fibre-matrix bond is much better, and the number of fibres in the microcracking zones is higher than in conventional fibre concrete. This has two most important consequences:

1. the tensile behaviour after the formation of the first macrocrack remains stable (Fig. 4.3), i.e. there is no "dip", such as in conventional FRC. The tensile stress (i.e. the carrying capacity) even increase further in most cases. This is the so-called "strain hardening", already mentioned in Chapter 3. Such a behaviour reminds to that of the conventional reinforced concrete loaded in tension, although the extent of the maximum stresses and strains that can be reached before the strain softening begins, is naturally lower in the case of HPFC.

2. it can be possible, that after the creation of the first macrocrack, it can be easier to create and open another macrocracks, than to continue to open the existing macrocrack. This phenomenon is known as the "multiple cracking". Multiple cracking is the consequence of an improved fibre-matrix bond, as well as of the relatively large number of fibres in the fracture zones. It was observed for the first time in [Aveston, Cooper, & Kelly, 1971], in cement-based composites with glass fibres. Later, it was registered in polypropylene fibre concrete, in e.g. [Li et al., 1992], as well as in steel fibre concrete in e.g. [Chanvillard, 2003].

The multiple cracking during macrocrack growth, was observed also in the case of Hybrid-Fibre Concrete. This phenomenon will be qualitatively described in this thesis, following the energy-based approaches of [Aveston, Cooper & Kelly, 1971], and of [Tjiptobroto & Hansen, 1992].

C) Bridging of macrocrack

Bridging of macrocrack begins when almost whole deformation is concentrated in a very narrow zone, with one single dominant crack. It is rather difficult to distinguish the clear beginning of this stage, especially if multiple cracks developed during the previous macrocrack growth stage. Anyhow, during multiple cracking, the total displacement (i.e. the total deformation), will more and more be localised at one dominant crack. This may be the first formed macrocrack, i.e. the first through-crack, as observed in [Tjiptobroto & Hansen, 1992] and [Mihashi et al., 2002], but not necessarily.

In plain concrete, the stage of bridging of macrocrack is very short, as the only bridging mechanism is a rather weak aggregate bridging [Van Mier, 1997].

In all types of fibre concrete, the fibres act much more efficiently as a crack bridging mechanism, by virtue of their strength, stiffness and shape. The bridging mechanism provided by the fibres is very important, because it prevents the catastrophic failure of fibre concrete, i.e. contributes significantly to the ductility and redundancy of this material.

The total crack bridging stress is the sum of the bridging stresses in all the individual fibres. The most important factors which affect this stress, are the geometry of the fibre (hooked-end or straight fibre), the quality of the frictional bond between fibre and concrete matrix, and the number and orientation of fibres that bridge the dominant crack. All these

factors will be included in the analytical model for bridging of macrocrack by fibres, which will be presented in detail in the section 4.6.

4.3 Existing analytical models for the tensile behaviour of FRC and HPFRCC

In this section, an overview of the existing analytical models for all four stages of the tensile response of FRC and of HPFRCC will be given. The models may be based on the micro- and mesostructural parameters (where the individual fibres and fibre-matrix interfaces are analysed), as well as on the macrostructural parameters (where the averaging of the action of all the fibres in a cross-section takes place).

4.3.1 Analytical models for microcracking and macrocrack growth stages

The earliest analytical models for these two initial phases of the tensile response of FRC, had mostly a qualitative character. The importance of fibre spacing in the initial phases of the tensile loading, was recognised already in the earliest beginning of the research on fibre concrete. In [Romualdi et al., 1964], it was found that the tensile stress is proportional to the inverse square root of the fibre spacing. Also, the importance of the fibre orientation with respect to the main tensile stress was explained. In [Soroushian et al., 1990], some new correlations between the achieved tensile strength and fibre spacing were found, for different fibre orientations.

The first analytical model for the development and growth of multiple cracks in continuous fibre composites, is the so-called ACK-Model [Aveston, Cooper and Kelly, 1971]. This model is based on the energy principle, where the micromechanical parameters are used to calculate the energy release rate independently for each fracture process during the formation and growth of macrocracks during the multiple cracking process.

This model was extended for high-performance cement composites with discontinuous fibres, in [Tjiptobroto & Hansen, 1993]. In this model, it was suggested, that multiple cracks form subsequently one by one, up to a certain saturation level. The energy, needed for the formation and opening of the first and of all other through-cracks, in a specimen with multiple cracks was determined. The fibre quantity, required to generate multiple cracking was subsequently calculated, and compared to the experimental results of flexural tests on DSP-concrete (concrete with Densified Small Particles, [Bache, 1987]).

One of the first analytical models for the microcracking stage of HPFRCC, is given in [Li and Leung, 1992], on the basis of which subsequently the so-called Engineered Cementitious Composite (ECC) was developed by the same authors. This model created a theoretical possibility to influence the tensile strength and the ductility of fibre concrete, by changing its composition, in terms of the necessary fibre content to achieve multiple cracking. The fibre orientation was however always taken as "random", which means that only 50% of the applied fibre quantity, is active in crack bridging. On the basis of this analytical approach, the

numerical procedure for the modelling of the tensile response of ECC was developed in [Kabele et al., 1996], which corresponded very well to experimentally obtained results.

In [Karihaloo, 1995], the formula was given for the uniaxial tensile strength of fibre composites. Later, in [Karihaloo, 1997], the analytical model for the strain hardening of fibre-cement composites was developed. The microcracks were presented as a double periodic array of discontinuities, bridged by the forces imposed by fibres. Compared to the experimental results, the model gave good predictions of the tensile response of HPFC.

4.3.2. Analytical models for bridging of macrocrack

Regarding that in this stage one dominant crack exists, the developed models apply mostly to the meso-scale, or to the macro-scale.

In the <u>meso-scale based models</u>, the bridging of the macrocrack is based on the number and orientation of fibres across the crack and on their individual pullout responses during crack opening. Analytical models for the flexural postcracking response of steel fibre concrete based on these facts, were developed in [Armelin et al., 1997] and [Van Gysel, 2000]. In both models, the individual fibre pullout responses were determined experimentally for different orientation angles of the fibres with respect to the main tensile stress. The models were calibrated on the results of flexural tests. The fibres were counted manually on the broken specimens. It was also assumed that an equal number of fibres possesses each analysed orientation angle, which in fact does not have to correspond to the reality.

In the <u>macro-scale based models</u>, the action of all fibres which bridge a crack, is observed as a whole, without taking into account the behaviour of each single fibre.

Two well-known macroscopically based models for the softening of fibre concrete are: the inverse analysis and the plastic-hinge method. Both of them are based on correlations between uniaxial tensile and flexural behaviour of FRC.

In the inverse analysis, the uniaxial tensile behaviour can be modelled on the basis of the results of flexural tests, which are easier to perform, but still rather difficult to interpret. The procedure was originally developed in [Hordijk, 1991] for conventional concrete, and extended by [Kooiman, 2000] for fibre concrete. Both models were based on three-point bending tests, taking into account that only one crack is present in the specimen. The inverse analysis based on curvature of flexural beams, was performed by [Casanova et al., 1996]. This analyses is more general, and can be used both if the flexural tests are performed as three- and as four-point bending tests. In both types of inverse analysis, a very good agreement with experimental behaviour of FRC was obtained. The nonlinear cracked hinge model, was developed for fibre concrete by [Olesen, 2001].

Other macroscopically based models are the approximate models for bending and uniaxial tension, developed by [Marti et al., 1999], and the tri-linear softening relationship for uniaxial tension, developed by [Kützing, 2000]. Both models are valid for conventional fibre concretes, with relatively low fibre volume quantities (up to ca. 40 kg/m^3). In analysis per-

formed by [Schumacher et al., 2003], very good correlation between experimental and modelled results of bending tests on self-compacting FRC, were obtained by means of both models.

Microcracking of HFC: a qualitative description

4.4.1 Introduction

In this section, a qualitative description will be given of the microcracking stage in Hybrid-Fibre Concretes (HFC) loaded in uniaxial tension. The first-cracking strength and the tensile strength of Hybrid-Fibre Concretes, with different types and volume quantities of fibres, will be correlated to the average fibre spacing.

The orientation of fibres will not be taken into account here, because it is rather difficult to isolate this factor from the results of the performed uniaxial tensile tests on HFC (sections 3.5 and 3.6). The scatter in the orientation of both short and long fibres was relatively low in the testing specimens. It can further be supposed that the quality of the fibre-matrix bond can be taken as constant (although this is not completely correct), because all the HFC mixtures tested in uniaxial tensile tests, had the same composition.

4.4.2 Efficiency of short and long fibres in HFC during microcracking

Fig. 4.4 illustrates and compares the efficiency of short and long fibres in increasing the first-cracking stress (and therefore also the tensile strength) of fibre concrete.
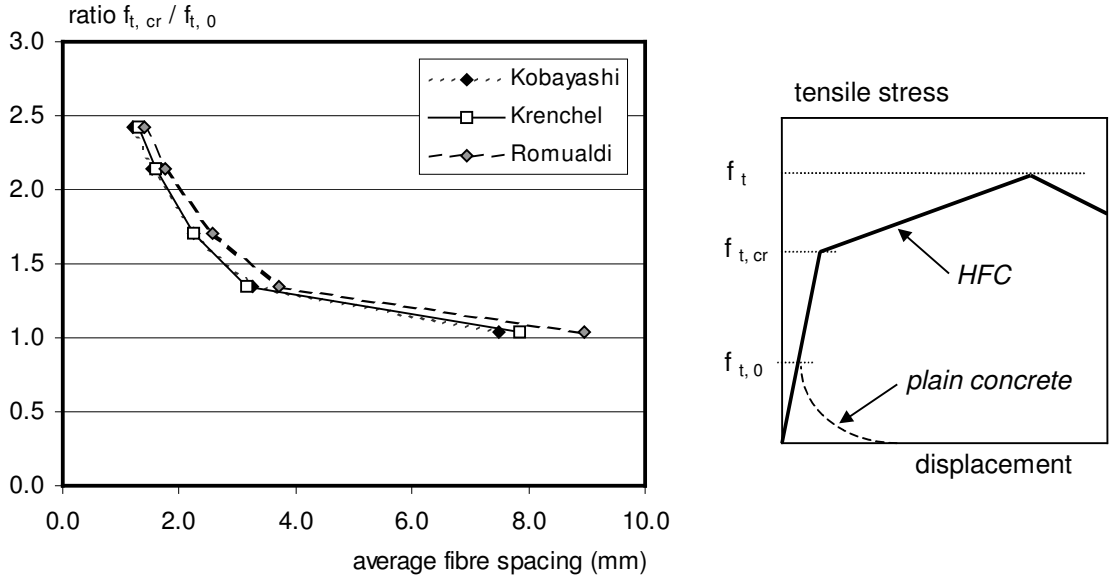
Fig. 4.4: Correlation between the average fibre spacing and the ratio of the first-cracking tensile stress of HFC ($f_{t,cr}$) and the tensile strength of plain concrete ($f_{t,0}$); the average fibre spacing was calculated using the equations of Kobayashi, Krenchel and Romualdi (given in chapter 2.5)

In this figure, the relation is given between the average fibre spacing and the ratio of the first-cracking tensile stress of HFC ($f_{t, cr}$) and the tensile strength of plain concrete ($f_{t, 0}$), with the same composition, but without fibres.

The average fibre spacing is calculated using the equations given in section 2.5 of this thesis. Three of the five available equations were chosen: [Kobayashi et al, 1976], [Krenchel, 1976] and [Romualdi et al., 1964]. The equation of Kobayashi is the only one that takes the real fibre orientation into account; another two have been developed for the random fibre orientation. Using these equations, it is not possible to calculate the fibre spacing if different types of fibres are present together in the cross section. Therefore, in concretes with two fibre types, the distance of only short fibres was taken into account, i.e. the influence of long fibres in the microcracking stage was neglected.

According to Fig. 4.4, the smaller the average fibre spacing, the higher the fibre efficiency will be. In the increasing of the tensile strength of Hybrid-Fibre Concrete, the short fibres can therefore be even 200 % - 250 % more efficient than the long fibres. This is a natural consequence of smaller length and diameter of short fibres, i.e. of their much higher number per volume quantity, compared to long fibres. Similar results were obtained by [Soroushian et al., 1990], as well as by [Akkaya et al., 1999].

Growth of macrocracks in HFC: a qualitative description

4.5.1 Introduction

In this section, the strain hardening observed during the growth of macrocracks in tensile fracture of Hybrid-Fibre Concrete, will be qualitatively described and analysed. The analysis will be based on the uniaxial tensile tests on different types of HFC, whose results are given in section 3.5. A special attention will be paid to the "multiple cracking" phenomenon, which was observed during the strain hardening phase.

As already pointed out, strain hardening is one of the most important phenomena, which distinguishes high-performance fibre concrete from ordinary fibre concrete. The fact that the tensile capacity of concrete increases in spite of crack formation, is very important at the structural level. As already pointed out, strain hardening in high-performance fibre concretes provides the redundancy after cracking, similarly like in classical reinforced concrete.

Multiple cracking is another advantage of high-performance fibre concrete. Instead of having one or a limited number of large wide cracks at an appropriate loading level (like in reinforced concrete), the elements made of high-performance fibre concrete can develop many very fine cracks. The crack width remains in this way far below the limit values, which is essential for a significantly improved durability of this material.

In this section, the influence of fibre spacing on the macrocrack growth will be analysed first, similarly to the analysis during the microcracking stage (section 4.4).

Subsequently, the fracture energy - based qualitative analysis of multiple cracking in fibre concretes, which contain one type of fibre (only long and only short fibres), will be given. The fracture energy needed to create multiple cracks will be determined. Both the micromechanical (fibre-matrix interface), as well as the macromechanical parameters (applied volume quantity of fibres and their orientation), will be taken into account in this analysis.

The main goals of this qualitative analytical modelling are:
−   to be able to estimate if multiple cracking in the analysed concretes will take place, depending on the mixture composition and the applied volume quantity of fibres. With this knowledge, the mixture composition of these concretes could further be adjusted, so that multiple cracking would always take place.
−   to provide a fundamental insight into the creation and the development of multiple cracks, and to perform a global analysis of the parameters which play the most important roles in this process.

4.5.2 Influence of short and long fibres on growth of macrocrack(s)

As the macrocracks are longer and wider than the microcracks, the question is whether short or long fibres are more effective as resistance mechanisms during the strain-hardening regime of Hybrid-Fibre Concrete.
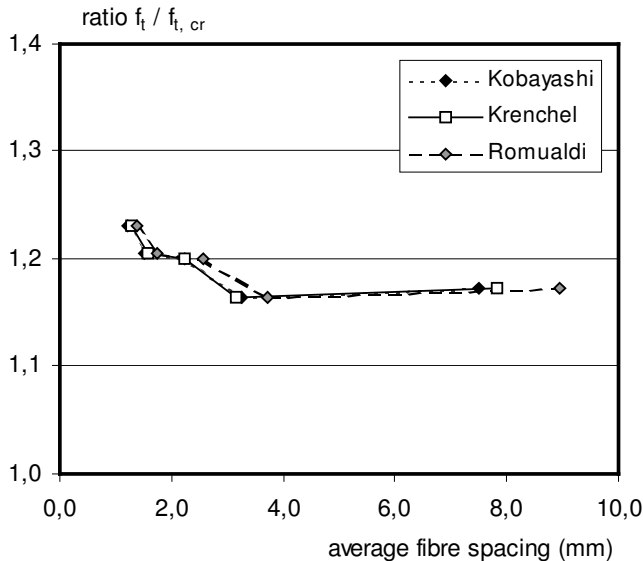
Fig. 4.5: The correlation between the average fibre spacing and the ratio of the tensile strength (f_t) and the first-cracking tensile stress of HFC ($f_{t, cr}$); the average fibre spacing was calculated using the equations of Kobayashi, Krenchel and Romualdi (given in chapter 2.5)

The relation between the average fibre spacing, and the fibre efficiency during the strain hardening stage, is given in Fig. 4.5. The fibre efficiency is herein expressed as the ratio of the tensile strength (f_t) and the first cracking stress ($f_{t, cr}$) of the appropriate type of Hybrid-Fibre

Concrete. For the average fibre spacing, the relations used previously in the section 4.4.2, are used here as well.

Obviously, short and long fibres have almost the same efficiency in increasing the tensile stress after cracking in Hybrid-Fibre Concrete, in contrast to the increase of the first-cracking strength (Fig. 4.4), where short fibres had a very dominant role. In average, an increase of the tensile strength of about 20% can be expected, which is again much less than the possible increase of the first-cracking strength (200% - 250 %, section 4.4).

4.5.3 Multiple cracking in HFC: energy-based approach

Qualitative observation of crack patterns in different types of Hybrid-Fibre Concrete

Different crack patterns were observed in the uniaxial tensile tests performed on Hybrid-Fibre Concretes with different types and volume quantities of fibres. The initial intention was to generate all cracks in the middle zone of the testing specimen, so that their propagation can be measured precisely. Therefore, dog-bone-shaped specimens were used in these tests.
In concretes with 1.0 vol.-% of long fibres (l/d = 60/0.7), a single crack was observed in almost all specimens. The crack path was in most cases approximately perpendicular to the direction of the main tensile stress.

In concretes with 2.0 vol.-% of short fibres (l/d = 13/0.2), multiple cracks were generated. Most of them were concentrated in the middle part of the specimen, within a narrow zone with a length of about 3 cm, where the highest tensile stresses act. The cracks were approximately perpendicular to the direction of the main tensile stress.

Also in all concretes with both short and long fibres (concretes No. 4, 5 and 6, Tab. 3.2), multiple cracking was observed, but in a much higher intensity compared to the concretes with short fibres only (Fig. 4.6). The cracks were distributed in a rather large zone, with a length of almost 10 cm.

This means that the Hybrid-Fibre Concrete was cracked not only in the zone of the highest tensile stresses, but also far outside this zone, where the average magnitude of tensile stress was about 50% lower than in the middle of the specimen. This might be a clue to the no-sensitivity of Hybrid-Fibre Concrete to stress-concentrations, similarly as observed in the case of ECC [Li et al., 2000]. Also, the total number of cracks was a several times larger than in concrete with short fibres only.
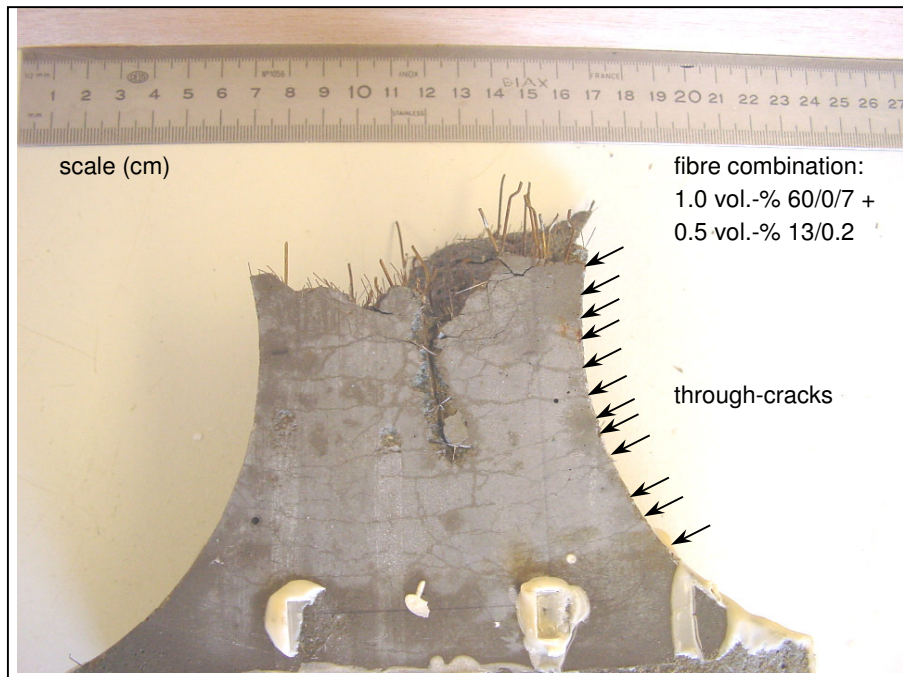
Fig. 4.6: Intense multiple cracking in Hybrid-Fibre Concrete with both short and long steel fibres, as observed in this research project (dog-bone shaped specimen loaded in tension)

Modelling of multiple cracking based on fracture energy

The energy-based analytical model for the analysis of the multiple cracking sequence, was firstly developed by [Aveston, Cooper and Kelly, 1971], for cementitious composites with continuous fibres. Their concept was universal, covering both the combination [*ductile fibre - brittle matrix*], as well as [*brittle fibre - ductile matrix*].

This analytical model was later upgraded by [Tjiptobroto and Hansen, 1992], for cementitious composites with discontinuous randomly oriented fibres. The main assumption of their analytical model is, that the first formed macrocrack (the first-through-cracks) in a concrete specimen, will also be the dominant failure crack. It was also assumed in this model, that the change of the initial tensile stiffness between the stages A and B in Fig. 4.1, corresponds to the formation of this first through-crack. The same assumption will be valid in the further text.

If the energy needed <u>to open</u> the first through-crack is higher than the energy needed <u>to create</u> another through-crack, than that another through-crack will be created. The process continues further for the third, fourth, etc. through-crack, up to the saturation level.

According to this model, only the first through-crack is foreseen <u>to be opened</u>. It is supposed that other through-cracks should be <u>only created</u> (Fig. 4.7). Therefore, the energy terms will be different for different types of cracks. For example, for the opening of the first through-crack, both the fracture energy needed to debond the fibres and to pull them out will be taken into account. However, for the creation of the second, third etc. crack, only the fibre-matrix debonding energy will be taken into account. Moreover, it is supposed in this model,

- 116 -

that the fracture energies needed to create the second, third, etc. through-crack, are approximately equal.
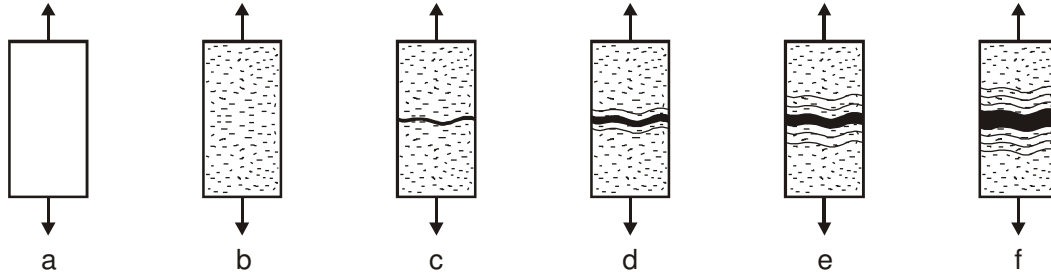
Fig. 4.7: Multiple cracking sequence, as assumed in the analytical model of multiple cracking, after [Tjiptobroto & Hansen, 1992]:   a) initial state;   b) microcracks;   c) the first through-crack;   d) the creation of second and third through-crack;   e) and f) only the first through-crack continues to open, as other through-cracks are only being created, up to a certain saturation level

The first formed through-crack can indeed be the dominant failure crack, as observed in [Mihashi et al., 2001] and [Tjiptobroto & Hansen, 1992]. In the tensile tests performed within this research project, this phenomenon could be observed in some tensile specimens as well (Fig. 4.6). However, in a number of tensile tests, very complex cracking patterns were detected, making a clear distinguishing of the cracking sequence almost impossible.

In general, much more research is necessary in order to determine the exact sequence of the development and spreading of cracks during multiple cracking. Therefore, it should strongly point out, that the analytical modelling of the multiple cracking in Hybrid-Fibre Concrete performed in the next section has exclusively a qualitative character, having as the main goal a better understanding of the multiple cracking phenomena.

Another very important remark related to the analytical modelling of multiple cracking, is that the analytical model of [Hansen & Tjiptobroto, 1992] is developed for high-performance fibre concretes with one type of fibre. The model in the present form can therefore not be applied to Hybrid-Fibre Concrete. The model will be applied only to concretes with only short and only long fibres, using the results of the uniaxial tensile tests on concretes No. 1, 2, 3 and 7 from Tab. 3.2. More research is necessary in order to extend the existing modelling equations and parameters to Hybrid-Fibre Concrete with two or more types of fibres.

Modelling concept

According to [Tjiptobroto & Hansen, 1992], and [Tjiptobroto, 1991], the energy E_{1-2} needed to open the first through-crack (i.e. the first macrocrack), can be expressed by:

$$E_{1-2} = \Delta U_{f-mc} + \Delta U_{fr} + U_{db} , \qquad\qquad [4.1]$$

where:

ΔU_{f-mc} : the increase of fibre strain energy by virtue of the action of the fibres in bridging the first through-crack;

ΔU_{fr} : the frictional energy, absorbed by virtue of the difference in strain (slip) of the fibres bridging the first through-crack and the concrete matrix which surrounds them;

U_{db} : the debonding energy, needed to destroy the elastic bond at the fibre-matrix contact.

The energy $E_2 = E_3 = \ldots = E_n$, required to form a new through-crack (denoted by number *2, 3, ..., n*), can be expressed as:

$$E_2 = E_3 = \ldots = E_n = G_m V_m + \Delta U_{f-mu} - \Delta U_{fm},\qquad [4.2]$$

where:

$G_m V_m$: the fracture energy of the matrix, required to create a new through-crack surface (where G_m is the matrix fracture energy, and V_m the matrix volume fraction);

ΔU_{f-mu} : the increase in the fibre strain energy, as a result of the bridging of cracks during multiple cracking;

ΔU_{fm} : the decrease of the matrix strain energy (since the strain in a cracked matrix is zero);

The basis of this modelling concept is given in Fig. 4.8. If the applied fibre volume quantity is higher than a critical fibre volume quantity ($V_{f,crit}$) for which $E_2 = E_{1-2}$, multiple cracking can appear.
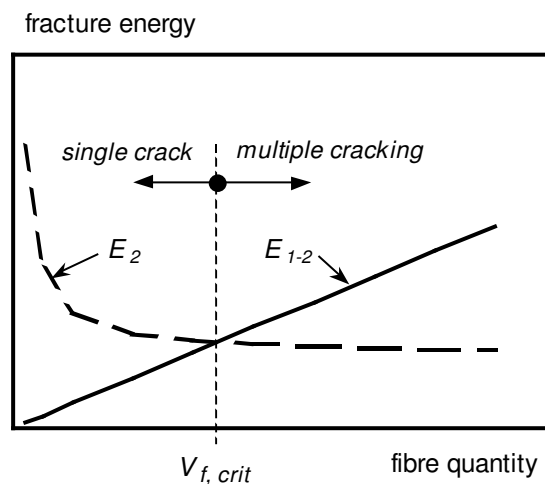
Fig. 4.8: The condition to achieve multiple cracking in fibre concrete, based on the fracture energy for the applied fibre volume quantity, according to [Tjiptobroto & Hansen, 1992]

The multiple cracks can be created up to a certain saturation point, which depends on the ratio of E_{1-2} and E_2 (Eq. 4.3). The total number of cracks n_{cr}, which is possible to create with the applied fibre volume quantity, can be calculated as:

$$n_{cr} = \frac{E_{1-2}}{E_2}.$$ [4.3]

After all the cracks have been generated, the first one will become dominant, and the tensile softening phase can begin.

In Equation 4.1:

$$\Delta U_{f-mc} = \frac{V_{ef}}{E_f} \left[\frac{7}{48} \frac{\tau_f^2 L_f^3}{r^2} - \left(E_f \, \varepsilon_{mu} \right)^2 \frac{L_f}{4} \right]$$ [4.4]

$$\Delta U_{fr} = \frac{V_{ef} \, \tau_f \, L_f^2}{4r} \left[\frac{\tau_f \, L_f}{3r \, E_f} - \frac{1}{2} \varepsilon_{mu} \right]$$ [4.5]

$$U_{db} = \frac{V_{ef} \, L_f \, G_{II}}{r}$$ [4.6]

in Equation 4.2:

$$\Delta U_{f-mu} = \frac{1}{24} E_f \, V_{ef} \, L_f \, \alpha \, (18 + 7\alpha) \, \varepsilon_{mu}^2$$ [4.7]

$$\Delta U_m = \frac{11}{24} E_m \, V_m \, L_f \, \varepsilon_{mu}^2$$ [4.8]

with:

$$V_{ef} = \eta \, V_f, \text{ and } \alpha = \frac{E_m \, V_m}{E_f \, V_f}$$ [4.9] and [4.10]

where (units *mm* and *N*):
V_{ef} = the effective volume quantity of fibres;
V_f = the applied volume quantity of fibres;
$V_m = 1 - V_f$ = the matrix volume fraction;
η = the coefficient of orientation of fibres, $(0 < \eta < 1, \eta = 1$ for fibres fully oriented in the direction of the main tensile stress, as explained in section 3.6);
E_f = the modulus of elasticity of the fibres $(E_f = 210000 \text{ N/mm}^2)$;
L_f = the fibre length;

r = the fibre radius;

G_m = the fracture energy of plain concrete, obtained from the tensile test (here approximate G_m = 0.108 N/mm);

ε_{mu} = the strain at which the first through-crack forms in the fibre concrete under consideration (corresponds to the first bending point at the diagram of uniaxial tensile response, Fig. 4.1);

τ_f = the average frictional stress at the fibre-matrix interface, which exists after the debonding at the interface has been finished;

G_{II} = the fracture energy released at the fibre-matrix interface during the debonding process (the fracture energy of the second (*II*) mode – i.e. of the shear fracture).

Parameter identification

The unknown parameters from the previous list are:

_ the frictional stress τ_f

– the debonding energy G_{II}

– the strain ε_{mu} at which the first through-crack forms.

These parameters will be determined in this section. Moreover, some of them will be varied, in order to observe their qualitative influence on the probability of multiple cracking in different types of fibre concretes developed within this research project.

Concerning the fibre orientation, both the real values, determined in section 3.6, as well as other possible values will be applied, in order to observe their influence on the cracking sequence of fibre concretes developed within this research project.

The frictional stress τ_f and the debonding energy G_{II}

The diagrams for the debonding and pullout response of single fibres (short and long), will be used for the determination of both the frictional stress at fibre-matrix interface, and the debonding energy. A detailed impression of the debonding and pullout phase is given in Fig. 4.9.a for short straight fibres, and in Fig. 4.9.b for long fibres, with and without hook.

As no own experimental results are available, in the case of long fibres (l/d = 60/0.7), the following parameters will be used (Fig. 4.9.b), based on the pullout behaviour of the same fibre type in a rather similar concrete matrix, from [Van Gysel, 2000]:

– the fibre slip at which debonding finishes Δ_d = 0,1 mm;

– the appropriate frictional pullout force at which the debonding finishes P_d = 100 N.

In the case of short straight fibres (l/d = 13/0.2), the scatter of the results is relatively large (Fig 4.9.a). This can be expected, due to the very low pullout forces (only about 10 - 20 N). Therefore, the parameters will be varied. First, the displacements (fibre slips) will be varied and the pullout forces will be kept constant, and subsequently the opposite will be done. These variations will provide an insight into the probability of multiple cracking of the fibre concrete with short fibres, for different qualities of the fibre-matrix bond.
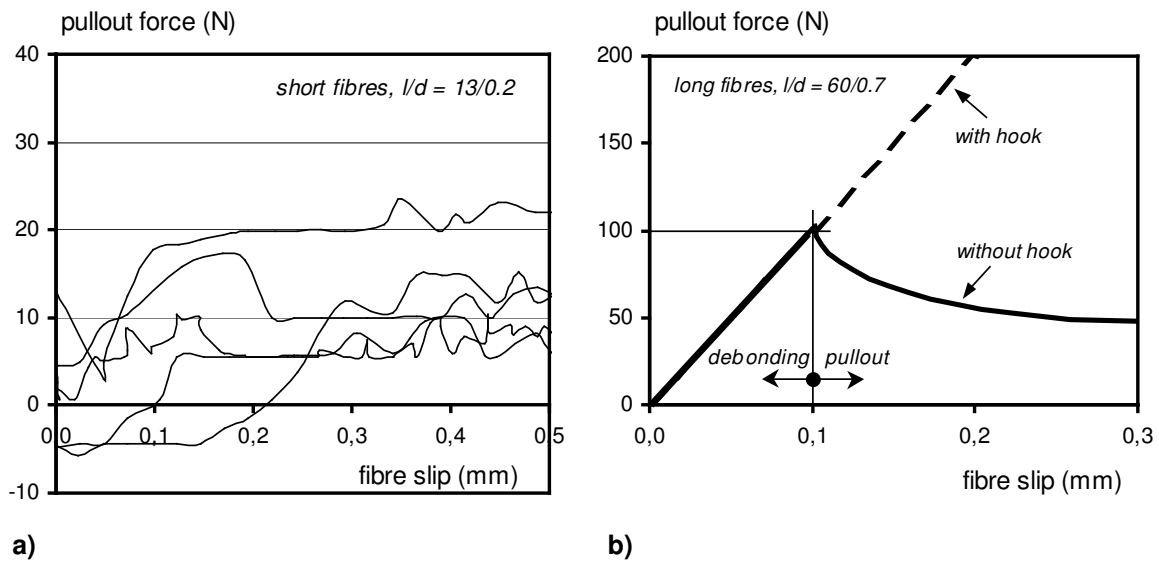
Fig. 4.9: Debonding and initial pullout stage of: a) short straight steel fibres, experimentally obtained (full results given in section 2.9); b) long steel fibres with and without a hook, assumed pullout behaviour based on [Van Gysel, 2000]

The variations of parameters for short straight fibres are given in Fig. 4.10. a and b. The parameters will be varied according to:

Variation 1:
- for the fibre slip at which the debonding finishes, three values will be applied:
  $\Delta_d = 0.010$ mm, 0.025 mm and 0.050 mm;
- the value of the frictional pullout force will be kept constant at the experimental average value of $P_d = 15$ N (approximately).

Variation 2:
- the fibre slip at which the debonding finishes, will be kept at $\Delta_d = 0.025$ mm;
- for the frictional pullout force, three values will be applied: $P_d = 10$ N, 15 N and 20 N.

Using these parameters, the average frictional stress can be calculated from:

$$\tau_{fr} = \frac{P_d}{A_{fr}^f}$$

[4.11]

where:

P_d =   the average measured frictional force present at the fibre-matrix interface after debonding is completed;

A_{fr}^f = the surface area of the fibre exposed to the action of the frictional stress, which will in this case be calculated using one half of the fibre length as an average debonded length of all fibres.
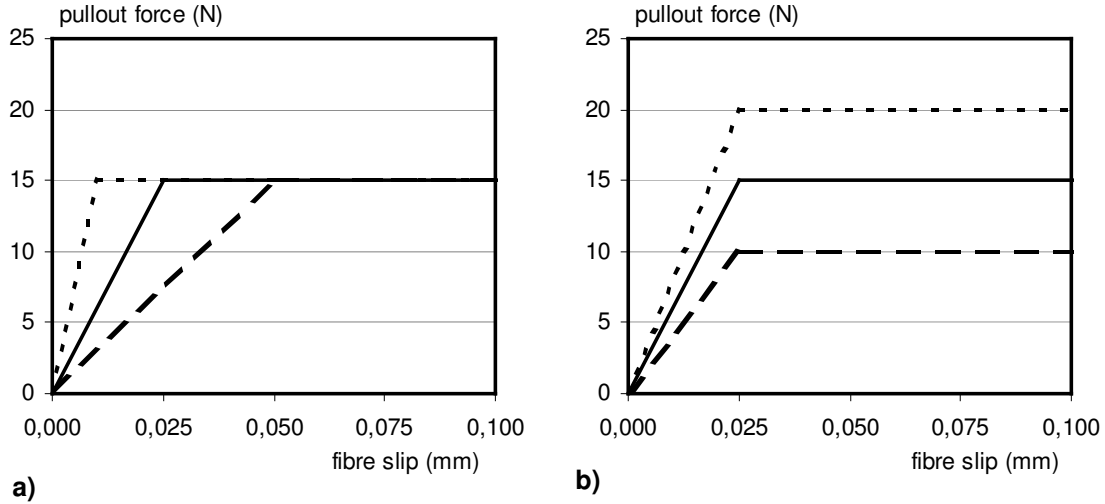
Fig. 4.10: The variations of parameters from the pullout tests of short straight fibres used in the model: a) variation of fibre slips at which fibre-matrix debonding finishes;   b) variation of the frictional pullout forces

The fibre-matrix debonding energy can be calculated from:

$$G_{II} = \frac{A_{debonding}^*}{A_{fr}^f}$$
[4.12]

where:

$A_{debonding}^*$ = the triangular surface area under the part of the fibre pullout diagram, which corresponds to the fibre-matrix debonding phase. This area will be calculated in each case separately, according to the applied variation of the fibre slip and the debonding force;

A_{fr}^f = the surface area of the fibre exposed to the action of the frictional stress, which will in this case be calculated using one half of the fibre length as an average debonding length for all fibres.

The strain ε_{mu} at which the first through-crack forms

The strain at which the first through-crack forms (the first macrocrack) in the fibre concrete under consideration (the bending point at the diagram of uniaxial tensile response), will be determined taking the measuring basis of $l_m = 105$ mm into account (in case of plain concrete $l_m = 35$ mm), from:

$$\varepsilon_{mu} = \frac{\delta_{mu}}{l_m}$$

[4.13]

The strains ε_{mu} depend on the applied fibre combination, and they are obtained either experimentally, or by linear extrapolation (Tab. 4.1).

Tab. 4.1: Values of the first-macrocracking strain ε_{mu} of fibre concretes with short and long fibres. The values given in bold are based on the results of the uniaxial tensile tests (section 3.5), all other values were obtained through linear inter- and extrapolation between the measured values

fibre quantity (vol.%)		δ_{mu}	ε_{mu}
13/0.2	60/0.7	(mm)	(%)
0	**0**	**0,004**	**0,0100**
1	-	0,006	0,0057
2	**-**	**0,009**	**0,0086**
3	**-**	**0,012**	**0,0114**
4	-	0,015	0,0143
-	**1**	**0,005**	**0,0048**
-	2	0,010	0,0095

The orientation of fibres

All calculations with the above mentioned parameters for concretes with short fibres only, will first be made with a constant orientation coefficient $\eta = 0.8$. This approximately corresponds to the average value of the orientation coefficient for short fibres ($\eta = 0.805$), as found in the orientation analysis, given in section 3.6.

After that, the orientation coefficients of $\eta = 0.5$ and $\eta = 1.0$ will be used as parameters in the model. In those analyses, the values of the fibre slip at which the fibre-matrix debonding finishes will be kept at 0.025 mm, and the appropriate frictional force at 15 N.

The goal is the quantitative determination of the influence of the fibre orientation on the multiple cracking of concretes with short fibres only. For concretes with long fibres only, the orientation coefficient $\eta = 0.87$ will be used. This corresponds to the value determined in the analysis of the fibre orientation (Section 3.6). This will be the only value to be used.

Application of the model to concretes with short and with long fibres

The fracture energies E_{1-2} and E_2, for concretes with different volume quantities of short fibres only ($l/d = 13/0.2$), are given in Fig. 4.11.

In Fig. 4.11.a, the fibre slip at which the fibre-matrix debonding is finished (Δ_d), is varied as Δ_d = 0.010 mm, 0.025 mm and 0.050 mm, according to Fig. 4.10.a. Obviously, the higher this debonding slip Δ_d is, the lower fibre quantity will be needed for achieving of multiple cracking. Taking into account that the multiple cracking was observed for concrete with 2.0 vol.-% of short fibres, it may be concluded that the fibre slip Δ_d is most probably higher than Δ_d = 0.01 mm for short fibres with l/d = 13/0.2.
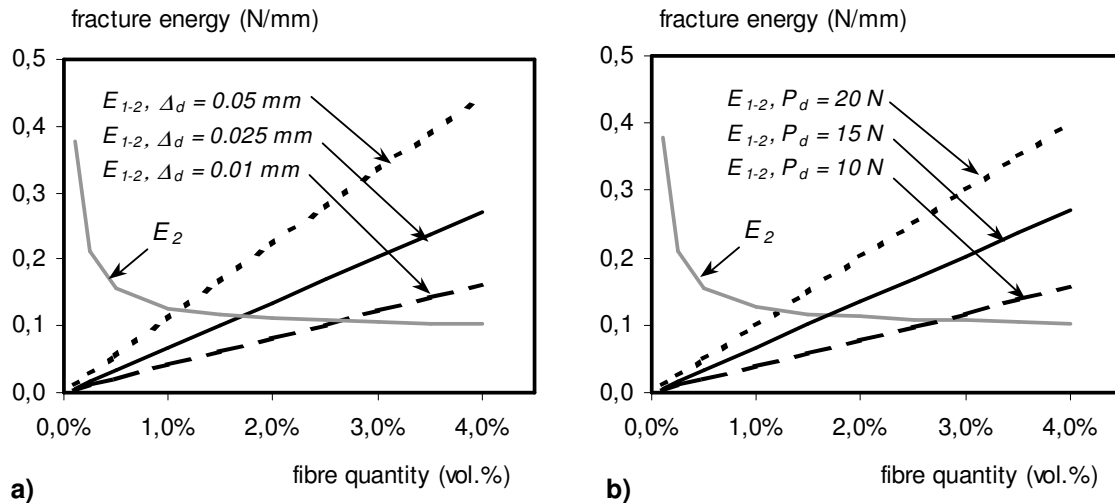
Fig. 4.11: The relations between the applied volume quantity of short fibres (l/d = 13/0.2) and fracture energies E_{1-2} and E_2 (the intersection point of E_{1-2} and E_2 diagrams marks the beginning of the multiple cracking), for variations of the parameters related to the fibre pull-out: a) frictional force P_d = constant, fibre debonding slip Δ_d varied (according to Fig. 4.10.a); b) frictional force P_d varied, fibre debonding slip Δ_d = constant (according to Fig. 4.10.b); the orientation coefficient of fibres equal to 0.8 in all cases

In Fig. 4.11.b, the fibre pullout force at which the debonding is completed (P_d), is varied as P_d = 10 N, 15 N and 20 N. This force is directly dependent on the quality of the fibre-matrix bond: the better the bond, the higher the force P_d will be. From Fig. 4.11.b, it can be concluded that the better is the fibre-matrix bond, the lower is the fibre quantity needed to achieve multiple cracking. Indeed, about 2 times more fibres are needed for multiple cracking, in the case where P_d = 10 N, compared to the case where P_d = 20 N.

The fibre orientation plays a very important role, not only for the tensile strength, but also for achieving multiple cracking in fibre concrete. In Fig. 4.12.a, three different values of the fibre orientation coefficient η are analysed: η = 1.0 (all fibres oriented in the direction of the main tensile stress), η = 0.8 (observed orientation of short fibres in tensile specimens), and η = 0.5 (random orientation of fibres).

Obviously, the more fibres are oriented in the direction of the main tensile stress, the less fibre quantity is needed to achieve multiple cracking. The differences in the required fibre quantity for the orientation coefficients 1.0 and 0.8 are relatively small (only about 0.2 vol.-%).

As the orientation of fibres gets closer to the random value ($\eta = 0.5$), the volume quantity required for multiple cracking will be about 2 times higher than in the ideal case ($\eta = 1.0$). For the orientation coefficient $\eta = 0.25$, the required fibre quantity for multiple cracking will be about 5 times higher than those for $\eta = 1.0$. This is another evidence of the importance of fibre orientation for the optimum tensile behaviour of fibre concrete.
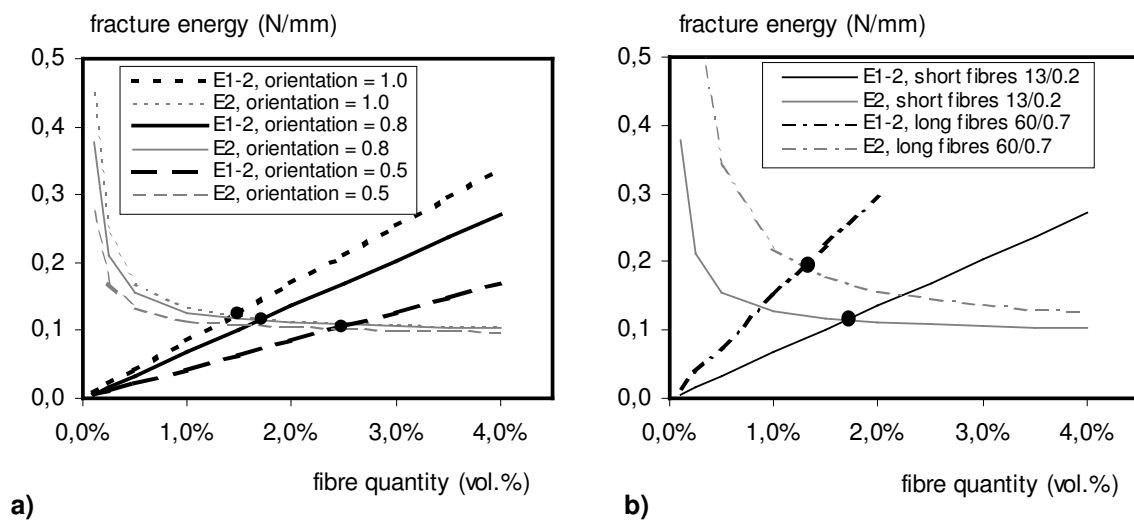
Fig. 4.12: The relations between the applied volume quantity of fibres and the fracture energies E_{1-2} and E_2 (the intersection point of the E_{1-2} and E_2 curves marks the beginning of multiple cracking), for: a) different orientation coefficients of short fibres (l/d = 13/0.2); b) concretes with either only short fibres (l/d = 13/0.2), or only long fibres (l/d = 60/0.7), with the orientation coefficient of fibres being equal to 0.8 in both cases

In Fig. 4.12.b, the comparison of required fibre content to achieve multiple cracking is given, in cases where only short fibres (*l/d* = 13/0.20), or only long fibres (*l/d* = 60/0.7) are applied. The same concrete matrix composition and the same coefficient of fibre orientation ($\eta = 0.8$) are used for both fibre types. Multiple cracking in concrete with long fibres is possible if the volume quantity of fibres is higher than 1.4 vol.-%, whereas in the case of concrete with short fibres, this quantity is equal to 1.7 vol.-%.

A better performance in multiple cracking of concretes with long fibres, is a consequence of the strong bond between the long fibres and the surrounding concrete matrix, as well as of the very low first macrocracking strain for concretes with long fibres only (Tab. 4.1).

4.5.4 Concluding remarks and discussion

Multiple cracking is one of the most important phenomena observed in the tensile response of Hybrid-Fibre Concrete, especially in relation to the durability of this material. The more cracks are being generated, the smaller their width will be, and therefore also the durability can be improved.

In this chapter, qualitative observations combined with the energy-based modelling of the multiple cracking in different types of Hybrid-Fibre Concrete and in concretes with one type of fibre were performed. In general, the appearance of the multiple cracking depends on the applied type and volume quantity of fibres, their orientation as well as on the quality of the concrete that surrounds the fibres. From the performed analysis, the following can be concluded:

1. Keeping all other parameters constant, the higher the applied fibre quantity, the more cracks can develop during multiple cracking.

2. The stronger is the bond between the fibres and the concrete (i.e. the higher the debonding slip and the maximum fibre pullout force), the lower is the volume quantity of fibres, that is required to generate multiple cracking.

3. The more fibres are oriented in the direction of the main tensile stress, the lower volume quantity of fibres is required to generate multiple cracking.

As already pointed out in the previous section, the here performed analytical modelling of multiple cracking has only a qualitative character. The model of [Hansen & Tjiptobroto, 1992] is based on the fact that in multiple cracking process, the first through-crack will always be the dominant one. The number of available evidences for this is still rather low. Even in this research project, no exact conclusion on the multiple cracking sequence could be made, due to a large complexity and variability of the observed cracking processes. The here presented analytical model should therefore be used only as a first estimate of the cracking process (single or multiple cracking), that can be expected for the applied fibre quantity and orientation.

It should also be pointed out, that although the multiple cracking was observed in Hybrid-Fibre Concrete (in the dog-bone-shaped tensile specimens), it does not mean that the same phenomenon will be present on the structural scale. However, based on the observation of multiple cracking in large-span prestressed beams subjected to bending, made of self-compacting fibre concrete with only about 40 kg/m³ fibres [Falkner et al., 2004], it can be expected that this phenomena will occur also in the structural elements made of Hybrid-Fibre Concrete.

4.6 Bridging of macrocrack in HFC: analytical modelling

In this section, the analytical model for crack bridging by fibres in Hybrid-Fibre Concrete loaded in uniaxial tension (also known as "tensile softening") will be presented.

The model with all its parameters and assumptions will be introduced first. The modelling of the tensile behaviour of concretes with one type of fibres (only short or only long) will be performed subsequently, in order to calibrate the unknown modelling parameters. Once all the parameters are known, the modelling of tensile behaviour of concretes, which contain both short and long fibres will be performed, and compared with the experimental results. Subsequently, a discussion and conclusions on the analytical model will be provided.

4.6.1 Introduction

The exact knowledge of the tensile softening phase for any type of FRC, is necessary for design calculations of the ultimate carrying capacity of structural elements. Depending on the applied types and amounts of fibres, as well as on the structural system (statically determined or undetermined) and on the loading conditions (bending, pure tension, etc.), the ultimate carrying capacity may be reached at rather large crack widths, because of the redistribution of stresses in FRC.

For example, within this research project, the ultimate flexural carrying capacity of small statically determined beams made of the Hybrid-Fibre Concrete, was achieved at crack widths of about 2.5 - 3.5 mm (section 3.4). Translated to the uniaxial tensile response, these points lay far in the softening phase. In statically undetermined structures, even larger values of these crack widths may be achievable. In conventional types of FRC, the softening phase may also be important for the calculations of the crack widths with respect to durability.

Another reason for the importance of the softening phase, is that structural elements made of high performance fibre concrete, often possess non-standard structural shapes and forms. This often requires the application of numerical modelling for their exact calculation (e.g. finite element modelling). In such a case, the full tensile softening response is usually one of the compulsory input parameters.

The analytical modelling of the uniaxial tensile response for different types of Hybrid-Fibre Concrete is performed within this research project. The analytical model is based on the pull-out response of fibres that bridge the dominant crack, taking into account their type (short or long fibres, or both combined), their number across the crack and their orientation with respect to the main tensile stress.

The main goals of this analytical model are:

- The simplification of the determination of uniaxial tensile behaviour for different types of Hybrid-Fibre Concrete; In the engineering practice, it is indeed possible to apply a lot of different types of steel fibres, in different volume quantities in HFC. Performing uniaxial tensile or flexural tests on HFC's with all possible fibre combinations and types, in order to determine the tensile properties, would not be practical. It is therefore very useful to be able to predict the tensile softening phase by appropriate models;

- To achieve a better understanding of the crack bridging stage in the uniaxial tensile response of different types of Hybrid-Fibre Concrete; The fundamental knowledge about the crack bridging mechanisms is still insufficient, especially in the case of high performance concretes reinforced with different types of steel fibres. A better understanding of the crack bridging processes, can serve to optimise of both the mixture compositions of fibre concrete, and the shape, dimensions and mechanical characteristics of steel fibres as well. The modelling results could also be extended further, to the analytical modelling of flexural or tensile behaviour of structural elements, made of both conventional FRC or high performance fibre concrete, in combination with e.g. standard steel reinforcement or prestressing reinforcement.

4.6.2 Description of the analytical model

Introduction

In this section, the basic principles, which will be used in the analytical model for bridging of macrocrack by fibres in HFC (tensile softening), will be explained. For the sake of simplicity, the analytical model will be introduced using a simple case of three fibres with different embedded lengths, that bridge a crack, as shown in Fig. 4.13.a.

For this simplified case, the following assumptions are made:
- all fibres are straight and oriented in the direction of the main tensile stress;
- all fibres have the same diameter;
- each fibre acts independently from the neighbouring fibres, i.e. there is no influence of the stress fields of neighbouring fibres on each other during the pullout process;
- for each fibre, the whole debonding and pullout process take place only on one side of the crack, i.e. the other part of the fibre remains intact. Therefore, the fibre slip (Δ) is equal to the crack width w, at each moment of the pullout process;
- the fibre slip w_0 as a result of only the initial debonding between fibre and matrix, is equal for all the fibres, independent on their embedded length;
- the larger is the fibre embedded length, the higher is the maximum pullout force (fibre *1*), and vice versa (fibre *3*) (Fig. 4.13.b);
- the pullout force remains constant during the frictional pullout phase of fibres.
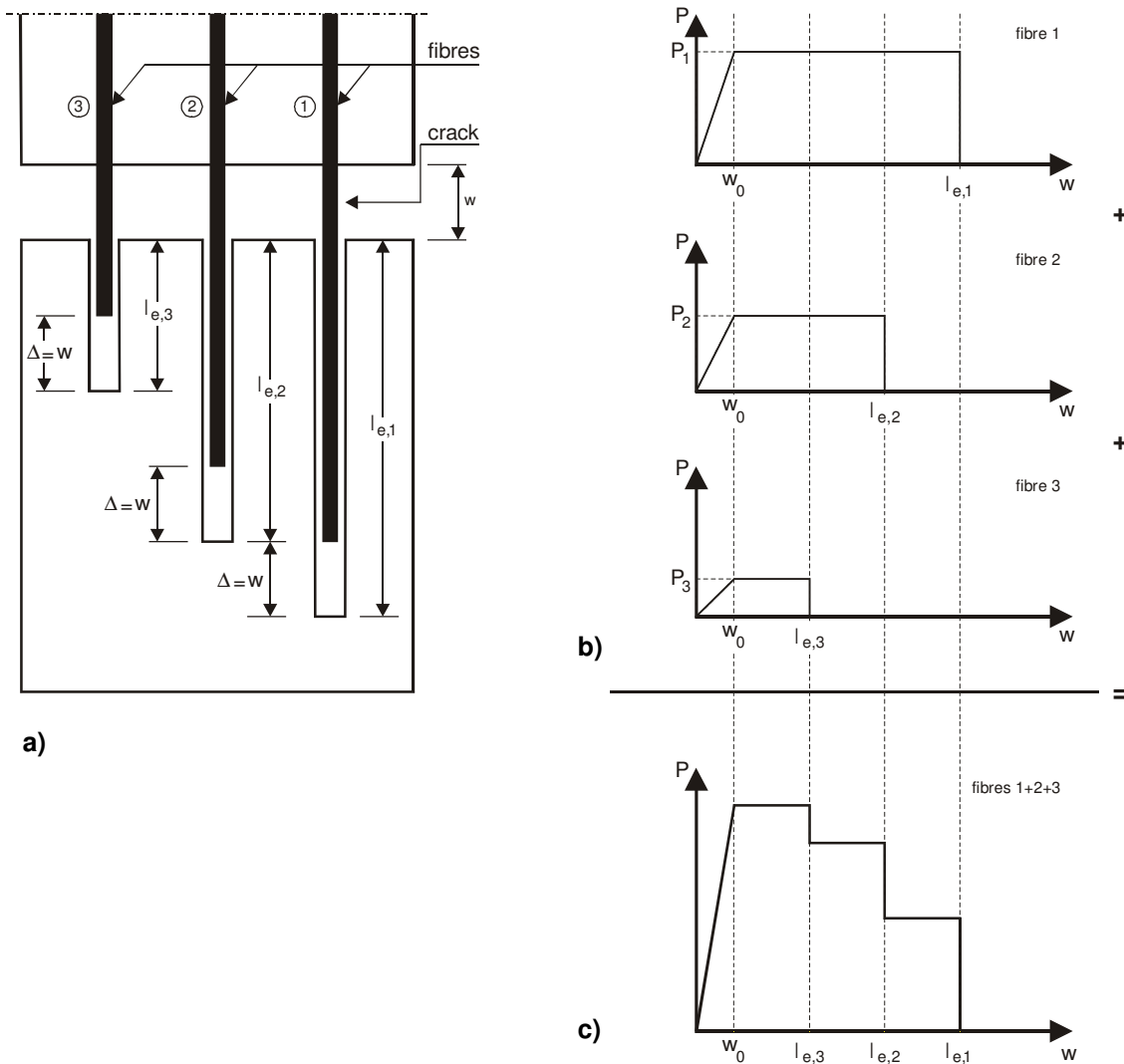
Fig. 4.13: a) Three independent straight fibres (marked as 1, 2 and 3) bridge a crack of width w, the fibres have different embedded lengths, and are oriented parallel to the direction of main tensile stress; b) The assumed individual pullout responses of fibres 1, 2 and 3, where P represents the pullout force, and w is the fibre slip (which is equal to the crack width); c) The arithmetic sum of the individual pullout responses of fibres (1+2+3)

In Fig. 4.13.b), the assumed individual pullout responses for each fibre are given. In Fig. 4.13.c), the arithmetic sum of these individual pullout responses is given. In both Fig. 4.13.b) and c), only the pullout phase of the diagrams, starting from $w = w_0$, will be of interest for this analytical model. The debonding of fibres (up to $w = w_0$), was already taken into account in the qualitative description of the macrocrack growth phase (Section 4.5), and will therefore not be considered in following text.

It will be further assumed, that after the dominant macrocrack has formed, the total deformation is concentrated only in this crack, i.e. all other eventually formed multiple cracks do not open any longer. The total tensile stress, which can be transmitted over the dominant mac-

rocrack, will then be equal to the sum of the tensile forces in all fibres, which bridge that crack.

Total transmitted bridging force

The arithmetic sum of all individual pullout forces of fibres (P), in relation to the crack width (w), i.e. the total tensile softening response of this fibre-concrete composite, is presented in Fig. 4.13.c. The maximum tensile bridging force, which can be transmitted across the crack, will not remain constant, primarily due to the pullout of fibres. The first decrease will be at the crack width $w = l_{e,3}$ when fibre **3** is pulled out, i.e. when this fibre becomes inactive in crack bridging. After that, similar decreases of the tensile force (tensile stress), will appear also after the crack width w reaches the embedded length of fibre **2** and **1.**

Therefore, the decrease of the tensile stress after the peak, known also as "tensile softening", is partly a consequence of the termination of the pullout process of fibres. If the pullout forces of individual fibres also decreases (i.e. do not remain constant after completed debonding), a faster decrease of the total bridging force will occur.

Number of fibres active in the crack bridging

The number of the fibres active in crack bridging at each value of the crack width ($n_{act}(w)$), is one of the parameters that determines the tensile softening of any type of FRC. If the total number of fibres is marked as n_{tot}, the probability $p(w)$ (from 0 to 1), that the fibres active in crack bridging may be found at any crack width w, can be expressed as (Fig. 4.14):

$$p(w) = \frac{n_{act}(w)}{n_{tot}}. \hspace{4cm} [4.14]$$
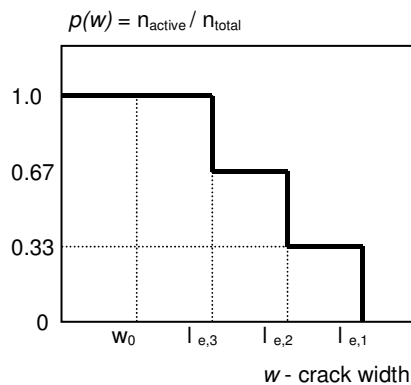
Fig. 4.14: The relative number of fibres active in crack bridging (p(w)), at any crack width w (according to Eq. 4.14 and related to the fibres in Fig. 4.13)

The value $p(w)$ represents also the cumulative distribution of the available embedded lengths of fibres.

Influence of fibre orientation on crack bridging

Most of the fibres in FRC elements are oriented under an angle with respect to the direction of the principal tensile stress.

The fibre in Fig. 4.15.a, is initially inclined at the angle α with respect to the direction of the force P (i.e. of the main tensile stress). As the crack opens, the <u>local bending</u> of the part of the fibre, which lays over the crack, will start.

The extent of the local bending of a fibre, depends in a general case on the crack width w. As the crack width increases, the fibre tends to bend more and more. If $\beta(w)$ is the bending angle at a crack width w, the following will be valid (Fig. 4.15.a):

$$w = 0 \quad \Rightarrow \quad \beta(w) = \beta_{max} = \alpha \qquad [4.15]$$

$$0 < w < \infty \quad \Rightarrow \quad \alpha > \beta(w) > 0 \qquad [4.16]$$

$$w = \infty \quad \Rightarrow \quad \beta(w) = \beta_{min} = 0 \qquad [4.17]$$

Clearly, the intensity of the local bending will depend on two main factors:

- the bending stiffness of the fibre (EI): within this research, steel fibres with diameters of 0.2 mm (short fibres) and 0.7 mm (long fibres) are used. The bending stiffness of long fibres is therefore about 150 times higher than that of short fibres.
- the tensile strength of the concrete matrix, which surrounds fibres: the higher this strength, the larger intensity of local bending may be expected, and vice versa.

For any modelling purpose, the following pullout relation can be used in the limit cases (Fig. 4.15.b):

- in the case of very small local bending of the fibre (i.e. approximately $\beta(w) = \alpha$), the pullout relation for the fibre aligned to the pullout force can be used.
- in the case of very large local bending of the fibre (i.e. approximately $\beta(w) = 0$), the pullout relation for fibre inclined at the initial angle α can be used.

In all cases in between these two limit cases, the pullout relations for fibres inclined at the angle $\beta(w)$ should be used.

The influence of the initial inclination angle is already evaluated in the Section 2.9 of this thesis, and it will be analysed in relation to the analytical modelling in the following section
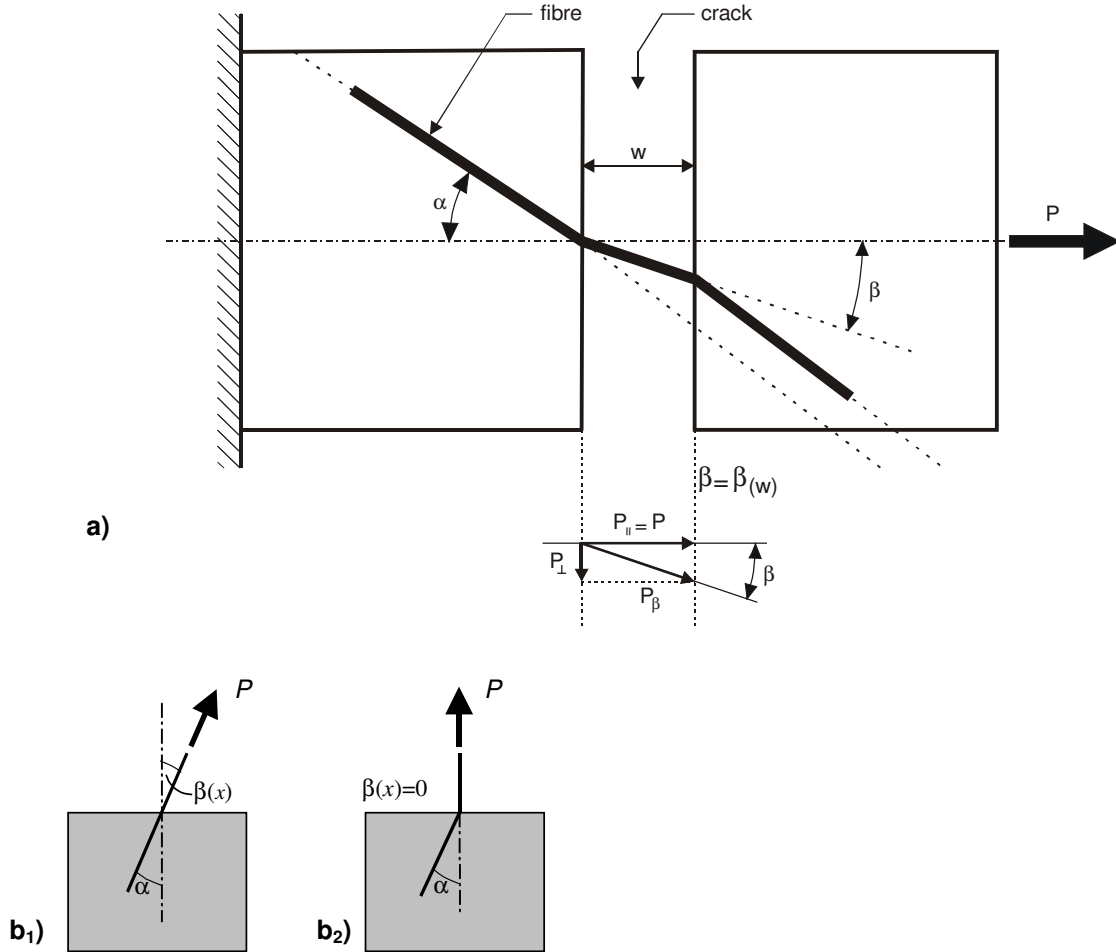
Fig. 4.15: a) Bridging of a crack by fibre, which is initially inclined at the angle α, and locally bent at the angle β across the crack, with respect to the principle tensile stress (i.e. tensile force P), with from here the resulting bridging force $P_{II} = P(w)$ b) limit cases of local bending of fibre across the crack: b_1) no local bending of fibre, $\beta(x)=\alpha$; b_2) full local bending of fibre, $\beta(x)=0$

The resulting crack bridging force generated by a single fibre (Fig. 4.15) at any crack width w, is:

$$P(w) = P_{\beta(w)} \cdot \cos \beta(w), \qquad\qquad [4.18]$$

where:

$P(w) = P_{II} =$ the horizontal component of the total bridging force, equal to the total tensile force that acts on the fibre-concrete composite element in Fig. 4.15;

$P_{\beta(w)} =$ total tensile force in the fibre inclined under the angle $\beta(w)$;

$\beta(w) =$ the angle of local bending of fibre across the crack.

General modelling equation

The resulting total crack bridging force *P(w)* at any crack width *w*, produced by the individual actions of all the fibres active at that crack width *w*, is equal to:

$$P(w) = \sum_{i=1}^{n(w)} P_i(w) \cdot \cos \beta_i(w), \qquad\qquad [4.19]$$

where:

$P(w)$ = the total crack bridging force generated by the fibres, at any crack width *w*
$P_i(w)$ = the pullout force generated by an individual fibre *i*, at a crack width *w*
$\beta_i(w)$ = the actual inclination angle of fibre *i* at a crack width *w*
$n(w)$ = the number of fibres active in the crack bridging, at any crack width *w*.

Equation 4.19 is valid under the basic assumptions, that there is only one dominant crack present in the fibre concrete element under consideration.

Although the situation of the crack bridging by fibres in Fig. 4.15 and 4.13, is given as a two-dimensional (2-D) drawing, the Equation 4.19 is in general valid for three-dimensional fibre orientation (3-D). This means that the 3-D values of the orientation angles of fibres given in Tab. 3.3 may be directly used in the Equation 4.19.

Still, a distinction should be made between two possible geometries of fibres in their length direction:
− the fibres with a 3-D rotational symmetry (e.g. cylindrical straight fibres);
− the fibres with no 3-D rotational (e.g. hooked-end fibres as applied in this research).

In the case of fibres with rotational symmetry (e.g. short straight fibres 13/0.2), the fibre which is in 3-D oriented at any angle α with regard to the main tensile stress, will always give the same pullout response, no matter of its orientation with regard to a reference straight line.

In the case of fibres without rotational symmetry, such as for example the fibres 60/0.7 with hooked-end, the pullout response may slightly differ depending on the orientation of the hook plane itself with respect to the direction of the main tensile stress. However, to the author's opinion, the differences in pullout responses of the same hooked-end fibres with different orientations of the hook planes at their ends are very small.

4.6.3 Parameter identification

In this chapter, all the modelling parameters, which appear in Eq. 4.19, will be identified and evaluated separately for concretes with only long and only short fibres.

In general, these parameters are:

the number of the fibres active in the crack bridging at any crack width w;
the pullout behaviour of aligned and inclined fibres, with different embedded lengths.

A complete tabular overview of all known and unknown modelling parameters is given in tabular form at the end of this section, see Table 4.2.

Number of long fibres active ine crack bridging

The number of long fibres active in crack bridging at any crack width w, can be directly derived from the measured visible lengths of long fibres on the fractured tensile specimens (section 3.6, Fig. 3.25). Under the assumption that the fibre debonding and pullout take place only on one side of the crack, the visible length of a fibre will be equal to the crack width at which that fibre was fully pulled out.

In Fig. 4.16.a, the ratio of the number of long fibres active in the crack bridging at any crack width w, and the total counted number of fibres as observed at the crack planes of tensile specimens, is given. The ratios for hooked-end fibres, with both fully and partly deformed hooks are given in a cumulative distribution, based on the determination of the visible fibre lengths in Fig. 3.25.
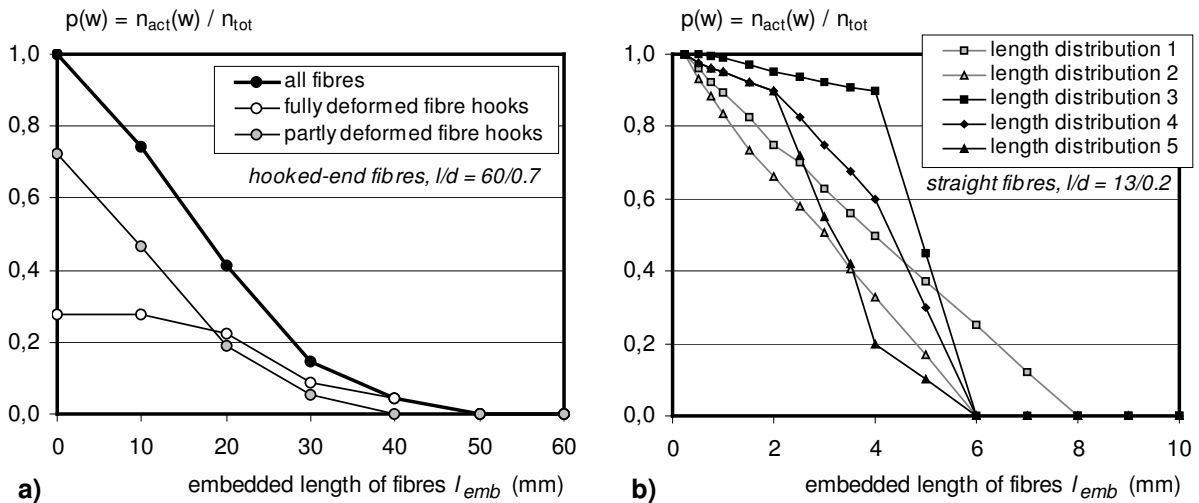
Fig. 4.16: The cumulative distribution of fibre embedded lengths, i.e. the ratio of the number of fibres active in the crack bridging at the crack width w, and the total number of fibres, for: a) Concrete with long fibres only (all fibres, and fibres with fully and partly deformed hooks) - determined from the diagram given in Fig. 3.25; b) Concrete with short fibres only – assumed different fibre length distributions (1 to 5) for the modelling purposes

Number of short fibres active in crack bridging

For concretes which contain only short fibres, the exact determination of the available embedded lengths of the fibres is technically very difficult, due to the large number of densely distributed fibres on the crack planes. Therefore, several distributions of the fibre embedded lengths will be assumed and applied in the model (Fig. 4.16.b).

The fibre length distribution No. 1, with $w_{max} = 8$ mm, corresponds to the determined distribution of long fibres, that ends approximately at 2/3 of the total fibre length (in this case, the total fibre length is $l_f = 13$ mm).

On the other hand, the crack path in the concrete with densely distributed short fibres, does not have to be similar to the crack path in the concrete with only long fibres. Therefore, other distributions of fibre embedded lengths, with $w_{max} = 6$ mm, will be applied as well (fibre length distributions No. 2 to No. 5).

The fibre length distribution No. 2 is almost linear, like the distribution No. 1. The dominant fibre lengths in the length distribution No. 3, are from 4 to 6 mm and in the distribution No. 5 from 2 to 4 mm. The distribution No. 4 is an approximately average case of the distributions No. 3 and No. 5.

It should also be pointed out, that in the specimens with short fibres, the total number of fibres was not counted at the crack surface, but determined automatically from the photo of the nearest cross-section, as explained in section 3.6.

Fibre pullout – general remarks

The pullout behaviour of a single fibre in a pullout test, and the behaviour of the same fibre in a fibre concrete, during its pullout during the crack bridging, are most probably never identical. Three most important reasons for these differences are:

1. In fibre concrete, each fibre is surrounded by other fibres and all the fibres act in and as a group during the crack bridging; in the pullout test, the fibre acts individually;

The only work on this phenomenon known to the author, is that of [Naaman & Shah, 1976], for steel fibres with a length of 30 mm. According to this work, the better the alignment of the fibres to the direction of the pullout force, the smaller the differences between the individual and the group action of fibres will be. In their experiments, the differences between single and group action of fibres become really visible from inclination angles of 45° and larger.

The orientation of all fibre types in the tensile specimens produced within this research project was rather close to the direction of the main tensile stress (from 15° to 32°, Tab. 3.3). Therefore, the fibre orientation does probably not have a significant influence on a group action of fibres in the testing specimens.

However, the spacing of short fibres is about 4 times smaller than the spacing of long fibres, for the same fibre volume quantity (Fig. 2.6). According to this, short fibres will therefore influence each other during pullout to a somewhat larger extent than long fibres.

Still, if long fibres act in a group, their hooks can cause in the initial stages of the pull-out a diagonal splitting fracture in the surrounding concrete. Therefore, also these fibres do influence each other when acting as a group.

The influence of both short and long fibres on each other when acting in and as a group, will be discussed more in detail in one of the following sections.

2. In fibre concrete, the fibre is embedded along its whole length in the concrete; in the pull-out tests performed in this research project, the fibre is embedded at one side in the concrete, and on the other side it is hold by a steel grip;

To the author's knowledge, the only comparison of the results of pullout tests of fibres, embedded at both and at one side in concrete, is given in [Bartos et al., 1994]. In these tests, both aligned and inclined fibres were tested. In general, somewhat lower maximum pullout forces were registered when the fibres were embedded in concrete from both sides, probably due to the debonding and eventual pullout of fibres from both sides of the "cracking plane". The differences in the maximum pullout forces were almost negligible for the inclination angles between 0° and 30°, while at inclination angles of 45° and 60°, the differences were about 15% and 30% respectively. The general pullout behaviour of the fibres was similar for both embedding conditions.

As in the tensile specimens produced in this research project, the fibres are oriented at angles from 15° to 32° with respect to the direction of the main tensile stress (Tab. 3.3), the influence of the embedding conditions will therefore be neglected.

3. For inclined fibres, another reason for different pullout behaviour, is the difference between the initial inclination angle α, and the actual local bending angle β across the crack;

This aspect was already mentioned in the previous sections, and these differences will be analysed in detail both for long and for short fibres in the following chapters.

Pullout of long fibres with fully deformed hook
The experimental results of the pullout tests on long fibres with fully deformed hook, and those in the modelling applied pullout behaviour of these fibres, are given in Fig. 4.17 a and b. The diagrams are based on the experimental results of the pullout tests on these fibres (see section 2.9).

For the modelling purposes, the following assumptions were made:
1. During tensile softening, the fibre pullout takes place only at one side of the crack, i.e. the fibre slip Δ is equal to the crack opening w;
2. The average orientation angle of long fibres in the tensile specimens is 29° (Tab. 3.3). Taking into account a rather high bending stiffness of the steel fibres with $l/d = 60/0.7$, the

minimum achievable bending angle β_{min} (Fig. 4.15), is assumed to be approximately one half of the average initial orientation angle, i.e. $\beta_{min} = 15°$;

3. Using the results of the pullout tests on aligned and inclined hooked-end fibres (section 2.9), the following possibilities will be assumed for bending angle of the fibre across the crack of a width w (Fig. 4.17):

− no bending: it is assumed that the fibre has such a large bending stiffness, that it does not bend in spite of its inclination with respect to the main tensile stress. Therefore, in this case the fibre pullout diagram for fibre inclined at 0° will be used.

− full bending: the bending stiffness of the fibre is so low, that from the early beginning of its pullout, the fibre is fully bent, i.e. inclined under the angle $\beta_{min} = 15°$; as a consequence of bending of fibre across the crack at this angle, higher values of pullout forces are obtained compared to aligned fibres.

− the average case - partial bending: the inclination angle of the fibre increases linearly from 0° at $w = 0$ mm, until $\beta_{min} = 15°$ at $w = 5$ mm, and after that remains constant.
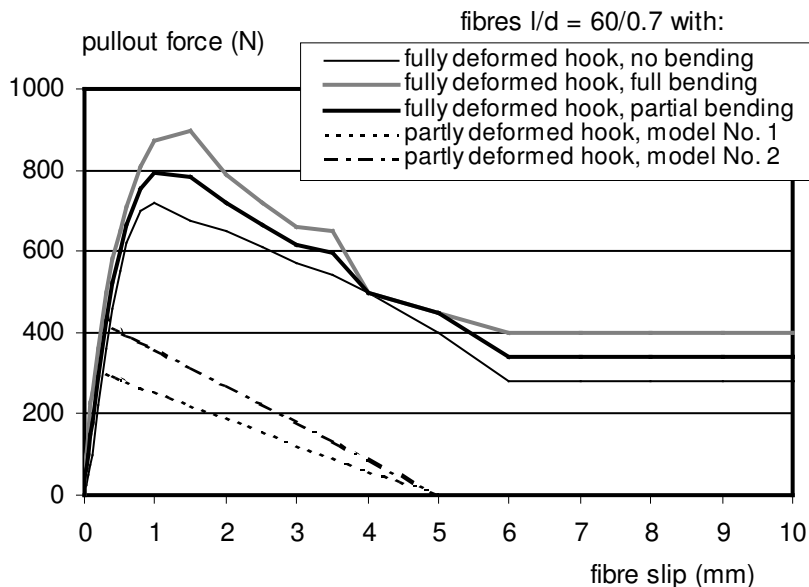
Fig. 4.17: The approximation of the pullout response of long hooked-end fibres (l/d = 60/0.7): full lines: fibres with fully deformed hooks, for different bending angles across the crack (0° (no bending), 15° (full bending), and the average case of the former two), based on the results of the pullout tests (section 2.9); dotted lines: fibres with partly deformed hooks, on the basis of the assumption on the combined fibre pullout and concrete fracture around fibre, as presented in Fig. 4.18.

4. As already pointed out in section 2.9, the pullout response of hooked-end fibres does not depend on the available fibre embedded length, for embedded lengths larger than 10 mm (which is approximately the hook length plus 5.0 mm). This was shown in [Markovic et al., 2002b], as well as in [Van Gysel, 2000];

5. The frictional pullout force decreases linearly to 0, starting from the 2/3 of the available full fibre embedded length, based on the results of the fibre pullout tests given in [Markovic et al., 2003b];

Pullout of long fibres with partly deformed hook

During the analysis of the number and orientation of fibres in the tensile specimens, a relatively large number of long hooked-end fibres with no hook deformation, was observed (section 3.6, Fig. 3.26).

Clearly, these fibres do provide a pullout resistance, but probably to a smaller extent compared to the fibres with fully deformed hooks. However, the experimental determination of the pullout response of fibres with partly deformed hooks is technically not possible.

For the modelling purposes, the following assumptions were made:
1. During tensile softening, the fibre pullout takes place only at one side of the crack, i.e. the fibre slip Δ is equal to the crack opening w;
2. According to the possible pullout scheme given in Fig. 4.18, a combination of fibre pullout and concrete fracture will occur. In both fibres, the pullout force increases in the initial phases of their pullout, until the beginning of the fracture of the concrete around one of these fibres. The possible reasons for concrete fracture can, for example, be a small embedded length of a fibre, inclination of a fibre, a locally poor quality of the concrete, and/or different combinations of these factors. As the surrounding concrete cracks, less and less pullout resistance is provided by these fibres. Their hooks will therefore remain un-deformed until the end of the pullout.
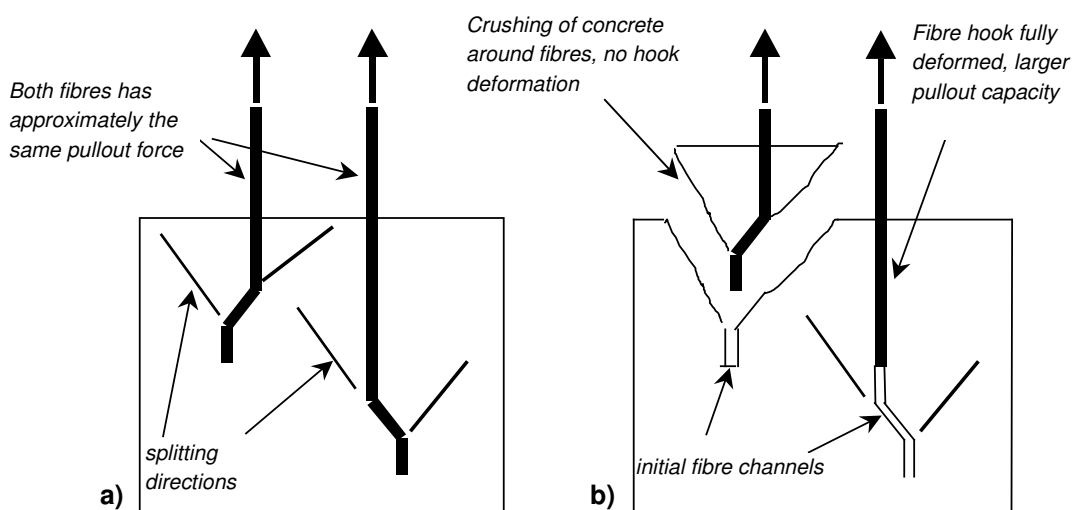
Fig. 4.18: Assumed possibilities of the pullout of hooked-end fibres: a) the initial stage of the pullout process, both fibres equally active;   b) concrete matrix around fibre with shorter em-

bedded length cracks, therefore this fibre is pulled out without hook deformation; while the hook of the fibre with longer embedded length is fully straightened and pulled-out.

The described fracture of concrete around hooked-end fibres does indeed take place. A lot of small broken pieces of concrete could be observed, during both tensile and flexural tests, especially when the concrete contained only long hooked-end fibres.
The maximum pullout force needed for only the debonding of a long hooked-end fibre with $l/d = 60/0.7$, is about 100 N, according to [Van Gysel, 2000]. The energy necessary to debond a fibre and to start the fracture of concrete around it, is certainly somewhat higher than the one needed only to debond the fibre. Therefore, two pullout curves are proposed in Fig. 4.17 for fibres with partly deformed hooks (assumed maximum pullout forces 300 N and 450 N), and they will be evaluated.

It should be pointed out as well, that the cracking of concrete around fibres with partly de-formed hooks (fibre No. 2 in Fig. 4.19), can have an influence on the pullout process of neighbouring fibres with fully deformed hooks. If the diagonal cracks in Fig. 4.19 cross the fibre No. 3 with fully deformed hook, than the pullout of that fibre will be finished at a crack width smaller than the visible embedded fibre length. Therefore, the visible fibre length l_{vis} will be larger than the real embedded length of the fibre l_{emb} (Fig. 4.19). The fi-bre No. 1 in Fig. 4.19 is located outside the influencing zone of the fibre No. 2, and there-fore for this fibre is $l_{emb} = l_{vis}$.
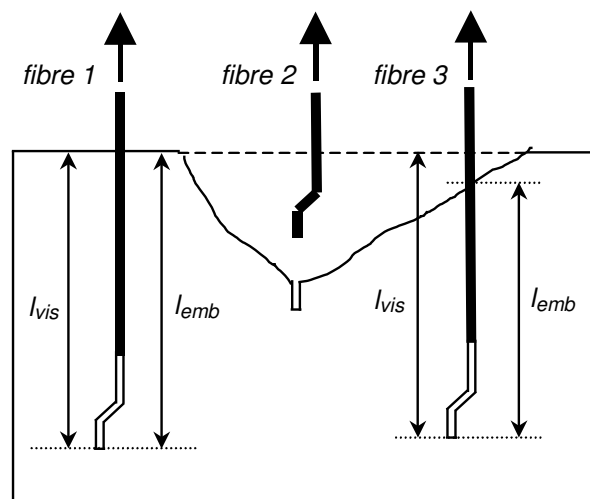
Fig. 4.19: The influence of fibres 1, 2 and 3 on each other: the inner cracking due to the pull-out of fibre 2 (with partly deformed hook) causes that the visible length (l_{vis}) of the fibre 3 with fully deformed hook is larger than its real embedded length (l_{emb}), i.e. $l_{emb} < l_{vis}$; for fibre 1 is $l_{emb} = l_{vis}$, because this fibre lies outside the influence zone of the fibre 2

According to Fig. 3.25.b, about 40 % of the hooked-end fibres have a visible embedded length larger than 20 mm. This means that there must be a tensile stress transfer at the displacement of 20 mm and more. However, in tensile tests, already at the displacement of about 20 mm, the tensile stress was equal to zero. Therefore, all the fibres with visible lengths larger than 20 mm were not active in crack bridging. The most probable reason is that their real embedded lengths are smaller than their visible lengths, which happens by virtue of the inner cracking of concrete around these fibres (Fig. 4.19).

This requires the modifications in the pullout diagrams of the fibres, but only at the values of the fibre slips larger than 10 - 20 mm. As only the initial part of the pullout process is of interest here, no modifications will be introduced, and this phenomenon will from now on be neglected in the analytical modelling.

3. As these fibres are active only at small crack widths, it can be supposed that they do not bend over the crack, i.e. $\alpha = \beta$ (Fig. 4.15).

Pullout of short straight fibres

The pullout curves for short straight fibres (l/d = 13/0.2) with different embedded lengths, which will be applied in the analytical modelling, are given in Fig. 4.20 and Fig. 4.21 a) and b).

As already explained, the scatter of the results of pullout tests on short fibres was rather large. Also, only a few comparable test results of other researchers on straight steel fibres are available [Van Gysel, 2000]. Therefore, for the modelling purposes, the following assumptions were made:

1. During tensile softening, the fibre pullout takes place only at one side of the crack, i.e. the fibre slip Δ is equal to the crack opening w;
2. The maximum pullout force P is proportional to the available fibre embedded length l_{emb}. The maximum forces in the pullout diagrams of fibres, given in Fig. 4.20 with dotted lines, are assumed first for the discrete values of the fibre embedded lengths of 2, 4, 6, 8, and 10 mm. This is done on the basis of the performed pullout tests on short fibres (Fig. 2.29.b) using the linear proportionality of fibre embedded lengths l_{emb} and pullout forces P, based on:

$$l_{emb} = 2 \text{ mm} \quad => \quad P = 10.0 \text{ N (assumed)};$$
$$l_{emb} = 6 \text{ mm} \quad => \quad P = 20.0 \text{ N (experimentally obtained - approximated).}$$
$$l_{emb} = 8 \text{ mm} \quad => \quad P = 25.0 \text{ N (experimentally obtained - approximated).}$$

After that, the average pullout response of fibres, whose embedded lengths lies between the two subsequent discrete embedded lengths (i.e. between 0 and 2 mm, 2 and 4 mm etc.), is determined as the arithmetic average value (full line diagrams given with grey line in Fig. 4.20).

The assumption on the linear proportionality between the pullout forces and the embedded lengths of fibres, is probably not completely correct, as the distribution of the shear stress on the fibre-matrix interface is non-linear. However, as the number of the existing experimental and analytical studies on the pullout behaviour of fibres with different embedded lengths is very limited ([Li & Stang, 1997], [Van Gysel, 2000]), and no one of them describes this process for steel fibres fully and in a unified way, it was decided to use the simple rules of linear proportionality.

3. Two possibilities for the frictional part of the pullout diagram will be tested; namely, a constant frictional pullout force (Fig. 4.20.a) and a linearly-decreasing frictional pullout force (Fig. 4.20.b).

A more-or-less constant pullout force was experienced during the frictional part of the pullout of single short fibres (Fig. 2.29.b). However, a decrease of the frictional pullout force is possible as well. This can happen because of the differences in the quality of the concrete in single fibre pullout tests and in the uniaxial tensile tests, as well as because of the weakening of the fibre action, if the fibres act in and as a group.
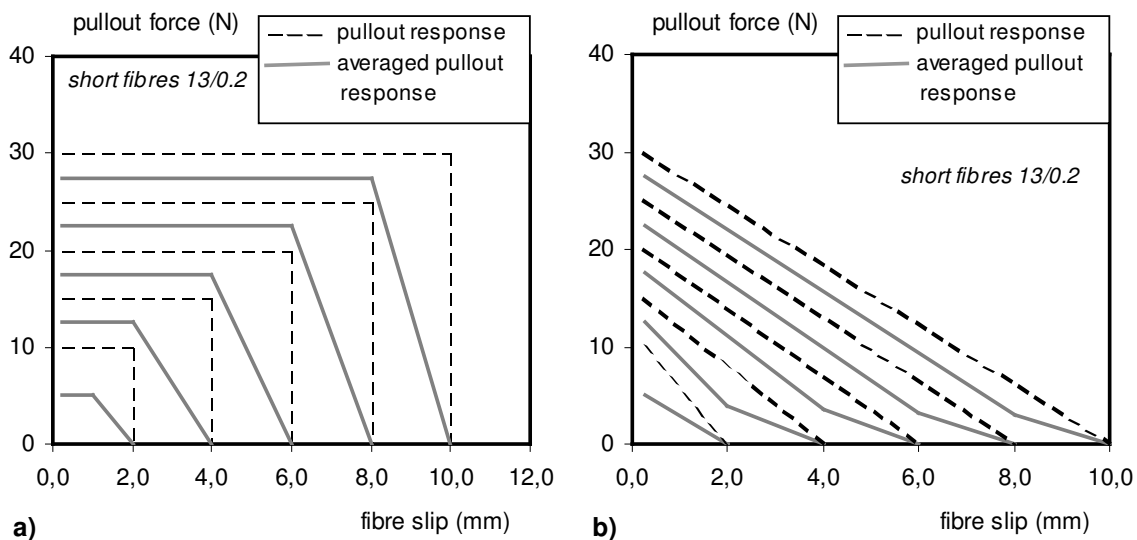
Fig. 4.20: The assumed pullout response of short fibres with embedded lengths l_{emb} = 2, 4, …, 10 mm (broken lines), and arithmetically averaged pullout responses for the fibres with embedded lengths l_{emb} = 0 to 2 mm, 2 to 4 mm, …, 8 to 10 mm (grey full lines), for: a) constant frictional pullout force;   b) linearly decreasing frictional pullout force

4. For the specimens with short fibres only, the average orientation angle of the fibres was about 32.5° (Tab. 3.3). The bending stiffness of the short thin fibres (l/d = 13/0.2) is about 150 times lower compared to the bending stiffness of the long hooked end fibres (l/d = 60/0.7). Therefore, it will be assumed that the short thin fibres will completely bend across the crack, from the early beginning of the crack opening, i.e. $\beta = 0°$ for $0 < w < w_{max}$ (Fig. 4.15).

In [Van Gysel, 2000 - Fig. III.38 to III.40], the results of the pullout tests on straight fibres (l/d = 30/0.5) inclined at 30° are described. Starting from the fibre slip (i.e. here from the crack width) of about 0.2 mm, the pullout force of inclined fibre was about 35% - 45% higher, compared to the same aligned fibre. This increase is a consequence of local bending of the fibre across the crack.

Based on these results, and taking into account that the average orientation angle of the fibres in the tensile specimens was approximately also 30° (like in [Van Gysel, 2000]), all the values of pullout forces in previously determined pullout diagrams, will be increased for 35%. The only exception will be made for the fibres with very short embedded lengths l_{emb} < 2.0 mm, where the influence of bending can be neglected. The final fibre pullout diagrams for different embedded lengths, are given in Fig. 4.21.a (constant frictional pullout force) and Fig. 4.21.b (linearly-decreasing frictional pullout force).
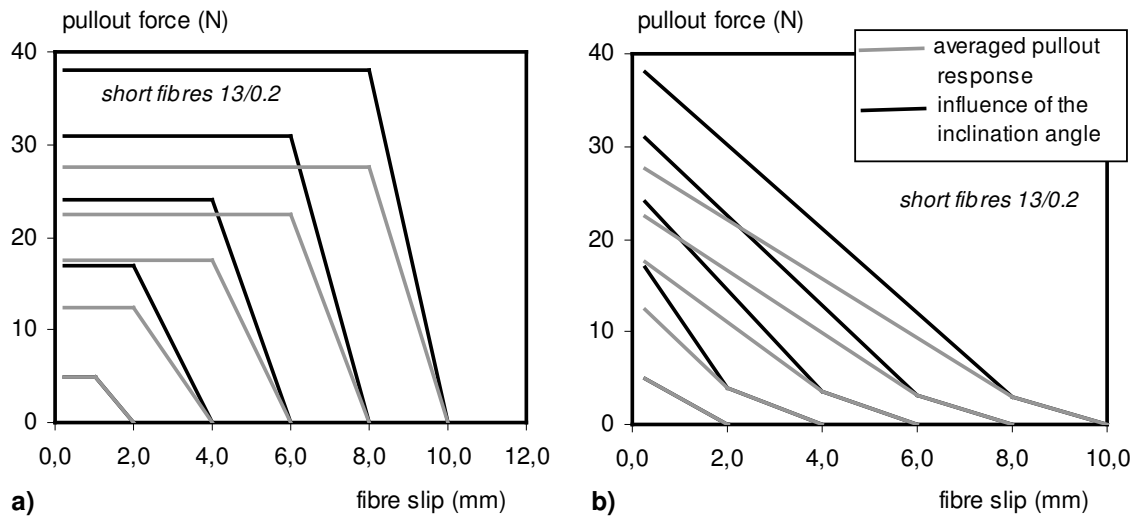
Fig. 4.21:   The initial (grey lines, from Fig. 4.20) and the increased pullout response of short fibres 13/0.2, by virtue of their inclination angle of 30° (black lines), which will be used in the analytical model: a) assumed constant frictional pullout force during the whole pullout process (as observed in the pullout tests on these fibres);   b) assumed linear decrease of the frictional pullout force, after its maximum value has been reached

Modelling procedure and summary of the modelling parameters

In the following sections, the results of the analytical modelling of the tensile softening will be shown. The procedure for the computation of tensile stresses in concretes with short, long and with short and long fibres together will be described as well.

The detailed examples of the computation procedures are given in tabular form as well, in the Appendix 4.A, using the tensile softening of Hybrid-Fibre Concrete as a case-study. This is therefore a general example, because the computation of tensile stresses generated by both short and long fibres is covered.

All known and unknown modelling parameters are given in Tab. 4.2, together with the short explanation on the constant and variable parameters in the modelling.

Tab. 4.2: Overview of the modelling parameters

FIBRE TYPE	PARAMETERS		WAY OF MODELLING
LONG FIBRES			
	Number of fibres		
		- fully deformed fibre hooks (Fig. 4.16.a)	= const.
		- partly deformed fibre hooks (Fig. 4.16.a)	= const.
	Orientation of fibres		
		$\beta_{min} = 15°$ (Tab. 3.3)	= const.
	Fibre pullout		
		- fully deformed fibre hooks (Fig. 4.17)	
		- no bending across the crack	to be varied in the model
		- partly bent across the crack	to be varied in the model
		- full bending across the crack	to be varied in the model
		- partly deformed fibre hooks (Fig. 4.17)	
		- Pmax = 300 N (model 1)	to be varied in the model
		- Pmax = 450 N (model 2)	to be varied in the model
SHORT FIBRES			
	Number of fibres		
		- length distribution 1 (Fig. 4.16.b)	to be varied in the model
		- length distribution 2 (Fig. 4.16.b)	to be varied in the model
		- length distribution 3 (Fig. 4.16.b)	to be varied in the model
		- length distribution 4 (Fig. 4.16.b)	to be varied in the model
		- length distribution 5 (Fig. 4.16.b)	to be varied in the model
	Orientation of fibres		
		$\beta_{min} = 30°$ (Tab. 3.3)	= const.
	Fibre pullout		
		- linear decrease of the pullout force during the frictional part of fibre pullout (Fig. 4.21.a)	to be varied in the model
		- constant pullout force during the frictional part of fibre pullout (Fig. 4.21.b)	to be varied in the model

4.6.4 Application of the model to concrete with long fibres only

The comparisons of the modelled unixial tensile behaviour, and the mean experimental results of the uniaxial tensile tests on concrete with 1.0 vol.-% of long fibres ($l/d = 60/0.7$), are given in Fig. 4.22 and 4.23 (up to the displacements of 2 mm and of 10 mm respectively).

According to Tab. 4.2, the following modelling parameters were used:
- first, the pullout behaviour of the fibres with fully deformed hooks was varied, depending upon their local bending across the crack (full, partial or no bending), as given in Fig. 4.17. For this purpose, the maximum achievable pullout force of the fibres with partly deformed hook, was taken as 300 N (model No. 1, Fig. 4.17);
- subsequently, the optimum local bending angle was chosen, and the pullout response of fibres with partly deformed hooks was varied according to Fig. 4.17 (model No. 1 with $P_{max} = 300$ N, and model No. 2 with $P_{max} = 450$ N).

The number of fibres active in crack bridging (the fibre length distribution), was kept constant (Fig. 4.16.a)
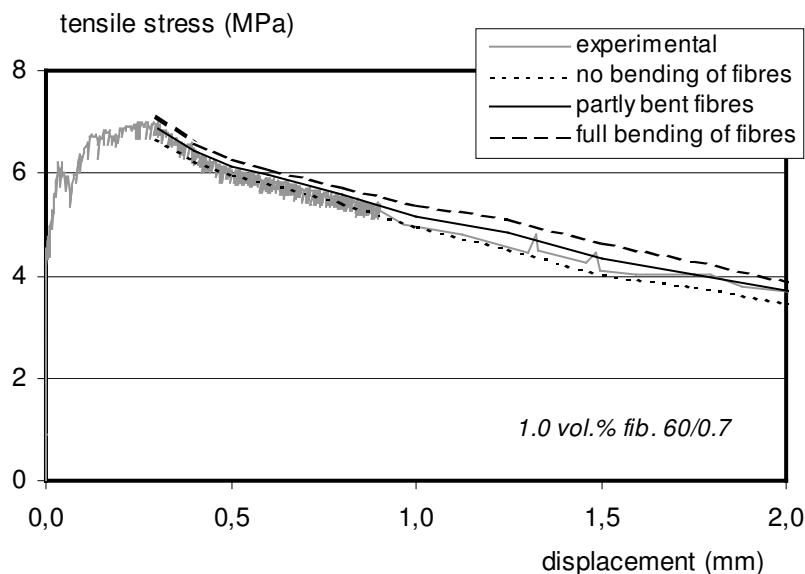
Fig. 4.22: Uniaxial tensile behaviour of concrete with 1.0 vol.-% of long fibres (l/d = 60/0.7), up to a displacement of 2.0 mm: comparison of mean experimental results and modelled tensile behaviour for different bending angles of the fibres across the crack (no bending, partly bending and full bending)

The tensile stress was calculated starting from a displacement of 0.3 mm, at which tensile softening approximately begins. Therefore, the number of fibres active in the crack bridging (Fig. 4.16.a), and the values of the pullout force (Fig. 4.17), were also taken into calculation starting from 0.3 mm. The calculations were made for discrete displacement values, with

steps of 0.1 mm between 0.3 mm and 1 mm, the step of 0.25 mm between 1 mm and 2 mm, the step of 0.5 mm between 2 mm and 5 mm, and further with steps of 1 mm up to the displacement of 40 mm.

Obviously, a rather good agreement between the experimental and the analytically modelled results could be achieved. The local bending of the fibres over the crack does not have such a large influence on the full tensile response (Fig. 4.22). This is primarily due to the relatively low number of fibres with fully deformed hooks in this concrete (only about 25 % of total number of fibres), for which this local bending was taken into account. As the scatter in the modelled tensile responses is very small, it is rather difficult to say for which local bending angle the best modelling agreement was achieved.

The comparisons of the modelled tensile responses with partly deformed fibres with P_{max} = 300 N (model No. 1, Fig. 4.17) and P_{max} = 450 N (model No. 2, Fig. 4.17), is given in Fig. 4.23. Obviously, much better agreement can be achieved using as P_{max} = 300 N (model No. 1).
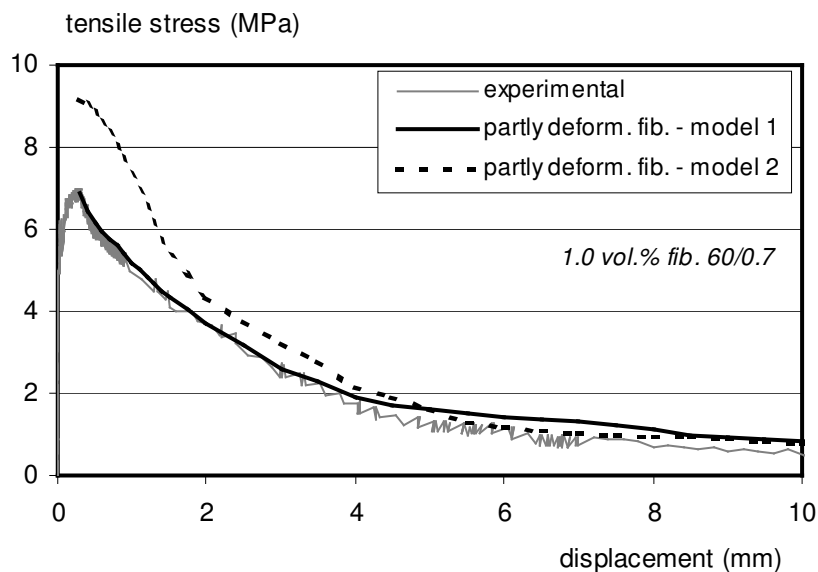
Fig. 4.23: Influence of the pullout behaviour of fibres with partly deformed hooks on the total uniaxial tensile behaviour of concrete with 1.0 vol.-% of long fibres (l/d = 60/0.7), according to the assumed pullout diagrams shown in Fig. 4.17 (model No. 1 and model No. 2)

At displacements larger than about 8 mm, the differences in modelled and experimental tensile stresses are somewhat larger than the initial values. This is probably the consequence of the inner cracking of the concrete that surrounds fibres with fully deformed hooks, as explained in Fig. 4.19.

4.6.5 Application of the model to concrete with short fibres only

The comparisons of the modelled uniaxial tensile behaviour, and mean experimental results of the uniaxial tensile tests on concrete with 2.0 vol.-% of short fibres (l/d = 13/0.2), are given in Fig. 4.24 and 4.25.

According to Tab. 4.2, the following modelling parameters were used:

− firstly, both a constant and a linearly decreasing fibre pullout force (Fig. 4.21.a and b), both of them using the fibre length distributions No. 1 (l_{max} = 8 mm) and No. 2 (l_{max} = 6 mm), given in Fig. 4.16.b;

− subsequently, only the linearly decreasing fibre pullout force (Fig. 4.21.b), using the fibre length distributions No. 3, 4 and 5, given in Fig. 4.16.b (each one with l_{max} = 6 mm, with different percentages of various fibre embedded lengths).

The tensile stress was calculated starting from a displacement of 0.5 mm. However, the number of fibres active in crack bridging (Fig. 4.16.a), and the values of the pullout force (Fig. 4.17), were taken into calculation starting from a displacement of 0.25 mm, which corresponds to the beginning of the tensile softening. The calculations were made at discrete displacement values, with steps of 0.25 mm between 0.5 mm and 1 mm, steps of 0.5 mm between 1 mm and 4 mm, and further with steps of 1.0 mm up to a displacement of 6 mm, i.e. of 8 mm.

Although the tensile softening of this concrete starts at a displacement of about 0.25 mm, it may be supposed that at this displacement there is still not one single dominant crack. The fibres, which bridge the multiple cracks developed during the strain hardening phase, are probably still partly active during an intermediate period, until one single crack becomes dominant. Here, it was supposed that this intermediate period extends from 0.25 mm to 0.5 mm, and therefore the calculations for the tensile softening response started from 0.5 mm.

The scatter in the uniaxial tensile behaviour of concrete with short fibres was rather high during the softening phase. Therefore, the mean experimental result will be the one, to which all the modelling results will be compared to.

The comparison of the experimental results and the modelled uniaxial tensile response for a concrete with 2.0 vol.-% of short fibres (*l/d* = 13/0.2), for the fibre embedded length distributions 1 and 2 (Fig. 4.16.b), and for both constant and linearly decreasing frictional pullout force of fibres (Fig. 4.21.b), is given in Fig. 4.24.

Obviously, a constant fibre pullout force results in a strong overestimation of the experimental results, no matter which fibre length distribution was used. The assumption of a linearly decreasing fibre pullout force, corresponds much better to the experimentally obtained results. However, the differences are for both fibre length distributions still rather large.
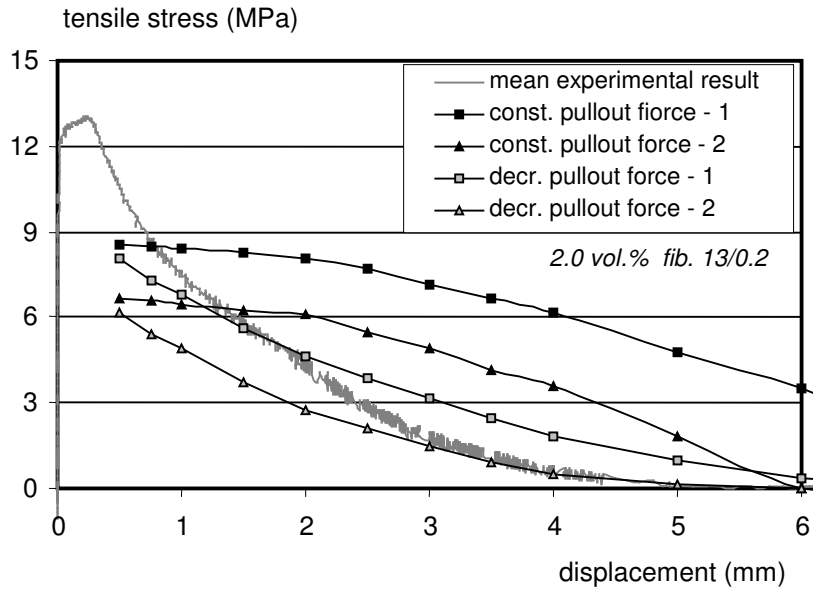
Fig. 4.24: Uniaxial tensile behaviour of concrete with 2.0 vol.-% of short fibres (l/d = 13/0.2): a comparison of the mean experimental result and modelled tensile behaviour for different fibre pullout diagrams (Fig. 4.21.b) and distributions of the fibre embedded lengths No. 1 and 2 (Fig. 4.16.b)
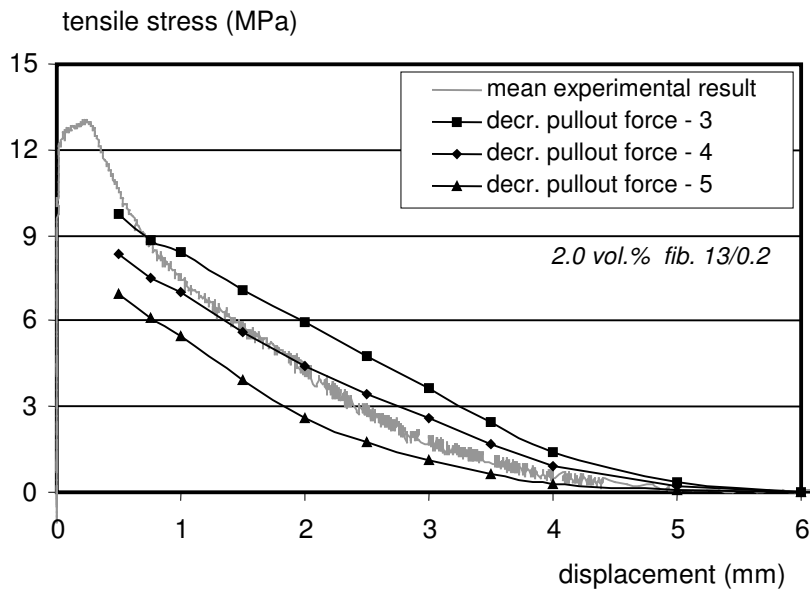
Fig. 4.25: Uniaxial tensile behaviour of concrete with 2.0 vol.-% of short fibres (l/d = 13/0.2): a comparison of the mean experimental result and modelled tensile behaviour for linearly decreasing pullout force (Fig. 4.21.b) and the distributions No. 3, 4 and 5 of fibre embedded lengths (Fig. 4.16.b)

In Fig. 4.25, the modelled uniaxial tensile responses with linearly decreasing pullout force (Fig. 4.21.b), for fibre embedded length distributions No. 3, 4 and 5 (Fig. 4.16.b), are given.

Obviously, the modelled results with the fibre embedded length distribution No. 4, for which the most of the available embedded lengths of the fibres lay between 2 and 6 mm, shows the best agreement to the experimental results. Also, the more shorter fibre embedded lengths are present, the lower the tensile stress during tensile softening will be (fibre length distribution No. 5), and vice versa (fibre length distribution No. 3).

In Fig. 4.25, using the fibre length distribution No. 4, the modelled results approximate the experimental results rather well starting from the displacement of 1.0 mm. However, between 0.5 and 1.0 mm, it was still not possible to achieve a good correlation, in spite of a rather large number of trials with many other fibre length distributions.

This may be a consequence of other modelling parameters, which is in this case only the fibre pullout force. A good correlation could indeed be achieved using somewhat higher fibre pull-out forces for fibre slips between 0.5 and 1.0 mm. This is however not well founded, taking into account the experimental pullout diagrams for short fibres (Fig. 2.29.b)

Another reason for the deviations between 0.5 mm and 1 mm, could be the still on-going intermediate period, between the reaching of the tensile strength, and the existence of one single dominant crack. It may therefore be possible that in concretes which exhibit the multiple cracking, the macrocrack growth phase does not end immediately after the tensile strength is achieved, but somewhat later. In such a case, the crack growth phase shown in Fig. 4.1, should be extended further to the tensile softening phase.

It should also be noticed that the assumption of no local bending of short thin fibres across the crack, would not be reasonable. In such a case, the fibre pullout forces would on average be about 30% lower than the pullout forces of the inclined fibres. Therefore, also the modelled tensile stresses would be about 30 % lower.

On the basis of these results, a theoretical influence of the number of fibres (i.e. of the applied fibre volume quantity) on the tensile softening response is determined, and given in Fig. 4.26. A constant fibre orientation angle of 30° was used in all cases. In addition, a linearly decreasing fibre pullout force and fibre length distribution No. 4 were applied.

Obviously, the more fibres are present in the cross section, the higher tensile stresses can be achieved in the softening phase. However, it should be taken into account that the higher is the fibre quantity, the more entrapped air will probably be present in the concrete matrix, i.e. the quality of concrete will be lower. Therefore, higher tensile stresses can be expected with more fibres (keeping their orientation constant), but the increase of these stresses will probably not be proportional, as shown in Fig. 4.26.
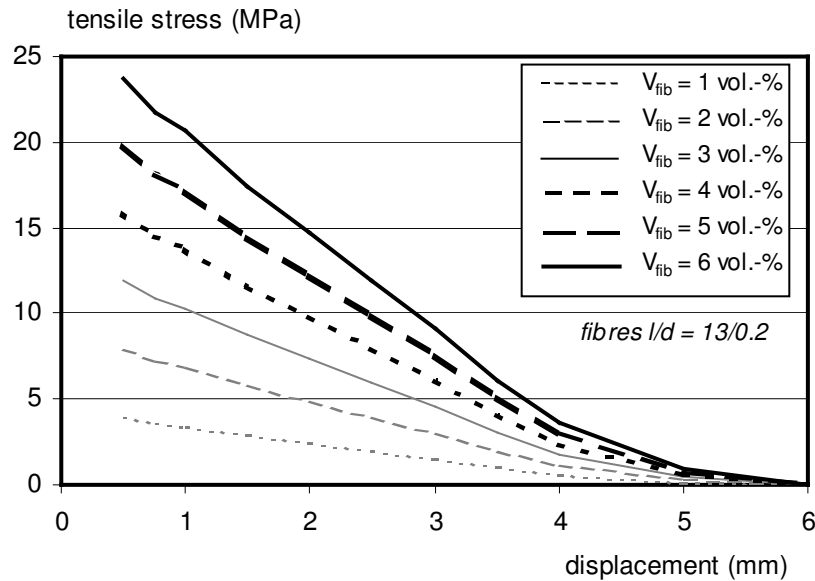
Fig. 4.26: The theoretical influence of the applied volume quantity V_{fib} of short fibres (l/d = 13/0.2) on the tensile softening response of concrete

4.6.6 Application of the model to concrete with both long and short fibres

Introduction

In the previous two sections, the modelling parameters were varied and calibrated, using the results of tensile tests on concretes with one type of fibres (short or long). In this section, these calibrated parameters will be applied in the analytical modelling of the tensile response of concrete with both short and long fibres.

The modelling will be performed for the hybrid-fibre concrete No. 5 (Tab. 3.2), which contains 0.5 vol.-% of short fibres (*l/d* = 13/0.2), and 1.0 vol.-% of long fibres (*l/d* = 60/0.7). The results of the uniaxial tensile tests on notched specimens, given in Fig. 3.20.b will be used as experimental reference for comparisons. The reason for choosing the results on notched specimens, is to avoid the eventual intermediate period between reaching of tensile strength and the development of one dominant crack, as observed in the un-notched speci-mens, used in tensile tests of concrete with short fibres (Fig. 4.25).

Parameter identification

Similarly as for concretes with one fibre type, also here the two main groups of parameters can be identified:
− the distribution of the embedded lengths of the fibres (both short and long)
− the pullout behaviour of the fibres (both short and long).

Distribution of embedded fibre lengths

The distribution of the embedded lengths of the long fibres (l/d = 60/0.7) can be derived from the diagrams given in Fig. 3.25. In Fig. 4.27, the ratio of the number of long fibres active at any crack width w, and the total number of fibres that bridge a crack, are given, both for fully and partly active fibres. By virtue of the presence of short fibres, much more long hooked-end fibres have fully deformed hooks, compared to the concrete that contains only long fibres (Fig. 4.16.a). The total number of long fibres will be taken from Tab. 3.3, as the average counted number in three tensile specimens (n_{tot} = 1.77 fibres / cm^2, i.e. n_{tot} = 107 fibres in the whole cross-section).

For short straight fibres (l/d = 13/0.2), the distribution of the embedded lengths No. 4 will be applied (Fig. 4.16.b), as calibrated in Fig. 4.25. The total number of short fibres per cm^2 of the cross-section of the specimens is given in Tab. 3.3 (the average value for two specimens is 11.15 fibres / cm^2).
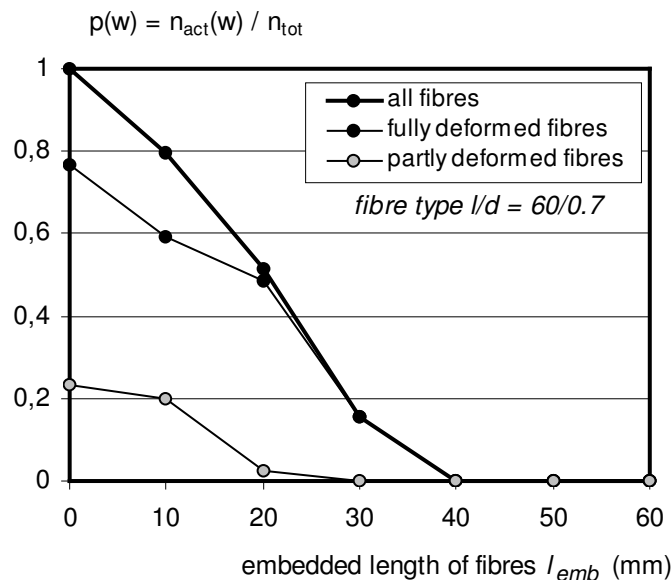
Fig. 4.27: The ratio of the number of fibres active in crack bridging at a crack width w, and the total number of fibres, for concrete with short and long fibres (all fibres, and fibres with fully and partly deformed hooks) - determined from the diagram given in Fig. 3.25

Pullout behaviour of fibres

In concrete with long fibres only, the influence of local bending of fibres across the crack was taken into consideration only for fibres with fully deformed hook (Fig. 4.17). As their number was relatively small, no significant influence of the local bending angle was observed in the modelling of tensile response (Fig. 4.22).

Therefore, all cases of the pullout of fibres with fully deformed hooks as given in Fig. 4.17, will also be taken into the consideration in the modelling of tensile response of hybrid-fibre concrete.

For the fibres with partly deformed hook, the pullout diagram with the maximum pull-out force P_{max} = 300 N will be used, according to the calibration given in Fig. 4.23.

According to [Markovic et al., 2003a], the pullout force of long hooked-end fibres increases if short fibres are present in the pullout medium (concrete). For the hooked-end fibres which were both aligned and inclined to the pullout force (i.e. to the main tensile stress), the presence of 2.0 vol.-% of short fibres resulted in an increase of the pullout force of about 30 % (Fig. 2.26).

Taking into account that the applied volume quantity of short fibres is 4 times smaller (0.5 vol.-%) in the concrete under consideration, an increase of the pullout force in each hooked-end fibre of: *(30 %) / 4 = 7.5 %* will be assumed. This assumption is therefore based on the linear proportionality between the applied quantity of short fibres and the pullout behaviour of long fibres.

Practically, this means that in the calculations, the tensile stresses generated by long fibres will be calculated first as if the presence of the short fibres does not influence the pullout behaviour of long hooked-end fibres. Subsequently, in such a way calculated tensile stresses will be multiplied by *1.075 (= 7.5 %)*.

For short fibres, the pullout response given in Fig. 4.21.b will be applied. Herewith, an inclination of the short fibres from the early beginning of the pullout process is assumed. Moreover, the pullout force decreases linearly during the pullout process. This pullout process was calibrated as the best one in simulating the experimental tensile softening behaviour of concrete with short fibres only.

Results of the analytical modelling

The comparisons of the modelled uniaxial tensile behaviour, and the mean experimental results of the uniaxial tensile tests on concrete with 1.0 vol.% of long fibres (*l/d* = 60/0.7) and 0.5 vol.-% of short fibres (*l/d* = 13/0.2), are given in Fig. 4.28.

The only parameter that was varied in the analytical modelling, was the pullout response of hooked-end fibres with fully deformed hooks (Fig. 4.17).

The tensile stress was calculated starting from a displacement of 1.0 mm, i.e. the point where tensile softening of HFC approximately begins. The number of fibres active in crack bridging (Fig. 4.16.a), and the values of the pullout force (Fig. 4.17), were also taken into account starting from 1.0 mm.

The calculations were made at discrete displacement values, with a step size of 0.1 mm between 0.3 mm and 1 mm, 0.25 mm between 1 mm and 2 mm and 0.5 mm between 2 mm and 5 mm. Further, a step size of 1 mm up to the maximum displacement of 40 mm was ap-

plied. First, the tensile stresses were calculated independently as a result of the action of short and of long fibres, and subsequently these values were summed.

tensile stress (MPa)
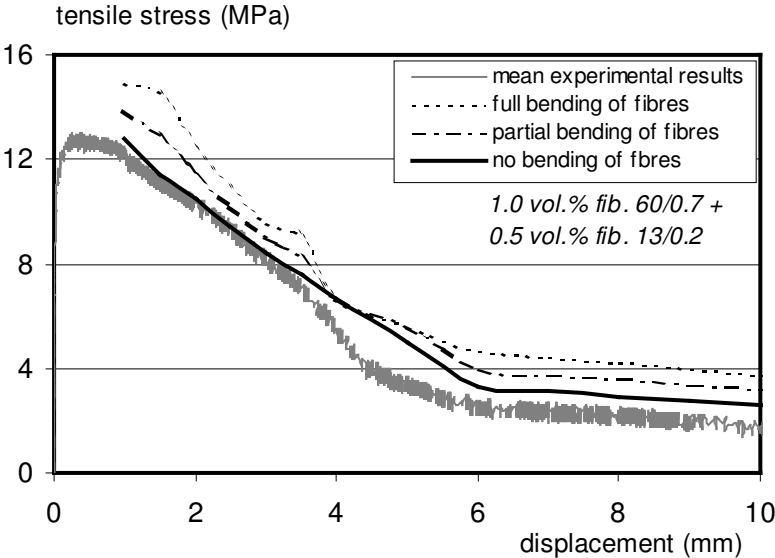
Fig. 4.28: Uniaxial tensile behaviour of concrete with 1.0 vol.% of long fibres (l/d = 60/0.7) and 0.5 vol.-% of short fibres (l/d = 13/0.2) up to the displacement of 10 mm: comparison of mean experimental results and modelled tensile behaviour, for different bending angles of the fibres across the crack (no bending, partial bending and full bending)

Obviously, the best correlation between modelled and measured tensile response was obtained with the assumption that there is no local bending of the fibres at all. With this assumption, the maximum modelled tensile stress was only 3 % higher than the experimentally obtained one. The first part of the descending branch (from 1.0 to 6.0 mm), as well as the characteristic bending point at the tensile diagram (at a displacement of about 6 mm), are very clearly pronounced in the modelled tensile response, with very low differences in comparison to the experimental results.

For the displacements exceeding 6.0 mm (second descendent branch), the modelled tensile stresses are about 20 % higher than the experimentally obtained values. This may be a consequence of the overestimated embedded lengths of the long fibres, as explained in Fig. 4.19, and as registered for concrete with long fibres in Fig. 4.23.

With the assumption of local bending of fibres (full or partial, section 4.6.2), neither the first descending branch, nor the characteristic bending point could be modelled properly. The differences in the modelled and experimental tensile stresses for displacements larger than 6 mm were also very large (about 100 %).

Synergetic effects

Synergy is the phenomenon where acting of two or more subjects together, leads to a better result, than the action of the same subjects independently of each other. Translated to Hybrid-Fibre Concrete, the synergy of short and long fibres leads to an improved tensile response of the Hybrid-Fibre Concrete, compared to the arithmetic sum of tensile responses of two concretes, one of which contains only long and other only short fibres (in the same volume quantities as the Hybrid-Fibre Concrete).

The short fibres contribute in two manners to the tensile softening behaviour of concrete containing both short and long fibres:

− direct contribution:
   - depending on the applied volume quantity of short fibres, they contribute to the total tensile stress during the tensile softening phase.

− indirect contribution:
   - much more long hooked-end fibres have fully deformed hooks during their pullout, by virtue of the presence of short fibres. Only a rather small quantity of short fibres can result in significantly higher number of long fibres with fully deformed hooks (e.g. the presence of 0.5 vol.-% of short fibres resulted that the number of long fibres with fully deformed hooks increased for about 250 %. This is obvious from the comparison of Fig. 4.27 (long fibres with short fibres and Fig. 4.16.a (only long fibres);

   - if present in concrete, short fibres can significantly improve the pullout behaviour of long hooked-end fibres, observed on individual basis (increase of the tensile force for about 30 %, Fig. 2.26). Therefore also the total tensile stresses during tensile softening behaviour of Hybrid-Fibre Concrete will be improved (in an indirect way).

These are the main reasons for the significant improvement in the tensile behaviour of the concrete with both short and long fibres (Fig. 4.28), compared to the concrete with long fibres only (Fig. 4.23).

In Fig. 4.29, the influence of the addition of 0.5 vol.-% of short fibres 13/0.2 to concrete containing 1.0 vol.-% of long fibres 60/0.7 is shown. Two cases are analysed:

− no synergy of fibre actions (the sum of the tensile stresses generated with both fibre types, given with dashed line);

− synergy of fibre actions (determined in the analytical modelling taking into account the contribution of the short fibres to the deformability and the pullout of long fibres, given with full line in Fig. 4.29).
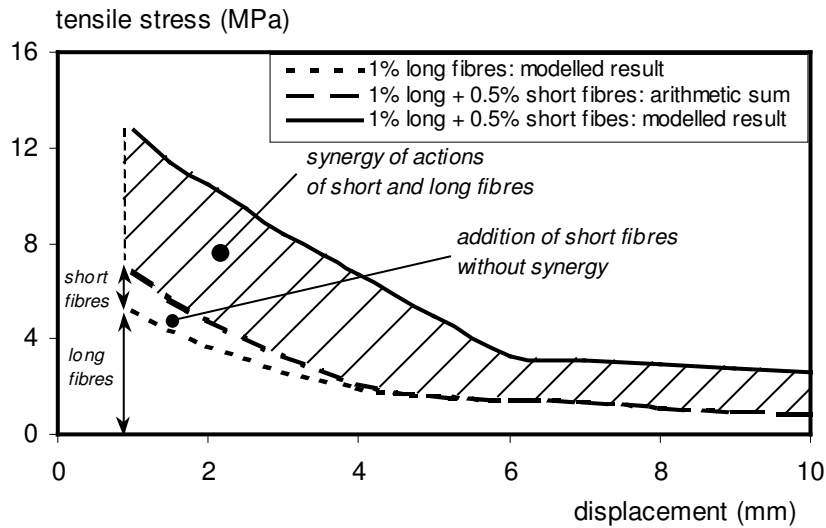
Fig. 4.29: Influence of the addition of 0.5 vol.-% of short fibres on the tensile behaviour of the concrete containing 1.0 vol.-% of long fibres, <u>without</u> synergy (arithmetic sum given with dashed line) and <u>with</u> synergy (modelled result given with full line, see also Fig. 4.28)

Clearly, the presence of short fibres contributes significantly to the improvement of the fibre pullout and deformability of the hooks of long fibres. Therefore, the total tensile stress generated during tensile softening is much higher compared to the tensile stress that can be achieved by independent action of fibres.

This is an analytical confirmation that combining different fibres in Hybrid-Fibre Concrete results in a significantly improved tensile softening behaviour in comparison with concretes with one type of fibre only.

Effect of the increase of volume quantity of short fibres

In the previous section it was shown that the presence of only 0.5 vol.-% of short fibres can significantly improve the tensile softening response of Hybrid-Fibre Concrete. In this section, the quantity of short fibres will be increased further to 1.0 vol.-%, 1.5 vol.-% and 2.0 vol.-%, in order to observe its influence to the tensile softening behaviour of Hybrid-Fibre Concrete. The quantity of long fibres will be kept constant at 1.0 vol.-%.

The modelled tensile softening behaviour for these concretes is shown in Fig. 4.30. The only modelling parameters that were varied, were:
− the pullout behaviour of long fibres 60/0.7 with fully deformed hooks (increased proportionally to the increase of the quantity of short fibres, based on Fig. 2.26);

- 154 -

– the volume quantity of short fibres.

tensile stress (MPa)
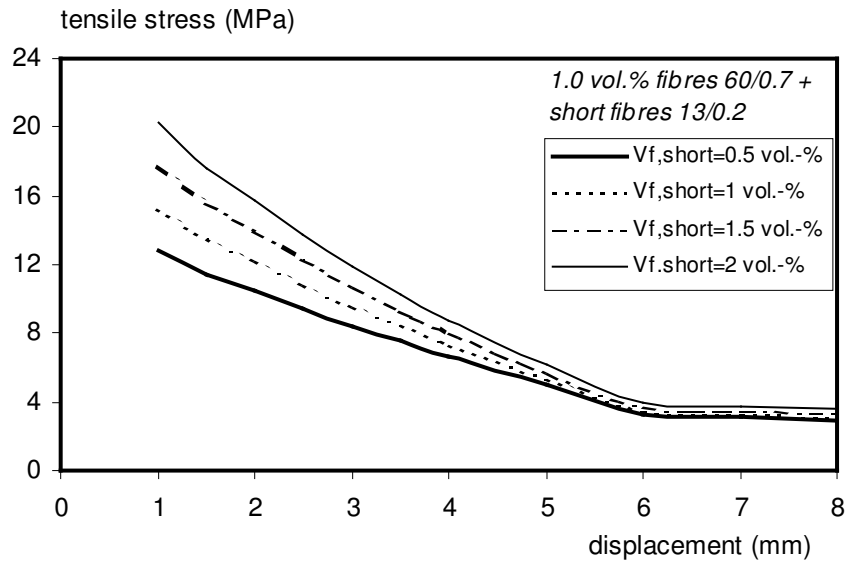
Fig. 4.30: The influence of the increase of the volume content of short fibres 13/0.2 on the tensile softening behaviour of concrete that contains 1.0 vol.-% of long fibres 60/0.7

Taking into account that no experimental data on the tensile behaviour of these concretes are available, all the *p(w)* values were taken the same as in the previous sections. Even the number of the fibres with partly deformed hooks was kept constant (as given in Fig. 4.27). However, with increasing amount of short fibres in concrete, more and more long fibres will show fully deformed hooks. Therefore, the modelling results will be at the safety side with such an assumption.

As shown in Fig. 2.26, the presence of 2.0 vol.-% of short fibres in concrete improves the pullout forces of long fibres with about 30 %. In Fig. 4.31, the influence of the improvement of the pullout behaviour of long fibres (by virtue of the presence of short fibres) on the total tensile stresses is shown. This improvement is therefore related only to the fibres with fully deformed hooks. The results are given for concretes that contain 1.0 vol.-% of long fibres 60/0.7, combined with 0.5 vol.-% and 2.0 vol.-% of short fibres 13/0.2.

Obviously, the more short fibres are present, the larger the improvement of the total tensile stress will be. In the case of low volume content of short fibres, the improvement is not that large (about 7.0 %). Therefore, the short fibres contribute mostly by increasing the number of long fibres with fully deformed hooks.

On the other hand, the improvement of the total tensile stress is about 18.0 %, if 2.0 vol.-% of short fibres are present in the concrete. Therefore, if short fibres are present in higher volume quantities, they have a double contribution to the improvement of the tensile stress during tensile softening: the pullout forces in long fibres are increased, as well as the number of long fibres with fully deformed hooks.

- 155 -
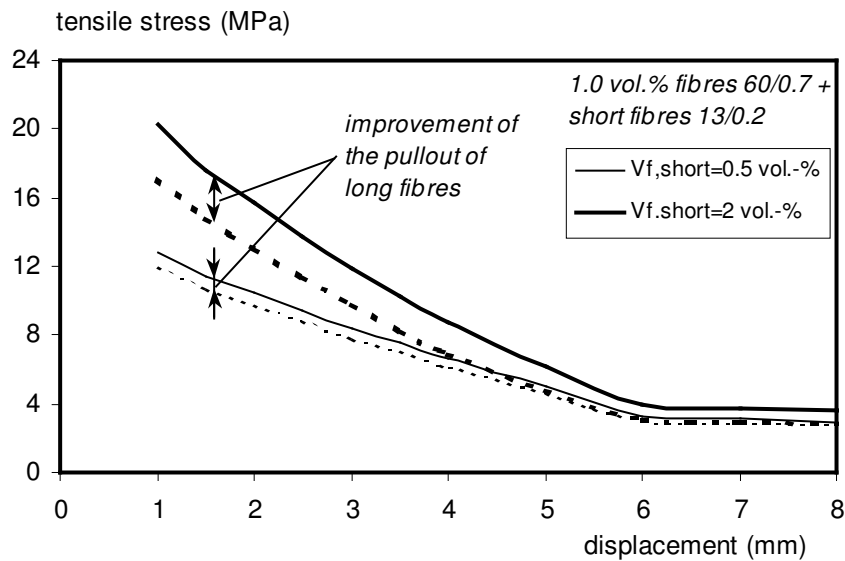
Fig. 4.31: The increase of the total tensile stress due to the influence of short fibres 13/0.2 on the improvement of the pullout forces in long fibres with fully deformed hooks, for different volume quantities of short fibres (0.5 vol.-% and 2.0 vol.-%) and constant quantity of long fibres (1.0 vol.-%)

4.7 Summary and concluding remarks

In this section, the analytical modelling of the tensile softening behaviour of concretes with one and two types of fibres is presented. The analytical model is based on number, orientation, pullout response and available embedded lengths of the fibres which bridge the dominant crack.

After the analytical model was introduced, the unknown parameters were determined from the tensile response of the concretes with one type of fibres (short and long fibres). Subsequently, the tensile response of concrete with two types of fibres was modelled using these parameters (or the parameters derived from the modelling parameters), and compared to the experimental results. The obtained modelled results corresponded in all cases rather well to the experimental results.

On the basis of the performed analytical modelling of the bridging of cracks by fibres in HFC, the following can be concluded:

General conclusions

1. With the exactly calibrated parameters, the modelled results correlate very well with the experimental ones, both for concretes with one and with two types of fibres. Therefore, the basic modelling equation 4.19, describes very satisfactorily the bridging of the crack by

- 156 -

fibres in fibre concrete during the tensile softening phase. This equation can most probably be used for any type of FRC with discontinuous fibres, no matter on fibre type or on fibre orientation.

2. Both short and long fibres influence each other rather strongly in fibre concrete, where they act in and as a group. The pullout behaviour obtained in the pullout tests on single fibres, is therefore not completely valid if more fibres act together near each other in a group.

3. The fibres inclined with respect to the main tensile stress, can in general show full, partial or no local bending over the crack. For each of these cases, the appropriate fibre pullout diagrams should be used.

Conclusions for concrete with short fibres only

4. For concretes with short fibres only ($l/d = 13/0.2$), the best correlation was obtained with the assumption of a linearly decreasing frictional pullout response of fibres. Such a response differs from the experimentally obtained constant frictional pullout response. This could be a consequence of the influence of the fibres on each other, by virtue of their small distance in the crack plane.

5. Short fibres inclined to the direction of the main tensile stress, probably start to bend locally over the crack immediately as the crack starts to open. This happens because of their low bending stiffness.

6. Local bending increases the fibre pullout forces of short fibres, and therefore also the total tensile stress for a fibre inclination angle of 30°. Therefore, according to the model, a better tensile softening response can be achieved if short fibres are oriented at 30°, compared to the fibres aligned with the main tensile stresses. Still, the experimental evidence for this is missing and should therefore be provided.

Conclusions for concrete with long fibres and Hybrid-Fibre Concrete

7. For concretes with long fibres, both the fibres with fully and with partly deformed fibre hooks should be considered in the analytical model, especially if many fibres possess partly deformed hooks. This happens often if only long fibres are applied in concrete. In that case, the pullout behaviour of fibres with partly deformed hooks determines to a large extent the total tensile behaviour of the fibre concrete under consideration.

8. In concrete with only long fibres, as well as in the concrete with both short and long fibres, according to the modelling results, no local bending of long fibres across the crack occurs. This is most probably the consequence of the large bending stiffness of these fibres.

Conclusions on synergy of short and long fibres in Hybrid-Fibre Concrete

9. Short fibres have triple contribution to the total tensile stress in tensile softening response of Hybrid-Fibre Concrete:

− they transmit tensile stresses across the crack (direct contribution);

− by virtue of the presence of short fibres, the number of long fibres with fully deformed hooks can be significantly increased (indirect contribution);

− by virtue of the presence of short fibres, the pullout behaviour of long fibres can be improved (indirect contribution).

10. In concrete with both short and long fibres, much more long fibres show fully deformed hooks. This happens by virtue of the presence of short fibres, even in rather low volume percentages. The full deformation of fibre hooks contributes significantly to the increase of the pullout forces in long fibres. This results in much higher tensile stresses that can be transmitted across the crack, compared to concrete without short fibres.

11. Not only the total number of fibres with fully deformed hooks, but also the pullout behaviour of each single long fibre with fully deformed hook is improved by the presence of short fibres.

12. On the basis of these facts, it may be concluded that there is a "synergy" of actions of short and long fibres in Hybrid-Fibre Concrete. "Synergy" means that the short fibres are "helping" the long fibres to generate as high tensile stresses as possible. Therefore, the combining of different types of fibres in the same concrete results in a better tensile (softening) behaviour compared to the concretes with one single type of fibre only. Similar conclusion apply also for flexural and uniaxial tensile tests.

Although a very good correlation between the experimentally obtained and the modelled results for Hybrid-Fibre Concrete is obtained (Fig. 4.28), it should be pointed out that a better understanding of the modelling parameters and the fracture processes in general is still necessary.

First, it should more accurately determine the pullout behaviour of short fibres, with variable embedded lengths and with different inclination angles. The assumptions made in this research project and related to the pullout behaviour of short fibres, resulted in a rather good prediction of the tensile softening response, but it should not be forgotten that those assumptions are mostly empirical.

Secondly, practical evidences on the local bending across the cracks for different types of inclined fibres, with different bending stiffnesses should be provided. The assumptions made in this research project seem to be logical from an empirical point of view, but there are still no firm evidences for them.

The contribution of fibres with partly deformed hooks to the total tensile response of fibre concrete does exist and should not be neglected. However, the pullout behaviour of these

fibres assumed here, is based on the experience, and should therefore be determined more accurately in the future.

For fibre concretes where multiple cracking is present, the full cracking sequence, as well as the point where the strain hardening stops and strain softening begins, should be accurately determined. As shown in Fig. 4.25 (concrete with only short fibres, with present multiple cracking), it was possible to obtain a proper correlation between the modelled and the experimental results starting from a displacement of about 1.0 mm, even though the decrease of the tensile stress (i.e. "per definition" the tensile softening) began at about 0.25 mm. This is probably a consequence of the not-terminated multiple cracking processes up to about 1.0 mm in this concrete.

In general, the analytical model for the tensile softening behaviour of different types of Hybrid-Fibre Concrete is based on a rather accurate determination of the numerous modelling parameters. This may require further complex experimental work.

As a first step, more fundamental understanding of these parameters is necessary. Subsequently, it is recommended to create reliable analytical models for as much parameters as possible in the future (fibre pullout behaviour, distributions of fibre visible lengths, etc.). The incorporation of the single parameters determined in such a way into the main model presented here, could improve the prediction of the tensile softening response for different types of Hybrid-Fibre Concrete.

CHAPTER 5:

UTILISATION OF HYBRID-FIBRE CONCRETE

5.1 Introduction

The first four chapters of this thesis are dedicated to the development of Hybrid-Fibre Concretes, with different types and volume quantities of fibres. The initially set demands concerning high tensile and flexural strength, pronounced ductility accompanied with multiple cracking as well as self-compactability and mixture stability in the fresh state, are fulfilled.

In this chapter, the possibilities for utilisation of Hybrid-Fibre Concrete in the engineering practice will be analysed. A short literature overview of the existing design methods and applications of both conventional FRC and HPFRCC will be given first. After that, a method of transition from the material scale to the structural scale will be proposed for Hybrid-Fibre Concrete, taking the fibre orientation as one of the crucial influencing factors. Subsequently, a case study related to the utilisation of Hybrid-Fibre Concrete for precast long-span prestressed girders will be presented and the results will be compared to the same utilisation case of classical concrete, from engineering and financial point of view. This will be followed by recommendations and conclusions with regard to the utilisation of Hybrid-Fibre Concrete.

The main goals of this analysis are to provide reliable design and production recommendations, as well as to point out the advantages of the utilisation of Hybrid-Fibre Concrete in engineering practice.

The idea of this chapter is to give a brief illustration of the possibilities of the utilisation of Hybrid-Fibre Concrete in engineering practice. This research area is still in development, and a significant portion of knowledge and experience should be gained in the future. Therefore, only the initial ideas and facts related to structural design with Hybrid-Fibre Concrete will be provided, without going much into details.

5.2 Design methods and utilisation fields of FRC and HPFC

5.2.1 Introduction

According to most national and international building codes, nearly all concrete structures can be designed if only two parameters are known: the compressive strength of the concrete and the yield strength of the steel (and prestressing) reinforcement.

Such a design concept cannot be applied in the case of fibre concrete. The reason for this is that the inner material structure of any type of fibre concrete is incomparable to the inner structure of conventional plain concrete. The post-cracking tensile capacity of fibre concrete is usually higher than that of the plain concrete. These facts can have a significant influence on most of the mechanical properties and therefore also on the design parameters needed for structural design (all values of the σ–ε diagram, E-modulus, shear resistance parameters, crack width control, mean crack spacing, etc.).

Several national and international research committees dealt with the development of recommendations for structural design, with both conventional fibre concrete (FRC), as well as with high-performance fibre concrete (HPFC). In this section, these recommendations will be presented first, and subsequently the utilisation fields and applications of FRC and especially of HPFC will be discussed.

5.2.2 Design methods for FRC and HPFC

The tensile behaviour of any type of fibre concrete can be characterised in different ways for design purposes in the engineering practice. In the so-called stress - strain method, the fibre concrete is considered to behave as a homogeneous continuum, both under tensile and compressive loading [Vandewalle, 2003]. The same method is incorporated into most of the building codes and standards for conventional reinforced concrete.

Due to its suitability and familiarity in standard engineering practice, this method was recommended by research committees for structural design with conventional fibre concrete, in [RILEM TC 162-TDF, 2003], [DBV-Merkblatt, 2001] and [SIA, 1998]. In [RILEM TC 162-TDF, 2003], the most comprehensive recommendations for the utilisation of FRC, based on numerous round-robin tests are given (production and testing methods, complete structural design principles and durability).

Existing design methods for structural design with high-performance fibre concretes (HPFC), are based on the stress - strain method too. The most comprehensive recommendations for structural design with HPFC are given by the French research group, in [AFGC & Setra, 2002]. In these recommendations, aspects like production and testing methods, structural design methods in SLS and ULS, durability and fatigue are discussed. However, the calculation procedures for crack width control as well as for the mean crack spacing are not given in these recommendations.

The design stress-strain curve proposed by [AFGC & Setra, 2002], with the numerical expressions for the appropriate design parameters in it, is given in Fig. 5.1.

According to this curve, the maximum linear elastic tensile strain $\varepsilon_{b,el}$ can be obtained from the maximum linear elastic tensile stress $f_{b,el}$ and the modulus of elasticity E. All other strains can be calculated from the characteristic length (L_{ch}), which is according to [AFGC & Setra, 2002] equal to $L_{ch} = 2H / 3$, where H is the height of the cross-section. No literature

source for such assumption for the value of L_{ch} is mentioned in these recommendations. The calculation of the post-cracking strains ε_{w1} and ε_{w2}, is based on the appropriate displacements w_1 (corresponds to the tensile strength f_b), and w_2 (corresponds to the stress where the softening diagram changes its slope. The ultimate strain $\varepsilon_{b,u}$ is dependent on the fibre length l_f. The values of stresses on the diagram, correspond to the appropriate values of stresses obtained in the uniaxial tensile tests, corrected with the safety factor.

$$\varepsilon'_{b,u} = 3.5\ \text{‰}$$

$$\varepsilon = \frac{\Delta L}{L_{ch}}$$

$$L_{ch} = 2H/3$$

$$\varepsilon_{b,el} = f_{b,el} / E$$

$$\varepsilon_{b,w1} = w_1 / L_{ch}$$

$$\varepsilon_{b,w2} = w_2 / L_{ch}$$

$$\varepsilon_{b,u} = l_f / (3L_{ch})$$
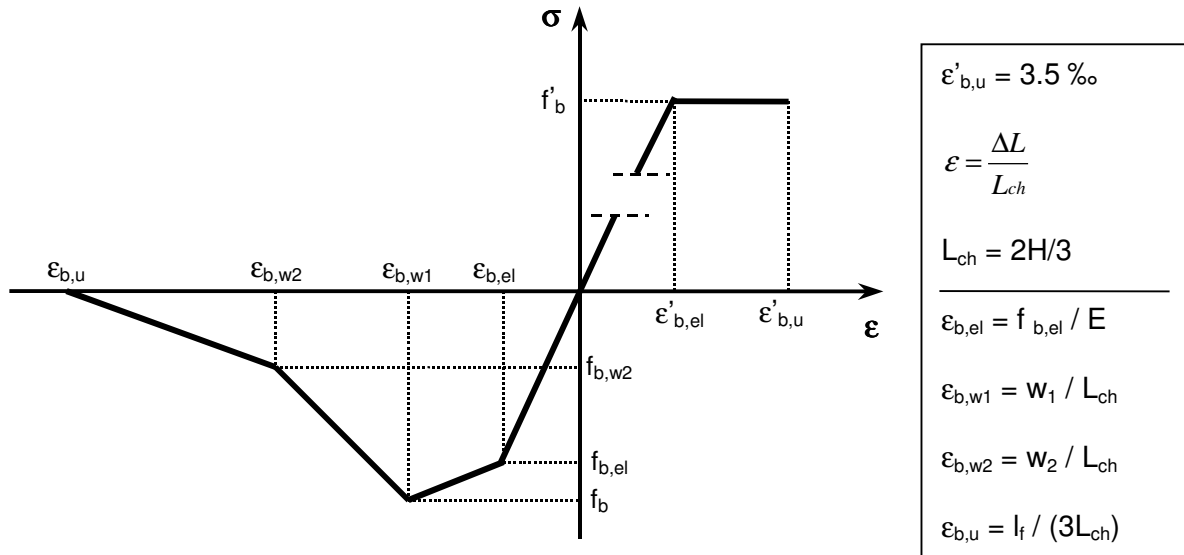
Fig. 5.1: Design stress-strain relation for high-performance fibre concrete, as recommended by [AFGC & Setra, (2002)], with the numerical expressions for the appropriate design parameters at the right-hand side

5.2.3 Utilisation areas and applications of FRC and HPFC

Although the research on fibre concrete started more than 40 years ago, the application of this material is in most European countries still limited to a rather low percentage of the total concrete production. Most of the applications cover cases with the special requirements for the crack width control and/or toughness and ductility, such as industrial floors, sewage and other pipes, specific types of pavements, etc. In these cases, the fibre concrete is always combined with conventional steel reinforcement. One of the first proposals for the application of conventional FRC where no steel reinforcement is necessary, is the application for the segments of bore tunnels [Kooiman, 2000]. Furthermore, according to [Grünewald, 2004] and [Teutsch et al., 2004], if the FRC is self-compacting, the production process of such tunnel segments can also be somewhat faster. Other examples of the successful application of fibre concrete with no conventional reinforcement is for foundation slabs on grade or slabs resting on a grid of piles, developed by [Destrée, 2000], [Sorelli, et al., 2004], [Beletti et al., 2004]. Self-

compacting fibre concrete with no reinforcement was sucessfully applied in long-span prestressed beam girders, developed by [Di Prisco & Plizzari, 2003].

The first high-performance fibre concrete (HPFC) was developed about 10 years ago, and in contrast to conventional FRC, both the number of realised applications of HPFC up to now and the number of innovative ideas, are very promising. The most appreciated properties of HPFC in structural design are the high compressive and tensile (flexural) strength, good workability, high toughness and ductility and especially (much) better durability compared to any conventional concrete.

Taking into account that a very strict quality control during the production is required, the most suitable utilisation area of HPFC is the pre-cast concrete industry. In most cases, the pre-cast concrete elements made of HPFC are prestressed, without conventional steel reinforcement. Possibilities for utilisation are medium- and long-span girders, plates and shells, structures where a high durability is required, heavily loaded elements (e.g. columns in high-rise buildings, connections between pre-cast concrete elements), composite steel-concrete structures, as well as for the rehabilitation and repair of existing structures.

Most of the realised structures using different types of high-performance fibre concrete up to now, are bridges with medium spans in Canada [Aiticin & Richard, 1996], France [Simon et al., 2002], Korea [Behloul, 2003] and in Germany (currently in the development phase) [Fehling et al., 2004], [Schmidt et al., 2004]. Two very successful architectural application are the shell structures for large-span thin roofs in Canada [CPCI, 2003], as well as in France [Thibaux et al., 2004]. Neither conventional, nor prestressing reinforcement was applied in these roof structures. Another interesting proposal was made by [Naaman, 1991], and extended by [Svermova, 2004], and it concerns the application of SIFCON for the corner zones of concrete frames, in order to increase their carrying capacity and to generate shear failure instead of tensile failure. Another examples of applications of HPFC are hot-water storage tanks [Reineck, 2002], strengthening of existing bridges [Walter et al., 2003], beams in aggressive environment, as well as many thin, light, pre-cast concrete products, such as staircases, balconies, etc.

In the Netherlands, a number of pilot-projects dealing with the utilisation of high-performance fibre concrete were realised. One of the most actual examples is a light, only 25 mm - thick canopy made of UHPC with steel fibres, covering an area of 9 x 9 m^2, containing no classic reinforcement [Van Herwijnen et al., 2005]. Another examples are thin, light and durable sheet piles without conventional reinforcement [Van der Veen et al., 2002], which can be used very efficiently instead of the conventional steel sheet piles. Another project dealt with the utilisation of HPFC for the rehabilitation and strengthening of orthotropic bridge decks, in order to solve the fatigue problems [Kaptijn, 2004].

Also, many other possible applications of HPFC were proposed, or are currently under development. The most interesting are the applications of HPFC for pre-cast concrete ele-

ments with long span [Aljeboury, 2005], the application of HPFC for different types of bridge girders [Vonk, 1999], as well as for the widening of existing bridges and viaducts [Van Blokland, 1997].

5.3. Hybrid-Fibre Concrete: From material to structure

5.3.1 Introduction

A correct transition of the material properties of any type of fibre concrete with regard to the applications at structural level, is of the highest importance with regard to the reliability of those structures. Any stress-strain relation obtained in the tensile and compressive tests, is basically valid only for the testing specimen. In structural elements, the number and orientation of fibres may be significantly different in comparison to the testing specimens. The initial stress-strain relation should therefore be corrected, according to the conditions which exist on the structural level. This is an important condition in order to be able to guarantee sufficient reliability of the structures made of fibre concrete.

In this section, the basic information on the transition from the material properties of Hybrid-Fibre Concrete for applications at structural level will be provided first. After that, a design stress-strain relation will be introduced and discussed with special consideration of the orientation of fibres.

5.3.2 Orientation of fibres and tensile response of testing specimens (material level)

Tensile fracture of any fibre concrete occurs there, where the resistance to the tensile stresses is minimal. This fracture is never located in one cross-section, but rather in the volumetric fracture zones of the testing specimens (or of the structural elements). As pointed out in section 3.2, the two most important parameters that determine the uniaxial tensile behaviour of any fibre concrete, are:
− the number of fibres in any cross-section, and
− the orientation of the fibres with respect to the principal loading directions, in these fracture zone(s).

These two parameters are basically independent of each other: for example, if the same number of fibres is present in the fracture zones of two specimens, they will have the same tensile response, only if the orientation coefficient of the fibres is the same as well.

However, these parameters do act together: a low number of optimally oriented fibres in a fracture zone, can result in the same tensile behaviour as the large number of not-suitably oriented fibres.

Obviously, it is rather difficult to distinguish how large is the individual influence of the number of fibres, and what individual influence of the orientation of fibres on the tensile behaviour of fibre concrete can be expected. The exact design approach, where both parameters are taken into account, would require a rather complicated method for conversion from the material to the structural scale. The design rules would then become too complex to be applied in engineering practice.

For the sake of simplicity, it will therefore be assumed in the following text, that the number of fibres in all of the produced elements (testing specimens and structural elements) is constant, and that only the orientation of the fibres has an influence on the tensile behaviour of the fibre concrete.

Only a very few research studies dealt with the exact quantification of the influence of these parameters on the tensile behaviour, such as [Van Mier et al., 1992] and [Behloul, 1996], and their results are shown in Fig. 5.2 a and b. In both cases, special casting and production procedures were applied, in order to align the fibres under the characteristic angles of 0°, 22.5°, 45°, 67.5° and 90°.
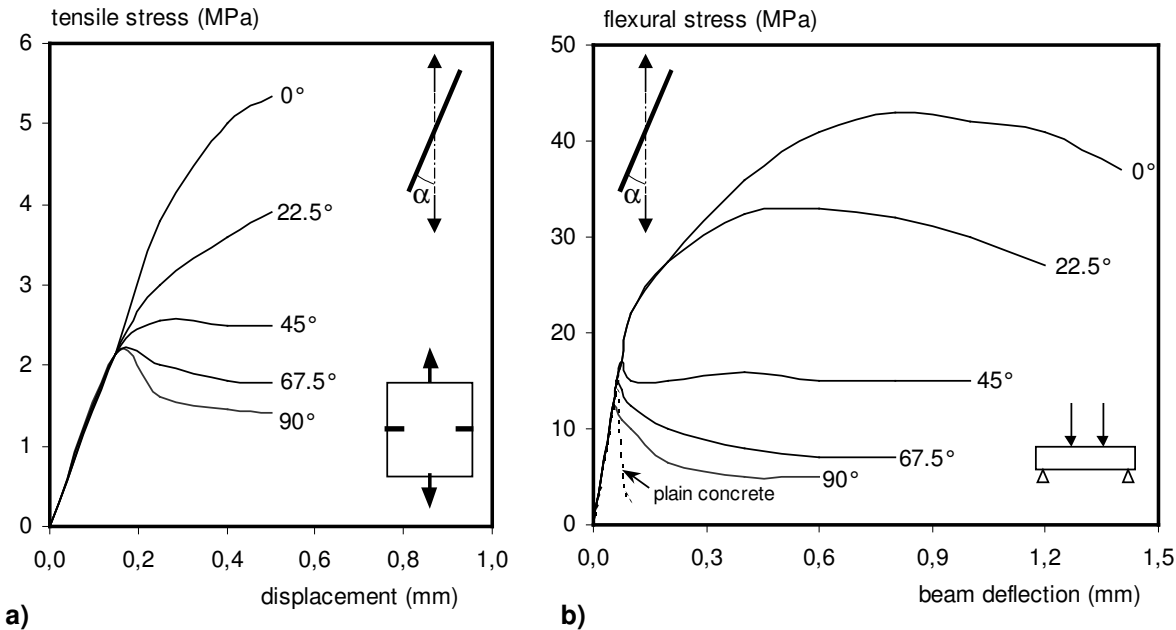
Fig. 5.2: The influence of the orientation angle α of fibres on: a) uniaxial tensile behaviour of SIFCON, after [Van Mier et al., 1992] (tests stopped at the displacement of 0.5 mm);   b) flexural behaviour of RPC, after [Behloul, 1996];   In both cases, the fibre orientation of 0° corresponds to the direction of the main tensile stress in the middle of the testing specimen

Obviously, for each fibre orientation, an independent stress-strain relation can be made. A general case of the schematic simplified tensile stress-strain relations for fibre concretes with fibres inclined at the characteristic angles of 0°, 22.5°, 45°, 67.5° and 90° with respect to the main tensile stress, is given in Fig. 5.3. These are qualitative stress-strain relations, valid only

for the testing specimens at the material level. These relations, with their characteristic values of strains (ε) and stresses (σ), will in the following section be used as a basis for the determination of the design stress-strain relation for Hybrid-Fibre Concrete at the structural level.
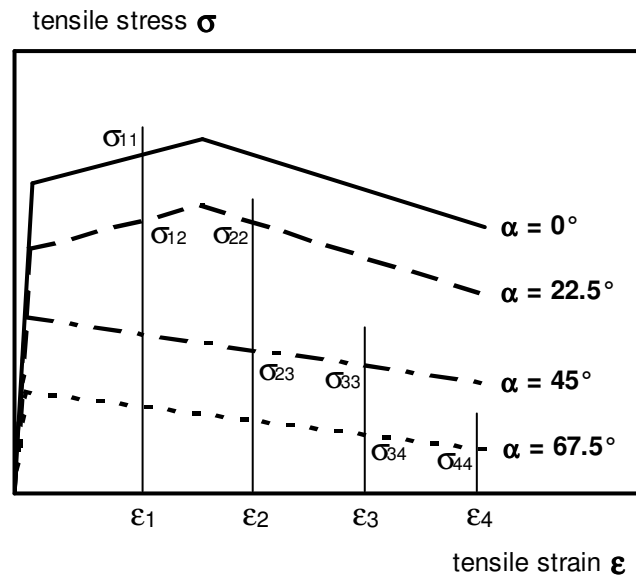
Fig. 5.3: General case of the qualitative uniaxial tensile stress-strain relations ($\sigma - \varepsilon$) for fibre concrete, with fibres inclined at given angles with respect to the main tensile stress, with characteristic strain (ε_1 to ε_4) and stress values (σ_{11} to σ_{44}) (these stress-strain curves are given only for illustration, and do not necessarily correspond to the experimental ones)

5.3.3 Orientation of fibres in the structural elements (structural level)

The difference between the orientation of the fibres in the testing specimens (material scale) and in the structural elements (structural scale), is a key issue for the determination of the design stress-strain relation for any type of fibre concrete.

The starting assumptions in the following analysis are:
- the fibre concrete under consideration is self-compacting;
- the quality of any type of self-compacting fibre concrete in terms of its mixture composition and workability, is the same in the laboratory and in the factory of pre-cast concrete.

It can always be expected that the orientation of the fibres in structural elements of any type of fibre concrete will be different from the orientation of fibres in tensile specimens. The main reasons for these differences are:
- It is relatively difficult to apply in industrial practice (i.e. in the factory of pre-cast concrete) the same casting process of fibre concrete as used under laboratory conditions;

- The shape of the structural element under consideration (e.g. large beams, plates, shells), is generally different from the shape of the tensile specimen;
- The way of flowing of fibre concrete and therefore the distribution and orientation of fibres caused by the flowing, will most probably be different in the tensile specimens compared to large structural elements, because usually different production processes have to be applied in these two situations;
- For structural elements, not only their shape, dimensions and production process, but also the presence of prestressing and/or conventional reinforcement has an additional influence on the flow of the fresh fibre concrete, and therefore also on the orientation of fibres; in testing specimens, no reinforcement is present;
- The general quality of production in the pre-cast concrete industry may be different from the one in the lab.

Therefore, one of the initial steps in the application of HPFRC on the structural level, is to produce a couple of the "pilot" structural elements in the pre-cast concrete factory. These structural elements should be used only for the determination of the orientation of fibres.

It is further recommended to select a number of characteristic cross-section(s) of these "pilot" elements in the longitudinal direction. This should be done in all specific zones of such an element, with special regard to the fibre orientation. These zones can be located where the variation of geometry (in longitudinal, transversal or vertical direction) is present, above the supports, etc.

The plane of each of these cross-sections should subsequently be divided into characteristic zones, in which the fibre orientation will be determined. The size of a characteristic zone should approximately correspond to the size of the area, within which a more-or-less constant orientation of fibres is expected. Therefore, as an independent characteristic zone, it should choose:

- each part of the cross-section with a constant geometry (constant width and/or height). The width and/or height should then be approximately comparable to the width and/or height of the testing specimens;
- each parts of the cross-section around reinforcement and/or openings;

Moreover, it should pay a special attention on the fibre distribution in corners of the cross-sections [Dupont, 2004], as well as in all other specific parts of a cross-section.

In the following part of the text, a theoretical example is given for the determination of the stress-strain relation for the T-cross-section of a girder made of FRC and loaded in e.g. bending. It should note that this is only a theoretical example, having as a main goal the illustration of the determination of the stress-strain curve.

For the sake of simplicity, it will be assumed that every characteristic zone of this cross-section has its own fibre orientation, as shown in Fig. 5.4.a. The design tensile stress-strain curve for the cross-section under consideration, is shown in Fig. 5.4.b. Again for the sake of

simplicity, it will be assumed that the average orientation angles of fibres in the characteristic zones are of 0°, 22.5°, 45°, 67.5° and 90°, just like in the initial testing specimens in Fig. 5.3.

The design stress-strain curve (for the cross-section), is based on the initial stress-strain curves for different fibre orientations in the testing specimens. For each characteristic zone in Fig. 5.4.a with an appropriate fibre orientation, the appropriate stress-strain curve, for the concrete with the same fibre orientation in Fig. 5.3 should be chosen.
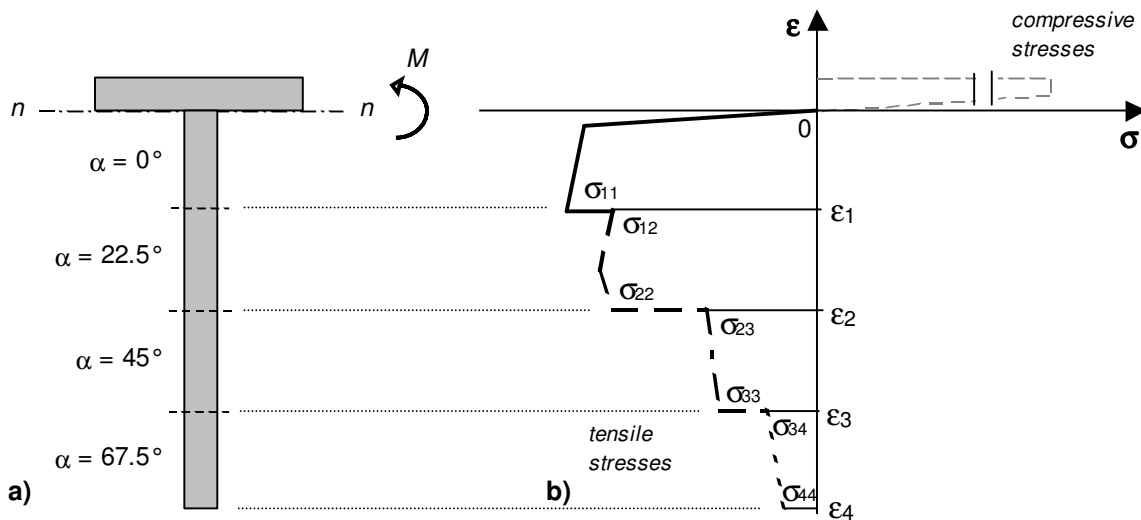
Fig. 5.4: A theoretical example for the determination of the stress-strain curve for a T cross-section of a FRC-girder loaded in bending (note that the position of the neutral axis and the values of the orientation angles α are taken only as an example, and therefore they do not have to correspond to the real fibre orientation in such a girder): a) Cross-section loaded in bending, with four different characteristic zones with different orientation angles of fibres (α); b) Appropriate design stress-strain relation (σ - ε) in tension for this cross-section, created using the characteristic stress-strain relations given in Fig. 5.3, taking the fibre orientation into account;

As shown in Fig. 5.4.b, for zone with the orientation angle $\alpha = 0°$, the stress-strain curve in Fig. 5.3 for $\alpha = 0°$ is chosen, up to the strain ε_1. After that, along the height of the section that corresponds to the characteristic zone with the orientation angle of fibres $\alpha = 22.5°$, the part between the strains ε_1 and ε_2 of the stress-strain curve for fibre orientation angle of 22.5° is chosen. The same procedure is valid for other characteristic zones of fibre orientation.

If the average orientation angles of fibres in the characteristic zones lie between the characteristic values of 0°, 22.5°, 45°, 67.5° and 90°, the appropriate stress-strain curves for these orientation angles should be calculated first. This can be done by using a linear interpolation

between the appropriate curves in Fig. 5.3. Subsequently, for the creation of the design stress-strain curve, the same procedure as explained herein should be used.

5.3.4. Alternative method for the determination of fibre orientation in rectangular cross-sections of structural elements

According to Section 5.3.3, the orientation of fibres in structural elements should be determined using the optical method, described in section 3.6. This procedure is in the first line very complex and time-consuming. It requires very skilled personal, and the question is if it will be accepted in such a form in the engineering practice. Moreover, the quality of the results depends on some technical factors (the quality of digital photos, the flashes area etc.).

Therefore, in this section an alternative method for the determination of fibre orientation will be presented, based on the theoretical model of [Soroushian et al., 1990]. By means of the equations developed in this work, it is possible to determine the fibre orientation in any rectangular cross-sections with dimensions b x h. The appropriate diagrams are given in Fig. 5.5.
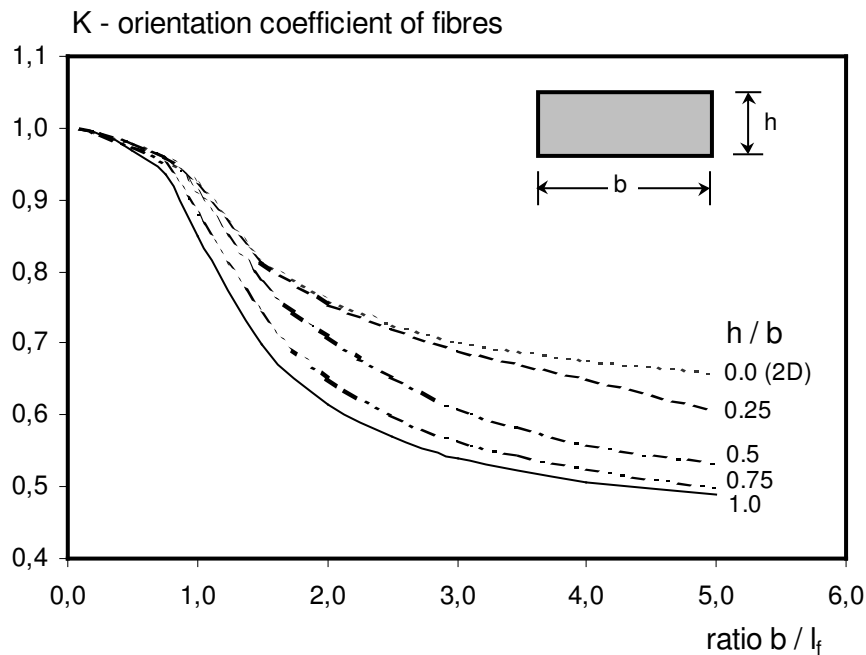
Fig. 5.5: The orientation coefficient of fibres in rectangular cross sections with dimensions b X h, taking the fibre length l_f into account, after [Soroushian et al., 1990]; the fibre orientation angle with respect to the main tensile stress α is equal to $\alpha = arccos\ K$ (e.g. K=1 => $\alpha=0°$; K=0.75 => $\alpha=41^o$; K=0.5 => $\alpha=60^o$)

A special feature of these equations (diagrams), is that it takes both the dimensions of the cross-section (b and h), and the fibre length (l_f) as the parameters. This is to the author's knowledge the most comprehensive model for the determination of fibre orientation up till now.

5.3.5. Summary: procedure for determination of design stress-strain relation for HFC

The full procedure for the determination of the design stress-strain relation for Hybrid-Fibre Concrete is summarised in Fig. 5.6. The proposed procedure is a combination of the experimental data related to the testing specimens (in the laboratory) and to the structural elements (in the factory of pre-cast concrete).

The recommended steps of this procedure are:

1. Determine the mixture proportions of HFC, mix it and test its workability;

2. If the consistence of concrete is self-compacting, compare the workability in laboratory and factory conditions, and make corrections if the differences are large; Moreover, in the factory and in the laboratory, the control of the workability of every charge of produced fibre concrete is essential;

3. Subsequently, cast the concrete in the same way in all testing specimens, so that the orientation of all fibres is approximately equal to the characteristic values of 0°, 22.5°, 45°, 67.5° and 90° with respect to the direction of main tensile stress. The possible casting procedures to achieve these orientations of fibres, are described in [Van Mier, 1992] and [Behloul, 1996].

4. Cast the concrete in the "pilot" structural elements, keeping the casting process constant for all of them;

5. In the lab: determine the mechanical properties (uniaxial tensile and compressive tests); Create the initial stress-strain relations for concretes with different orientation angles of fibres (valid only on the material level, i.e. for the selected specimen size and geometry), taking the standard deviation of the experimental results into account; Also control the actual fibre orientation.

   In the factory: choose the characteristic cross-section(s) of the produced structural elements, and determine the orientation of fibres in the characteristic zones of these cross-sections, using the optical method described in the section 3.6, or the analytical approach described in section 5.3.4;

6. Compare the orientation of fibres in the characteristic zones of the cross-section of the structural elements, to the characteristic orientation of fibres in the testing specimens, and make the necessary corrections.

Another interesting question is related to the repeatability of approximately constant fibre orientation in all produced structural elements. Even if the casting process is constant, the fibre orientation determined in a couple of the "pilot" structural elements, does not have to remain the same in thousands of other structural elements which will be produced in the future.

However, if the quality of self-compacting Hybrid-Fibre Concrete can be kept at constant level, a very high probability exist that the fibre orientation will indeed remain constant in all produced structural elements. If the rheological properties of fresh mixtures of Hybrid-Fibre Concrete are constant, the fresh mixtures will flow always in the same way, and will

therefore disperse the fibres always in the same or very similar patterns. Therefore, the self-compactibility of HFC is in the moment the best possible guarantee of the repeatability of fibre orientation and distribution in the structural elements.

The quality control of the fresh mixtures of Hybrid-Fibre Concrete deserves therefore a great importance in the engineering practice, exactly because of these facts.

LABORATORY **FACTORY OF PRE-CAST CONCRETE**

```
LABORATORY                              FACTORY OF PRE-CAST CONCRETE

   ┌─────────────────────┐                 ┌─────────────────────┐
   │ Mixture proportioning│                │ Mixture proportioning│
   │  and mixing of HFC   │                │  and mixing of HFC   │
   └─────────────────────┘                 └─────────────────────┘
            │                                       │
   ┌─────────────────────┐                 ┌─────────────────────┐
no │   Is the mixture     │             no │   Is the mixture     │
   │  self-compacting?    │                │  self-compacting?    │
   └─────────────────────┘                 └─────────────────────┘
            │ yes                                   │ yes
   ┌─────────────────────────┐             ┌─────────────────────┐
   │ Casting of testing      │             │ Casting of pilot     │
   │ specimens, fibre        │             │ structural elements  │
   │ orientations: 0°, 22.5°,│             └─────────────────────┘
   │ 45°, 67.5°, 90°         │                       │
   └─────────────────────────┘             ┌─────────────────────────┐
            │                               │ Determination of        │
   ┌─────────────────────┐                 │ orientation of fibres   │
   │ Testing of mechanical│                │ in cross-sections of    │
   │ properties (uniaxial │                │ these structural        │
   │ tension, compression)│                │ elements                │
   └─────────────────────┘                 └─────────────────────────┘
            │
   ┌─────────────────────┐
   │ Control the          │
   │ orientation of fibres│
   │ in tensile specimens │
   └─────────────────────┘
            │
   ┌─────────────────────────┐
   │ Initial stress-strain   │
   │ relations for different │
   │ fibre orientations      │
   └─────────────────────────┘

           ┌───────────────────────────────┐
           │ Comparison of orientation of  │
           │ fibres in structural elements │
           │ and testing specimens         │
           └───────────────────────────────┘
                        │
           ┌───────────────────────────────┐
           │ Design stress-strain relation │
           └───────────────────────────────┘
```

Fig. 5.6: Recommended procedure to determine the design stress-strain relation of Hybrid-Fibre Concrete (and of any other fibre concrete), combining of the experimental data from the material (laboratory) scale, and the structural scale (pre-cast concrete plant)

5.3.6. Alternative procedure for determination of design stress-strain curve for fibre concrete

The previously presented procedure for determination of the influence of fibre orientation on tensile response of fibre concrete, is based on the experimental measurements of fibre orientation in the structural elements. In this section, the alternative procedure recommended by [AFGC & Setra, 2002], will be presented and discussed.

In this procedure, no exact determination of the fibre orientation is required, but rather the comparison of the mechanical (tensile) properties of the testing specimens in the lab, and of the drilled specimens from the structural elements. Only one stress-strain curve of the testing specimens is required, with one appropriate value of the fibre orientation. The correction factor K is than equal to:

$$K = \frac{\sigma_{theo}}{\sigma_{str}},$$ (5.1)

where:

σ_{theo} = tensile (or flexural) strength obtained on the testing specimens

σ_{str} = tensile (or flexural) strength obtained on the specimens drilled from the appropriate "pilot" structural elements.

Further, according to the recomendations of [AFGC & Setra, 2002], all the values at the initial stress-strain curve of the testing specimens should be divided by the factor K. This factor is then by definition always larger than 1 ($K > 1$).

The recommendation of [AFGC & Setra, 2002] can obviously give higher design values of tensile stress, compared to the procedure for Hybrid-Fibre Concrete described previously in this section. From that point of view, the recommendation of [AFGC & Setra, 2002] clearly overestimates the design values of stresses. This recommendation can therefore be used only in cases, where the fibres have constant orientation along the whole cross-section of the structural element under consideration.

Another weak point of the recommendation of [AFGC & Setra, 2002], is that the maximum design tensile stresses are obtained if the orientation of fibres in the testing specimens and in the structural elements is the same. Only in such a case is $K = 1$, in all other cases is $K > 1$, i.e. the design values of tensile stresses must be reduced.

However, in Chapter 4 of this thesis it was shown that the fibre orientation, which is slightly different from the direction of the main tensile stress, may have a positive influence on tensile softening (and probably also hardening) behaviour of Hybrid-Fibre Concrete. The pullout of long hooked-end fibres inclined at 15° and 30°, resulted at 15 - 25% higher maximum pullout forces and a better total pullout energy compared to the aligned fibres (Sections 2.9 and 4.6.6). The similar tendency exists for short fibres as well (Section 4.6.5). Therefore, tensile stresses do not necessarily have to be reduced if $K < 1$. Obviously, from this point of

view, the recommendations of [AFGC & Setra, 2002] may lead to the underestimation of the design tensile stresses.

5.3.7. "Typenprüfung": Design by Testing

Introduction

Both described procedures for the determination of load-carrying capacity of HFC structural elements are rather complex from the technical point of view and require a rather long period of time and highly skilled workers. Therefore, it can not be expected that the full analysis can be accepted and performed always accurately in the engineering practice.

Therefore, an alternative procedure will be proposed herein: the so-called "Typenprüfung" (testing of typical elements), or in free translation "Design by Testing". The "Typenprüfung" is based on pilot testing of the appropriate type of structural elements on the 1 : 1 scale, in order to set up the general design rules for the whole product series of that type of structural elements.

The "Typenprüfung" originates from German engineering practice, and it is related to the so-called "Allgemeine Bauaufsichtliche Zulassung" (General building permission of the construction surveillance authority). This permission can be put up for any kind of civil engineering products. We will limit us here to the products of the pre-cast concrete industry.

The producer of e.g. pre-cast concrete elements, can ask for this permission, if the product under consideration does not fall under the valid building codes and regulations. This procedure is used often for innovative pre-cast concrete products, if for example their load-carrying capacity can not be determined accurately using available methods, or if these elements are made of a new type of building material.

The procedure itself consists of testing of the series of structural elements by a certified testing authority or laboratory. The main goal of the tests is to control if the elements satisfy with regard to the existing building regulations and codes. The results of these series of tests may be extended further: appropriate tables and diagrams can be made based on the test results. They can then be used as a kind of a special building code or a special building regulation.

There are numerous examples of the civil engineering products which require testing by "Typenprüfung": prestressed hollow floor plates, different types of steel anchors, various reinforcement bars, wire net for the protection of stone sliding etc.

Application of "Typenprüfung" to the pre-cast elements of Hybrid-Fibre Concrete

"Typenprüfung" can be a very suitable method for the determination of the load-carrying capacity and of other design relevant properties of the pre-cast elements (e.g. beam girders, plates and shells) made of Hybrid-Fibre Concrete.

First, more such pilot-testing elements should be cast in the laboratory, and subsequently the testing of their load-carrying capacity should be performed. The testing itself must be performed according to exactly determined rules. The basic testing demands would be:

− the applied loading scheme should cause the maximum static influences (moments and forces, i.e. stresses and strains) in a structural element
− all relevant design parameters should be recorded during testing (not only the ultimate load-carrying capacity, but also e.g. the load for which the deflection of a girder exceeds the limit serviceability value should be recorded);
− the applied testing procedure should be constant for all elements.

It is also important to be able to make comparisons between the behaviour of different girders: the casting process should then be kept as constant as possible for the elements belonging to the same testing series.

This procedure can lead to the design diagrams and tables, which can subsequently be used efficiently in the engineering practice for structural design. In these diagrams, the relations between the actual fibre orientation and the maximum load-carrying capacity may be given, for constant dimensions of the cross-section and constant area of the prestressing reinforcement.

On the other hand, the interaction diagrams (M - N) for the cross-sections of HFC structural elements can be made as well. With these diagrams, it would be possible to determine the necessary fibre quantity for a given cross-section and loading of a structural element.

5.4 Case study: Application of Hybrid-Fibre Concrete for pre-cast concrete elements

5.4.1 Introduction

From the tests performed on different types of Hybrid-Fibre Concrete (HFC) it is clear that this material has many advantages compared to any other conventional concrete and fibre concrete. This material can be very suitable for the utilisation in the pre-cast concrete industry.

In this section, a case study related to the design of different long-span prestressed girders made of Hybrid-Fibre Concrete will be presented. The project tasks and the design parameters will be given first. Subsequently, the results of the case study will be shown and discussed. At the end, the conclusions will be drawn.

The idea of this section is only to give a brief illustration of the possibilities of utilisation that Hybrid-Fibre Concrete offers. Detailed calculation procedures and parameters with the detailed technical drawings of the designed girders, are given in [Aljeboury, 2005].

5.4.2 Project tasks, design parameters and procedures

The case-study on the utilisation of Hybrid-Fibre Concrete for different types of pre-cast prestressed concrete girders with long span, was made as a part of the MSc-thesis at the TU Delft, by [Aljeboury, 2005].

The main goal of this case-study is to show how large the compensation of the material costs can be, if pre-cast concrete elements having different types of cross-sections are produced, using the Hybrid-Fibre Concretes with different quantities of fibres. Other goals of this case-study are:

− a detailed analysis of all relevant design rules for high-performance fibre concrete proposed by [AFGC & Setra] (especially of the stress-strain relation), and their application to Hybrid-Fibre Concrete;
− the full automation of the calculation of the relevant design parameters (ultimate flexural and shear carrying capacity of the cross sections with variable dimensions), by means of computer programmes;
− the optimisation of the standard shapes of the cross sections with respect to both the ultimate carrying capacity and the minimum cross-sectional area
− a preliminary calculation of material costs of girders made of different types of Hybrid-Fibre Concrete, and comparison of these costs to the material costs of girders made of conventional concrete C55/65.

The studied types of cross-sections, with the span of the girders and the applied types of concrete are given in Tab. 5.1. The girders are in all cases simply supported beams. The applied types of concrete are:

- conventional C55/65;
- Hybrid-Fibre Concretes developed within this research project, which contains [0.5 vol.-% of short fibres 13/0.2] + [l.0 vol.-% of long fibres 60/0.7]; this is mixture No. 5 in Tab. 3.2, its uniaxial tensile response is shown in Fig. 3.18, and the analytical model of the tensile response is given in Section 4.6 (Fig. 4.28).

The uniformly distributed vertical load was applied for all types of girders. The intensity of this load (Tab. 5.1), was the same for girders made of both types of concrete. For different spans of the girders, the dimensions of the cross-sections and the quantity of prestressing steel were varied, in order to satisfy the design conditions.

Tab. 5.1: Basic geometrical properties of designed girders and applied types of concrete for their production

Type of cross section of girder	Span of the girder (m)	Applied types of concrete
I - girder	20 to 40	- concrete C 55/65 - HFC with 0.5% short and 1% long fibres
T - girder	12 to 20	- concrete C 55/65 - HFC with 0.5% short and 1% long fibres
STT - girder	20 to 40	- concrete C 55/65 - HFC with 0.5% short and 1% long fibres

In design calculations, it is required to calculate the height of the compressive zone of the cross-section, so that equilibrium of the inner forces and bending moments exists [Walraven et al., 1998]. These calculations are based on numerous iteration procedures, and they are fully automated by virtue of a computer programme written in the programming language Matlab.

The input parameters of this programme are the mechanical properties and the cross-sectional area of the applied concrete, prestressing steel and conventional reinforcement (the last only in case of C55/65), as well as the chosen span and the heights of the cross-sections. The output results are the internal bending moment of the cross-section in SLS and in ULS, the ultimate shear capacity as well as the characteristic stresses and strains in the cross-sections both in the ULS and in SLS. One of the requirements in the ULS was that the failure takes place in the reinforcement (ductile failure).

The following parameters were varied during the calculation, according to the required span of the beam:
- the height of the cross-section;
- the width of the upper flange (slab), proportional to the height of the cross-section;
- the width of the lower flange (slab), where the prestressing reinforcement is placed;
- the thickness of the web;
- the quantity of the prestressing reinforcement;

The height of the upper flange (slab) was proportional to the height of the cross section, and the height of the lower flange (slab) was kept constant during the calculation

In the design calculations, the recommendations of [AFGC & Setra] have been followed, except with regard to the orientation of the fibres. An appropriate fibre orientation was assumed taking into account the dimensions of the different parts of the cross-section and the applied fibre length, using the diagrams, developed by [Soroushian et al, 1990] and given in Fig. 5.5. Each of the chosen cross-sections which are in Tab. 5.1 can be divided into a number of rectangular parts: the slab (flange) and the web. Following the diagrams in Fig. 5.5, and the maximum fibre length $l_f = 60$ mm, the following orientation coefficients η of fibres are assumed:

−   in the slab (flange): $\eta = 0.66$;
−   in the web: $\eta = 0.80$.

The stress-strain relations were subsequently created following the explanation given in Fig. 5.4.

5.4.3 Results

Cross-sectional area and height

In this section, the results of the calculations of the cross-sections of girders made of Hybrid-Fibre Concrete and of conventional concrete C 55/65 will be presented. In Fig. 5.7 to 5.9, for each analysed cross-section, the relation of the span and the cross-section area is given, both for the structural solutions in Hybrid-Fibre Concrete and in conventional concrete C55/65. The schemes of the designed cross-sections is included in each diagram as well, for the structural solutions in both concretes.

For I girders, an about 3 times smaller cross-sectional area can be obtained, if these girders are made of HFC (Fig. 5.7). The total weight of the I girders made of HFC is therefore about 3 times lower compared to girders made of C 55/65. The height of the cross-section is about 35 % lower in case of HFC.
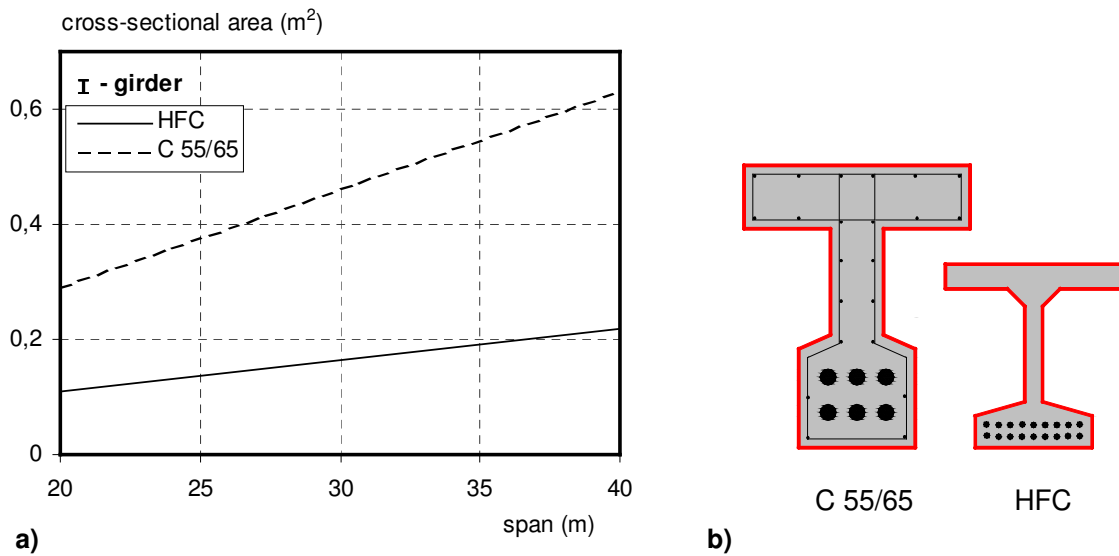
Fig. 5.7:   a) The relation between span and cross-sectional area of I girders made of Hybrid-Fibre Concrete (HFC) and of conventional reinforced concrete C 55/65;   b) The scheme of the cross-sections of girders in HFC and C55/65

The differences in the cross-sectional area of the T girders made of HFC and C55/65 are somewhat lower (Fig. 5.8): about 2 times less material is needed in the case of HFC girders. The depth of the HFC girder is about 10 % smaller than that of the T girder made of C 55/65.
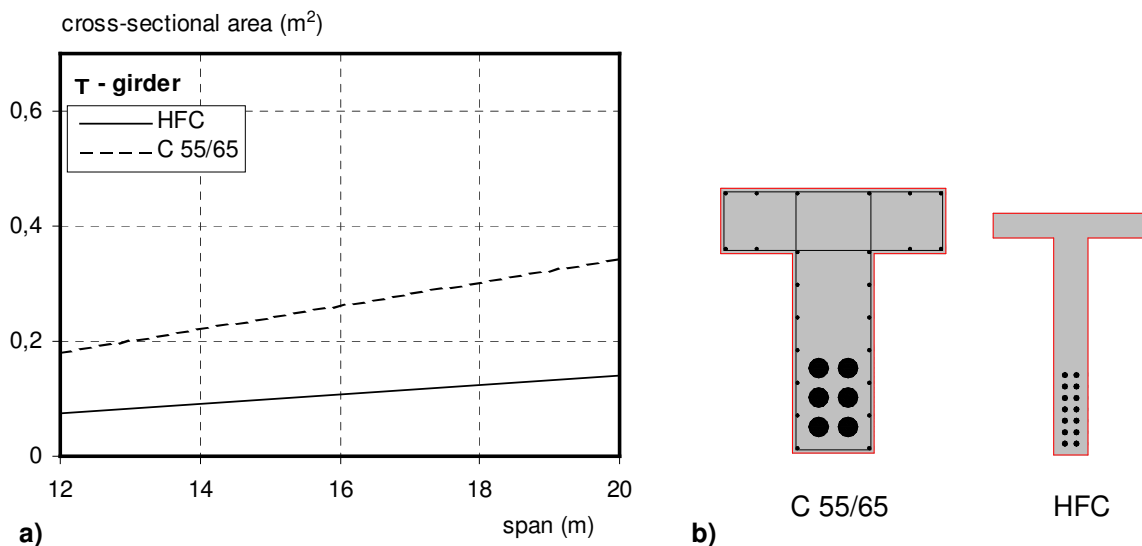
Fig. 5.8:   a) The relation between span and cross-sectional area of T girders made of Hybrid-Fibre Concrete (HFC) and of conventional reinforced concrete C 55/65;   b) The scheme of the cross-sections of girders in HFC and C55/65

The I cross-section is obviously more "efficient", by virtue of the larger distance of the centroids of the tensile and compressive forces in the cross-section.

The largest reduction of the cross-sectional area and therefore also of the weight of girders, can be achieved using the rather non-compact cross-section of the so-called STT-girder (Fig. 5.9). In this case, the possible weight reduction is about 420 % if the girder is made of Hybrid-Fibre Concrete. The girders made of HFC have also a two times smaller height of the cross-section, compared to the girders made of C 55/65.
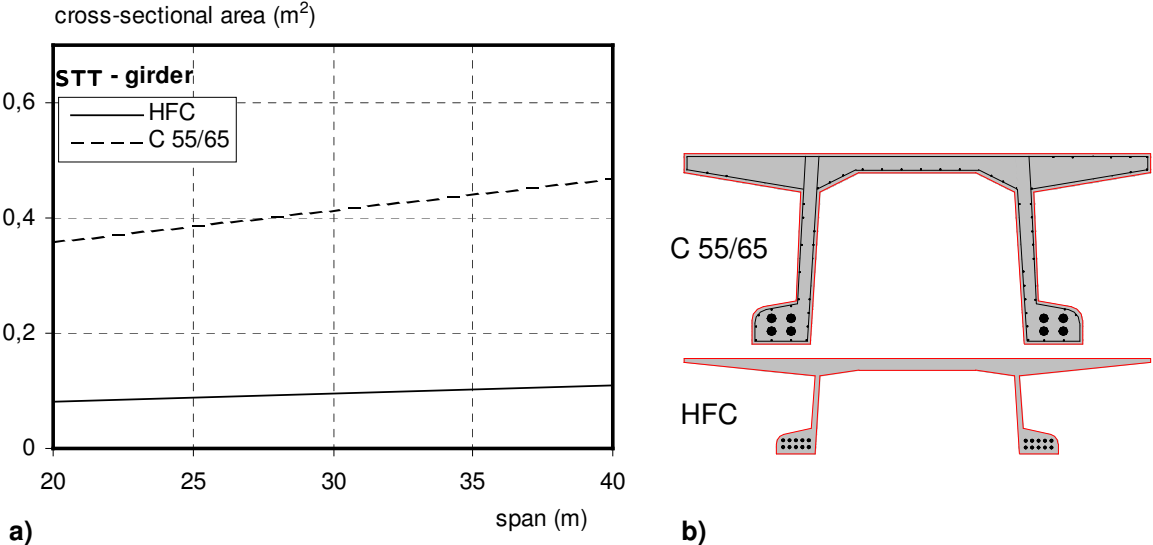
Fig. 5.9: *a) The relation between span and cross-sectional area of* STT-*girders made of Hybrid-Fibre Concrete (HFC) and of conventional reinforced concrete C 55/65; b) The scheme of the cross-sections of girders in HFC and C55/65*

Quantity of prestressing steel and of conventional passive reinforcement
In general, the required quantity of prestressing steel is lower in the case of girders made of Hybrid-Fibre Concrete (HFC), although the compressive strength of HFC is higher compared to the compressive strength of C55/65. The reason for this is the smaller height of the cross-section of HFC girders.

The difference in the needed quantity of prestressing steel is about 15% for both I and T cross-section, and this difference is approximately constant, i.e. independent on the span of the girder. For the STT girder, the difference is even higher: the quantity of the prestressing steel can be reduced with about 30%, if these girders are made of Hybrid-Fibre Concrete.

It has been shown as well, that no conventional passive reinforcement is needed for girders made of Hybrid-Fibre Concrete. The main role of the passive reinforcement in prestressed concrete structures is to provide resistance to:

- shear stresses;
- cracking due to the loading in the service conditions (SLS);
- cracking due to the creep and shrinkage of concrete.

For all these reasons, fibres provide enough resistance, taking their actual orientation into account:

- it was shown in the case-study, that the thickness of the web should be larger than a minimum value, in order to provide enough resistance to the shear forces;
- according to Fig. 3.12, the first-cracking flexural stress in Hybrid-Fibre Concrete is about 3 times higher than that of plain concrete (thus also of classical reinforced concrete). Therefore, the total load in the SLS, acting on the HFC girder, can also be about 3 times higher than the load acting on the C 55/65 girder, for the same (or similar) height of these girders. After the optimisation of the dimensions of the cross-section, even no conventional reinforcement was needed in the contact zone of the web and the cantilevers, in the upper flange of the STT-girders (Fig. 5.9.b);
- no conventional steel reinforcement was needed to resist the creep and shrinkage deformations in HFC girders as well. These deformations were calculated following the recommendations of [AFGC & Setra, 2002].

Conventional steel reinforcement will most probably be needed only in the anchoring zones at both ends of girders.

Limit crack width, deflections and vibrations

The maximum crack width in the serviceability limit state is important with respect to the durability of structures. There is still no procedure to calculate the crack width for structural elements made of high-performance fibre concrete without conventional reinforcement. However, because multiple cracking occurs (Fig. 4.6), it can be expected that for the same load intensity, the crack width in structural elements made of Hybrid-Fibre Concrete will be smaller than the crack width in conventional concrete structures.

As the designed structural elements are suitable for applications such as roof elements, the maximum allowed deflections u_{max} for the roof girders with span L in the SLS, are taken from the Dutch Building Code NEN 6702, as $u_{max} = 0.004\ L$. For the self-weight and the live load in the SLS, this condition is satisfied for all analysed spans of the I and T girders made of Hybrid-Fibre Concrete. For the STT-girders, the condition is satisfied for spans up to about 28.0 m. Therefore, for larger spans, the cross-section of these girders should be further optimised. The same is valid for the local stability (buckling) of the rather thin webs of the STT - girder.

In this case-study, it was supposed that all designed structural elements will be subjected to static loading during their service life. The effects of dynamic loading were not considered. This point deserves special attention for the applications in dynamically loaded structures (e.g. bridges), taking into account that the thin and light structural elements made of

Hybrid-Fibre Concrete could possess a lower stiffness than conventional concrete elements. A further optimisation of the cross-sections may be required in such cases.

5.4.4 Summary: HFC versus conventional concrete

The feasibility of the application of any new building material should always be based on the integral reduction of the costs, which can be achieved by utilisation of that material. One of the first examples of the integral cost analysis for ultra high performance concrete, was given in [Racky, 2004].

In this case-study, the direct reduction of the material costs by virtue of the utilisation of Hybrid-Fibre Concrete will be evaluated quantitatively. The total reduction of the integral costs, will be analysed qualitatively.

Quantitative comparison of direct material costs

According to the analysis made in this case-study, Hybrid-Fibre Concrete with 1.5 vol.-% of steel fibres is about 4 times more expensive than concrete C 55/65 with a standard mixture composition (without costs of steel reinforcement in C 55/65). This calculation is based on the average prices of the applied building materials, dating from June 2004.

A full compensation of the costs is directly achieved in the STT-girders, where about 4.2 times less material is needed for HFC - girders (Fig. 4.8). A rather high direct compensation of the material costs is possible also in the case of I - girders.

Qualitative comparisons of integral costs

Hybrid-Fibre Concrete possesses rather high tensile and flexural strength, whereas the ductility is significantly pronounced. Moreover, in the fresh state the material is self-compacting with a very rapid development of the compressive strength.

In spite of the rather high price per m^3, Hybrid-Fibre Concrete is from the economical point of view very attractive. By virtue of the significantly improved mechanical properties, it is possible to design very thin and light structural elements in HFC. As already mentioned, the weight of such elements, and therefore also the quantity of the Hybrid-Fibre Concrete needed to produce them, is a couple of times lower than the quantity of conventional concrete needed to produce the same type of structural elements. It is therefore possible to compensate the rather high material costs of Hybrid-Fibre Concrete by rather low quantities of the material needed to produce structural elements.

Another high advantage of the structural elements in Hybrid-Fibre Concrete, is that in most cases no conventional reinforcement is needed. This means further reduction of the costs of the reinforcement. Moreover, the total production time can significantly be reduced, because the activities related to the designing, assemblage and placing of the conventional steel reinforcement are often rather time-consuming.

Hybrid-Fibre Concrete has a very rapid increase of the compressive strength after casting: just 24 hours after casting, a compressive strength of about 80 MPa can be achieved. The produc-

tion process as well as the installation of the pre-cast elements at the building site, can therefore be accelerated significantly.

As structural elements in Hybrid-Fibre Concrete are thin, much more of them can be placed on the transport at the same time, compared to the elements made of conventional concrete, which means further reduction of the total costs.

At the building site, it is relatively easy to handle and to assemble the structures using thin and light structural elements made of Hybrid-Fibre Concrete. The construction time is therefore shorter, which has positive influence not only on the total costs of the engineering project, but also on the surroundings of the building site and on the environment.

The demands for the durability of structures are becoming higher and higher nowadays. The main reason for this, are the relatively high maintenance costs of the existing structures. It can be expected that the durability of Hybrid-Fibre Concrete is better compared to conventional concrete and normal fibre concrete, although still no appropriate experimental data are available. The main reason for this expectation is the very intense multiple cracking (Fig. 4.6), observed in almost all parts of the dog-bone shaped testing specimens used in the uniaxial tensile tests on Hybrid-Fibre Concrete. With an improved durability, the maintenance costs of structures can also be significantly reduced.

5.5 Summary and concluding remarks

In this section, the essential principles related to structural design with Hybrid-Fibre Concrete are introduced and illustrated by means of a case study on pre-cast long-span girders.

Existing design methods, recommendations and examples of utilisation of high-performance fibre concrete were given first. Subsequently, the effect of fibre orientation on the tensile response of fibre concrete was analysed. After that, this analysis was used to create design stress-strain relations for Hybrid-Fibre Concrete, based on different orientations of fibres in the characteristic zones of the structural elements. Finally, a case study dealing with the utilisation of Hybrid-Fibre Concrete in long-span pre-cast prestressed girders with different types of cross-sections was presented, and the most important results were discussed.

From the performed analysis, the following conclusions can be drawn:

1. For any fibre concrete, the uniaxial tensile response and therefore also the stress-strain relations, are different for different orientations of fibres in the testing specimens. Therefore, the initial step to obtain the design stress-strain curve in tension, are the uniaxial tensile tests on the specimens, in which the fibres are inclined at a couple of possible characteristic angles (e.g. 0°, 22.5°, 45°, 67.5° and 90°) with respect to the main tensile stress. On the basis of these tests, the initial stress-strain relations for all applied fibre orientations should be derived.

2. The <u>design stress-strain relation</u> for Hybrid-Fibre Concrete is based on the orientation of fibres in the characteristic zones of the cross-section of a structural element. First, the average fibre orientation in a number of characteristic zones of the cross-section(s) of the "pilot" structural elements made of Hybrid-Fibre Concrete should be derived. The design stress-strain relation can then be obtained by joining together the parts of the initial stress-strain relation, with fibre orientation corresponding to the orientation of fibres in the characteristic zone. It is also possible to deterimine the fibre orientation using a simplified charts which cover different fibre lengths and different dimensions of cross-sections (Fig. 5.5).

3. Alternative procedure for the determination of design stress-strain relation recommended by [AFGC & Setra, 2002], is not valid in general. The correction of the stress-strain relations based on the linear proportionality of the stresses in testing specimens and in the structural elements is not acceptable in general case.

4. A German structural testing method known as "Typenprüfung", can be used to get a direct evidence of the carrying capacity and mechanical behaviour of structural elements. This method can be useful and practical to perform in the engineering practice, especially if structural elements are made of innovative (or not enough known) materials, such as HFC.

5. The performed case-study showed that Hybrid-Fibre Concrete is very suitable for application in long-span pre-cast prestressed girders. Compared to girders made of conventional concrete C 55/65 with the same span and load, girders made of Hybrid-Fibre Concrete have substantially smaller cross-sectional area and weight, the needed quantity of prestressing steel is lower and no passive reinforcement is required. The rather high material costs of HFC girders can therefore be fully compensated by its significantly improved mechanical properties.

6. For girders made of Hybrid-Fibre Concrete, the normative design parameters will often be the deflection, or the local stability, or the shear resistance. This can be significantly different compared to the girders made of conventional concrete, where usually the ultimate bending moment is the normative design parameter.

7. During the production of structural elements in Hybrid-Fibre Concrete (and in all similar types of high-performance fibre concrete), the quality control has to be at a very high level, in order to guarantee the reliability of structures.

The herein presented procedure for obtaining the design parameters for Hybrid-Fibre Concrete, gives real and reliable design parameters. The procedure is based on comprehensive experimental work in the lab and on the structural elements. This could eventually be simplified.

In the lab, with the exact knowledge on the pullout behaviour of the inclined fibres, the results of the tensile tests for different fibre orientations could be modelled.

On the structural scale, the knowledge of the flowing processes of the self-compacting fibre concretes, would enable an accurate prediction of the number and orientation of the fibres in different zones of the structural elements with different and/or variable shapes. This could accelerate significantly the whole design process.

CHAPTER 6:

CONCLUSIONS AND FUTURE PROSPECTS

6.1 Conclusions

The research project presented within this PhD-thesis, was focused on the development and utilisation of high-performance Hybrid-Fibre Concrete. The main features of Hybrid-Fibre Concrete are its significantly improved tensile strength and ductility compared to conventional fibre concretes. Combined with the self-compactability in the fresh state, these features make the Hybrid-Fibre Concrete a very attractive material for the utilisation in pre-cast concrete industry.

In the introductory **Chapter 1**, the research project and its contents and goals are presented.

The basic principles of the mixture composition of Hybrid-Fibre Concrete, as well as the analytical model for the preliminary determination of the mixture proportions of Hybrid-Fibre Concrete, are given in **Chapter 2**. The interactions between aggregate grains and different types of fibres were studied, based on packing densities of dry aggregate-fibre mixtures. Subsequently, the amount of cement needed to apply with different types and volume percentages of fibres was determined, in order to obtain self-compacting fibre concrete mixtures. Pullout tests on single fibres were performed after that as well, in order to optimise the concretes, so that the fibres can give an optimum performance during pullout.

From workability tests on fresh mixtures, the self-compacting ones were selected and their mechanical properties in bending and in uniaxial tension were determined in **Chapter 3**. The tests were performed using the concretes with only short, only long, as well as a number of concretes with both short and long fibres. The number and orientation of fibres in testing specimens were determined after the tests, and subsequently related to the test results.

Qualitative analyses of the microcracking and the multiple cracking in Hybrid-Fibre Concrete, as well as the analytical model for calculating the softening behaviour of Hybrid-Fibre Concrete subjected to uniaxial tension, are presented in **Chapter 4**. This model is based on the pullout behaviour of fibres as well as on their number and orientation. The calibration of unknown modelling parameters was performed for concretes with only short and only long fibres. These parameters were subsequently used for analytical modelling of the uniaxial tensile

response of Hybrid-Fibre Concrete containing both short and long fibres. For this type of concrete, the synergy of short and long fibres was observed.

Finally, in **Chapter 5**, the principles and possibilities related to the utilisation of Hybrid-Fibre Concrete in engineering practice were discussed. Stress-strain relations for HFC with different fibre orientations within a cross-section were developed, followed by a case study on the utilisation of Hybrid-Fibre Concrete for different pre-cast prestressed concrete elements with medium and large spans, without conventional reinforcement.

The following conclusions can be drawn from this research project:

1. The workability of fresh Hybrid-Fibre Concrete mixtures depends mostly on the interactions between fibres (their type and volume percentage) and of the applied volume percentage and grading of aggregate and cement. Packing density of dry aggregate-fibre mixtures is not very much affected by the addition of fibres, if only fine-grained aggregate is applied (e.g. $D_{max} = 1$ mm). A higher amount of cement in the fresh mixtures allows for using higher fibre quantities, while keeping the mixtures self-compacting. The maximum applicable quantity of short fibres is rather large (more that 4.0 vol.-%), and of long fibres somewhat lower (about 1.0 vol.-%), in order to guarantee the self-compactability of Hybrid-Fibre Concrete mixtures.

2. The efficiency of single fibres in the pullout tests from different concrete matrices as the pullout media, can be used to optimise the mixture composition of the pullout media. Low water-binder ratios and the presence of short steel fibres in the pullout medium, resulted in improved pullout efficiency of long hooked-end fibres.

3. In both flexural and uniaxial tensile tests, the same fibre action was observed: higher volume quantities of short fibres lead to higher tensile (flexural) strength; higher volume quantities of long fibres result in more pronounced strain hardening (ductility).

4. There are strong indications that the uniaxial tensile (flexural) strength as well as the strain hardening behaviour (ductility) of Hybrid-Fibre Concrete depends much more on the applied combination of fibres than on the applied fibre volume content. Combining more different fibre types together in one concrete offers much more possibilities for the optimisation of the uniaxial tensile (flexural) behaviour.

5. The scatter in both the uniaxial tensile (flexural) behaviour, and in the number and orientation of fibres was very low, so that it was not possible to determine accurately the appropriate relations between these parameters.

6. Smaller spacing between the fibres leads to more intensive microcracking, i.e. the higher the first cracking tensile strength of Hybrid-Fibre Concrete will be. Multiple cracking can appear during the strain hardening phase, if the fracture energy required to open the first through-crack is larger compared to the fracture energy needed to create another through crack. The multiple cracking process depends on the fracture energy of the concrete matrix without fibres, as well as on the quality of the bond between fibres and the surrounding concrete matrix, and on the number and orientation of fibres.

7. By means of the analytical model developed in this research project, the tensile softening behaviour of Hybrid-Fibre Concrete was modelled very accuratelly. According to this model, the tensile capacity of HFC during tensile softening phase, depends basically on the pullout behaviour of short and long fibres that bridge the dominant crack, as well as on their number and orientation on the cracking planes.

8. In Hybrid-Fibre Concrete, a high level of synergy of short and long fibres exists. "Synergy" means that the short fibres are "helping" the long fibres to generate as high tensile stresses as possible. Therefore, the combining of different types of fibres in the same concrete results in a better tensile (softening) behaviour compared to the concretes with one single type of fibre only.

9. Short fibres have triple contribution to the total tensile stress in tensile softening response of Hybrid-Fibre Concrete:
    − they transmit tensile stresses across the crack (direct contribution);
    − by virtue of the presence of short fibres, the number of long fibres with fully deformed hooks can be significantly increased (indirect contribution);
    − by virtue of the presence of short fibres, the pullout behaviour of long fibres can be improved (indirect contribution).

10. The design stress-strain relation should be created taking into account the actual average fibre orientation in each representative part of the cross-section of a structural element. The uniaxial tensile behaviour (i.e. the stress-strain relations) of concrete elements with the characteristic fibre orientations (e.g. 0°, 22.5°, 45°, 67.5° and 90°) should be known in advance, so that the stress-strain relations for the actual fibre orientation can be interpolated between them. Alternative priodedures

11. Hybrid-Fibre Concrete is very suitable for the utilisation in the pre-cast concrete industry, taking into account that a rather good quality control is necessary. The case-study performed within this research project, showed that it is possible to design light thin prestressed concrete elements using Hybrid-Fibre Concrete, without any conventional reinforcement. In comparison to the similar elements made of conventional concrete, the initial costs of the material itself are fully covered by the significantly reduced weight of

the elements. The total cost reduction is even higher, taking into account the absence of the reinforcement, the cheaper transport of the pre-cast elements and the durability, which is most probably significantly improved compared to the conventional concrete.

12. The decisive structural design criteria for HFC - structures can often be different compared to classical reinforced concrete structures. By virtue of the thickness of the structural elements made of Hybrid-Fibre Concrete, it can happen that the deflections, response to the dynamic actions, or the shear resistance are the decisive design criteria.

6.2 Future prospects

Within this research project, a solid basis for the development and utilisation of Hybrid-Fibre Concrete has been made.

Regarding the further development on the <u>material scale</u>, the following points are recommended for future research:

- **Further improvement of the properties of steel fibres:** the bond between steel fibres and concrete can be improved by roughening the fibre surface. Moreover, it should analyse new shapes and geometries of both short and long fibres. In the first line, it should vary the aspect ratios (length/diameter) of steel fibres, and investigate their influence on the workability and on the tensile behaviour. The anchorage mechanisms could be applied on the short fibres as well. It should also investigate alternative anchorage mechanisms and fibre shapes for Hybrid-Fibre Concrete (waved fibres, fibres with enlarged ends, twisted fibres), combined with clear ideas on the strength of bond and the way of deformation of these fibre types. Research results covering some of these topics are already published in [Stähli et al., 2004 b].
- **The application of synthetic fibres in high-strength concrete matrices which already contain steel fibres:** synthetic fibres (PVA, PVE) are usually much thinner and shorter than steel fibres. The spacing between them can therefore be very small, which can increase tensile strength of fibre concrete. Research results covering some of these topic are already published by [Nakamura et al., 2004].
- **Further optimisation of granular composition of high-performance fibre concretes:** the final goal is that the applied fibres can be homogeneously accommodated between the aggregate grains, and that at the same time (highly flowable) self-compacting mixtures can be produced. Moreover, not only blast-furnace slag, but also other cement types and filler materials should be applied and their influence on the workability and the bond between fibres and concrete should be investigated. Some of these aspect are covered in the publications by [Borneman & Schmidt, 2002], [Geisenhanslüke & Schmidt, 2004].
- **Development of relations between the rheology of the fresh HFC mixtures and properties of HFC at the material scale:** the workability of HFC (and of all other types of

FRC) has most probably a very important influence on the micro-mechanical properties, such as e.g. bond strength between fibres and concrete. Therefore, also the tensile properties depend on the rheology. A more exact relation between rheology and micro-mechanical properties should therefore be determined.

– **All these proposals should lead to the decrease of a rather large gap between the tensile and compressive strength of HFC:** in genreal, this can probably be done by increasing the water-binder ratio, in order to decrease the compressive strength of Hybrid-Fibre Concrete. At the same time, the tensile strength should be increased, through application of appropriate types and amounts of fibres, such as proposed in this sub-section. The decrease of the gap between the tensile and compressive strength of HFC would effect a more rational utilisation of this material in the structures [Van Mier et al., 1991].

Regarding the further development on the <u>structural scale</u>, the following points are recommended for the future research:

– **Further development of testing methods and tests set-ups for the determination of the tensile properties of Hybrid-Fibre Concrete:** the basic principle for the testing of HFC should be, that the material is tested as it appears in the real structures [Van Mier, 2004 b]. This is of importance with regard to the number and orientation of fibres, which are the key parameters for the tensile response of Hybrid-Fibre Concrete and any other fibre concrete.

– **Development of relations between the rheology of the fresh HFC mixtures and properties of structural elements made of HFC:** more knowledge on the orientation of short and long steel fibres in different types of structural elements (beams, plates, shells, columns) for different casting procedures is required. It should try to relate the viscosity and the flow direction of fresh HFC mixtures with the fibre orientation in a computational (quantitative) way. Some research results covering this topic are already provided in [Grünewald et al., 2002 a], and [Stähli et al., 2004 b] and [Karihaloo et al., 2005].

– **The research on the repeatability of the fibre distribution and orientation in the structural elements:** after the optimum casting process is known, it should make clear if such a casting proces results in a more-or-less constant number and orientation of fibres in a number of structural elements (repeatability). Subsequently, in the pre-cast concrete factories, it should standardise the casting process and the quality control for the pre-cast elements made of Hybrid-Fibre Concrete.

– **All existing design methods for different types of loading (bending, shear, punching, etc.) should be evaluated experimentally and theoretically**.

– **The shapes of the cross-sections of the structural elements made of Hybrid-Fibre Concrete should further be optimised.** This is especially important with regard to the the more optimal utilisation of the material in the tensile and compressive zone, as well as with regard to the behaviour of structures in serviceability limit state (deflections and vi-

brations). Some of the pioneer ideas in this direction are proposed by [Walraven, 2002] and [Jungwirth & Mutoni, 2004].

– **Behaviour of HFC in structures during their service life should be investigated.** More research on durability, fire resistance and fatigue of HFC and UHPFC is recommended. Some pioneer works in these areas are published in [Schmidt et al., 2002], [Dehn et al., 2003] and [Lappa et al., 2004]. Another interesting research area with regard to durability is the possible self-healing phenomenon in Hybrid-Fibre Concrete. If applied in a right way, self-healing materials could open a completely new era in the material science, and contribute to tremendous improvements in the sustainable development.

REFERENCES

Adeline, R., Cheyrezy, M. (1998): "La passarelle de Scherbrooke. premier ouvrage d'art en BPR", in 13th Congress of FIP, Amsterdam, pp. 343-348

AFGC & Setra (2002): "Ultra High Performance Fibre-Reinforced Concretes - Interim Recommendations, Working group BFUP, Reference Setra: F0211

Akkaya, Y., Shah, S.P., Ankenman, B. (2001): "Effect of Fiber Dispersion on Multiple Cracking of Cement composites", in Journal of Engineering Mechnanics, Vol. 127, No. 4, pp. 311-316

Aljeboury, A. (2005): "Applicability of ultra-high performance fibre concrete in structures", MSc-Thesis No. 737, Section of Concrete Structures, Delft University of Technology

Armelin, H.S., Banthia, N. (1997): "Predicting the Flexural Postcracking Performance of Steel Fiber Reinforced Concrete from the Pullout of Single Ibres", ACI Materials Journal, Vol. 94, No. 1, pp. 18-31

Aveston, J., Cooper, G.A., Kelly, A. (1971): "Single and Multiple Fracture: The Properties of Fibre Composites", in Conference Proceedings of National Physical Laboratory, pp. 15-24, IPC Science and Technology Press Ltd.

Bache, H.H. (1987): "Compact Reinforced Composite Basic Principles", in CBL Report No. 41, Aalborg Portland Cement Industries, Denmark

Banthia, N, Trottier J.F. (1991): "Deformed steel fiber - cementitious matrix under impact", Cement and Concrete Reseearch, Vol. 21, No. 1, pp. 158-168

Bartos, P.J.M., Duris, M. (1994): "Inclined tensile strength of steel fibres in a cement-based composite", Composites, Vol. 25, No. 10, pp. 945-952

Behloul, M. (1996 a): "Tensile behaviour of Reactive Powder Concrete (RPC)", 4th Int. Symp. Utilization of High Strength/High Performance Concrete, Paris, pp. 1375-1381.

Behloul, M. (1996 b): "Analyse et modelisation du comportement d'un materiau a matrice cimentaire fibree a ultra hautes performances (Betons de Poudres Reactives)", Phd-Thesis, L'Ecole Normale Superieure de Cachan (Genie Civil), C.N.R.S., Universite de Paris VI (in French)

Behloul, M., Lee, K.C. (2003): "Ductal Seonyu footbridge", fib Journal "Structural Concrete", Vol. 4, No. 4, pp. 195-201

Bekaert Factories (2000): "Product Information: Dramix Fibres", Bekaert BV, Zwevegem, Belgium

Beletti, B., Cerioni, R., Plizzari, G. (2004): "Fracture of SFRC slabs on grade", in 6th Rilem Symposium on Fibre Reinforced Concrete (BEFIB 2004), Varenna, pp. 723-733 (RILEM, ISBN: 2-912143-51-9)

Bentur A., Diamond S., Mindess S. (1985): "Cracking Processes in Steel Fiber Reinforced Cement Paste", Cement and Concrete Research, Vol. 15, No. 2, pp. 331-342

Bentur, A., Mindess, S. (1990): "Fibre reinforced cementitious composites", Elsevier Applied Science, London, 1990, ISBN 1-85166-393-2

Billberg, P. (2002): "SCC Mix Design Method", 2002 Summer School on Rheology and Self-Compacting Concrete, Technical University of Denmark, Lyngby

Bischop, J., van Mier, J.G.M. (2002): "Drying shrinkage cracking on cement based materials", HERON, vol. 47, No. 3, pp. 163-184

Blokland, G. van, (1997): "Verbreding van viaducten in Beton van Reactief Poeder", MSc-Thesis, Section of Concrete Structures, Delft University of Technology (in Dutch)

Borneman, R., Schmidt, M. (2002): "The role of powders in concrete", in 6th International Symposium on the Utilization of High Strength / High Performance Concrete, Leipzig, pp. 863-873 (ISBN: 3-934178-18-9)

Boulay, C., Rossi, P., Thalian, J.-L. (2004): "Uniaxial tensile tests on a new cement composites having a hardening behaviour", in 6th Rilem Symposium on Fibre Reinforced Concrete (BEFIB 2004), Varenna, pp. 61-69 (RILEM, ISBN: 2-912143-51-9)

Brite-Euram Project BRPR-CT98-0813 (2002): "Test and Design Methods for Steel Fibre Reinforced Concrete", ISBN: 90-5682-358-2

British Standard BS 812: Part 2 (1975): "Methods for testing aggregate", British Standard Institute, London

Casanova, P., Rosi, P. (1996): "Analysis of metallic fibre-reinforced concrete beams submitted to bending", Journal Materials and Structures, Vol. 29, pp. 354-361

Chanvillard, J., Aiticin, P.-C. (1992): "On the modelling of the pullout behaviour of Steel Fibres", in 1st International RILEM-Workshop on High Performance Fibre Reinforced Cement Materials (eds. H.W. Reinhardt, A.E. Naaman), RILEM Proceedings 15, pp. 388-406

Cheyrezy, M., Maret, V., Frouin, L. (1995): "Microstructural Analysis of RPC (Reactive Powder Concrete)", Cement and Concrete Research, Vol. 25, No. 7, pp. 1491-1500

CPCI (Canadian precast and prestressed concrete institute), 2003: "New canopies at the Shawnessy station in Calgary" (source: www.cpci.ca)

De Larrard, F. (1999): "Concrete Mixture Proportioning: a scientific approach", E&FN Spon, London and New York, ISBN 0 419 23500 0

De Larrard, F., Sedran, T. (1994): "Optimization of ultra-high-performance concrete by using a packing model", Cement and Concrete Research, Vol. 24, No. 6, pp. 997-1009.

Di Prisco, M., Plizzari, G., Meda, A., Sorelli, L. (2003): "Application of FRC for long-span prestressed roof girders", in in International RILEM Workshop "Test and Design Methods for SFRC: Background and Experiences", TU Bochum, pp. 98-107 (RILEM, PRO 31, based on the work of RILEM TC-147 TDF)

Dehn, F., König, G. (2003): "Fire resistance of different fibre reinforced HPC", 4th International Workshop on HPFRCC, Ann Arbor, pp. 189-205, ISBN: 2-912143-38-1

Destrée, X. (2000): "Structural application of steel fibre as princpal reinforcing: conditions - design - examples",Proc. of the 6th Int. RILEM-Symposium on Fibre Reinforced Concrete - BEFIB 2000, Lyon, pp. 328-337

Deutscher Beton- und Bautechik-Verein (DBV) (2001): DBV Merkblatt Stahlfaserbeton (in German)

Fehling, E., Bunje, K., Leutbecher, T. (2004): "Design relevant properties of hardened Ultra High Performance Concrete", 1st Int. Symp. on Ultra High Performance Concrete, Kassel, pp. 327-338, (Die Deutsche Bibliothek, ISBN: 3-89959-086-9)

Fehling, E., Schmidt, M., Bunje, K., Schreiber, W. (2004): "Ultra-High Performance Composite Bridge across the River Fulda in Kassel - Conceptual Design, Design Calculations and Invitation to Tender", 1st Int. Symp. on Ultra High Performance Concrete, Kassel, pp. 69-75, (Die Deutsche Bibliothek, ISBN: 3-89959-086-9)

Geisenhanslüke, C, Schmidt, M. (2004): "Methods for Modelling and Calculation of High Density Packing for Cement and Fillers in UHPC", in 1st Int. Symp. on Ultra High Performance Concrete, Kassel, pp. 303-313, (Die Deutsche Bibliothek, ISBN: 3-89959-086-9)

Groth, P. (2000): "Fibre Reinforced Concrete", PhD Thesis, Department for Construction Technology, Lulea University of Technology, ISSN: 1402-1544

Grünewald, S., Walraven J.C. (2000): "Self-Compacting Fibre-Reinforced Concrete", Report 25.5-00-11, Stevinlab, TU Delft

Grünewald S., Walraven J.C. (2002 a): "Self-compacting fibre reinforced concrete - orientation and distribution of steel fibres in beams", Report 25.5-02-33, Section of Concrete Structures / Stevinlab, TU Delft

Grünewald S., Walraven J.C. (2002 b): "High-Strength Self-Compacting Fibre Reinforced Concrete: Behaviour in Fresh and in the Hardened State", in 6th International Symposium on High-Strength/High-Performance Concrete, Leipzig, pp. 977-991

Grünewald, S., Walraven, J.C. (2002 c): "Erfahrungen mit Faserbetonen in den Niederlanden", in 2. Leipziger Fachtagung "Innovationen im Bauwesen - Faserbeton", Leipzig, pp. 237-251

Grünewald, S. (2004): "Performance-based design of self-compacting fibre reinforced concrete", PhD Thesis, Department of Concrete Structures, Delft University of Technology, ISBN: 90-407-2487-3

Guererro, P., Naaman, A.E. (2000): "Effect of Mortar Fineness and Adhesive Agents on Pullout response of Steel Fibres", ACI Materials Journal, Vol. 97, No. 1, pp. 12-20.

Holschemacher, K., Dehn, F., Klotz, S., Weiße, D. (2004): "Ultra High Strength Concrete under Concentrated Loading", in 1st Int. Symp. on Ultra High Performance Concrete, Kassel, pp. 471-481

Hoy, C. W. (1998): "Mixing and mix proportioning of fibre reinforced concrete", PhD-Thesis, University of Paisley (British Library, Thesis No. DX200558)

Jungwirth, J., Mutoni, A. (2004): "Structural Behaviour of Tension Members in UHPC", in 1st Int. Symp. on Ultra High Performance Concrete, Kassel, pp. 533-547

Kabele, P., Horii, H. (1996): "Analytical model for fracture behaviour of pseudo-strain hardening cementitious composites", JSCE-Proceedings, No. 532 / V-30

Kaptijn, N. (2004): "A new bridge deck for the Kaag bridges: the first CRC application in cibil infrastructure", in 1st Int. Symp. on Ultra High Performance Concrete, Kassel, pp. 49-59

Karihaloo, B.L. (1995): "Fracture Mechanics and Structural Concrete", Monography, Longman Science and Technical, London, UK

Karihaloo, B.L., Wang, J. (1997): "Micromechanical modelling of strain hardening and tensile softening in cementitious composites", Journal of Computational Mechanics, Vol. 19, pp. 453-462

Karihaloo, B.L., Fehling, E., Stiel, T. (2004): " Effects of Casting Direction on the Mecjhanical Properties of CARDIFRC®", in 1st Int. Symp. on Ultra High Performance Concrete, Kassel, pp. 481-495, (Die Deutsche Bibliothek, ISBN: 3-89959-086-9)

Kelly, A. (1974): "Microstructural parameters of an alligned fibrous composite", Conference on Composites - Standards, Testing and Design, Teddington, National Physical Laboratory, pp. 5-14

Kennedy, C.T. (1940): "The Design of Concrete Mixes", ACI Proceedings, Vol. 36.

Kobayashi, K., Cho, R. (1976): "Mechanics of Concrete with randomly oriented discontinious fibres", 2nd International Conference on Mechanical Behaviour of Materials, Boston, pp. 1938-1942

Kooiman, A.G. (2000): "Modelling Steel Fibre Reinforced Concrete for Structural Design", PhD Thesis, Department of Concrete Structures, Delft Univversity of Technology, ISBN: 70-73235-90-X

Krenchel, H. (1976): "Fibre Reinforcement", Technical Report, Akademisk Forlag, Copenhagen

Kützing, L. (2000): "Tragfähigkeitsermittlung stahlfaserversterkter Betone", PhD Thesis, Institut für Massivbau, University of Leipzig (in German)

Lappa, E.S., Braam, C.R., Walraven J.C. (2004): "Static and fatigue bending tests on UHPC", in 1st Int. Symp. on Ultra High Performance Concrete, Kassel, pp. 449-461 (Die Deutsche Bibliothek, ISBN: 3-89959-086-9)

Li, V.C., Leung, C.K.Y. (1992): "Theory of Steady-State and Multiple Cracking of Random Discontinious Fiber Reinforced Brittle Matrix Composites", in ASCE Journal of Engineering Mechanics, Vol. 118, No. 11, pp. 2246-2264

Li, V.C., Stang, H. (1997): "Interface Property Characterization and Strengthening Mechanisms in Fiber Reinforced Cement Based Composites", in Advanced Cement Based Materials, No. 6, pp. 1-20

Löfgren, I. (2004): "The wedge splitting test - a test method for assessment of fracture parameters of FRC?", in 5th International Symposium on Fracture Mechanics of Concrete and Concrete Structures (FraMCoS), Vail, Colorado, pp. 1155-1162 (RILEM, ISBN 0-87031-135-2)

Markovic, I., Van Mier, J.G.M., Walraven J.C. (2002 a): "Single fiber pullout from the hybrid fiber reinforced matrices", in 6th International Symposium on the Utilization of High Strength / High Performance Concrete, Leipzig, Vol. 2, pp. 1175-1187, ISBN: 3-934178-18-9

Markovic, I., Van Mier, J.G.M., Grünewald, S., Walraven J.C. (2002 b): "Characterization of Bond Between Steel Fibres and Concrete - Conventional Fibre Reinforced Versus Self-Compacting Fibre Reinforced Concrete",

in 3rd International Symposium "Bond in Concrete - from research to standards", Budapest, pp. 520 - 529, ISBN 963 420 714 6

Markovic, I., Van Mier, J.G.M., Walraven J.C. (2003 a): "Development of High Performance Hybrid Fibre Concrete", in 4th International Workshop on HPFRCC, Ann Arbor, pp. 277-300, ISBN: 2-912143-38-1

Markovic, I., Van Mier, J.G.M., Walraven J.C. (2003 b): "Experimental Evaluation of Fibre Pullout From Plain and Fibre Reinforced Concrete", in 4th International Workshop on HPFRCC, Ann Arbor, pp. 419-436, ISBN: 2-912143-38-1

Markovic, I., Van Mier, J.G.M., Walraven J.C. (2003 c): "Self-compacting Hybrid-Fibre Concrete", in 3rd International Symposium on SCC, Reykjavik, pp. 763-776, ISBN: 2-912143-42-X

Markovic, I., Van Mier, J.G.M., Walraven J.C. (2004 a): "Tensile Behaviour of High Performance Hybrid-Fibre Concrete", in 5th International Symposium on Fracture Mechanic of Concrete and Concrete Structures (FraMCoS-5), Vail, Colorado, Vol. 2, pp. 1113-1121, ISBN: 0-87031-135-2

Markovic, I., Van Mier, J.G.M., Walraven J.C. (2004 b): "Tensile Response of High Performance Hybrid-Fibre Concrete", in 6th Rilem Symposium on Fibre Reinforced Concrete (BEFIB 2004), Varenna, pp. 1341-1353 (RILEM, ISBN: 2-912143-51-9)

Marti, P., Pfyl, T., Sigrist V., Ulaga, T. (1999): "Harmonized Test Procedures for steel FRC, in ACI Materials Journal, Vol. 96, No. 6, pp. 676-685

Marti, P. (2002): "Empfehlungen für Stahlfaserbeton", in Festschrift zum 60. Geburtstag von Prof. Dr.-Ing. H. Falkner - Betonbau: Forschung, Entwicklung und Anwendung, Schriftenreihe des IBMB, TU Braunschweig, Heft 142, pp. 213-221 (in German)

Mc Kee, D.C. (1969): "The Properties of an Expansive Cement Mortar Reinforced with Random Wire Fibres", PhD Thesis, University of Illinios

Midorikawa T., Pelova G., Walraven J.C. (2001): "Application of "Water Layer Model" to Self-Compacting Mortar", in 2nd International RILEM Symposium on SCC, Tokyo

Mihashi, H., Otsuka, K., Kiyota, M., Mori, S. (2002): "Observation of multiple cracking on micro and meso level", in JCI International Workshop on Ductile Fiber Reinforced Cementitious Composites (DFRCC), Gifu University, Japan, pp. 121-127

Mobasher, B., Stang, H., Shah, S.P. (1990): "Microcracking in Fiber Reinforced Concrete", in Cement and Concrete Research, Vol. 20, pp. 665-676

Naaman A.E., Shah, S. (1976): "Pullout mechanism in Steel Fiber Reinforced Concrete", Journal of Structural Division (ASCE), Vol. 102, No. 8, pp. 1537-1548

Naaman, A.E. (1999): "Fibers with slip hardening bond", High Performance Fibre Reinforced Cement Materials (eds. H.W. Reinhardt, A.E. Naaman), RILEM Publicatons PRO 6, pp. 371-387

Naaman, A.E., Najm, H. (1991a): "Bond-Slip Mechanisms of Steel Fibres in Concrete", ACI Materials Journal, Vol. 88, No. 2, pp. 135-145

Naaman, A.E., Namur, G., Alwan, J., Najm, H. (1991b): "Fiber Pullout and Bond Slip. I: Analytical Study", Journal of Structural Engineering (ASCE), Vol. 117, No. 9, pp. 2769-2790

Naaman, A.E., Namur, G., Alwan, J., Najm, H. (1991c): "Fiber Pullout and Bond Slip. II: Experimental Validation", Journal of Structural Engineering (ASCE), Vol. 117, No. 9, pp. 2791-2800

Naaman, A.E., Reinhardt H.W. (1995): "Characterization of high performance fiber reinforced cement composites - HPFRCC", in 2nd International RILEM-Workshop on High Performance Fiber Reinforced Cement Composites, Ann Arbor, pp.1-21

Nakamura, S., Van Mier, J.G.M., Masuda, Y., (2004): "Self-compactability of hybrid-fibre concrete containing PVA fibres ",in 6th Rilem Symposium on Fibre Reinforced Concrete (BEFIB 2004), Varenna, pp. 527-539 (RILEM, ISBN: 2-912143-51-9)

Nemeeger, D. (1999): "Zelfverdichtend Staalvezelbeton", Proceedings Constructuersmiddag 1999 in Ede, Ned. Betonvereniging, Gouda (in Dutch)

NEN 6720 (Nederlands Normalisatie-instituut): Voorschriften Beton TGB 1990 (Constructieve eisen en rekenmethoden – VBC 1995), 1995 (National Netherlands regulations for concrete structures) (in Dutch)

Nordenswan, E. (2002): "Measurements of packing density of steel spheres using the IC Tester", Engineering consulting company "Consolis Technology", Finland, unpublished results-private communication

Okamura, H., Ozawa, K., Ouchi, M. (2000): "Self-compacting concrete", fib-Journal "Structural Concrete", Vol. 1, No. 1, pp. 3-17

Olesen, J. F. (2001): "Fictitious Crack Propagation in Fiber-Reinforced Concrete Beams", Journal of Engineering Mechanics, Vol. 127, No. 3, pp. 272-280

Orange, G., Dugat, J., Acker, P. (2000): "Ductal : New Ultra-high Performance Concretes - Damage Resistance and Micromechanical Analysis", 5th International Rilem Symposium on Fibre Reinforced Concretes BEFIB, Lyon, pp. 781-790.

Pfyl, T. (2003): "Tragverhalten von Stahlfaserbeton", PhD-Thesis, Institute for structural engineering (IBK), Swiss Federal Institute of Technology (ETH), Zurich (in German)

Pinchin D.J., Tabor D. (1978): "Interfacial Contact Pressure and Frictional Stress Transfer in Steel Fibre Concrete", in Testing and Testing Methods of Fiber Cement Composites, The Construction Press, UK, pp. 337-344

Plizzari, G., Sorelli, L., Meda A. (2004): "Uni-axial and bending tests for the determination of fracture properties of FRC", in 5th International Symposium on Fracture Mechanics of Concrete and Concrete Structures (FraMCoS), Vail, Colorado, pp. 1163-1171 (RILEM, ISBN: 0-87031-135-2)

Prado, E.P., Van Mier, J.G.M. (2003): "Effect of particle structure on mode I fracture process in concrete", in Engineering Fracture Mechanics, Vol. 70, pp. 1793-1807

Racky, P. (2004): "Cost-effectiveness and sustainability of UHPC", in 1st Int. Symp. on Ultra High Performance Concrete, Kassel, pp. 797-805, (Die Deutsche Bibliothek, ISBN: 3-89959-086-9)

Reineck, K-H. (2002): "HPC Hot-water Tanks for the Seasonal Storage of Solar Heat", in 6th International Symposium on the Utilization of High Strength / High Performance Concrete, Leipzig, pp. 739-753, ISBN: 3-934178-18-9

Richard, P. (1996): "Reactive Powder Concrete - a new ultra-high-strength cementitious material", 4th Int. Symp. Utilization of High Strength/High Performance Concrete, Paris, pp. 1343-1349.

Richard, P., Cheyrezy, M. (1995): "Composition of Reactive Powder Concrete", Cement and Concrete Research, Vol. 25, No. 7, pp. 1501-1511

Richard., P., Cheyrezy, M. (1995): "Composition of Reactive Powder Concretes", Cement and Concrete Research, Vol. 25, No. 7, pp. 1501-1511

RILEM TC 162-TDF (Chairlady: L. Vandewalle) (2000): "Test and Design Methods for Steel Fibre Reinforced Concrete - Draft Recommendations", in Materials and Structures, Vol. 33, No. 1, pp. 3-5.

Robins, P., Austin, S., Jones, P. (2002): "Pullout behaviour of hooked-end steel fibres", Materials and Structures, Vol. 35, No. 8 (August), pp. 434-442

Romualdi J., Mandel, J. (1964): "Tensile Strength of Concrete Affected by uniformly distributed and Closely Spaced Short Lengths of Wire Reinforcement", Journal of the American Concrete Institute, Vol. 61, No.6, pp. 657-671

Rossi, P., Acker, P., Malier, Y. (1987): "Effect of steel fibres at two stages: the material and the structure", Materials and Structures, Vol. 20, pp. 436-439

Rossi, P., Renwez, S. (1996): "High Performance Multi-Modal Fiber Reinforced Cement Composites (HPMFRCC)", 4th Int. Symp. Utilization of High Strength/High Performance Concrete, Paris, pp. 687-694.

Sato, Y. (1999): "Mechanical Characteristics of High Performance Fibre Reinforced Cement Based Composites", Internal Report, TU Delft, Faculty of Civil Engineering and Geosciences, Section of Concrete Structures

Sato, Y., Walraven, J.C., van Mier, J.G.M. (1999): "Mechanical Characteristics of Multi-modal Fibre Reinforced Cement Based Composites", 5th Int. Symp. on Fibre Reinforced Concrete BEFIB, Lyon, (eds. P Rossi et al.), RILEM, pp. 791-800

Schmidt, M., Fehling, E., Bormeman, R., Middenhof, B., (2001): "Ultra-Hochleistungsbeton: Herstellung, Eigenschaften und Anwendungsmöglichkeiten", in Beton- und Stahlbetonbau, Jahrgang 96 (2001), Heft 7, pp. 458-467 (in German)

Schmidt, M., Fehling, E., Teichmann, Th., Bunje, K. (2002): "Durability of Ultra High Performance Concrete (UHPC)", in 6th International Symposium on the Utilization of High Strength / High Performance Concrete, Leipzig, pp. 1367-1377, ISBN: 3-934178-18-9

Schmidt, M., Fehling, E. (2003): "Ultra-Hochfester Beton: Perspektive für die Betonfertigteilindustrie", Beton- und Fertigteiltechnik, 2003 / No. 3, pp. 16-29

Schönlin, K. (1988): "Ermittlung der Orientierung, Menge und Verteilung der Fasern im Faserbeton", in Beton- und Stahlbetonbau, Vol. 83, No. 6, pp. 168-171 (in German)

Schumacher, P. (2002): "Three-Point Bending Tests on Self-Compacting Fibre Reinforced Concrete Beams", Stevinrapport No. , Department of Concrete Structures, TU Delft

Schweizerischer Ingenieur- und Architecten-Verein (SIA) (1998): "Richtlinie 162/6: Stahlfaserbeton"

Shah, S.P., Betterman, L.R., Oyang, C. (1995): "Fiber-Matrix Interaction in Microfiber-Reinforced Mortar", Advanced Cement-Based Materials, No. 2, pp. 53-61

Shah, S.P., Balaguru P.N. (1992): "Fiber-reinforced cement composites", McGraw-Hill, New York, 1992, ISBN   0-07-056400-0

Shiotani, T., Bisschop, J., Van Mier, J.G.M. (2003): "Temporal and spatial development of drying shrinkage cracking in cement-based materials", in Engineering Fracture Mechanics, Vol. 70, No. 12, pp. 1509-1525

Simon, A., Hajar, Z., Lecointre, D., Petitjean, J. (2002): "Realization of two road bridges with Ultra-High-Performance Fibre Reinforced Concrete, in 6th Int. Symp. on High Strength / High Performance Concrete, Leipzig, pp. 753-768

Sorelli, L., Meda, A., Plizzari, G., Rossi, B. (2004): " Experimental investigation of slabs on grade: steel fibres vs. conbventioonal reinforcement", in 6th Rilem Symposium on Fibre Reinforced Concrete (BEFIB 2004), Varenna, pp. 1083-1093 (RILEM, ISBN: 2-912143-51-9)

Soroushian, P., Lee, C. (1990): "Distribution and Orientation of Fibers in Steel Fibre Reinforced Concrete", in ACI Materials Journal, Vol. 87, No. 5, pp. 433-439

Stähli, P., Van Mier, J.G.M. (2004 a): "Three-fibre type hybrid-fibre concrete", in 5th International Symposium on Fracture Mechanics of Concrete and Concrete Structures (FraMCoS), Vail, Colorado, pp. 1105-1112 (RILEM, ISBN: 0-87031-135-2)

Stähli, P., Van Mier, J.G.M. (2004 b): "Rheological properties and fracture processes of HFC", in 6th Rilem Symposium on Fibre Reinforced Concrete (BEFIB 2004), Varenna, pp. 299-309 (RILEM, ISBN: 2-912143-51-9)

Stang, H., Olesen, J.F. (2000): "A Fracture Mechanics based Design Approach to FRC", in 5th Int. RILEM-Symposium on Fibre Reinforced Concrete - BEFIB 2000, Lyon, pp. 315-324

Stang, H. (2003): "Scale Effects in FRC and HPFRCC structural elements", in 4th International Workshop on HPFRCC, Ann Arbor, pp. 245-259, ISBN: 2-912143-38-1

Svermova, L. (2004): "Development of self-compacting SIFCON", PhD-Thesis, ACBM, University of Paisley, Scotland, 2004

Teichman, T. Schmidt, M. (2004): "Influence of the packing density of fine particles on structure, strength and durability of UHPC", in 1st Int. Symp. on Ultra High Performance Concrete, Kassel, pp. 313-325, (Die Deutsche Bibliothek, ISBN: 3-89959-086-9)

Thibeaux, T., Simon, A., Hajar, Z., Chanut, S. (2004): "Construction of an UHPFRC thin shell structure over the Millau viaduct toll gates", in 6th Int. RILEM-Symposium on Fibre Reinforced Concrete - BEFIB 2004, Varenna, pp. 1183-1195 (RILEM, ISBN: 2-912143-51-9)

Tjiptobroto, P. (1992): "High-Performance Fibre Reinforced Cement Based Composites", PhD Thesis, University of Michigan, Ann Arbor

Tjiptobroto, P., Hansen, W. (1993): "Tensile Strain Hardening and Multiple Cracking in High-Performance Cement Based Composites Containing Discontinious Fibres", in ACI Materials Journal, Vol. 90, No. 1, pp. 16-25

Trottier, J.-F., Banthia, N. (1994): "Concrete reinforced with Deformed Steel Fibres, Part 1: Bond-Slip Mechanisms", ACI Materials Journal, Vol. 91, No. 5, pp. 435-446

Van der Veen, C. (2002): "Ontwerpen in beton met zeer hoge sterkte", PAO engineering course "Nieuwe Betonsoorten", TU Delft, 2002 (in Dutch)

Van Gysel, A. (2000): "Studie van het uittrekgedrag van staalvezels ingebed in een cementmatrix met toepassing op stalvezelbeton onderworpen aan buiging", PhD Thesis, Laboratory Magnel for Concrete Research, University of Gent (in Dutch)

Van Herwijnen, F., Felt, R. (2005): "Prefabricated canopy in Ultra High Performance Concrete", 18th BIBM (Bureau International du Béton Manufacturé) International Congress, Amsterdam, The Netherlands, pp. 60-64, (Publisher BFBN, ISBN: 3-7625-3607-4)

Van Mier, J.G.M., Timmers, G. (1991): "Shear fracture in slurry infiltrated fibre concrete (SIFCON)", 1st RILEM/ACI Workshor on HPFRCC, Mainz, pp. 253-265 (RILEM)

Van Mier, J.G.M. (1997): "Fracture Processes of Concrete: Assesment of Material Parameters for Fracture Models", Monography, Publisher: CRC Press, Boca Raton, ISBN 0-8493-9123-7

Van Mier, J.G.M. (2004 a): "Reality behind fictitious cracks?", in 5th International Symposium on Fracture Mechanics of Concrete and Concrete Structures (FraMCoS), Vail, Colorado, pp. 11-30 (RILEM)

Van Mier, J.G.M. (2004 b): "Cementitious composites with high tensile strength and ductility through hybrid fibres", in 6th Rilem Symposium on Fibre Reinforced Concrete (BEFIB 2004), Varenna, pp. 219-238 (RILEM, ISBN: 2-912143-51-9)

Vandewalle, L. (2003): "Design with $\sigma - \varepsilon$ Method", in International RILEM Workshop "Test and Design Methods for SFRC: Background and Experiences", TU Bochum, pp. 31-47 (RILEM, Publication No. PRO 31, based on the work of RILEM TC-147 TDF)

Vandewalle, L., Dupont, D. (2004): "Comparison between the round plate test, and the RILEM 3-point-bending test", in 6th Rilem Symposium on Fibre Reinforced Concrete (BEFIB 2004), Varenna, pp. 101-111 (RILEM, ISBN: 2-912143-51-9)

Vonk, E. (2000): "Structural Design of Bridges using RPC", MSc-Thesis, Section of Concrete Structures, Delft University of Technology

Wallevik, O. (2002): "Course on Rheology - Rheology of Cement Suspensions", The Icelandic Building Research Institute, Reykjavik

Walraven, J.C. (2002): "From High-Strength to High-Performance to Defined-Performance Concrete", 6th International Symposium on High-Strength/High-Performance Concrete, Leipzig, pp. 77-91

Walraven, J.C. (2004): "Designing with ultra-high strength concrete: basics, potential and perspectives", in 1st Int. Symp. on Ultra High Performance Concrete, Kassel, pp. 853-865, (Die Deutsche Bibliothek, ISBN: 3-89959-086-9)

Walraven, J.C. (2005): "Precast concrete: benefits from new developments in concrete technology", 18th BIBM (Bureau International du Béton Manufacturé) International Congress, Amsterdam, The Netherlands, pp. 14-17, (Publisher BFBN, ISBN: 3-7625-3607-4)

Walraven, J.C., Galjaard, J.C. (1997): "Voorgespannen Beton", Betonpraktijkreeks 3, BetonPrisma, 's-Hertogenbosch, ISBN 90-71806-34-0 (in Dutch)

Walter, R., Stang, H., Gimsing, N.J., Olesen, J.F. (2003): "High-performance composite bridge decks using SC FRC", in 4th International Workshop on HPFRCC, Ann Arbor, pp. 495-505, ISBN: 2-912143-38-1

Wei S., Mandel J.A., Said S. (1986): "Study of the Interface Strength of Steel Fibre Reinforced Cement Based Composites", ACI Journal, Vol. 83, pp. 597-605

APPENDIX A

Computation procedure for the analytical modelling of the tensile softening response of Hybrid-Fibre Concrete (results given in Section 4.6.6)

In this Appendix, the procedure for the computation of tensile stresses in Hybrid-Fibre Concrete which contains 1.0 vol.-% of long fibres 60/0.7 and 0.5 vol.-% of short fibres 13/0.2 will be given. This procedure covers therefore the general case of the analytical modelling of tensile softening of a concrete with two fibre types.

The modelling parameters were calibrated from the tensile softening response of concretes which contain one type of fibre. The modelling of the tensile softening response of concretes with one type of fibre is basically the same as the one of the Hybrid-Fibre Concrete which is presented in this Appendix. The calibrated parameters will be directly applied for the modelling of the tensile softening response of Hybrid-Fibre Concrete.

This computation procedure consists of more steps, covering the contribution of long and short fibres to the total tensile softening response of Hybrid-Fibre Concrete. The result of these computations, are the tensile stresses produced by fibres during tensile softening of Hybrid-Fibre Concrete. These stresses depend basically on the total number of fibres (i.e. on the applied fibre volume quantity), the number of fibres active in the crack bridging at the crack width w, and on the pullout of fibres. For both long (60/0.7) and short (13/0.2) fibres, the computations were performed in tabular form, using the programme Excel.

The computation procedure for the tensile stresses produced by fibres 60/0.7 (long hooked-end fibres) is as follows (detailed computation and diagrams given in Tab. 4.A.1):

STEP 1: CONTRIBUTION OF FIBRES WITH FULLY DEFORMED HOOKS:

1.1. From the pullout diagrams of the single fibres 60/0.7 inclined under angles of 0º and 15º (Fig. 4.17), determine the values of the pullout forces at appropriate displacements (i.e. crack widths) w (starting from $w = 0$ mm, to $w = 20$ mm). These pullout forces do not depend on the fibre embedded length, if it is larger that 10 mm (for explanations, see Sections 4.6.4 and 2.9.6);

1.2. Determine the average value of the pullout forces for these two inclination angles. Regarding the local bending of fibre across the crack, the case with inclination angle of 0º corresponds to "no bending", the case with inclination angle of 15º to "full bending" and the average case corresponds to gradual bending of a fibre across the crack (Fig. 4.15);

1.3. Determine the ratio $p(w) = n_{act}(w) / n_{tot}$ starting from $w = 0$ mm to $w = 20$ mm. $p(w)$ is the probability that a fibre will be active in the crack bridging at a crack width w (Eq. 4.14). The determination of this probability is based on the visible (i.e. embedded) lengths of fibres at the crack surface. The determination of $p(w)$ is described in Section 4.6.3;

1.4. Knowing the total number of fibres that crosses the crack, and using p(w), determine the number of fibres active in the crack bridging at the crack width (displacement) w;

STEP 2: CONTRIBUTION OF FIBRES WITH PARTLY DEFORMED HOOK:

2.1. From the calibrated pullout diagram of these fibres (Fig. 4.17 and Section 4.6.4), determine the values of the pullout forces at appropriate displacements (i.e. crack widths) w (starting from $w = 0$ mm, to $w = 5$ mm);

2.2. Determine the ratio $p(w) = n_{act}(w) / n_{tot}$ for these fibres (similarly as explained herein under 1.3.);

2.3. Determine the number of fibres active in the crack bridging at the crack width (displacement) w (similarly as explained herein under point 1.4.);

STEP 3: DETERMINATION OF THE TOTAL TENSILE STRESS:

3.1. The total tensile stress at a displacement (crack width) w produced by fibres with fully and partly active hook can be determined using Eq. 4.19. Tensile stress is equal to the product of the pullout force present in each single fibre and the number of active fibres at that displacement (crack width) w.

3.2. For long fibres, this product has to be additionally multiplied with 0.075 (0.075 = 7.5 % = 30 % / 4), to account for the increase of the fibre pullout forces by virtue of the presence of short fibres in concrete (a detailed explanation for this can be found in Section 4.6.6).

3.3. In the case where no local bending of fibres is present, the tensile stresses has to be additionally multiplied with the cosines of the full inclination angle (= 26.4º) as explained in Fig. 4.15, so that the influence of the fibre orientation can be taken into account.

3.4. In the case where local bending of fibres is present from the starting point of tensile softening, the influence of the orientation angle has to be taken into account as well. The values of the tensile stress should be multiplied with the cosines of the angles of 15º and 7.5º (Fig. 4.15);

The computation procedure for the tensile stresses produced by fibres 13/0.2 (short straight fibres) is as follows (detailed computation and diagrams given in Tab. 4.A.2):

STEP 4: DETERMINATION OF TOTAL TENSILE STRESSES

4.1. Determine pullout forces in fibres with different embedded lengths (l_{emb} = 0 mm to 12 mm, with step of 2 mm). The calibration of these forces was performed in Section 4.6.5.

4.2. Determine the ratio $p(w) = n_{act}(w) / n_{tot}$ for these fibres. The calibration of this ratio was performed in Section 4.6.5. This ratio has here the same role as for the long fibres (explained under point 1.3.);

4.3. Determine the total tensile stress developed by the fibres for each displacement (crack width) w, using Eq. 4.19. The idea of using this equation is the same as defined herein under point 3.1.

4.4. According to the calibration of parameters (Section 4.6.5), all short fibres are fully bent across the crack from the starting point of the tensile softening. Therefore, the tensile stresses should not be additionally multiplied with the cosines of the local bending angle, as it was the case for long fibres.

STEP 5: TENSILE SOFTENING RESPONSE OF HYBRID-FIBRE CONCRETE

The computed total tensile stresses produced by short and long fibres should be added to each other. The total tensile softening response of Hybrid-Fibre Concrete is obtained in this way.
Further variations of the variable modelling parameters (e.g. applied fibre volume quantity) are possible (result of computation shown in Fig. 4.30 and 4.31)

REMARKS ON THE ANALYTICAL MODELLING OF TENSILE RESPONSE IN CASE OF SINGLE CRACK AND MULTIPLE CRACKS

CASE 1: Fracturing during the complete tensile response of Hybrid-Fibre Concrete (microcracking phase not taken into account) is governed by a single crack (valid e.g. for here tested tensile specimens with long fibres only, as well as for all notched tensile specimens):

as the fibre pullout starts immediately after the formation of the first (and most probably the only) through-crack, the value $p(w)$ start to decrease already from $w = 0$, both for short and for long fibres. However, as this analytical model accounts only for the tensile softening of Hybrid-Fibre Concrete, the tensile stress is shown starting from the displacement of 1.0 mm, which approximately corresponds to the beginning of the tensile softening.

CASE 2: Tensile fracture is governed by the multiple cracking during the macrocrack growth phase, and subsequently by a single dominant crack during the whole tensile softening phase (valid e.g. for here tested tensile specimens with only short fibres and specimens with both short and long fibres):

The pullout of fibres will probably exist by virtue of the opening of each of the multiple cracks, but it can be neglected until the point where the tensile softening begins. From this point on, fibre pullout takes place. Therefore, the reduction of the ratio $p(w)$ should start at the displacement where the tensile softening begins.

GENERAL REMARK: As pointed out in Section 4.6.2, the displacements during the elastic and microcracking phase will be neglected, because they are very small compared to the total displacements achieved in these tensile tests.

CALCULATION FOR FIBRES 60/0.7 (long hooked-end fibres)

applied volume quantity:	1.0	vol.-%	
total number of fibres:	98	fibres	(counted, Tab. 3.3)
average orientation angle:	26.4	degrees	(measured, Tab. 3.3)
average orientation angle:	0.461	rad	

cell	A	B	C	D	E	F	G	H	I	J	K	L
1		FIBRES WITH FULLY DEFORMED HOOKS					FIBRES WITH PARTLY DEFORMED HOOKS					
2	displacement	single fibre pullout forces Pi (N)			ratio p(w)	number of fibers	single fibre	ratio p(w)	number of fibers	tensile stress developed		
3	(mm)	for inclination angles (°) (Fig. 4.17)			(Fig. 4.27)	active in crack bridging	pullout forces Pi (N)	(Fig. 4.27)	active in crack bridging	by fibres inclined under angle (°)		
4		0°-15°	15°-15°	7.5°-15°						0°-15°	15°-15°	7.5°-15°
5	0	0	0	0	0.770	75.5		0.230	22.5			
6	0.005	10	40	25	0.770	75.5		0.230	22.5			
7	0.01	15	75	45	0.770	75.4		0.230	22.5			
8	0.025	25	100	62.5	0.770	75.4		0.230	22.5			
9	0.05	50	150	100	0.769	75.4		0.230	22.5			
10	0.075	75	225	150	0.769	75.3		0.230	22.5			
11	0.1	100	250	175	0.768	75.3		0.230	22.5			
12	0.2	220	360	290	0.766	75.1		0.229	22.5			
13	0.3	360	500	430	0.764	74.9	300	0.229	22.5	6.62	8.68	7.65
14	0.4	460	580	520	0.762	74.7	270	0.229	22.4	7.94	9.71	8.83
15	0.5	550	650	600	0.761	74.5	240	0.229	22.4	9.11	10.58	9.84
16	0.6	620	710	665	0.759	74.3	220	0.228	22.4	10.03	11.34	10.68
17	0.8	700	810	755	0.755	74.0	180	0.228	22.3	10.97	12.56	11.76
18	1	720	870	795	0.751	73.6	150	0.227	22.2	11.07	13.24	12.15
19	1.5	675	895	785	0.742	72.7	115	0.226	22.1	10.14	13.28	11.71
20	2	650	790	720	0.732	71.7	90	0.224	22.0	9.55	11.53	10.54
21	2.5	610	720	665	0.723	70.8	75	0.223	21.8	8.81	10.34	9.58
22	3	570	660	615	0.713	69.9	50	0.221	21.7	8.04	9.28	8.66
23	3.5	540	650	595	0.704	68.9	32.5	0.220	21.5	7.45	8.94	8.20
24	4	500	500	500	0.694	68.0	20	0.218	21.4	6.77	6.77	6.77
25	5	400	450	450	0.675	66.2	5	0.215	21.1	5.22	5.87	5.87
26	6	280	400	340	0.656	64.3	0	0.212	20.8	3.54	5.05	4.30
27	7	280	400	340	0.637	62.4	0	0.209	20.5	3.44	4.91	4.17
28	8	280	400	340	0.618	60.6	0	0.206	20.2	3.33	4.76	4.05
29	9	280	400	340	0.599	58.7	0	0.203	19.9	3.23	4.61	3.92
30	10	280	400	340	0.580	56.8	0	0.200	19.6	3.13	4.47	3.80
31	11	280	400	340	0.561	42.8		0.197	19.3	2.35	3.36	2.86
32	12	280	400	340	0.542	40.0		0.194	19.0	2.20	3.15	2.67
33	13	280	400	340	0.523	37.3		0.191	18.7	2.05	2.93	2.49
34	14	280	400	340	0.504	34.5		0.188	18.4	1.90	2.71	2.31
35	15	280	400	340	0.485	31.8		0.185	18.1	1.75	2.50	2.12
36	16	280	400	340	0.466	29.0		0.182	17.8	1.60	2.28	1.94
37	18	280	400	340	0.428	23.5		0.176	17.2	1.29	1.85	1.57
38	20	280	400	340	0.390	18.0		0.170	16.7	0.99	1.42	1.20

PULLOUT FORCES IN FIBRES

pullout force (N)

long fibres with:
- fully deformed hook, no bending
- fully deformed hook, partly bent
- fully deformed hook, full bending
- partly deformed hook - model 1
- partly deformed hook - model 2

fibre slip (mm)

RATIO p(w)
(number of fibres active in crack bridging at crack width w)

$p(w) = n_{act}(w) / n_{tot}$

- all fibres
- fully deformed fibres
- partly deformed fibres

fibre type l/d = 60/0.7

embedded length of fibres l_{emb} (mm)

TOTAL TENSILE STRESS

tensile stress (MPa)

- full bending of fibres
- partial bending of fibres
- no bending of fibres

1.0 vol.% fib. 60/0.7

displacement (mm)

CALCULATION FOR FIBRES 13/0.2 (short straight fibres)

applied volume quantity:	0.5	vol.-%		
total number of fibres:	540	fibres	(measured, Tab. 3.3)	
average orientation angle:	34.6	degrees	(measured, Tab. 3.3)	
average orientation angle:	0.604	rad		

cell	A	B	C	D	E	F	G	H	I	J	K	L	M	N
1	displacement	pullout forces in fibres with initial embedded length (mm) (Fig. 4.21)					ratio p(w), fibres with different embeddedd lengths (mm) (Fig. 4.16.b)					total number of fibers active in crack bridging	total tensile force	**total tensile stress**
2	(mm)	0-2	2-4	4-6	6-8	8-10	0-2	2-4	4-6	6-8	8-10		(N)	**(MPa)**
3	0	5	17	24	31.0	38	0.1	0.3	0.6	0.0	0.0	540.0		
4	0.25	5	17	24	31	38	0.075	0.3	0.6	0.0	0.0	526.5	10800	**2.20**
5	0.5	4.25	15	23	30	37	0.0625	0.3	0.6	0.0	0.0	519.8	10054	**2.05**
6	0.75	3.5	13	21	28.5	35.5	0.05	0.3	0.6	0.0	0.0	513.0	9028	**1.84**
7	1	3	11.5	20	27.5	34.5	0.025	0.3	0.6	0.0	0.0	499.5	8424	**1.72**
8	1.5	1.5	7.5	17	25	32.5	0	0.3	0.6	0.0	0.0	486.0	6743	**1.38**
9	2	0	4	14.5	22.5	30	0	0.225	0.6	0.0	0.0	445.5	5346	**1.09**
10	2.5	0	3	11.7	20	27.8	0	0.15	0.6	0.0	0.0	405.0	4155	**0.85**
11	3	0	2	9	17.8	25.7	0	0.075	0.6	0.0	0.0	364.5	3078	**0.63**
12	3.5	0	1	6	15.5	23.2	0	0	0.6	0.0	0.0	324.0	1985	**0.41**
13	4	0	0	3.5	13	21	0	0	0.3	0.0	0.0	162.0	1134	**0.23**
14	5	0	0	1.7	8	16.5	0	0	0	0.0	0.0	0.0	275	**0.06**
15	6	0	0	0	3.25	12	0	0	0	0.0	0.0	0.0	0	**0.00**
16	7	0	0	0	1.6	7.5	0	0	0	0.0	0.0	0.0	0	**0.00**
17	8	0	0	0	0	3	0	0	0	0.0	0.0	0.0	0	**0.00**
18	9	0	0	0	0	1.5	0	0	0	0.0	0.0	0.0	0	**0.00**
19	10	0	0	0	0	0	0	0	0	0.0	0.0	0.0	0	**0.00**

PULLOUT FORCES IN FIBRES

pullout force (N)

short fibres 13/0.2

fibre slip (mm)

RATIO p(w)
(number of fibres active in crack bridging at crack width w)

$p(w) = n_{act}(w) / n_{tot}$

short fibres 13/0.2

embedded length of fibres (mm)

TOTAL TENSILE STRESS

tensile stress (MPa)

0.5 vol.-% short fibres 13/0.2

displacement (mm)
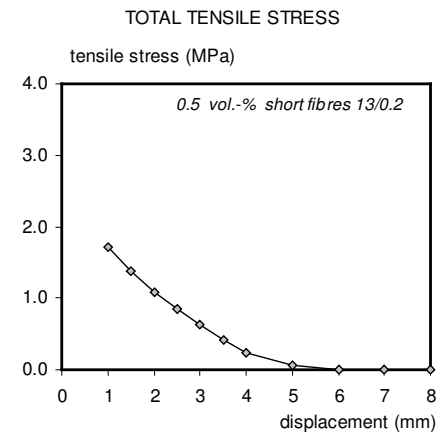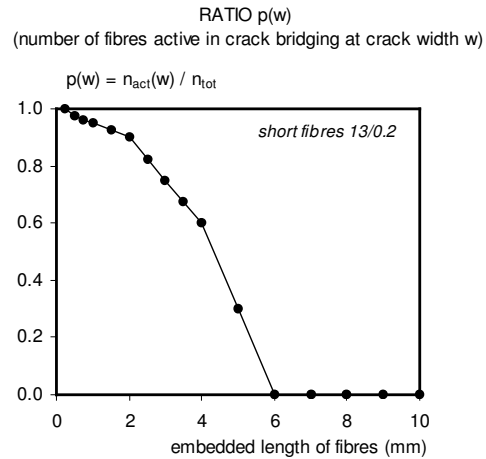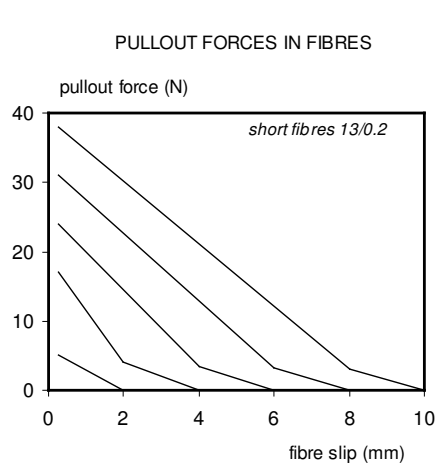
LIST OF SYMBOLS AND NOTATIONS

Capital Roman Letters:

$Af,1$	= surface area of the cross section of a single fibre	[mm^2]
D	= diameter	[mm]
D_{agg}	= diameter of the aggregate grain	[mm]
D_{aver}	= arithmetically average aggregate grain size	[mm]
D_f	= nominal fibre diameter (Eq. 3.1)	[mm]
D_{f2}	= length of the longer axis of the elliptical cross-section of a fibre	[mm]
D_{max}	= maximum aggregate grain size	[mm]
E_{1-2}	= energy needed to create the first crack in the multiple cracking sequence of HFC	[Nmm]
E_2	= energy needed to create the second and al other cracks in the multiple cracking sequence in HFC	[Nmm]
E_f	= the modulus of elasticity of the fibres (E_f = 210000 N/mm^2);	[N/mm^2]
G_{II}	= the fracture energy released at the fibre-matrix interface during the debonding process (the fracture energy of the second (II) mode – i.e. of the shear fracture)	[Nmm]
G_m	= the fracture energy of plain concrete, obtained from the tensile test (here approximate G_m = 0.108 N/mm);	[Nmm]
$G_m V_m$	the fracture energy of the matrix, required to create a new through-crack surface (where G_m is the matrix fracture energy, and V_m the matrix volume fraction in %)	[Nmm]
K_i	= compaction index of grain class i	[-]
M	= bending moment	[Nm]
N	= total number of fibres present in the cross-section of a FRC element	[-]
N	= normal force	[N]
P	= pullout force in fibre	[N]
$P(w) = P_{ll}$	= the horizontal component of the total bridging force, equal to the total tensile force that acts on the fibre-concrete composite element in Fig. 4.15;	[N]
$P_{aligned}$	= pullout force in the fibre aligned to the direction of tensile stresses	[N/mm^2]
$P_{inclined}$	= pullout force in the fibre inclined to the direction of the tensile stresses	[s]
$P_{\beta(w)}$	= total tensile force in the fibre inclined under the angle β (w);	[N]
PD_{exp}	= experimentally determined packing density	[-]
PD_{nd}	= non-disturbed packing density	[-]
S	= spacing of fibres in a cross-section of a FRC specimen	[mm]
U_{db}	the debonding energy, needed to destroy the elastic bond at the fibre-matrix contact	[Nmm]
V_{cont}	= the volume of the container	[m^3]
V_d	= ratio of disturbed volume of container and total volume of container	[-]
V_{ef}	= the effective volume quantity of fibres;	[-]
V_f	= fibre volume percentage	[N/mm^2]
V_f	= the applied volume quantity of fibres;	[-]
$V_m = 1 - V_f$	= the matrix volume fraction;	[-]
V_{nd}	= ratio of non-disturbed volume of container and total volume of container	[-]
Vol_{agg}	= the volume content of aggregate in a unit volume of the mixture	[-]
Vol_{fib}	= the volume content of fibres in a unit volume of the mixture	[-]
W	= resistance moment of the cross section	[m^3]

Small Roman Letters:

a_{ij}	= loosening (opening) coefficient for interactions between grains	[-]
b	= width of the cross- section of a structural element	[mm]
b_i	= virtual packing density of i class of grains	[-]
b_{ij}	= wall-effect coefficient for interactions between grains	[-]
d	= fibre diameter	[mm]

E_b	= modulus of elasticity of concrete	[N/mm²]
$f_{b,el}$	= tensile strength of HFC for the design stress-strain relation	[N/mm²]
$f_{b,w2}$	= tensile strength of HFC for the design stress-strain relation	[N/mm²]
f_b	= tensile strength of HFC for the design stress-strain relation	[N/mm²]
f_b'	= compressive strength of HFC for the design stress-strain relation	[N/mm²]
f_{cc}	= compressive strength of concrete	[N/mm²]
f_t	= uniaxial tensile strength of concrete	[N/mm²]
$f_{t,0}$	= tensile strength of plain concrete	[N/mm²]
$f_{t,cr}$	= first-cracking strength of FRC loaded in unaixial tension	[N/mm²]
f_y	= tensile strength f steel fibres	[mm]
h	= height of the cross section of the structural element	[mm]
k_w	= disturbance coefficient for a dry packing of aggregate (and fibres)	[-]
l	= fibre length	[mm]
l/d	= fibre aspect ratio	[-]
L_{ch}	= characteristic length	[mm]
L_{db}	= debonded length of a single fibre during its pullout	[mm]
l_{max}	= selected maximum visible fibre length for different fibre length distributions	[mm]
l_{vis}	= visible (i.e. pulled-out) length of fibre at the fracture plane of a specimen (after the performed test)	[mm]
m_{cont}	= the weight of empty container	[kg]
m_{full}	= the weight of full container	[kg]
$n_{act(w)}$	= the number of fibres active at the crack bridging for the crack width w	[-]
n_{tot}	total number of fibres present in the cracked cross section	[-]
$p(d)$	= probability that a hook of a long fibre will be fully straightened (fully deformed) during the crack opening	[-]
$p(l_{vis})$	= probability that a fibre with a visible (i.e. pulled-out length) l_{vis} can be found at the fracture plane of a specimen (after the performed test)	[-]
$p(w)$	= the probability that the fibres active in crack bridging may be found at the crack width w	[-]
r	= the fibre radius	[mm]
t_{50}	= flowing time of fresh concrete mixture from Abrams cone needed to reach a circle with a diameter of 50 cm	[N/mm²]
w	= crack width	[mm]
y_i	= the volume of i- type grains divided by total solid volume	[-]
y_i	= the experimental packing density of i class of grains	[-]

Capital Greek Letters:

Φ	= packing density of a granular mixture	[-]
Δ	= fibre slip during pullout	[mm]
ΔU_{f-mc}	: the increase of fibre strain energy by virtue of the action of the fibres in bridging the first through-crack;	[Nmm]
ΔU_{f-mu}	the increase in the fibre strain energy, as a result of the bridging of cracks during multiple cracking	[Nmm]
ΔU_{fr}	the frictional energy, absorbed by virtue of the difference in strain (slip) of the fibres bridging the first through-crack and the concrete matrix which surrounds them	[Nmm]
ΔU_{fm}	the decrease of the matrix strain energy (since the strain in a cracked matrix is zero)	[Nmm]

Small Greek Letters:

α	= the angle of inclination i.e. orientation of a fibre	[-]
$\beta(w)$	= the angle of local bending of an inclined fibre at the crack width w	[°]
$\beta(w)$	= the angle of local bending of fibre across the crack.	[°]
β_{max}	= maximum local bending angle of the fibre across the crack	[°]
β_{min}	= minimum local bending angle of the fibre across the crack	[°]
ε	= strain in general	[-]
$\varepsilon_{b,el}$	= the limit elastic tensile strain of HFC for the design stress-strain relation	[-]

$\varepsilon_{b,el}{}'$	= limit elastic compressive strain of HFC for the design stress-strain relation	[-]
$\varepsilon_{b,u}$	= ultimate tensile strain of HFC for the design stress-strain relation	[-]
$\varepsilon_{b,u}{}'$	= ultimate compressive strain of HFC for the design stress-strain relation	[-]
$\varepsilon_{b,w2}$	= tensile strain of HFC at the crack width w_2 for the design stress-strain relation	[-]
$\varepsilon_{b,w1}$	= tensile strain of HFC at the crack width w_1 for the design stress-strain relation	[-]
ε_{mu}	= the strain at which the first through-crack forms in the fibre concrete under consideration (corresponds to the first bending point at the diagram of uniaxial tensile response, Fig. 4.1);	[-]
γ_{agg}	= specific weight of aggregate (here 2.6 kg/dm^3)	[kg/dm^3]
γ_{fib}	= specific weight of fibre steel (here 7.85 kg/dm^3)	[kg/dm^3]
γ	= specific weight	[kg/m^3]
η	= the coefficient of orientation of fibres, ($0 < \eta < 1$, $\eta = 1$ for fibres fully oriented in the direction of the main tensile stress, as explained in section 3.6);	[-]
η	= factor in Eq. 2.1 for triangular and square fibre array	[-]
σ	= stress in general (tensile or compressive)	[mm]
τ	= shear stress along the fibre matrix interface	[N/mm^2]
τ_f	= the average frictional stress at the fibre-matrix interface, which exists after the debonding at the interface has been finished	[N/mm^2]

LIST OF ABBREVIATIONS

HFC	Hybrid-Fibre Concrete
FRC	Fibre Reinforced Concrete
HPC	High Performance Concrete
HPFC	High Performance Fibre Concrete
HSC	High Strength Concrete
HCFC	High Strength Fibre Concrete
UHSC	Ultra-High Strength Concrete
UHPC	Ultra-High Performance Concrete
UHPFC	Ultra-High Performance Fibre Concrete
UHPFRC	Ultra-High Performance Fibre Reinforced Concrete
SCC	Self-Compacting Concrete
CC	Conventional Concrete
SCFRC	Self-Compacting Fibre Reinforced Concrete
MMFRC	Multi-Modal Fibre Reinforced Concrete
RPC	Reactive Powder Concrete
PC	Portland Cement
LVDT	Linear Variable Displacement Transducer (displacement measuring device)
SLS	Serviceability Limit State
ULS	Ultimate Limit State
ISO	International Organisation for Standardisation
NEN	Nederlands Normalisatieinstituut – Netherlands Institute for Standardisation
DIN	Deutsches Institut für Normung - German Institute for Standardisation
ACI	American Concrete Institute
AFGC	L'Association Française de Génie Civil - French Society for Civil Engineering
RILEM	Réunion Internationale des Laboratoires et Experts des Matériaux, Systèmes de Constructions et Ouvrages - International Union of Laboratories and Experts in Construction Materials, Systems and Structures
SIA	Schweizerischer Ingenieur- und Architektenverein - Swiss Society of Engineers and Architects

C U R R I C U L U M   V I T A E

Name:	Ivan Marković
Born:	12 June 1976 in Aleksandrovac (Serbia)

Academic education:

Institution:	University of Belgrade, Faculty of Civil Engineering, Belgrade, Serbia
Period:	October 1995 – September 2000
Main disciplines:	Structural Engineering (Concrete Structures, Steel Structures, Structural Mechanics). Graduated with highest honours.

Exchange Program:

Institution:	Brandenburg University of Technology (BTU), Department of Steel Structures, Cottbus, Germany (based on DAAD Scholarship)
Period:	August 1999 – December 1999
Main disciplines:	Steel Structures

Employment:

Institution:	Delft University of Technology, Faculty of Civil Engineering and Geosciences, Department of Concrete Structures and Microlab, Delft, The Netherlands
Period:	October 2000 – October 2004
Main disciplines:	- PhD-Research on High Performance Hybrid-Fibre Concrete - Teaching activities (courses on Prestressed Concrete) - Supervision of MSc-thesis related to the applications of Hybrid-Fibre Concrete

Institution:	"Witteveen + Bos" Engineering Consultants, Department of Under-ground Infrastructure, Amsterdam, The Netherlands
Period:	from October 2004
Main disciplines:	- Specialised structural engineering related to the interactions between buildings and structures, soil and underground structures - Structural engineering, Projectmanagement, Concrete technology

Memberships:

Member of 10 national and international societies and working groups related to structural engineering, concrete structures, concrete mechanics and concrete technology.

Contact: i.markovic@witbo.nl and imarkovic@gmx.net .